

University of New Mexico

UNM Digital Repository

Anthropology ETDs

Electronic Theses and Dissertations

7-1-2010

THE HUMAN SKULL: DEFINITION BY INTEGRATIONIST AND MODULAR MODELS

John Y. Anderson

Follow this and additional works at: https://digitalrepository.unm.edu/anth_etds



Part of the [Anthropology Commons](#)

Recommended Citation

Anderson, John Y.. "THE HUMAN SKULL: DEFINITION BY INTEGRATIONIST AND MODULAR MODELS." (2010). https://digitalrepository.unm.edu/anth_etds/4

This Dissertation is brought to you for free and open access by the Electronic Theses and Dissertations at UNM Digital Repository. It has been accepted for inclusion in Anthropology ETDs by an authorized administrator of UNM Digital Repository. For more information, please contact disc@unm.edu.

**THE HUMAN SKULL: DEFINITION BY
INTEGRATIONIST AND MODULAR MODELS**

BY

JOHN YARD ANDERSON

B.S., Anthropology, University of California - Berkeley, 1994
M.S., Biological Anthropology, University of New Mexico, 1996

DISSERTATION

Submitted in Partial Fulfillment of the
Requirements for the Degree of

**Doctor of Philosophy
Anthropology**

The University of New Mexico
Albuquerque, New Mexico

July, 2010

John Y. Anderson

Candidate

Anthropology

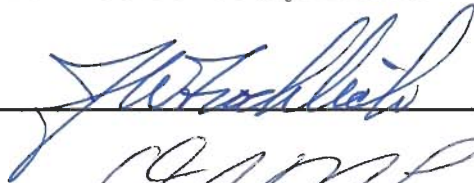
Department

This dissertation is approved, and it is acceptable in quality and form for publication:

Approved by the Dissertation Committee:

Michael W. Graves

, Chairperson





ED TD

Michael W. Graves

DEDICATION

To my parents, Dr. John A. Anderson and Sylvia Anderson, and to Lisa—they know why.

ACKNOWLEDGMENTS

What student of biological anthropology would I be not to thank the two figures who have meant the most to me in my learning career: Drs. Tim White of Berkeley and Erik Trinkaus of Washington University. To those who read this, they need no introduction—their knowledge spans the entire range of development of the genera and species that portray our past through their rare fossils.

With no less gratitude to my advisors at the University of New Mexico, I thank Drs. Powell, Bedrick, Froehlich, and Pearson; without their support and insight this dissertation would not only have not been possible, it would have been no fun at all. I especially thank Joe Powell who became my dissertation chair when Erik moved to Washington University. To my advisor, colleague, and friend Dr. Gary Richards and his wife Dr. Rebecca Jabbour I owe an unpayable debt of comradeship and respect. I thank Professor Teri Rosenbaum at the University of Utah for assistance with cross-sectional geometry and analysis in SCION, and Professor Paul O'Higgins for access to Morphologika in the earliest stages of its development.

I would like to acknowledge Mr. Mario Ruiz, the graphic artist who assisted me with several of the figures in this dissertation. I also thank Ms. Bettina Behrens for her gracious loan of her three-dimensional Calypso digitizer and for many fruitful discussions on evolutionary biology.

Finally, to all who study human evolution with the required sense of wonder and awe inspired by our position as a species, sometimes precariously placed, sometimes exalted, I say cheers.

**THE HUMAN SKULL: DEFINITION BY
INTEGRATIONIST AND MODULAR MODELS**

BY

JOHN YARD ANDERSON

ABSTRACT OF DISSERTATION

Submitted in Partial Fulfillment of the
Requirements for the Degree of

**Doctor of Philosophy
Anthropology**

The University of New Mexico
Albuquerque, New Mexico

July, 2010

ABSTRACT
THE HUMAN SKULL:
DEFINITION BY INTEGRATIONIST AND MODULAR MODELS

The human mandible and cranium are parts of an integrated cranial complex. These regions are also major components of the modular system, which comprises multiple semi-autonomous areas within the body. Integration and modularity express structure and function across various hierarchical levels of organization in the body and are thus definable as two non-exclusive ways of viewing somatic structure. What is integrated at one level may be a separable, modular unit at another. This dissertation statistically examines the interface between integration and modularity as partitioned through various hierarchical levels in the human skull, including the mandible. This examination is framed as a suggestion for new definitions of modularity, both through properties and attributes.

Cranial integration is usually defined as the degree to which cranial elements or regions are integrated across the skull, and modularity is defined as areas of localized integration within the skull. Modules result from changing function through time in an evolutionary context, thus being definable as areas of functionally driven, localized integration. Modules are also heritable, possessing a higher degree of internal organization than non-modular regions. Therefore modules are heritable areas of the skull, definable by function, which are more integrated within themselves than non-modular regions. Under this view modules are inherited patterns of integration, whether genotypic or phenotypic, resulting in the hypothesis that modules are constrained regions of morphology which are resistant to change within a taxonomic level such as species but necessarily express change across species.

This dissertation proposes the new definition of modularity through an examination of the patterned internal structure of modules in multiple groups of modern human skulls. Results presented in this dissertation suggest modularity as currently defined in biology lacks rigor. A testable, scientific definition of modularity can only be defined in the context of arguments which are driven by both attributes and properties. This dissertation attempts to show that modules represent areas of invariance to axes of population and sex, that the human mandible fails several key tests for being described as a module, and that modularity itself may be secondary to an even more fundamental, constrained pattern of development in the skull. Finally, it is shown dimensionality of measurements themselves (two-dimensional versus three-dimensional) is, in itself, a predictor for analysis of the shape of modules in the skull. Disregard of any of the above factors would ultimately prevent accomplishment of the goal of a robust definition of the human skull from a scientific perspective.

PREFACE

The human skull is one of the most studied shapes in history, yet the biological meaning of its expression is continually contested. One of the major questions in biological anthropology generally and paleoanthropology in particular concerns the role cranial integration plays in creating our overall cranial shape. Is the skull best regarded as one indivisible unit or as a collection of semi-competing integrated entities? Is the conception of “parts” even meaningful in the study of the skull? How? The cranium and mandible form one unit, yet the traditional view of “the cranium” and “the mandible” operates on the assumption the mandible is different from the skull in some obvious though unstated way—perhaps because it moves? Equally “obvious” is that without some form of integration chewing for sustenance would be impossible. But how does (and did) this integration come about?

Mastication is a complex process. Parts must fit together: severe disproportion between the cranium and mandible would compromise function and would be eventually be evolutionarily deleterious. Mastication also involves more than just the mandible and face; the neurocranial muscle attachment points, basicranial articulations, and nasopharyngeal spatial requirements are also parts of the system. The difficulty of inclusion of the mandible as part of the complex cranial system comes not just from the fact it moves, but also from the fact there are several other unique aspects to its morphology. The mandible is unique in being the only part of the skull moved by muscles, unusual in its being completely sheathed by muscles, and also remarkable in its being nearly weightless compared to the forces that move it. All these factors combine to

describe a structure that is, or might be, a perfect representation of Wolff's Law, that is, a structure that is little more than an osseous representation of forces produced for the role of mastication (Wolff, 1891). But, as with all other cranial elements, the mandible is more than a simple biomechanical device. If mechanical force were the only predictive variable for morphology, analysis would be complete and Wolff's Law would explain the mandible and cranium perfectly, that is, as shape schematized to production by only by one factor—biomechanical force. However, schematization here produces oversimplification, because the skull also exhibits the aspect of integration both within and across cranial parts or modules. Schematization of a complex, multifunctional entity such as the skull fails because much of the variability of morphology may not derive from biomechanical force but from other factors such as modularity and integration. The aspect of schematization forms a primary reason the skull is studied in this dissertation; the skull we observe is an integrated whole, and schematization is not informative in the broad sense.

The skull in general has several functions, and the mandible also represents more than one, having spatial aspects such as accommodation of respiration and participation in a counterpart system of cranial relationships (Hans and Enlow, 1996; Chinn et al., 2006; Weinstein, 2008). As outlined below, evolutionary modeling of body structures is currently argued in terms of modularity, being defined as a partitioning of somatic systems into a hierarchy of interconnected parts (Mitteroecker and Bookstein, 2007; Wagner, et al., 2007). The mandible is one of these somatic parts, yet no part or module of the body or skull exists in isolation. Patterned internal structure of modules in multiple groups of modern humans suggests modularity can only be defined in the context of

arguments which are driven by both attributes and properties and that modules should represent areas of independence in evolutionary trajectory. This form of modeling is indispensable in describing the modern human skull. However, although it is assumed that modularity explains cranial organization, definition of modularity itself is at an early stage. Presently it is not known whether modules encompass all of skull morphology or whether there are “extra-modular” areas within the cranium or mandible themselves. Much cranial research describes the face as an entity separate from the neuro- or basicranium yet fails to address the fact the splanchnocranium forms as a unit composed of the maxilla and the mandible. Many three-dimensional morphometric analyses and modular analyses of the skull exclude the mandible even though definitions of cranial modularity are based on levels of integration within and across cranial elements. These analyses are thus compromised because they omit a major component of the masticatory system. The face (including the mandible) maintains an integrated relationship that must be addressed for statistical significance if estimates of integration or modularity are being performed (Ackermann and Cheverud, 2004; Ackermann, 2005; Polanski and Franciscus, 2006).

This dissertation addresses the above issues by modeling the skull as resultant from and predictive of morphology arrayed at various hierarchical levels. The organization is as follows: Chapters 1 and 2 review the history of cranial research and examine the development and expression of the concept of modularity. Chapter 3 begins a series of chapters examining the hierarchical partitioning of the skull. Modules of the skull and their integration are examined using a series of linked hypotheses which are then tested

using statistical modeling including Cronbach's Alpha, partial least squares, and analysis of covariance structure using the Flury hierarchy. In general outline, cranial organization (including the mandible) is analyzed first using model-free hypotheses testing the relationship of "macromodules" of the face, base, skull, and mandible. Next, functional divisions of the skull are examined as modules and results are used to provide a functional definition of modularity through properties rather than solely by attributes. This definition is used to test recent suggestions organizational schema such as *bauplans* represent modular patterns and that phylogenetic analysis in *Homo* would be improved through the use of modules rather than whole-cranial structure (González-José et al., 2008). Chapter 5 examines this idea by comparing results from the pattern of modern human cranial modularity to representatives of hominine evolution. Modules may be genus- or subfamily-specific entities (as obliquely referred to in González-José et al., 2008). Results in Chapter 4 suggests that robusticity is best defined as the way size increases without modular reorganization of shape. In testing functional relationships it is shown that shape remains organized in the same way across human populations and sex, usually becoming more robust rather than reorganizing the shape itself in responding to function. Finally in Chapter 5 it is demonstrated that dimensionality of measurements used to define modules is an important, and sometimes overlooked, factor. This factor can skew any research using covariance matrices as representatives of cranial structure, including modules. Penultimately, cranial nerve patterning is explored as the underlying formative pattern of the skull, with the possibility that modularity itself is constrained by this pattern. If so, the present functional organization of the skull begins quite early in the Hominoidea, constraining even the less conserved pattern of modularity itself. Finally,

the expectations and limitations of current modular theory are described, with further avenues of research also suggested.

TABLE OF CONTENTS

FRONT MATTER	Page
DEDICATION	iii
ACKNOWLEDGEMENTS.....	iv
ABSTRACT	vi
PREFACE... ..	viii

CHAPTERS	Page
1 INTRODUCTION: THEORY AND BACKGROUND	1
2 PARTICULATE AND STRUCTURAL MODELS OF MODULARITY	28
3 HIERARCHICAL COMPARISONS OF CRANIAL REGIONS.....	46
4 FUNCTIONAL MODULAR PROPERTIES: TESTING HYPOTHESES OF MODULAR STRUCTURE	109
5 MODULAR APPLICATION AND IMPLICATIONS.....	157
6 SUMMARY AND CONCLUSION	192

APPENDICES	Page
A	SAMPLE COMPOSITIONS BY LOCATION196
B	METHODOLOGY 202
C	STATISTICS214
D	MORPHOLOGIKA 2.5223
E	CRANIAL BREADTH DISCRIMINANT ANALYSIS232
LITERATURE CITED234

TABLE OF FIGURES

Number	Title	Page
1-1	Integrated Skull Schematic of the Craniofacial/Mandibulomaxillo Relationship	7
1-2	Invariant Cranial Relationships (PM, NHA) That Not Only Cross Modular Units But Are Formed by Them.....	9
1-3	Progression to Piltdown—Linear Schema; Manifested Example of a Paradigm.....	10
1-4	D’Arcy Thompson Introduced Three-Dimensional Modeling As a Series of Morphing Coordinate Systems.....	13
1-5	An Illustration of the Underlying Logic of Discriminant Function.	15
1-6	Slide Showing Three-Dimensional Morphing of Liang Bau 1 Mandible	22
2-1	Pleiotropic Modularity	35
2-2	Parcellation and Integration	36
3-1	Measurements Used on the Mandible in the Fortext Sample	66
3-2	Scree Plot for the 47 Corrected Measurements of Howells Data	77
3-3	Scores Graph for Partial Least Squares Analysis of Facial Morphology Explained by the Neurocranium	78
3-4	Parallel Coordinate Plot of the Mandible and Cranium in 144 Individuals	80
3-5	PLS Scores Plot for Mandible by Skull Overview	81
3-6	Fortext Male/Female Plot.....	85
3-7	Howells Male/Female Plot.....	86

3-8	Bimodal Distribution of 3D Points in Males versus Females for the Howells Dataset	88
3-9	Analysis (Mahalanobis Distances)	89
3-10	Three-Dimensional Plot of the Face Using Howells Data.....	90
3-11	Results for Cranial Base.....	92
3-12	Results for Mandible.....	92
3-13	Results for Mandible (14 Measures), Circumpolar Samples.....	93
3-14	Single Variable Decomposition.....	96
3-15	Face, 3D Scatterplot.....	98
3-16	Skull, Canonical Plot Using Linear Discriminant Method	99
3-17	Mandible, Canonical Plot Discriminant Analysis	100
4-1	Cranial Base Angle (CBA)	121
4-2	Bivariate Fit of Mand14 by Face14	139
4-3	Partial Least Squares Scores for Face14 and Mand14.....	140
4-4	PLS Scores Plot for Mandible by Skull Overview	141
4-5	Bivariate Fit of Mand14 by Base14 (JMP Plot)	142
4-6	Partial Least Squares Scores for Mand14 and Base14 (JMP Plot)	143
4-7	Ellipsoid 3D Parallel Coordinate Plot of the Mandible, Face, and Base	144
4-8	Contour Plots for the Mandible in Males and Females	149
5-1	PLS	165
5-2	Bivariate Fit of Cor8 by Ram8	165

5-3	Anterior Facial Block and Mandible.....	171
5-4	Area Bounded by Facial Foramina	176
5-5	Anterior View of Constrained Area	177
5-6	Lateral View of Foramina	177
5-7	Positional Relationships.....	184
5-8	Three-Dimensional Partial Least Squares Scores	185
5-9	Bilateral Facial Partial Least Squares Scores	186
A-1	Locations of Fortext Populations.....	199
A-2	Locations for NMNH and AMHN Individuals Measured.....	200
B-1	Illustration of Axes Used to Calculate Polar J	203
B-2	Sample Illustration of Mandibular Molds.....	204
B-3	Illustration of Mandibular Points Used in Fortext	209
B-4	Illustration of Cranial and Mandibular Points Used in Fortext.....	210
C-1	The Application of Cronbach's Alpha	216
C-2	Flury Hierarchy	217
C-3	The Application of the Flury Hierarchy	219
C-4	The Application of Stepwise Linear Regression	221
C-5	The Application of PLS Regression.....	222
D-1	The Projection of Three-Dimensional Coordinates into Tangent Two-Dimensional Space Can Be Analyzed Using Multivariate Techniques	225
D-2	Lateral Mandible Analyzed in Chapters 3, 4, and 5.....	227

D-3	Oblique View Mandible Analyzed in Chapters 3, 4, and 5	228
D-4	Anterior Facial Block, Analyzed in Chapters 4 and 5.....	228

LIST OF TABLES

Number	Title	Page
3-1	Measurements Used in the Howells Dataset.....	62
3-2	Measurements Used with the Hanihara Dataset.....	64
3-3	Cronbach's Alpha – All Measurements in the Howells Dataset.....	72
3-4	Cronbach's Alpha – Males in the Howells Dataset.....	72
3-5	Cronbach's Alpha – Females in the Howells Dataset	72
3-6	Cronbach's Alpha – Size-Corrected Data for the Entire Howells Dataset Males and Females	73
3-7	Cronbach's Alpha – Comparison of the Neurocranial “Skull” Only	73
3-8	Cronbach's Alpha – Comparison of the Face Only	74
3-9	Cronbach's Alpha – Comparison of the Base Only	74
3-10	Cronbach's Alpha – Skull+Face+Base.....	76
3-11	Flury Decomposition of Three Cranial Regions	77
3-12	Partial Least Squares – Percent Variation Explained by the Neurocranium	79
3-13	Flury Decomposition of the Matrices of the Skull and Mandible	79
3-14	Partial Least Squares – Percent Variation in the Mandible Explained by the Skull	81
3-15	Flury Hierarchy – Howells Dataset	83
3-16	Flury Hierarchy – Complete Set Hanihara's Data	84
3-17	Flury Hierarchy for Whole Skull, Males versus Females Howells Dataset.....	86

3-18	Flury Decomposition of Chi Square (Step-Up and Model Building Approaches) Howells Data, Cranial Base, 7 Measurements.....	90
3-19	PC Eigenvalues for Cranial Base.....	93
3-20	PC Eigenvalues for Face.....	94
3-21	PC Eigenvalues for Mandible	94
3-22	Face and Mandible Responding Together to High Biomechanical Force on PC1	95
3-23	Counts for Group Membership for Actual Rows by Predicted Columns from Discriminant Function	97
3-24	Whole Skull, Flury Decomposition of Chi Square (Step-Up and Model Building Approaches) for Circumpolars	102
3-25	Cranial Base Only, Flury Decomposition of Chi Square (Step-Up and Model Building Approaches) for Circumpolars	102
3-26	Neurocranium, Flury Decomposition of Chi Square (Step-Up and Model Building Approaches) for Circumpolars	103
3-27	Face Only, Flury Decomposition of Chi Square (Step-Up and Model Building Approaches) for Circumpolars	103
4-1	Landmark Points for Morphometric Measurements	123
4-2	Major Functional Predictive Factors for Morphology.....	127
4-3	Stepwise Fit – Skull42 (42 Landmark Points, Combination of the Face, Base, and Mandible)	129
4-4	Stepwise Fit – Skull28 (28 Landmark Points, Whole Skull Exclusive of Mandible).....	131
4-5	Stepwise Fit – Mand14 (Including Base and Face)	133
4-6	Stepwise Fit – Mand14 (with Face and Base Joined As Skull28)	134
4-7	Stepwise Fit – Face14.....	136

4-8	Stepwise Fit – Base14.....	137
4-9	Orthogonal Regression of Face14 and Mand14	139
4-10	Partial Least Squares – Percent Variation Explained for Face14 and Mand14	140
4-11	Orthogonal Regression of Face14 and Base14	141
4-12	Orthogonal Regression of Mand14 and Base14	142
4-13	Partial Least Squares – Percent Variation Explained for Mand14 and Base14.....	143
4-14	Multivariate Correlations across Face, Base, and Mandible.....	144
4-15	Principal Components / Factor Analysis on Correlations across Face, Base, and Mandible.....	144
4-16	Pairwise Correlations among Mandible, Face, and Base.....	145
4-17	Effects of Functional Factors on Partitions of the Skull	146
4-18	Flury Hierarchy of Whole Skulls of Circumpolar and Non- Circumpolar Populations (CPC Shows Eskimos Compared to Skull of Others, CPC=2).....	152
4-19	Flury Hierarchy of Mandible in Circumpolar Populations Compared to All Other Samples (Mand14).....	153
4-20	Flury Hierarchy of Circumpolar Facial Module	154
5-1	Flury Hierarchy of the Ramus Compared with the Corpus.....	164
5-2	Partial Least Squares – Percent Variation Explained, Corpus by Ramus.....	165
5-3	Orthogonal Regression of Cor8 by Ram8.....	165
5-4	Stepwise Fit for Factors Producing Ramus	168

5-5	Stepwise Fit for Factors Producing Cor8	169
5-6	Points Used by Gonzalez-José et Al. (2008) for Face, in Common with This Dissertation's Morphologika Dataset	172
5-7	List of Specimens (from Gonzalez-José et Al. 2008)	173
5-8	Flury Hierarchy of Modern <i>Homo Sapiens</i> fersus Non-Homo (12 Facial Measurements)	174
5-9	Flury Hierarchy of Modern <i>Homo Sapiens</i> against Pleistocene <i>Homo</i>	174
5-10	Stepwise Fit for Foraminal Pattern in Morphologika 2.5	178
5-11	Flury Hierarchy Comparing Face—Modern Humans against Archaic <i>Homo</i>	188
5-12	Flury Hierarchy Comparing Face—Modern Humans against Archaic <i>Homo</i>	188
5-13	Flury Hierarchy of Man14 (3D)	190
5-14	Flury Hierarchy of Man9 (2D)	191
B-1	Howells Craniometric Measurements Used	211
B-2	Population Coding Used	213
D-1	Morphologika 2.5 Digitizing Points	229
E-1	Discriminant Function Analysis Illustrating Effect of Breadth Measurements	233

CHAPTER 1

THEORY AND BACKGROUND

The human mandible and face are part of an integrated cranial complex as suggested by Olson and Miller (1958). Integration in the skull across elements is constrained by canalization in the sense of Waddington (1942, 1957), which predicts developing biological structure maintains a degree of relationship through life derived from initial developmental states. This inherited pattern in the cranium and mandible is also represented through modular structure, in which several key functional units make up the basic organizational level of the skull (Polanski and Franciscus, 2006; Mitteroecker and Bookstein, 2007, 2008; Wagner et al., 2007). Integration and modularity can be defined as two organizational views of the same structure. Cranial integration is usually defined as the degree to which cranial elements or regions are integrated across the skull, whereas modularity is usually defined as integration within the different functional units of the skull. Some researchers stress the integrated aspect of the skull, while others focus on the modular aspect. The underlying significance of either analysis is that phylogenetic, populational, and structural arguments ultimately resolve to the different ways the skull is partitioned.

Although the skull is integrated, the modular structure means it has a complex substructure, organized as the sum of semi-autonomous parts. At the level of the individual or small population this autonomy is expressed as variability; individual skulls in populations vary widely. At larger scales this highly variable autonomy can be shown to be constrained into patterns of variation. Here, groups of regional and then continental

groups of skulls show a degree of similarity across sex and population, and it is at this scale similarities rather than differences in skulls become observable. The question becomes where the areas of constraint of variation in forming this patterned variation in the human skull occur. We see differences in individual skulls, yet by consolidating we eventually form groups which exemplify and then transcend smaller partitions into regional and finally continental patterns. This patterning results from the variable expression of the modules in the skull. Modules are the way constraint limits the degree to which skulls vary across population and sex. The boundaries of the modular pattern range between the one extreme where the skull is totally integrated (which would permit no functional derivation and no modules) to the other extreme where a skull would be totally modular (in which all function and microfunction would be a distinguishable entity).

This dissertation proposes modules constitute regions of stable forms within this spectrum, between an uninformative whole and trivial atomization. The working definition in this dissertation is that modules are inherited patterns of integration. Because the control of a phenotype is primarily genetic, this definition would seem to be a trivial observation, that of course it is the pattern in the genes that is inherited. Yet the complexity of the definition increases for the phenotype because the control of genetic expression of the phenotype is also genetic (or epigenetic). However, the definition of a module as an inherited pattern of integration is useful because the corollary is that a non-random, inherited morphological pattern such as a module will exhibit aspects of invariance as compared to non-modular regions. These patterns of invariance can be expected to have expression across population and sex, the primary axes of variation in

the human skull. Under this view, modules that are integrated, inherited, and constrained should exhibit the quantifiable property of invariance within species. This is a testable property, not a qualitative attribute.

Current modular theory seeks to explain how evolution has changed parts of complex interrelated systems through time without disruption, and modularity is demonstrated as the mechanism (Wagner and Altenberg, 1996). Modules have many definitions, and several key ones are summarized in Mitteroecker and Bookstein (2008:943): modules “[1)] collectively serve a common functional role, (2) are tightly integrated by strong pleiotropic effects of genetic variation, and (3) are relatively independent from other modules.” Similarly Klingenberg and colleagues (2001:11) describe modules as morphological structures that “are made internally coherent by manifold and strong interactions among their component parts, but are relatively independent from other modules and have relatively weak or few connections with other parts of a system.” Both these definitions serve to underscore the fact that modules are localized areas of integration. This definition explains how evolution in the skull can proceed; change in subregions does not necessitate the genomic reorganization of the entire system to produce effect (by extension such areas are not likely to develop randomly either in evolutionary sequence or ontogeny). Given this, it seems the first question to ask would be what are the temporal and/or spatial boundaries of modules, that is, the shared attributes and testable properties by which they can be defined?

Modules are defined in multiple ways, both in ontogeny and in evolutionary formation of morphology. Bastir, Rosas, and O'Higgins (2006) described the chronological constraint of developing modules in ontogeny; the adult skull is a result of a sequence of changes in modules of the skull. At the other end of the spectrum it has been pointed out this pattern of modularity has shown what is called herein "taxon-specificity," or the (assumed) propensity for invariance within, rather than across species. (For an explanation of how developmental modularity becomes evolutionary modularity see Cheverud, 1996). As Polanski and Franciscus (2006:348) point out, "Evolutionary biology has long maintained that morphological systems go from being more integrated to more modularized throughout evolution." In other words, as new functions emerge, the pattern of the skull becomes increasingly more modular. Not only is the skull modularized, but modularity itself is not constant across time, with taxon-specificity discriminating modules by varying above the level of the species as function changes (see González-José et al., 2008).

Modules are usually represented by covariance matrices which represent phenotypic morphology (Ackermann, 2005; Polanski and Franciscus, 2006; Mitteroecker and Bookstein, 2007, 2008; Wagner, et al., 2007; Bastir, 2008; Martínez-Abadías, et al., 2008). Change in the relationship of these entities can be generalized as scaling to "lines of least resistance" in phenotypic change through evolution (Erouhmanoff and Svensson, 2008). Most evolutionary change in taxa is modeled as occurring through this small-scale modification of existing structure, rather than as major reorganization. Current theory suggests this change "along lines of least resistance" is mirrored in covariance structure similarities such as proportionality (Schluter, 1996; Renaud, et al.,

2006). This in turn leads to the hypothesis, tested here, that modular regions should not only exhibit internal integration, but that the structural pattern of the covariance matrices across sex and population should maintain relative invariance within the same species.

Looked at in this way, modularity is a constrained aspect of morphology within the species, and stabilizing selection should serve to maintain modular shape, invariant across axes of population and sex. At evolutionary nexuses, subtle functional reorganization occurs, minimized as much as possible (constrained) to prevent systemic disruption. It is hypothesized here modular covariance matrices (proportionality, not equality) truly change only upon speciation, rather than (allometrically) within species. Testing this idea requires clear-cut definitions of modules both by attributes (qualitative), and properties (quantitative). At present, criteria defining modularity are not well specified. Without a robust definition for modules both by attributes they must possess and by statistical testing of quantifiable physical properties across sex and population, modularity can derive from a circular definition—we define the point used to measure structure arbitrarily and get the results we expect. An example of the difficulty in defining modules is underscored by a recent statement from Bastir (2008:50): “Modules are integrated by local cranial factors such as purely spatial proximity.” Such statements resolve to a non-functional definition without boundaries, hence unusable.

Therefore definition of modularity must proceed from both high level and low level analysis to be “exhaustive” (Bastir, 2008). Higher level explanations of form ultimately lead to adaptationist arguments, lower level to over-atomized, concretized models.

Neither higher level nor lower level explanations are both necessary and sufficient. In modular analysis an overemphasis on higher level complexity means an over-reliance on what is called herein “definition by attribute” or shared features. Over-reliance on lower level models leads to over-emphasis on what is referred to here as “definition by property,” which ultimately would be measurement without theory (for a good overview of the issue see Bastir, 2008). Here, property refers to the measurable, quantifiable aspects of morphology. Attributes can be referred to as qualities entities possess, which are not amenable to mensuration and quantification in the same way as properties. Currently, modules are defined by statistical relationship, by attributes, and by generalized, non-specified reference to function. Modules defined in these ways do not form objective entities that are capable of repeatability in testing nor entities that have biological meaning. This thesis defines modularity based on a view of the skull as a series of partitioned yet integrated craniofacial structures organized in a hierarchy.

Why study the mandible?

It is important to define the mandible separately in terms of cranial modularity first for several reasons. First, the mandible is frequently found isolated in archaeological context because it is the densest cranial element—e.g., see Oase (Trinkaus et al., 2003); Ohalo II (Herskovitz et al., 1995); Tignief (Temifine) 1–3 (Arambourg and Hofstetter, 1963); Tabun 1, 2 (McCown and Keith, 1939). The mandible is thus better represented in the hominid fossil record than most other bones (Wolpoff, 2000). A better understanding of the structural relationships between the mandible and skull (see Figure 1-1) would therefore lead to a greater degree of success in predicting skull morphology in fossils

from isolated mandibula through reverse-engineering and retro-design prediction (see Bastir et al., 2005).

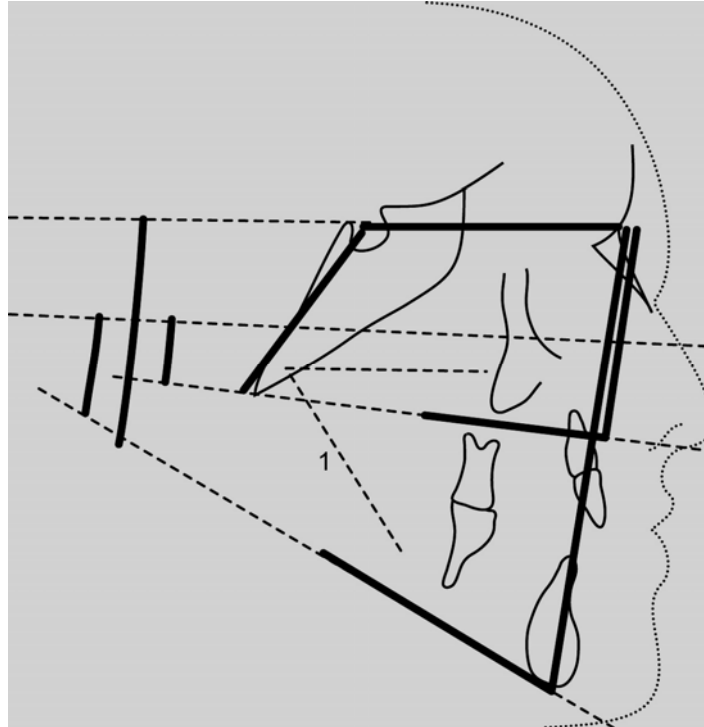


Figure 1-1. Integrated Skull Schematic of the Craniofacial/Mandibulomaxillo Relationship. Illustration shows angles, points of comparison, and cross-integrated mandibular and cranial boundaries.

Second, the mandible is frequently modified in clinical maxillofacial reconstruction, and it is the integrated nature of the mandible with other aspects of the maxillofacial and cranial systems that is most important here. Modification of the cranial system produces sequelae downstream in morphology, and further understanding the relationship between the mandible and skull may provide valuable insights into understanding integrated developmental relationships. These patterns of growth and integration underlie adult skull morphology. A clearer understanding of how the face forms in a manner integrated within the remainder of the skull and at the same time represents a module with different

functional requirements from other elements of the cranium will allow predictions of end-stage results in facial reconstruction to be more robust.

Last, understanding the mandible as both integrated and modular may help resolve longstanding questions in medicine, such as the meaning of invariant relationships in skull formation (Hans and Enlow, 1996; Zollikofer and Ponce de Leon, 2002; Bastir et al., 2004; O'Higgins et al., 2006). Invariant relationships—such as the above neutral axis of the orbits (NHA) to the pterygomaxillary (PM) suture line, the cranial base angle relationship to a host of planes and features, and other factors outlined below (see Figure 1-2)—can only be predicted by regarding the skull as an integrated and modular unit. Confirmation of the role and morphology of the mandible in producing and being produced by those relationships is a current effort in medicine generally and to a growing degree in biological anthropology as well (e.g., Bastir and Rosas, 2005). Finally, currently it is not understood whether modules themselves are best understood as variable aspects of cranial morphology across major divisions of morphology such as population or sex, or whether modules are themselves representatives of invariant relationships. For example, is it the modules themselves that respond to ecogeographical patterning such as in the nasal region, or is it regions outside the actual module that vary?

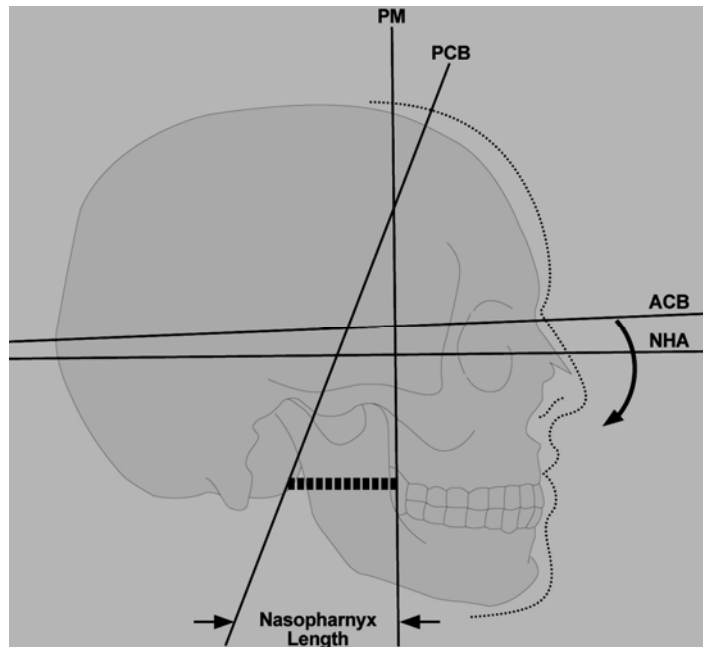


Figure 1-2. Invariant cranial relationships (PM, NHA) that not only cross modular units but are formed by them.

History of Mandibular Research

Cranial research has a history, which fact affects the models and methods employed in study. The hypotheses tested in this dissertation derive from a continuously developing research program, and the history of past efforts is important background for interpretations. Cranial study is approached from numerous scientific and medical disciplines with great time depth. The commonality of these approaches is that they all deal to some degree with the way the skull is shaped and how it changes through time, both in ontogeny and in evolution generally. As new hypotheses are tested, the agreed-upon meaning (or paradigm) of cranial shape changes through time. As models and techniques develop, the way we view the skull changes. And as knowledge expands, new research questions and directions are formulated. Thus it is to the history of this endeavor we must then look for this direction of thought. This process is germane to modular and

morphometric study, as both subdisciplines of evolutionary theory and statistical application respectively are relatively new and are therefore subject to the forces which affect expanding areas of research (outlined below).

In this way, then, the history of cranial research can be viewed as a progression of preconceptions, conjectures, insights, hypotheses, and agreed-upon facts subject to interpretation. However, because the subject reflects our beliefs about how we came to be ourselves, it is perhaps more subject to interpretational bias than other areas. For example, the most famous case of scientific fraud occurred within the field of cranial study. Piltdown resulted from the fact that everyone “understood” brain development was more important than mere postcranial bipedality and occurred first (depicted in Figure 1-3).

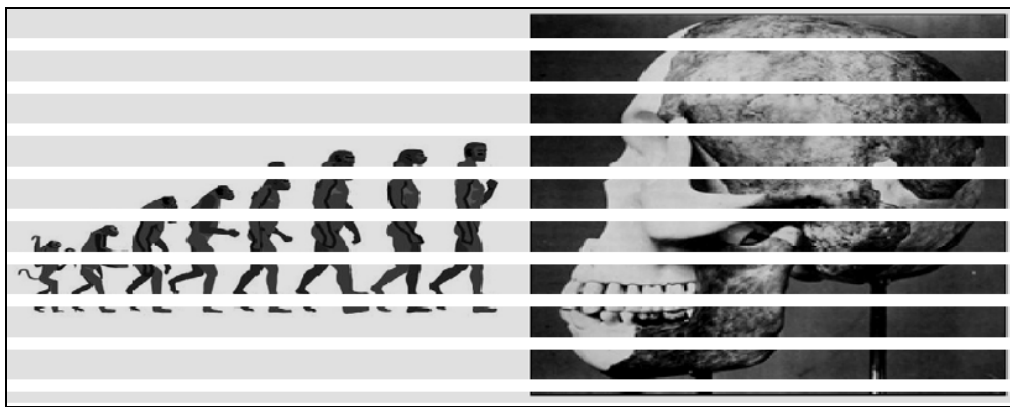


Figure 1-3. Progression to Piltdown—linear schema (l); manifested example of a paradigm (r)

The entire Piltdown affair has been previously well discussed and shows how a preconception can be written into scientific certainty until new techniques rectify the

prevailing consensus surrounding a particular interpretation of a process (Weiner, 2003). Current modular and maxillofacial research is in no way less susceptible to such factors of preconceptions and early under- or over-application of results from data. Yet another example of misapplied results is found in the literature of cranial modeling which looks at levels of integration and modularity in the skull without assessing population or sex as possibly confounding factors (Bookstein et al., 2003; Polanski and Franciscus, 2006) and without first ascertaining whether trajectories are the same across these partitions. This is an important question because currently it is not understood whether cranial modules (including the mandible) are representatives of invariant relationships (invariant across sex and population), such as the neutral axis of the orbit at 90 degrees and the pterygomaxillary suture line (PTM; PM line). Other examples of invariance include the positively allometric relationship of neurocranial expansion to orbital distance and the developmental sequence of maturation in the skull with the midline cranial base preceding the lateral base and that in turn preceding facial and mandibular maturation (Bastir et al., 2006). If the mandible and other areas of the skull tested here represent invariant modules, a degree of resistance to effects of population and sex needs to be tested, not merely assumed.

Even as the paradigm of brain expansion preceding bipedality has now reversed, there is evidence of another paradigmatic shift, from the view of the mandible as a relatively unimportant structure incidentally attached to an expanding neurocranium to a view of the mandible as being integrally involved in this expansion. That is to say, current modeling suggests constraint of the neurocranium by the masticatory apparatus may have

had to relax before brain expansion could occur (Leakey et al., 2001; Stedman et al., 2004; Bastir and Rosas, 2004).

History

A brief review of the history of mandibular research is useful for understanding the pressures that produced current theories. The history of mandibular research can be roughly divided into five periods, including the current period. Within the sequence (outlined below) there is a progression of increasing complexity in models and sophistication. The formative period (Period I) began with early systematic anatomy in the late nineteenth century and continued into the early twentieth century. Period II dates from the early twentieth century until the 1940s. This second period was marked by an increasing sophistication of statistical techniques, with the beginnings of multivariate statistics. Period III began in the later twentieth century (1970s) and continued to the late pre-millennial era (1990s). During this period mandibular research was marked by the introduction of Enlow (1968) and Moss's Counterpart and Functional Matrix hypotheses (1962). Period IV, discussed at length in Chapter 5, overlaps late Period III and is marked by what some have termed a "revolution" in the field—morphometrics and the application of three-dimensional modeling to paleontological and neontological research. Period V is our current position, a time when modularity is the preeminent topic to discuss in terms of explanatory modeling, and three-dimensional modeling is *de rigeur*. Again, however, full definitions of modules and full examination of the implications of three-dimensional modeling are lacking.

Period 1: Late 19th–Early 20th Centuries

In Period I, conceptual development began. Fossil mandibulae were first noted and described as differing from the modern mandible. Thus began one of the hallmarks of mandibular and craniofacial research, notation of difference without systematic definition of those differences. This first period was marked by formalization of anatomy, a growing appreciation of the differences in Neanderthal cranial form as compared with modern humans, and beginning evolutionary conceptualizations. At that time the formal idea of variability was not present. The skull, face, and mandible were not studied broadly enough for researchers to understand at first why or how Neanderthal and modern human skulls and mandibles differed, only that they did so. D’Arcy Thompson began three-dimensional modeling during this period as a series of morphing coordinate systems (see Figure 1-4).



Figure 1-4. D’Arcy Thompson introduced three-dimensional modeling as a series of morphing coordinate systems.

During this period modern human mandibular morphology was being robustly described for the first time, although anatomical descriptions, even of centers of growth in the face, are found as early as J. Hunter’s (1771) *The Natural History of the Human*

Teeth. During this period the contentions over Neandertal mandibular morphology began (Humphrey, 1866; Biondi, 1890), continuing to the present (Rak et al., 2007; Wolpoff, 2007). The insufficiency of models in this period resulted from the fact that study was conducted almost entirely by medical doctors, which limited the scope of the studies to medical applications, with no appreciation yet possible of normal population variation.

Period II: Early 20th Century–1940s

Period II was marked by an increasing sophistication of statistical techniques (see Figure 1-5), with the beginnings of multivariate statistical analysis, population genetic theory (New Synthesis, Mayr, 1947), a growing awareness of the importance of using biologically relevant points in measurement, and the beginnings of robust statistical descriptions of populations. An increase in the number of available fossil samples drove a new emphasis on studying neontological and paleontological human variability. This period was marked by insufficiency of models because cranial integration was not yet appreciated, biomechanical explanations for somatic form were rampant, and evolution was not yet widely discussed in terms of process. In Period II representative samples of fossil *Homo* mandibula continued to increase, pre-*Homo* mandibular material became plentiful, and clinical maxillofacial study in medicine began to study the mandible in a framework to modify developmental processes.

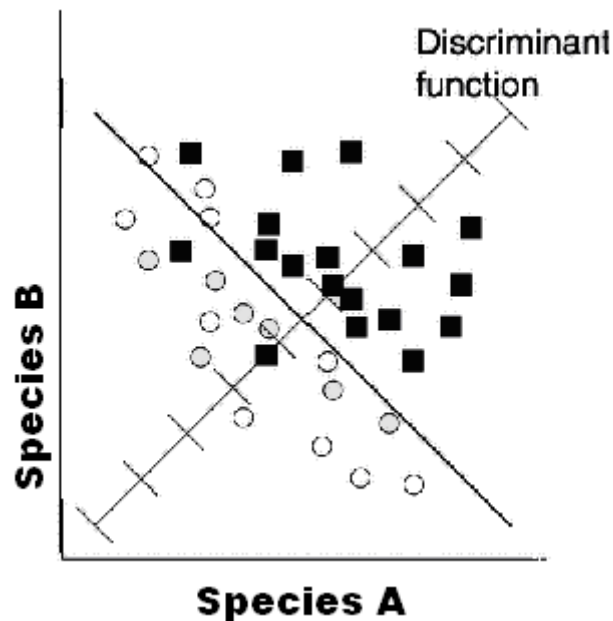


Figure 1-5. An illustration of the underlying logic of discriminant function. Without computers, such analysis was an intractably arduous process.

Period II also left the mandible relatively unstudied because of the received wisdom that this element did not need intensive study, as it was believed worthless as a population discriminator (see review in Humphrey et al., 1999). Much of the work in biological (physical) anthropology in this period was concerned with separating populations based on abilities and gross anatomy. Although the political reasons for attempting to use the mandible as a population discriminator waned after Weidenreich's compelling critiques of his contemporaries' science in the 1930s, there was and still is controversy over the mandible as a discriminator (Weidenreich, 1936). Howells (1973) found crania to differentiate populations with 92% accuracy using 70 measurements, while Humphrey et al. (1999) found mandibles to discriminate populations at 74.3% accuracy using 13 measurements. The role of the number of measurements in increasing the technique's accuracy is still unclear; however, generally, the more measurements the

better (see Jantz and Owsley, 2003). Wright (1992) found an accuracy of 74% using Howells's cranial data with fewer measures (i.e., 33 measures rather than 70).

Period III: 1940s–late 1990s

In Period III, statistical applications on computers became common, multivariate statistics became ubiquitous, and medical imaging (i.e., CAT and PET scans) became common (though sample sizes for the most part prevented application in paleontological study). Mandibular research began to address the complexity of biological structures.

This shift in the late twentieth century was not, however, merely a change driven by technical advances. It derived from the work of Olson and Miller ([1958] 1999); Moss (1962, 1997a,b,c,d); Enlow and colleagues (1969, 1971, 1982, 1996); Cheverud (1982, 1984, 1995, 1996; Cheverud and Midkiff, 1992); and Wagner (1996) which argues, persuasively, that the mandible must be studied as part of the facial and cranial skeleton. Large-scale investigations of functional morphology began (with one researcher, arguably, publishing significant results on every skeletal element of the human body in a paleontological context), computers, explosion of new species in human paleontology (thus bringing the still hotly debated role of species reticulation or anagenesis into play), multivariate statistical techniques and packages (originally mainframe versions), ontogeny and pathology in the fossil record, and formational processes.

The common thread underlying the three periods, going on into the beginning of the fourth, was that mandibular research did not look to an integrative framework for modeling. This situation was particularly true for anthropology and paleoanthropology. The traditional separation of biology (paleontology) and human biology (medicine) delayed the recognition of certain factors—such as modifications of head form through

surgical interventions, analysis of occlusion type (Angle Class), and analysis of dietary elements—as important in producing the morphology preserved in fossils, which in turn delayed such factors becoming integrated into models of cranial form. The lack of appreciation of the mandible as a cranial element allowed a great deal of mandibular research to simply focus on the mandible as a schematized entity.

Although the appreciation that the mandible must be studied as part of the entire cranial system was growing in anthropology during this period, it is to medicine that the original change to integrative frameworks should be ascribed.

The description of Period IV will benefit from a summary of the two main types of models that emerged from the work performed during Periods I–III: biomechanical and non-mechanical or spatial models.

Biomechanical Models: History of the Mandible as Mechanical Structure

In research Periods I and II, mandibular morphology was described by reference to functional requirements for mastication. This type of description treated the mandible as a mechanical device. Beginning late in Period III (approximately the 1980s), an awareness grew among researchers that mandibular form represented the interplay of structural and biomechanical factors in producing and maintaining occlusion. Research demonstrated that mandibular form could not be adequately described by schematic models derived from engineering analysis. Despite these caveats or reservations, the biomechanical approach was nevertheless perceived as necessary, because at that time there was as yet no real analytic framework to transcend these simple models. Simply looking at the mandible as an isolated unit could offer a useful idealization of biological

form, yet no totally mechanistic modeling of biological structure proved sufficient to reflect biological complexity (Smith RJ, 1982).

Mechanical models explained mandibular and facial morphology by reference to force production vectors operating to produce mastication (Greaves, 1978; Hylander, 1977, 1979; Hylander and Johnson, 1994; Weijs, 1989; Weiss and Hillen, 1986; Daegling, 1989; Spencer and Demes, 1993; Spencer, 1998, 1999). Under these assumptions the mandible was idealized as a simple bent beam (Symons, 1951) and as a simple bent beam with differentiated areas extending for muscle attachment (Weijs, 1989). It was further modeled as a simple bent beam with attached muscle insertions and representative stress points at expected areas of greatest loading (Weishampel, 1993; Spencer, 1998; Greaves, 1978), and then as this same bent beam with the addition of the areas of muscle insertion on the cranium (Antón, 1994; Kiliardis et al., 1995). The mechanical model worked well for simplified versions of mandibular and craniofacial morphology because the craniofacial complex must transmit force. However, the strictly functional/mechanical model was insufficient because (as mentioned before and detailed below) the face and mandible initially form as a structural unit, with primary innervation patterns, relationship of the jaws, and other factors discussed below continuing to unite the two entities through development.

Diet directly affects mandibular and facial morphology through functional mastication. As has long been observed in other taxa, dietary consistency affects facial morphology; recently Lieberman's study (2007) on a facial analogue of humans (Hyrax) demonstrated ventral (inferior) and posterior portions of the face loaded differentially,

depending on diet. That study thus verified results gained for the last 70 years showing mandibular plasticity in response to dietary factors (discussed previously; citations earlier). Nicholson and Harvati (2006) observed that results in their study of the mandible suggested food processing and use of the dentition in high-latitude populations drove some of the major differences in populations. Marriog and Cheverud (2005) have also shown trophic level is more predictive of morphological covariance among non-human primates (*Cercocebus*) than species membership. (Ideally diet would be controlled for in this dissertation, but here, as in most cases, diet cannot be determined.) However, for the most part here, skeletal material dating from before the fairly recent turn to softer, processed diets is used, and the assumption is made that diet is roughly held constant in the past populations used. (Descriptions of the populations included in this study appear in Appendix A.)

Biomechanical Models of Mandibular Morphology II: History of Mandibular Plasticity

Early in the 1940s, during Period II of mandibular research, the mandible was demonstrated to be plastic in response to dental loading. Hrdlička's belief that the mandible was a structure totally responsive to masticatory loading and hence of little use for phylogenetic analysis was widely held. Hrdlička further described the mandible as having "no relation to head shape," which perpetuated the view that the mandible was best studied as an isolated element (Hrdlička, 1940a,b). Thus the view continued until the change to integrative modeling that mandibular shape is homogenous compared to the remainder of the skull, due to the plastic nature of the bone in response to loading for mastication. The exact nature of this plasticity is still debated (Cheverud, 1995). The mandible during this period was sometimes described with exasperation. Various

described as the “lost step child of physical anthropometry” (Troc, in Hrdlička, 1940a), or as the “devil-spawned” aspect of cranial development, (apocryphal; cite in Rak, 1998; though attributable to William Straus, according to Clark Howell¹), the mandible continued to vex clinical and anthropological investigators.

Beginning late in Period II through early Period III of mandibular research, there were *in vivo* and *in vitro* experiments demonstrating mandibular plasticity in various taxa and populations of modern humans. Clinical research detailed the associations between muscle position, size, force, and portions of the craniofacial complex through coronoid manipulation, fusion of the condyle, condylar osteotomy, and dietary change in human and non-human taxa. Dietary changes were demonstrated to produce differential expression in the craniofacial complex in humans and non-humans (Washburn, 1947; Avis, 1959; Beecher and Corruccini, 1981a,b; Sarnat and Engel, 1985; Isberg et al., 1986). In modern humans, pronounced temporal change in craniofacial dimensions was found in samples from the same geographic locale. Facial change through masticatory effects, particularly through inferred dietary change, was observed (e.g., Seddon, 1984; Carlson, 1985). Although there was a growing interest in the mandible as plastic in response to differential force-production levels in various taxa and populations, the view of mandibular morphology as predictable only from force, either through differential dietary regimes or clinical manipulation through dental appliances, was still in full effect.

Non-Mechanical Models of Mandibular Morphology

Mandibular morphology began to be seen as a complex response to extra-mandibular factors as well as force in this latter part of Period II. Clinical research began

¹ The actual citation reads: “God created the skull—but the Devil made the mandible.”

demonstrating the inter-correlations of the cranium and body to the craniofacial complex itself. The splanchnocranium began to be examined as part of a whole-body system. Clinical analysis of modern craniofacial form showed multiple operant factors affected the craniofacial complex and consequently the mandible. These factors included posture (Huggare and Houghton, 1996), length of cervical spine (Houston, 1988), proportionate size of maxilla/mandible (Lin, 1993), the cranial base angle (Martone et al., 1991; Dibbets, 1996), head type (with dolichocephaly being associated with a vertically high face and mandible), and nasopharyngeal size (Wenzel et al., 1989). Obviously explanation of all these factors required more than the mechanical model. After including force from the muscle arms, it is impossible to increase knowledge of biological complexity without going to models that regard morphology as a structure integrated with portions of the face (maxilla, basicranium [Cheverud, 1995]) and then, at the next level of complexity, as a structure integrated with the entire skull. Finally modeling must include the relationship with the entire body (Hans and Enlow, 1996). As soon as structural/spatial requirements are included in models of mandibular morphology, complexity increases.

Period IV: 1990s–2000s

Period IV, discussed in Chapters 3–5 of this dissertation, marks what some have termed a “revolution” in the field—morphometrics and the application of three-dimensional modeling to paleontological and neontological cranial and mandibular research (see Figure 1-6). As outlined in succeeding chapters, it remains to be seen whether morphometrics has attained the status of a true revolution. As will become evident, small sample sizes and occasionally overlooked factors long demonstrated

important in morphological analysis—sex and population (allometry)—are sometimes discarded in perhaps rash over-application of new technology.

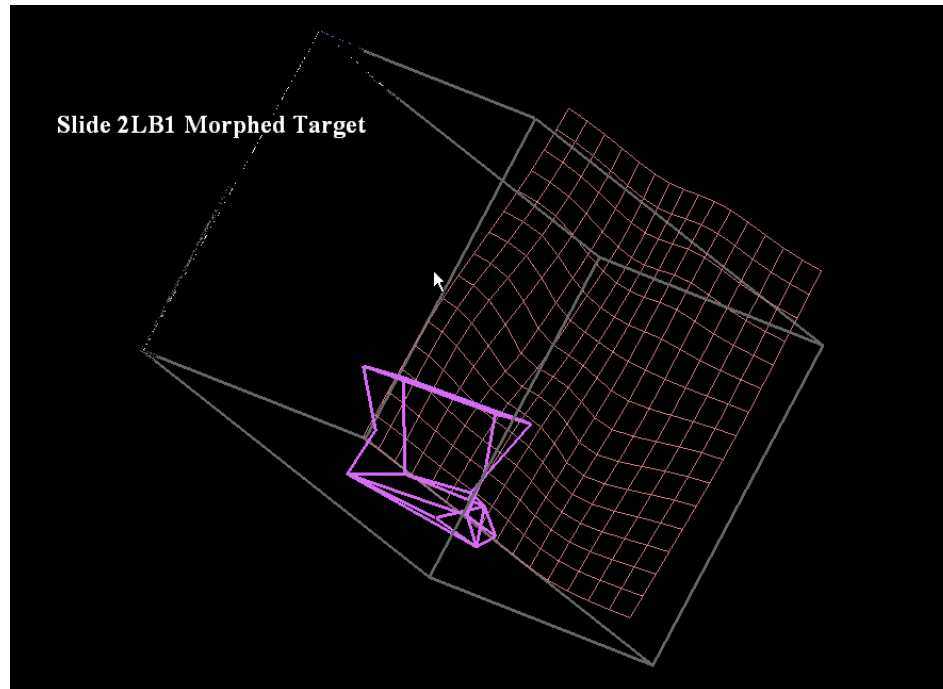


Figure 1-6. Slide showing three-dimensional morphing of Liang Bau 1 mandible from reference shape, Morphologika (Anderson 2007).

History of Structural and Modular Modeling

The penultimate era in mandibular research began when researchers turned to the examination of the mandible as part of an integrated, structural cranial system. Structural requirements predict the mandible reflects more than bite force. Given that the skull (particularly the face) and mandible develop together and participate in a mutually interdependent system, it became necessary to analyze cranial morphology as a unit. In this period of mandibular research, the evolution of the body began to be approached from a structuralist position. A structuralist holds that cranial and somatic organization results from integration across elements of the developing organism rather than through simple Darwinian inheritance (Wake and Larson, 1987; Churchill, 1996, 1998; Wagner,

1996). Under this model, the skull is constrained in expression of morphology because integration of cranial elements must be maintained.

The structuralist position thus reflects integrationist modeling. Change occurred because it became apparent the human mandible and face are part of an integrated cranial complex as initially suggested by Olson and Miller ([1958] 1999). Genetic and/or phenotypic integration of the cranium and mandible has been demonstrated in the Rodentia (Zelditch, 1987; Leamy et al., 1999; Mezey et al., 2000), the Sicuridae (Roth, 1996), and Sanguinas (Cheverud, 1996; Ackermann and Cheverud, 2000). Integration has also been demonstrated in Hominoids (Bromage, 1992; Ravosa and Shea, 1994), in Plio-Pleistocene hominins (*Paranthropus robustus*, McCollum, 1999), and in other members of the genus (Bromage, 1989). Cranial integration has been proposed as an operant factor in later mid-Pleistocene *Homo hiedelbergensis* mandibula (Rosas, 2001) and referred to in study of the basicranium and cranial base angle (Lieberman, Mowbray, and Pearson 2000). Cranial integration has been demonstrated in modern humans by anteroposterior and annular neurocranial deformation, with attendant modification of the basi- and splanchnocranium (Cheverud and Midikoff, 1992; Kohn et al., 1995; Antón, 1989). Thus there is wide general acceptance for morphological integration of cranial elements in mammals and primates (Leamy et al., 1999).

In late Period IV three major lines of evidence emerged to suggest structural integration is an important factor in describing mandibular morphology.

1. ***Primary formation of the human splanchnocranium is from the first branchial arch, stimulated by neurectoderm, through mesenchymal aggregation and differentiation, in a metamerical process of induction by Hox and non-Hox***

homeobox genes (Hall, 1999; Kuratani, 2003). Cranial skeletal derivation is from chondrocranial and dermatocranial elements (Hanken and Hall, 1998), with the splanchnocranial portion of the cranium inducted through neurectoderm and the neurocranium and basicranium inducted through paraxial mesoderm. The face thus derives in an integrated trajectory ontogenetically distinct from the remainder of the cranium, constrained by induction through the nervous system. The development of the cranial nerves proceeds and is uniquely associated to skeletogenesis in eutherian and non-eutherian mammals, contra the musculature (Anderson LC et al., 1991; Smith K, 1996). The innervation pattern of the cranial nerves precedes basicranial and neurocranial expansion, with both of the latter processes in turn positively allometric to ethmomaxillary expansion (Lieberman, Ross, and Ravosa, 2000), which tracks increasing body mass. These integrated and constrained processes occur prior to formation of full dental eruption and development of adult masticatory function in *Homo* (Kean and Houghton, 1987). In humans, the development of the brain and neurocranium outpace masticatory function, the brain being 90% of its adult size in comparison to 40% for the jaws at age 5 (Washburn, 1947; Hanken and Hall, 1998). Thus, formation of the craniofacial complex is hierarchical and masticatory factors are constrained to accommodate prior states in the ethmomaxillary, basicranial, and neurocranial regions (Kean and Houghton, 1987).

2. ***The craniofacial complex in *Homo* reflects factors common to mammalian and primate cranial evolution.*** In mammals, the relatively decoupled regions of the splanchno-, basi-, and neurocranium of the generalized tetrapod became

integrated, as the complex palato-quadrate masticatory articulation changed to dentary-squamosal contact (Wake, 1993). Concomitantly, in mammals the adductor musculature relocated and reoriented, allowing relaxed loading vectors. These changes underlay the mechanical constraint in the neuro- and basicranium, due to the reorganized mechanically stressed masticatory region of the primitive tetrapod, to allow incorporation of masticatory chondrocranial elements into the inner ear (Hall, 1999). In mammals generally and in primates particularly, the main forces acting through the adductor musculature, through the re-orientation supero-inferorally, produced a restructured rostrum, and reduced biomechanical stress on the basicranium (Demes and Creel, 1988). Mammals generally thus exhibit a fundamentally integrated cranium and mandible. Further development of this structural pattern presumably allowed sufficient relaxation of constraint to facilitate selection for increased neural tissue to produce the quasi-spherical neurocranial shape common to higher primates. This basic pattern of structural integration is common to the Hominoidea and Australopithecus and is pronounced in later *Homo* (Wake and Larson, 1987; Vrba, 1996; Smith K, 1996), though currently the common pattern of integration between these various primate species has remained unexamined.

3. ***Invariant relationships within the cranium of the Hominoidea support the hypothesis of integrated structural effects in the craniofacial complex of primates.*** Hans and Enlow's (1996) model of "architectonic balance" and research by Cheverud (1982, 1984, 1995, 1996) and Wagner (1996) emphasize modularity in evolution and predict occlusal relationships are maintained by integration of

developing modules in ontogeny. Support for this model lies in the results from a variety of studies in human and non-human primates. These results include stability of the pterygomaxillary suture line (PTM line) separating the anterior and posterior face in humans (Hans and Enlow, 1996; Lieberman, Ross, and Ravosa 2000), a neutral axis of the orbit oriented at 90° in primates (Ravosa and Shea, 1994), a high correlation of the minimum breadth of the ramus and nasopharyngeal size, with integration of facial prognathism and maxillary arch length (Smith RJ, 1984), and the demonstrated presence of anterior and posterior “facial blocks” in modern humans (Bastir et al., 2004, 2005). Such relationships are explicable only by reference to an integrated cranium. Bromage (1992) has demonstrated invariant cranial relationships in *Pan troglodytes*. McCollum (1999) has successfully analyzed the Paranthropine face in terms of an integrated architectonic model, showing that the vertical expansion of the palate exhibits constraint by the integrated process of mandibular rotation common to hominins. Kappleman (1996) has demonstrated high correlation of body mass and orbital size in primates and humans, which can only be explained as extra-cranial somatic effects being represented by the cranium itself. The total pattern of these results suggests that invariant relationships in primate craniofacial modular architecture result from an integrated cranium with a common conserved pattern of hierarchical constraint.

Donald Enlow was the primary architect of structuralist and integrationist modeling in humans: his theory of architectonic balance/counterpart theory holds that equilibrium is maintained throughout the skull in development. The parts of the neurocranium,

splanchnocranium, and basicranium (modules) increase in size, change shape, and remodel in tandem. Enlow's Period III –IV work, deriving from clinical maxillofacial research, incorporated information from evolutionary biology through demonstration of structural effects and also demonstrated structuralist modularity in ontogeny. The late Period III thus marked the beginning of empirical testing of structuralist theory. James Cheverud's clinical work in the Rodentia and Sanguinas provided similar supportive evidence for structuralist genetic effects in the phenotype in non-human mammals. The structuralist relationships in the modern human face demonstrated by Hans and Enlow (1996) are hypothesized to result from modular integration, maintained by genotype-phenotype "mapping," through epigenetic factors such as pleiotropy (Cheverud, 1996; Wagner, 1996; Ackermann and Cheverud, 2000).

Period V: The Present

Our present period, V, could be the beginning of a "post-morphometric revolution" expansion period, perhaps marked by return to emphasis on population and sex as predictive factors in morphometric analyses (see Chapter 5 for more discussion). Modularity, as the key conceptual framework, requires explicit testing of statistical relationships AND examination of trajectories derived from large-scale data. If thought of as a "post-morphometric" time, Period V is when empirical observations from morphometrics across multiple disciplines are examined for results mirroring and expanding theory. A primary goal of this period is the formation of a robust definition for modularity. As outlined in the preface and detailed in Chapter 2, currently the concept of modularity lacks robustness of definition and mature theory.

CHAPTER 2

PARTICULATE AND STRUCTURAL MODELS OF MODULARITY

Chapter 1 established that both biomechanical and integrative factors underlie cranial morphology. The history of cranial research was introduced to outline the sequence of increasing complexity of models and applications in cranial study. The concept of historicity was introduced as the framework for modular analysis. As detailed therein, there is a progression from early anthropological analysis of isolated cranial specimens to presently forming hypotheses of the patterns of cranial integration within populations. There is also a correlation between that progression and the state of scientific knowledge of the time (thus an effect of paradigmatic shifts). This chapter sets the concept of modularity in an evolutionary context and defines it as proceeding through both development and function (using as an example Donald Enlow's model of architechtonic/counterpart balance [Hans and Enlow, 1996]). Further, relationships of cranial integration, modularity, and invariant cranial relationships are used to make predictions which underlie the hypotheses which are then tested in Chapter 3.

As was also discussed in Chapter 1, simply reducing craniomandibular morphology to a series of lever arms and relationships of force production variables—though a necessary functional analysis—does not sufficiently account for the morphology of the mandible or the cranium. Several lines of evidence were used to demonstrate that morphological integration of the skull is a necessary predictive factor for describing the relationships of cranial morphology. Here in Chapter 2, this aspect of morphological integration is examined under particulate and structuralist models of evolutionary process.

The discussion in Chapter 1 of invariant cranial relationships within the Hominoidea underscored the most important question regarding modularity, that is to say, whether modules belong to a class of invariant cranial relationships underlying cranial form—thus belonging to a class of *bauplan*. Recently González-José et al. (2008) treated modules as entities representative of genus (or sub-family). Therein it was demonstrated that changes in modules broadly represent the patterning of accepted phylogeny within the Hominoidea. Although representatives of various taxa were few and the modules are somewhat ill-defined (as discussed here later), results are generally what would be expected if modules represent an invariant form of morphology within a given taxonomic level. By extension, if this idea is sound, then within taxa the relationships of parts of the skull (modules) should be invariant and taxon-representative. Further, this invariance may be resistant to allometric or population effects in the same way cranial base angle, neutral axis of the orbits, and other parts of the skull are, in effect, taxon-specific cranial absolutes. This idea has not yet been tested at the species level as this dissertation does in Chapters 3–5, because the idea is relatively new. Before testing this idea, it is necessary to see how factors in evolution would have served to create and maintain modularity at various levels in taxa.

Particulate and Structuralist Models of Evolution

In order to show the relationship of integration to modularity, particulate and structuralist models of cranial evolution are compared below.

Particulate Models

Particulate evolution, under which parts of the skull evolve independently, cannot be used to explain modularity. Nonetheless, the modern human skull results from evolutionary change which sometimes has been modeled, implicitly or explicitly, as particulate. The particulate model of evolutionary change, operates through natural selection acting directly on specific characters in isolation (Wake and Larson, 1987; Churchill, 1996 [see also Brace's model of dental reduction 1963; Brace et al. 1987]). This evolutionary model can be very useful for explaining individual factors such as dental reduction, realignment of the *mm temporalis* in Neanderthals, development of the chin, increasing encephalization (Brace, 1979; Antón, 1994; Spencer, 1998, 1999; Schwartz and Tattersal, 2000; Wolpoff, 2000), and other expressions of cranial morphology. However, many structural properties of an integrated cranium are emergent at different hierarchical levels and cannot be easily described as the result of selection on single characters (Hall, 1999). Therefore definition of craniomandibular evolution through a series of isolated steps in the mandible and craniofacial complex is ultimately uninformative.

Oversimplifying complexity through use only of a particulate model of selection is reductionist because even an apparently simple process such as mastication is multifactorial. Mastication occurs through muscular stimuli, spatial relationships with the remainder of the skull, and ultimately, the need for maintenance of homeostasis and organismal integration. Change through time across these factors cannot be subsumed into a series of isolated steps, because sequential transformation of any biological structure must accommodate adjacent structure or integrated processes. Under the most

extreme form of the particulate model, the biomechanical, the face would have evolved only as the aggregate of response to changing mechanical requirements.

There unquestionably was selection for masticatory factors such as dentognathic reduction and neurocranial expansion in the Pleistocene as would be predicted by the particulate model of evolutionary process. At the same time structural integration constrained morphology through time by stabilizing selection on the remainder of the skull. Direct selection as expressed under a particulate model can be differentiated from stabilizing selection in regards to formation of morphology. Direct selection causes morphology to change in response to environmental conditions, shifting mean morphology towards an adaptive peak. Stabilizing selection serves to maintain morphology (under an optimal fitness model) at that given adaptive peak (Fisher, 1930; Welch and Waxman, 2003). This maintenance of morphology occurs through external stabilizing selection maintaining homogeneity of interaction between the phenotype and external environment, each peak of optimal fitness thus representing an idealized “perfect match” between a biological structure or behavior and the environment. At the same time, the second aspect of stabilizing selection—internal stabilizing selection—operates by co-adaptation of features (or modules) and expresses the relationship or constraint of the phenotype to expressed internal processes.

In Chapter 1, it was demonstrated this internal stabilizing selection can be considered canalization in the sense of Waddington (1957; see also Cheverud, 1996; Marroig and Cheverud, 2001; Flatt, 2005). In the mid-to-later Pleistocene the human skull was beginning to change in response to both cultural factors such as extra-oral processing of

food and non-cultural factors such as ecogeographical change. The adaptive peaks that mark the durable grade-level adaptation in *Homo ergaster/erectus* represents change partially in response to particulate factors such as extra-oral processing of food (cooking) or paramasticatory activities. These particulate factors were constrained by major modular-influencing factors such as climatic adaptation, increasing body size, neurocranial expansion, and ethmomaxillary reorganization. This constraint through internalizing selection has been indirectly addressed in research examining the role of natural selection versus neutral selection models (Harvati and Weaver, 2006). If differences in cranial form through time can be demonstrated as resulting from modular changes, both sides in the debate over neutral versus direct selection could be correct. The skull can be responding to selection of a few different functions yet seem to be representing neutral selection due to modular invariance, producing a pattern suggesting either.

The integrated skull responded to selection as outlined in the broad sense in Cheverud's model of hierarchical integration. Cheverud (1996) divides integration into three interrelated categories: functional/developmental, genetic, and evolutionary. In the Pleistocene the skull responded to new developmental and functional masticatory and encephalization factors, with effects probably constrained through pleiotropy. These functional associations were inherited through time as modules, eventually uniting and becoming entities exhibiting evolutionary integration, themselves stabilized (or canalized) in time through stabilizing selection.

Structuralist Models

As shown above, particulate change in single systems becomes part of changes in structural hierarchies of organization. Particulate versus structural hypotheses have been addressed by Melanie McCollum (1999). Mandibular ramal height and anterior temporalis position in *Australopithecus boisei* have been considered to represent a response to energy-deficient substrate in taxa eating large amounts of rhizomes and foliage. The deep palate of “robust” Australopithecines is considered by McCollum (1999) to be a consequence of their vertically tall mandibular ramus, formed by the spatial requirements for maintaining an anterior rotation of the maxilla. Under a structuralist model the palate must expand inferiorly, yet the superior, nasal portion is constrained to maintain congruence with body size and cannot simply increase. Therefore the palate deepens as a response to the tall mandible. The face does not directly respond to mastication as under a particulate model, but is responding to integrative structural factors. These results suggest structural factors are as important as direct selection for mastication, the traditional explanation for the highly unusual face of the robust Australopithecines. In the non-robust Australopithecines, the palate depth does not increase, as the constraint imposed by the premaxilla-vomer contact does not exist. It is also possible to explain the “low infraorbital foramina” of the robust Australopithecines as maintaining their position as the entire upper face moved superiorly.

These structuralist arguments thus reflect modular theory in predicting that constraint of direct selection for substrate use is in turn constrained by intra-cranial relationships. These arguments may even be “pre-modular” if, as tested in Chapter 5, the fundamental pattern in taxa is represented by the cranial nerves (CN), which are specific to given taxa. CN patterning and positioning may in itself constrain facial development (Anderson

2000) or even modular development. Recently Bastir and Rosas have modeled structural change in Neanderthals and modern humans. In a series of articles dating from 2002 through 2005 they demonstrate how morphology is explainable in both taxa by reference to Donald Enlow's partitioning of the cranium into a series of interconnected, structurally integrated modules.

Under a structuralist model then, evolution of the craniofacial complex occurred in the context of selection constrained (canalized) by the genotypic-phenotypic interface. Selection under a structuralist model can be considered constrained by the degree to which the genome responds to mutation. Pleiotropic structural effects can be used to predict that the modern human skull arose through the favorable action of compartmentalization, in which aspects of the genome were affected by random mutations in modules (compartments), with selection acting in these modules rather than on the whole body. This type of change is modeled as allowing modularized systemic change, with the entire system therefore being less likely to be compromised due to unfavorable mutations (Wagner and Altenberg, 1996; Cheverud, 1995). As Wagner and Altenberg (1996) and Cheverud (1996) point out, selection acting on mutations across the genome will tend to fail by producing deleterious effects across an already integrated structure. If all systems were affected equally by any one mutation the probability is greater that all mutations would be deleterious given that they would disturb "complexity in balance," or, as Wagner (1996:328) puts it, "On average further improvements on the system must not compromise past achievements."

Thus, in order for parts of the skull to respond differentially to selective pressures it must be partitionable. Once the skull is partitioned, selection can then act differentially.

Mosaic evolutionary change occurs because of the relative independence of cranial regions or modules (Raff, 1996). Cheverud's (1996; Ackermann and Cheverud, 2004). Similarly, Wagner's (1996) model of cranial integration explains cranial structure as resulting from semi-independent modules united by constraint imposed from above on developmental program.

The modern human skull thus retains aspects of Pleistocene (and earlier) developmental constraints maintained through time by stabilizing selection acting on modules associated by pleiotropy. The action of pleiotropy is modeled as the way that natural selection acts on the cranium in the context of constrained structural factors (see Figure 2-1).

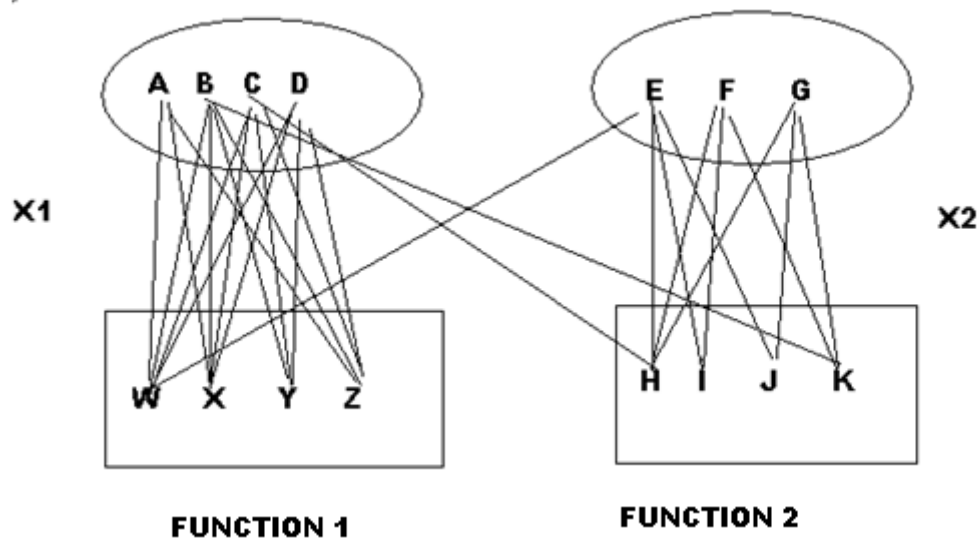


Figure 2-1. Pleiotropic Modularity (after Wagner and Altenberg 1996:988). Function 1 and Function 2 are controlled by pleiotropic genes, primarily WITHIN functional character complexes (modules) rather than ACROSS them.

Evidence suggests pleiotropy as the original functional mechanism by which metazoans evolved from protozoans with subsequent effects at all taxonomic levels (Wagner, 1996). In protozoan communities there is a 1:1 correspondence between gene

program and cell; mutation affects each cell similarly. Metazoans are modeled as diverging from protozoans by breaking the 1:1 correspondence. Pleiotropy thus means single or few genes can control multiple functions; mutation can then occur at one genetic locus and effect change throughout part of the system (in modules) without affecting all other systems.

Pleiotropy can affect trait complexes in two ways, through parcellation and integration. In parcellation, trait complexes have a reduction in the number of controlling genes “inter complex” (i.e., among complexes such as the skull and mandible or the ramus and corpus) with maintenance of pleiotropic effects “intra complex” (see Figure 2-2). Conversely, in integration, coevolution of characters related by new functions cause formerly unrelated traits to integrate and subsume into modules.

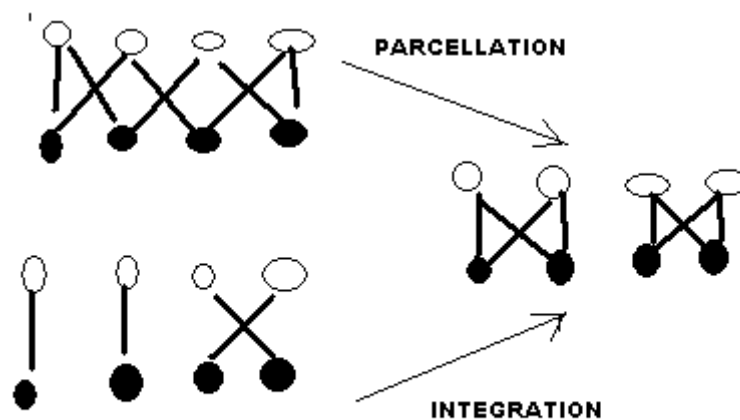


Figure 2-2. After Wagner and Altenberg (1996:973). Parcellation and integration as processes cause change in gene-character correspondence. Similar modules can result from either parcellation or integration.

Presently it is unclear whether the evolution of the skull and mandible can be ascribed to coevolution in the mode of either parcellation or integration or both modes. It may be that the skull and mandible decoupled through parcellation, or it may be that in the

change from *Australopithecus* the (possibly) formerly decoupled skull (now driven by cranial expansion) integrated with a reducing masticatory complex (mandible). Given the essentially integrated nature of the mandible and maxilla (discussed in Chapter 1 and in the following section), it seems more probable that parcellation was the primary process.

Modularity as process has been delineated in Polanski and Franciscus (2006); however within that research only one form of modularity, that derived by disassociation, is mentioned: “[A] process that may be responsible for widely observed patterns of mosaic evolution in general ...is based on morphological dissociation, i.e., an evolutionary shift in ontogeny where individual traits or functional units (F-sets) acquire a degree of genetic and developmental independence” (Polanski and Franciscus, 2006:38). This is an oversimplification since formerly integrated functional complexes do not necessarily “acquire” independence—in the case of pleiotropy by integration, already independent modules unite to form further integrated modules.

Currently modularity, originally referred to as compensatory interaction (Sofaer, 1972) and/or compensatory mechanisms (Gould and Garwood, 1969), is a widely discussed topic in biology, as modularity brings the study of development back into widespread currency (Orr, 2005). As Orr points out, the study of modularity is neither novel enough nor new enough as a concept to be considered a true scientific revolution as defined by Kuhn, but in demonstrating relationships of the developing organism genetically modularity may provide the final “step” in allowing a fully integrative biology.

Modular explanations of craniofacial organization have great explanatory power in that they provide a way to explain variability (the propensity to vary at the genetic level) in the skull as distinct from variation, which is the realized phenotypic expression of the

genome. As an evolving function of the genome, variability can be used to explain integration, canalization, and developmental constraints as an evolutionary expression of the degree to which the genotype “maps” onto the phenotype (Wagner and Altenberg, 1996). These constraints cannot come from the developmental structures themselves but result from pleiotropic effects in the genome (Cheverud, 1996).

Modularity As Realized by Both Development and Function

In order to robustly describe the mandible in terms of the overall cranial system, it is necessary to delineate functional effects that derive from selection—in neo-Darwinian terms, in contrast to structuralist requirements that have contributed to mandibular morphology. This dichotomy can be reduced to development versus function.

Currently there is no consensus on how to partition function from developmental process in producing integration. As González-José et al. (2005:177) observe, “[It] is not clear whether the integrative processes can be separated into functional vs. developmental.” This uncertainty is unfortunate, because, as Ackermann (2002) points out (following Strait, 2001), prior studies have shown developmental effects are more likely to produce homologous characters for phylogenetic reconstruction than later developing functional ones. In mice, developmental integration precedes functional integration (Zelditch, in Ackermann, 2002). Marroig and Cheverud (2001) ascribe equal weighting to functional and developmental characters in matrix comparison, while others such as González-José et al. (2005) weight them separately.

Cranial modules must therefore be described at several functional levels; if there is no agreement as to the interplay of developmental and functional factors it is primarily due to level of analysis being unspecified. The first level of modular definition is of course,

the distinction made between the mandible and the skull (cranium). This division may make sense intuitively, as the mandible does not reside “inside the skull,” but both ontogenetic and functional definitions of modularity argue against it. Given that the mandible and maxilla form together in ontogeny and that both exhibit a common function, there is little information to be gleaned from separating cranial modules in such a broad fashion. However, in Chapter 3 the relationship of the skull to the mandible is performed in the “model-free” hypothesis testing.

The second level of modular definition is the traditional separation of the skull into the splanchnocranium, dermatocranium (neurocranium), and basicranium, (face, braincase, and cranial base, or “S/D/B”). Defining characteristics of the modules in this organizational scheme include an autonomous genetic organization, hierarchical organization, specific location, and connection to other modules (Raff, 1996). To this list McCollum (1999) would add the attribute of sequential transformations in development. All these definitions apply well, in a broad sense, to the traditional S/D/B modules. For example, modules such as the face are genetically programmed autonomously, apart from the dermatocranium and basicranium (through differential Hox gene induction patterns, Kuratani, 2005). There is intermodular hierarchical organization: the structure of the face follows the more rapidly expanding dermatocranium and nasal region (Kean and Houghton, 1987; Franciscus and Trinkaus, 1988). The S/D/B modules occupy specific cranial regions. Connection to other modules is demonstrable for the dermatocranium and basicranium in that annular deformation of the former causes coronal expansion of the latter at the glenoid fossa (Cheverud and Midkiff, 1992). Finally sequential transformations in development are evident. The mandible, dermatocranium, and

basicranium all change radically in processes such as chondrogenesis and/or intermembranous ossification and later, senescence. The question thus becomes whether these regions, although sharing criteria advanced for modules, actually represent them.

Modules of the skull can be further subdivided. For example, McCollum (1999) proposes a division of the skull into modules of the neurocranium, the nasal region, and the oral apparatus. Bastir and Rosas (2005) recognize the traditional “S/D/B” distinction as useful, then distinguish two further basicranial modules (midline and lateral). Moss (1962, 1997a, 1997b, 1997c, 1997d) also makes further divisions of the S/D/B.

Modularity thus faces a definitional problem of over- or under-prescription. Identifying too few modules means too little partitioning of the different regions of the skull, while identifying too many means an integrated structure becomes atomized. The question becomes what form modularity may take—modules organized into the S/D/B on a macro-scale, modularity as proposed under Enlow’s model of architectonic balance (which is a definition of modularity across the traditional S/D/B; this model receives additional examination below), or modularity in multiple units within the S/D/B boundaries of the skull (also discussed in the next section). It is necessary to define modularity itself in these neo-traditional and functional ways.

Modularity Tested under Model-Bound Hypotheses

Modularity is discussed by Polanski and Franciscus (2006). Results therein suggest a decoupling of the face and braincase (splanchno- and dermatocranium), with integration higher within the neurocranium in modern humans, in contradistinction to the pattern observed in other members of the Hominoidea. These results are described as contra that

of Ackermann (2005) in finding a high level of integration within the face of *Homo*. As Polanski and Franciscus point out, results of cranial integration appear to be highly affected by which f-sets (functional matrices, or modules in the broad sense) are chosen. Franciscus and Polanski suggest the apparently paradoxical results of their study and Ackermann's stem from the possible inclusion of measurements from the more integrated neurocranium in Ackermann's study. It is here suggested that rather than sampling neurocranial measures, Ackermann's variables possibly included more facial measures with a previously undescribed level of integration resulting from function. This hypothesis is tested by the inclusion of the mandible in the facial module in Chapter 3. It is also suggested, as discussed above, differences in integration patterning with modules are taxa-specific. If so, differential inclusions of taxa will skew results, and there is reason to assume results as in Polanski and Franciscus for *Homo* will not be comparable to results for all of the Hominoidea.

Corpus and ramal areas of the mandible have been distinguished as separable morphological (modular) units in *H. heidelbergensis* (Rosas, 2001). This builds on prediction under an integrated architectonic model suggesting the ramal width should correlate with nasopharyngeal requirements (Smith RJ, 1982) as well as body mass (Estenson, 1999) and the middle cranial fossa (Hans and Enlow, 1996). Further, Klingenberg (2004) has suggested the murine mandible can be regarded as a dual portion architectonic system. Bastir and Rosas (2005) have demonstrated anterior and posterior facial "blocks" in which the mandible is regarded as an intrinsic part of the system. These invariant relationships across traditionally defined separate areas cannot be explained without reference to functionally mediated modularity.

Enlow's Model: Development and Function in the Framework of Modularity

Probably the best example of a combined developmental and functional approach is Enlow's work on the skull. Here, developmental effects are shown to derive from function. Enlow's model posits that development across the modules of the skull acts to maintain the function of perfect occlusion. In many cases the division of developmental versus functional entities seems an arbitrary division. Klingenberg et al. (2003) has followed a different approach, showing that matrices derived from fluctuating asymmetry of the murine skull have a different structure than that derived from later functional aspects of the system. Klingenberg suggests the genetic developmental pattern represented by fluctuating asymmetry underlies and differs from the later developing functional pattern. In his view patterns of fluctuating asymmetry represent development, while general morphological matrices represent developmental AND functional effects.

While Cheverud's (e.g., 1996) and Wagner's (e.g., 1996) research emphasizes modularity in evolution, Enlow's (e.g., 1968, 1996) model of "architectonic balance" (also known as the "counterpart" model) explains modularity as expressed in function. Enlow's model is elegant in explaining development and function in the holistic sense, in that development of the craniofacial system or module incorporates other cranial regions to provide normal occlusion. This constraint of modules by function suggests a way to define modules without naming too many entities and thus atomizing structure. Under Enlow's model (1996), aspects of the splanchnocranium, dermatocranium, and basicranium are functionally constrained to maintain ideal occlusion. The function of occlusion thus unites the modules of the major regions.

Enlow's model predicts that the anterior cranial fossa (ACF), the nasomaxilla, and the corpus of the mandible develop as a unit, through integrated depositional/resorption patterns, while the middle cranial fossa, nasopharynx, and ramus develop as a unit. Because it incorporates aspects of all the S/D/B modules operating in an integrated manner, constraint by function reflects pleiotropic effects, thereby encompassing the particulate biomechanical model while also including structural integration.

Enlow's model offers a finer-grained analysis of the skull than the traditional S/D/B organization, without the risk of overatomizing structure. An example of overatomizing structure would be to describe the mandibular ramus and corpus as completely separate units and disregard the fact that at higher organizational levels they represent an integrated structure. Although at varying levels of organization one can argue that the mandible is a module, the face is a module, and the skull is a module, Enlow's model predicts that modules should be described as functionally developed entities. This functional definition is not usually mentioned in modular research, and much research only uses the cranium exclusive of the remainder of the skull to test integrative hypotheses. If Enlow's model is fully explanatory it is a mistake to analyze the skull while missing a major component of its organizing morphology. In short, if Enlow's model is correct, then cranial modules are not capable of being analyzed using traditional definitions of cranial regions; they are a highly visible artifact, rather than real biological entities. The role of the mandible as either a module *in toto* or consisting of two is examined in Chapter 3.

Defined functionally, the mandible is a "dually composed" module that is highly affected by biomechanical function, rather than simply a representation of biomechanical

force. It is part of a system best described as the posterior and anterior craniomandibular system, in conjunction with the middle and anterior cranial fossae. Under Enlow's model, cascade effects from the middle cranial fossa drive the nasopharyngeal and ramal morphology, the system being hafted onto the face through the pterygomaxillary suture (PTM). The line through the PTM and the lingual tuberosity on the internal corpus/ramus interface separate the posterior from the anterior facial areas. Bastir and Rosas (2005) suggest a decoupling of the internal and external mandibula in evolution, in accordance again with a structuralist modular hypothesis for the organization of the skull.

Generation of Hypotheses

The summary of background research and theory from Chapters 1 and 2 suggests some general craniomandibular relationships that can be used to generate hypotheses:

- ◆ The mandible shares cranial shape through developmental structural factors, yet retains an element of later manifesting function. Areas of the mandibular module(s) used for force production may load in multivariate space differently from non-force production areas.
- ◆ Mandibular modules related to the production of force for mastication may highly co-vary with both the muscles to produce that force and the dentition. Non-masticatory regions or modules may not co-vary in the same pattern. This prediction can be tested by separating the mandibular measurements from the cranial ones. Structural modules/regions with little involvement in masticatory force production (e.g., those of the cranial base angle, nasopharynx, nasomaxilla, angulation of the anterior and middle fossae, and body) should show an integrated pattern that may subsume part of the mandibular module(s).

- ◆ Finally, and most importantly, it is suggested that integrative levels within the skull may be demonstrated to not follow traditional definitions at all. It may well be that partitioning of the skull into regions best defined by an “architectonic” model is more explanatory than any other hierarchical separation.

The specific predictions above lead to a series of hypotheses testing the effects of cranial integration in human mandibular morphology. Establishing whether cranial integration is a stronger factor in predicting mandibular morphology than biomechanical requirements requires testing linked hypotheses in a series of exclusions. This is the topic of Chapter 3.

CHAPTER 3

HIERARCHICAL COMPARISONS OF CRANIAL REGIONS

Chapter 1 examined historical factors in modeling cranial morphology. Chapter 2 outlined models of evolutionary change. Modularity was introduced as a model to explain the factors of cranial integration outlined in Chapter 1. Further, modularity was described as the functional partitioning of the skull resulting from evolutionary factors. Modularity was thus presented as the functional partitioning of the skull into units exhibiting evolutionary independence. It was suggested the pattern of modularity may be taxon-specific, in that modules within a given taxon may maintain a degree of invariance across partitions of sex and population. This invariance was hypothesized to result from canalization of the skull through time from inherited structural constraint of modules. Canalization results from developmental modularity leading to evolutionary modularity through time, providing a path from mutation to stabilization of functional cranial forms (as outlined by Cheverud, 1996). It was further suggested that this structural canalization into modules constrains how function is expressed across regions of the skull (Flatt, 2005). Modules constrained by this heritable functional organization (sometimes referred to as *bauplans*) may cause localized stability of cranial form. This in turn means modules can be hypothesized as heritable taxon-specific areas of integration in the skull which are invariant across sex and population to a degree higher than that found in non-modular regions.

This chapter begins to test these hypothesized properties of modules given the information introduced above. If the skull is organized in a hierarchy the first goal is to analyze how the modules of the skull are bounded. Building on the historical factors in

the development of modular theory it is possible to model modular expression in large-scale units of the skull such as the mandible or cranium. At this highest level of the hierarchy of the skull are also traditional divisions of the skull—face, mandible, and base. Here the term “macromodule” is introduced for these traditional partitions of the skull because it remains to be seen which, if any, can rightfully be considered modules. Testing the property of invariance of modules within species begins by testing the relationships of these macromodules.

As pointed out in the earlier chapters, reference to modularity without creating testable hypotheses of relationship (through properties) is circular. The first step here is to analyze large-scale partitions of the skull to demonstrate their relationships, testing to see whether integration patterns within or across modules. This is also necessary because modules are frequently defined below this level of traditional partitions (macromodules) of the skull (Hans and Enlow, 1996; Bastir et al., 2004; Bastir et al., 2006). Without a clear explication of the way integration and modularity play out at higher levels, an examination of relationship at lower levels is uninformative. These examinations of higher level structure form the basis for the next step in the hierarchy, defining functional relationships as in Chapter 4 of this dissertation. It is thus necessary to examine levels of the hierarchy of organization before beginning to look at function as the predictor for morphology as outlined in Chapter 2 and tested in Chapter 4. Therefore the first hypotheses tested here in Chapter 3 concern relationships of form and can be considered “model free” in that they do not directly address the factors that cause them.

The macromodules are tested for integration patterns across several axes of population and sex using four primary sources of data. Data come from the well-known W.W. Howells dataset (1996; $n = 2554$); from T. Hanihara (used with permission, $n = 113$); from a lab-collected and literature-derived dataset prepared by this author for the dissertation called Fortext ($n = 150$); and from a morphometric three-dimensional dataset collected at the American Museum of Natural History (AMNH), the National Museum of Natural History (NMNH), and the Maxwell Museum of Anthropology ($n = 180$). (Details of the samples' locations and their compositions are in Appendix A.) The possible areas of invariance proposed as modules are tested for covariance structure integrated within, not across, cranial regions (Klingenberg, 2004). This is done by a series of comparisons using Cronbach's Alpha and partial least squares analysis (PLS) and then an examination of covariance structure using the Flury hierarchy. (Complete details of statistical procedures used and analysis expanding upon the use thereof is in Appendix C.) Mitteroecker and Bookstein (2008) have demonstrated that covariance matrices for definition of modularity can only be robustly compared when using same numbers of points. Therefore the primary analyses in both multivariate and morphometric datasets use equivalent numbers of points.

It would be ideal to simply use Howells's data ($n = 2554$, both males and females) to test these hypotheses of relationship across the skull, as Howells's data has been used in the past for integrative, phylogenetic, and modular studies (Polanski and Franciscus, 2006; Manica et al., 2007; Schillaci, 2008). However, the Howells dataset lacks mandibular information. Conversely, simply using Hanihara's data would be acceptable, since it includes mandibular data as well as cranial, but the Hanihara data used here are

solely Asian and solely male. The third dataset (Fortext, $n = 150$) addresses these problems: it has mandibular data, it has males and females, yet it has few variables even while the data are global in scope, as are Howells's data. Therefore a combination of datasets is employed here. Results from individual datasets are compared—using a combination of information drawn from all these sources makes it possible to partition variation sufficiently to show patterns of integration and possible invariance in the skull.

It is important to use data from the whole skull, including the mandible, to examine modular structure because primary comparisons of modules frequently compare the splanchnocranium (face) to the dermatocranium (neurocranium or braincase) (Polanski and Franciscus, 2006; Ackermann, 2005; Martínez-Abadías et al., 2008; Bastir, 2008). Failure to include the mandible as part of the splanchnocranium when comparing to the skull amounts to excluding a great deal of a developmentally integrated system. Currently there are no estimates as to how this exclusion affects the covariance structure used to test hypotheses of relationship of both form and modularity, so this dissertation provides these estimates in Chapters 3–5. It is also hoped that use of the mandible in forming rigorous hypotheses of relationship will help clarify the issue of whether it is the level of taxonomic analysis being used or measured point attribution that causes contradictory results in degrees of integration present in the face and braincase (for these opposing results see Ackermann, 2005; Polanski and Fransiscus, 2006; for further discussion see Mitteroecker and Bookstein, 2007). Full-skull data including the mandible are obviously more informative in these contexts than only data for the face and neurocranium.

The above problem of comparing levels of integration within the proposed modules of the skull mentioned above (such as within the dermatocranium or basicranium) primarily results from a definitional problem of over- or- under-prescription. Many current modular studies (and studies using modular implications such as phylogenetic reconstruction) do not define (or adequately define) proposed modules in a biological sense (for critiques of this issue see modular embryological, populational, and phylogenetic analyses in Ackermann, 2002; González-José et al., 2008; Eroukmanoff and Svensson, 2008).

The real difficulty here is defining what form modularity may take. Modules can be organized into the splanchnocranium/dermatocranium/basicranium (S/D/B) on a macro-scale (Bastir et al., 2004; Polanski and Franciscus, 2006; Mitteroecker and Bookstein 2007; Bastir, 2008). Modularity is proposed under Enlow's model of architectonic balance (a definition of modularity across the traditional S/D/B boundaries [Hans and Enlow, 1996]). Modularity is also proposed for multiple units within the S/D/B boundaries of the skull (such as the nasal module—see Franciscus and Trinkaus, 1988, 1995; Bastir et al., 2006; McCollum, 2007; Bastir, 2008; Martínez-Abadías et al., 2009).

Clearly the solution to this over- and under-production of differentially defined modules must come from application of the hierarchical principle. Hierarchy allows analysis at multiple levels, thus reducing complexity to a tractable problem. Related to systems theory, hierarchy theory models somatic organization as a series of “holons,” which are compositions of nested and integrated subsystems, themselves consisting of subsystems with consecutively decreasing orders of complexity (discussed in Bastir, 2008). It is probably impossible to address the complexity of the skull, the interplay and integration of multiple cranial elements, and the role of the mandible without the use of a

hierarchy of organization. Entities at one level in a hierarchy may be discrete at one level and integrated at another. Here, using a hierarchy is necessary to avoid another potentially serious problem in the definitions of modules, the inclusion of spatially proximal areas into modules based solely on proximity, a problem illustrated in such statements as this from Bastir (2008:50): “Some modules are integrated by local cranial factors such as purely spatial proximity.” This inclusion of simple spatial proximity into modules creates definition without boundaries, and thus an untestable definition. As mentioned in the Preface and Chapter 2, robust definitions of modules need aspects of both qualification (attributes) and quantification (properties). The dual aspect of definition is necessary for such a biological process as outlined in the Preface and Chapter 2, because the skull is organized in a hierarchy.

Hierarchical Levels

The first level of organization into a hierarchy is the traditional distinction between the mandible and the skull. As was pointed out previously, many researchers have observed this dichotomy, making distinctions between the use of the mandible versus the skull for such topics as population discrimination and construction of phylogenies (discussed in Humphrey et al., 1999). As was also pointed out earlier, observable and traditional differences such as this basic partitioning may make little sense in examining integrated structures with similar embryological origins, because such a relationship is not directly visible. Divisions such as the cranium and the mandible may make sense intuitively, as the mandible does not reside inside, or form the wall of, the skull, but both ontogenetic and functional definitions of integration (and modularity) belie this. Given that the mandible and maxilla form together in ontogeny and that both exhibit a common

function, there may be little information to be gleaned from separating cranial modules in such a broad fashion.

The second level of macromodular definition is the traditional separation of the skull into the splanchnocranium, dermatocranium (neurocranium), and basicranium (face, braincase, and cranial base, or “S/D/B”). Development of these traditional regions follows “attributive” definitions of modules as proposed by Raff (1996)—autonomous genetic organization, hierarchical organization, specific location, and connection to other macromodules. To this list McCollum (1999) adds the attribute of sequential transformations in development. All these definitions apply well, then, to the traditional S/D/B partitioning. For example, regions such as the face are genetically programmed autonomously, apart from the dermatocranium and basicranium (through differential Hox genes—i.e., mesenchymal—induction patterns; see Kuratani, 2005). The S/D/B macromodules occupy specific cranial regions. Following Raff, connection to other macromodules is demonstrable for the dermatocranium and basicranium in that annular deformation of the former causes coronal expansion of the latter at the glenoid fossa (Antón, 1989; Cheverud and Midkiff, 1992). Finally sequential transformations in development are evident. The mandible, dermatocranium, and basicranium all change radically in processes such as chondrogenesis and/or intermembraneous ossification and later, senescence. However, simply demonstrating the traditional partitions of the skull have some of the above attributes of modules does not prove that in fact they are.

At the third level the skull can be even further subdivided. For example, McCollum (1999) proposes a division of the skull into modules of the neurocranium, the nasal region, and the oral apparatus. Bastir et al. (2005) recognize the traditional S/D/B

distinction as useful, then distinguish two further basicranial modules (midline and lateral). Moss (1962, 1997a, 1997b, 1997c, 1997d) also makes further divisions of the S/D/B as discussed in Chapter 2. Further, there may be intermodular (or intramacromodular) hierarchical organization: in ontogeny the structure of the face follows the more rapidly expanding dermatocranium and nasal region (Kean and Houghton, 1986; Franciscus and Trinkaus, 1988; Ackermann and Cheverud, 2004). These complex relationships, again, point out the necessity of objective definition of both the biological entity being defined (element, module, or macromodule) and the level of analysis (hierarchical location). The commonality of large-scale partitioning is that the traditional S/D/B and mandibular macromodules have not been tested as equal entities in a hierarchy in modern humans. It is possible to talk of S/D/B differences in the broad sense, but without first looking at the relationship of the mandible to the other parts of the skull (as in the first partition above), an analysis of the relationship of the mandible to the S/D/B partitions is not robust.

Population

Population is a differential factor in the mandible and cranium that must be addressed in regarding them as initial examples of modules. Studies have shown relatively weak associations between populations when looking at the similarities of the mandible based on nearest neighbor clustering (Humphrey et al., 1999, which continues observations made since Hrdlička, 1940). This suggests that mandibular variability is not patterned in a strict ancestor-descendant relationship. Thus it is different from that in the skull, which apparently exhibits a center-edge dispersal from an initial African radiation (see Manica, Balloux, and Hanihara, 2007, although also see John Hawks's [2007] online critique).

Although early modern human populations such as Skhul and Qafzeh are morphological candidates for ancestors to all human populations, they group most closely with Middle Paleolithic populations in the mandible in many aspects of analysis (Nicholson and Harvati, 2006). This result would not be expected if the mandible is truly a module, as taxon-specificity would make this unlikely.

Results presented below show different parts of the mandible respond to different factors, again pointing out the need to establish whether the mandible can be considered a module or if it is actually formed of two modules, as suggested by counterpart analysis and results in non-human taxa (Klingenberg, 2004; Cheverud, 2004 on the murine mandible; Rosas and Bastir, 2004 on Neanderthal). Patterning shows ramus height tends to be variable within and across hominine groups, whereas ramal breadth is more stable (Schreiner, 1935; Weidenreich, 1936). Nicholson and Harvati (2006) found two major morphologies of the mandible: one with a relatively supero-inferiorly thin and antero-posteriorly elongate corpus; the other with a broad ramus and sloped margin. Ramal height is primarily a function of masticatory stress (Weidenreich, 1936; Hylander, 1977; McCollum, 1999) whereas ramal breadth is more correlated with nasopharyngeal spatial requirements in recent humans (Smith, 1983; Hans and Enlow, 1996; Anderson, 1998; Estenson and Anderson, 1998; Estenson, 2004). Humphrey et al. (1999) showed slightly better ability to distinguish populations using the mandible than previous studies. Humphrey left open in that study the question of whether the results derived from numbers of points used for measuring, rather than biological reality. (Interestingly, Rosas and Bastir [2004; above] have demonstrated independent trajectories of the supra- and infra-mandibular nerve morphology in *Homo* groups, proposing a separation of these

possible modules by the pattern of innervations, an idea explored more completely here in Chapter 5.) On the other hand, population itself is a strong predictive factor in the mandible. Nicholson and Harvati (2006) found population effects in the first three components of their analysis of the mandible, particularly in circumpolar populations with high dental loading. One of the hypotheses tested below concerns modularity in these populations of humans.

Allometry

Allometry is the other factor that may confound a property-based definition of cranial modules, particularly in the mandible. Male mandibles are larger on average than female, with Weidenreich (1936) concluding that modern human female mandible size averaged 92.4% of male size. There have been many fruitless attempts in the past to differentiate hominoid and hominine taxa based on mandibular morphology based on size (also discussed in Rak et al., 2002). Within *Pan* and *Homo* most of the differences in mandibles are found in overall size rather than in differential form (Wood, 1976; Wood, Li, and Willoughby, 1991). However, Rosas and Bastir's (2002) two-dimensional analysis of cranial shape (including the mandible) found significant differences in male and female form. In their *two-dimensional* analysis, Bastir and Rosas found shape as explaining 53% of variation in the skull and mandible, with size contributing 35%.

Mandibular form may represent an area of relative stability of form compared to other regions of the skull. This is suggested by data in Franciscus and Trinkaus (1995). Their results on mandibular measurements suggest Neanderthal mandibular proportions are similar to modern human; results mirror those derived from Hrdlička (1940a,b,c). Hrdlička's sample comprises 2,363 modern human mandibles and was analyzed for

overall ramal proportions. The overall sample of ramus breadth divided by mandibular length values gives a result of 0.374, extremely close to a value from JY Anderson (unpublished data) of 0.369. This figure also accords with that obtained by using Franciscus and Trinkaus's (1995) results from an archaic *Homo* sample. Because all three examples accord with a common ramus proportion of approximately 0.370, the hypothesis of significant differences in modern human and Neanderthal mandibles in this aspect is not supported. These data, also consistent with those derived by using data from Kaifu (1998a,b) and Pinhasi (2000), suggest some aspects of mandibular form are constants. If so, they would presumably be resistant to change given their possible expression of modularity (however, as outlined previously, there is a longstanding argument against the mandible as a single module).

The hypotheses tested below (H_{01} and H_{02}) examine the relationships of the skull to determine first whether the skull *in toto* is more integrated or more modular. Intuitively it is obvious parts of the skull differ yet without testing all parts together for level of integration within and across major subdivisions (such as the S/D/B and mandible) modularity cannot be assessed. As with all divisions in the skull, if the mandible integrates completely with other cranial regions such as the face or base it cannot be described as having a separate evolutionary pathway and hence would fail the test of modular independence.

A further test (H_{03} below) is done to see if populations expressing high dental loading through masticatory and paramasticatory use follow the general pattern in the skull tested here. Here covariance matrices of various partitions of the skull in a hierarchy are made

without an analysis of function which may be driving the morphology. Chapter 4 examines factors producing the morphology at the various levels of the hierarchy.

Model-Free Hypotheses

Model-free hypotheses test the prediction of differences between macromodules of the cranium and mandible. They are formulated without biological or functional explanation for organization, and simply test statistical relationships, primarily covariance matrix structure. The model-free hypotheses are thus an analysis of Platonic, idealized form and could be applied to any two-part three-dimensional entity to see if differences are across or within structure. Initial data exploration is through sequential examination of the covariance matrices from Principal Component Analysis (PCA) using the statistical platforms Paleontological Statistics Program (PAST) and JMP to define Cronbach's Alpha. Cronbach's Alpha is here used as an exploratory measure of the relationship of variables integrated within the macromodules (Cronbach, 1951). Cronbach's Alpha is not a standard technique: its statistical power is weak and it is uninformative if used for different numbers of measured points, being susceptible to numbers of comparisons. Here it is used only with similar numbers of points and only to examine relationships and form, not test, hypotheses. The mathematical underpinnings of Cronbach's Alpha are reviewed in Appendix C Statistics.

The hypotheses are tested using statistical analysis through sequential comparisons of covariance matrices using PAST (Hammer, 2007) and JMP (SAS). Further, the covariance matrices are tested for internal structure and integration using the Flury hierarchy (Flury, 1983; Arnold and Phillips, 1999; Ackermann and Cheverud, 2000). The

Flury hierarchy provides a means to assess not only significance of differences of covariance matrices, but how the similarity (or difference) is structured. Full details supporting the use of the Flury hierarchy appear in Appendix C Statistics.

Hypotheses

H₀1: There are no different levels of integration between and across macromodules of the skull including the mandible.

This is a simple hypothesis of no difference and is not model-bound. Rejection of H₀1 is of interest, as it would demonstrate the mandible and the other macromodules can simply be regarded as equally integrated cranial elements. This hypothesis also indirectly tests results in Martínez-Abadías et al. (2009) suggesting there are no statistically significant differences among the heritabilities of facial, neurocranial, and basal dimensions. As suggested here, the heritable part of morphology may be described as the module. If so, radically different heritabilities would be difficult to explain, as all three parts are inherited. Rejection of the hypothesis means the investigation should continue. It would be impossible to later describe differences in cranial and mandibular form as predicted by functional biomechanical or structural factors should there be no differences to begin with. Acceptance of this hypothesis would also preclude any further modular analysis, because failure to find areas of differential integration would mean the skull is totally integrated.

H₀2: No mandibular and/or cranial multivariate or morphometric modular male/female differences exist across sex.

H₀2 could nearly be considered a “model-bound” hypothesis. However, no explanation or expectation of differences is here included. Testing this hypothesis directly tests the assertion that cranial regions including the mandible are not simply (allometrically) “scaled-up” female mandibles. Testing this hypothesis also addresses the acceptability or non-acceptability in grouping covariance matrices across sex in phylogenetic or evolutionary scenarios.

H₀3: No mandibular and/or cranial multivariate or morphometric modular craniomandibular population differences exist across samples from circumpolar populations.

H₀3 could also nearly be considered a “model-bound” hypothesis, in that there is evidence that the mandible and skull do vary by population to a degree based on masticatory and paramasticatory use (Harvati and Weaver, 2006). However, no explanation or expectation of differences is here included. This hypothesis simply tests population as a factor.

Prior evidence also suggests that H₀1, H₀2, and H₀3 will be rejected, as measurements of cranial integration derived from Howells’s (1989) cranial dataset indicate higher levels of cranial integration therein rather than those found in prior studies of mandibular integration (Anderson, 2000). Additionally comparisons between major areas of the skull have shown differences in covariance structure (Polanski and Franciscus, 2006; Ackermann, 2005). Anderson (2000) previously examined H₀1 and H₀2 using Cheverud’s

(1984) matrix decomposition and total eigenvalue methods in a smaller dataset, with inconclusive results.

Methodology

Hypothesis testing consists of comparisons of both multivariate and morphometric analysis from a global craniometric dataset (W.W. Howells's craniometric dataset); a subset of T. Hanihara's craniometric dataset (males only, Asian populations only); a lab-measured and literature-derived linear multivariate dataset (Fortext); and finally a three-dimensional morphometric dataset collected for this dissertation at AMNH and NMNH (the Smithsonian). All details about the samples and definitions for the measurements appear in Appendices A–C.

Howells's Data

Analysis of the skull using Howells's (1996) dataset consisted of 21 linear measurements (see Table 3-1). Fourteen of these replicated the three-dimensional cranial structure as discussed in Polanski and Franciscus (2006). Attention was paid to the dimensionality of the measurements, with variables in length-width-height axes used in equal numbers. This step is to prevent any one plane from over-influencing analysis, and it is necessary because analysis of form using only two dimensions is not robust, given the three-dimensional nature of the skull (see Chapter 5). These 14 measurements, divided into two subsets of 7 measurements, were used to describe the skull and the face in three dimensions. An additional seven-variable subset was constructed describing the cranial base. One of each subset of points overlapped with another; however, as is detailed below, the significance of results showing differences across groups (as is expected when comparing unintegrated regions; see Klingenberg et al., 2003) is enhanced

by cross-sample inclusions, which tend to drive integration up rather than down. Comparisons of integration in interregional covariance will actually overestimate the amount of integration across the regions because of one or two shared measurement points across the datasets. Therefore results here showing little relationship across macromodular regions are conservative. If results were ambiguous the redundant points were eliminated, and the analysis was repeated with 6 measurements and no redundant points. If results differed significantly from those using all 7 measurements, they are reported.

Table 3-1. Measurements Used in the Howells Dataset (definitions follow Howells 1989)

Location	Measurement Type	Measurement Landmarks
Neurocranium ("Skull")	<ul style="list-style-type: none"> • Cranial length • Maximum cranial breadth • Maximum frontal breadth • Frontal chord • Parietal chord • Cranial height • Basion-nasion length 	<ul style="list-style-type: none"> • Glabella-opisthocranion (GOL) • Euryon-euryon (XCB) • At coronal suture (XFB) • Nasion-bregma (FRC) • Bregma-lambda (PAC) • Basion-bregma (BBH) • Basion-nasion (BNL)
Face	<ul style="list-style-type: none"> • Facial height • Orbital height • Orbital breadth • Nasal breadth • Bimaxillary breadth • Lower facial projection • External palate breadth 	<ul style="list-style-type: none"> • Nasion-prosthion (NPH) • Perpendicular to orbital long axis (OBH) • Ectoconchion-dacryon (OBB) • Alare-alar (NLB) • Zygomaxillare-zygomaxillare (ZMB) • Basion-prosthion (BPL) • Alveolar border – greatest breadth (MAB)
Base	<ul style="list-style-type: none"> • Cranial height • Biauricular breadth • Biasterionic breadth • Basion-prosthion length • Mastoid height • Mastoid breadth • Foramen magnum length 	<ul style="list-style-type: none"> • Basion-bregma height (BBH) • Biauricular breadth (AUB) • Biasterionic breadth (ASB) • Basion-prosthion length (BPL) • Across mastoid (MDH) • Across mastoid (MDB) • Sphenobasion-opisthion (FOL)

Hanihara's Data

Analysis of the skull also used (by permission) Hanihara's dataset derived from male Asians ($n = 116$; see Table 3-2). The dataset consisted of 20 linear measurements. The first 14 (of the skull and face respectively) are the same as those used in Howells. Hanihara's data were used to extend results using Howells's measurements in the skull and face and to provide mandibular information lacking in the Howells dataset. Six mandibular measurements were also used, and results from the three regions (skull, face, mandible) were compared for Cronbach's Alpha, covariance matrix integration, and covariance measure structure, as was done for Howells's data. As with Howells's data, measurements used from Hanihara also preserved the dimensionality of the measurements, with variables in length-width-height axes used in equal numbers. The cranial base was not analyzed because measurements are not the same as in Howells, and therefore analysis on sex and population factors could not be performed. Final analysis used the CPCP (the Common Principal Components Program; see Arnold and Phillips, 1999; Phillips and Arnold 1999) to assess matrix structure similarities.

Table 3-2. Measurements Used with the Hanihara Dataset (definitions follow Howells 1989, except for mandible, which follow Martin and O'Brien 1939)

Location	Measurement Type	Measurement Landmarks
Neurocranium ("Skull")	<ul style="list-style-type: none"> • Cranial length • Maximum cranial breadth • Maximum frontal breadth • Frontal chord • Parietal chord • Cranial height • Basion-nasion length 	<ul style="list-style-type: none"> • Glabella-opisthocranion (GOL) • Euryon-euryon (XCB) • At coronal suture (XFB) • Nasion-bregma (FRC) • Bregma-lambda (PAC) • Basion-bregma (BBH) • Basion-nasion 3 (BNL)
Face	<ul style="list-style-type: none"> • Facial height • Orbital height • Orbital breadth • Nasal breadth • Bimaxillary breadth • Lower facial projection • External palate breadth 	<ul style="list-style-type: none"> • Nasion-prosthion (NPH) • Perpendicular to orbital long axis (OBH) • Ectoconchion-dacryon (OBB) • Alare-alar (NLB) • Zygomaxillare-zygomaxillare (ZMB) • Basion-prosthion (BPL) • Alveolar border – greatest breadth (MAB)
Mandible	<ul style="list-style-type: none"> • Ramus breadth • Mandibular Length • Condyle Height • Bicondylar Breadth • Bigonial Breadth • Symphysis Height 	<ul style="list-style-type: none"> • M71 (RAM) • M681 (ML) • M70 • M65 (BICON) • M66 (BIGON) • M69 (SYMHGT)

Fortext

A multivariate analysis of a lab-measured and literature-derived dataset of 12 measurements of the skull and mandible used an equally weighted series of 6 mandibular

and 6 cranial linear measurements, $n = 150$. (Sample composition, measurements used, and methodological information are given in the Appendices.)

The measurements used on the mandible are illustrated in Figure 3-1; those used for the cranium are in Appendix B Methodology. These measurements were chosen for biological relevance (Type 1 measurements; O'Higgins, 2000) and for an equal contribution in the length-width-height axes of the skull overall to define spatial relationships (Polanski and Franciscus, 2006). This dataset was analyzed using PAST (Hammer, 2007). PCA, PLS, and Flury hierarchy and matrix comparisons were performed using PAST and JMP (SAS, 2009) and CPCP (Arnold and Phillips, 1999; Phillips and Arnold, 1999). Some analyses were run size-corrected to remove the well-known allometric effect of the first principal component associated with size.

statistical analysis. (Description of Morphologika 2.5 and three-dimensional morphometrics in Appendix D, Chapter 5, and O'Higgins, 2000). Matrices derived from the mandible, face, and base were compared by the Flury hierarchy as outlined below.

Data Analysis

Howells's and Hanihara's data were analyzed by extracting the covariance matrices from various partitions of the skull, using PAST. These covariance matrices were loaded into the CPCP (see Stepan, 1997) using the Flury hierarchy (Flury, 1988) from Phillips and Arnold (1999; see also Arnold and Phillips, 1999). Common Principal Component (CPC) analysis tests more than simple equivalence of covariance matrices. The prediction that areas of the skull exhibit modularity was tested under the assumption that covariance matrices with similar structure (proportional or identical, as outlined below) fail the test of modularity in being integrated within themselves, thus forming one large module, rather than showing separation from other skull regions. CPC analysis tests whether matrix structure below the level of equality is proportional or less (a full description is in Appendix C). Two or more covariance matrices are compared using the knowledge that a given level of similarity of matrix comparisons across the matrices must include similarity at the levels below. The CPC analysis thus tests hierarchical hypotheses of relationship.

As an example, consider Matrix A might be equal to that of B except that each element of the $(p, *p)$ matrix is multiplied by a single constant. This defines proportionality; here multiplication by a constant represents simple matrix (scaling) differences. Therefore

matrices with similar eigenvectors (matrix structure) but a proportionally different constant such as simple allometric size are proportional.

Comparisons below this level can show similarity in any sequentially lower structural integration. This ranges from all principal components in common (CPC model) down to, eventually, $p-2$ components shared. In knowing the principal components are orthogonal to one another, we already know $p-1$. Back in the other direction, towards structural homogeneity, proportionality (represented by equality minus the scaled relationship) is only exceeded by matrix equality in which eigenvectors and eigenvalues are equal. Matrix equality thus bounds the hierarchy if proportionality is exceeded by total equivalence of the matrices.

The methodology here uses the fact that Flury hierarchy proportionality represents a test of the scaling relationship of the matrices compared, excluding any eigenstructure differences (thus it is an example of multivariate allometry [see Klingenberg and Zimmermann, 1992]). This scaling relationship of matrices can be generalized as representing “lines of least resistance” in phenotypic change in evolution (Erouhkmannoff and Svensson, 2008). Most evolutionary change in taxa is modeled as occurring through this small-scale modification of existing structure, rather than as major reorganization.

Current theory suggests this change “along lines of least resistance” is mirrored in these covariance structure similarities (Schluter, 1996; Renaud et al., 2006). Analysis here applies and extends this theory to module comparison in the hierarchy. Flury hierarchy proportionality means eigenstructure is similar in the comparison (eigenvectors are similar, while eigenvalues differ—see Ackermann and Cheverud, 2000). Module

comparison exhibiting proportionality does not indicate reorganization, as the matrix has not changed “shape” (eigenvectors), only “size” (eigenvalues). Therefore true modules should never share proportionality of matrices as that would indicate integration across the modules and violates the central tenet of modularity, internal integration rather than shared.

If Flury hierarchical comparisons show proportionality across partitioning then modules are the same. Obviously the covariance structure of different morphological shapes will show differences. Theory predicts those differences will have a hierarchy and predicts the level of least difference (line of least resistance) will be at the level of proportionality. Again, this application is based on evidence suggesting most species and population divergence occurs along the “lines of least resistance” in which covariance change from one entity to another at the level of population exhibits the pattern of simple “size” modification of the matrix, rather than a major reorganization of the matrix (Erouhmanoff and Svensson, 2008). As stated before, the logic is that structure as defined by the covariance matrices is congruent if proportional. This congruence of structure cannot be expected in taxa within an evolving lineage if function dictates change in structural relationships—changing function reorganizes structure. Here it is suggested this reorganization occurs within modular levels above species (see González-José et al. 2008). This suggestion is tested in Chapter 5.

In addition to comparison of covariance matrices extracted from Howells’s, Hanihara’s, and Fortext’s data, procrustes superimposition and PCA on 200 individuals (a global sample) were performed using Morphologika 2.5. The loadings of the individuals on the principal components were compared in generalized PLS extracted as

canonical variates and compared using the JMP program (from SAS 2009). This extraction was done to establish the amount of explanation of various proposed modules/macromodules to each other. For example, an assessment of the amount of explanation of the morphology of the mandible by the face and cranial base separately and individually was performed. As with eigenvalues, successive canonical variates explain successively smaller amounts of total variation; therefore the first root is the largest. First roots of the extracted canonical variates from the mandible, face, and base were compared for explanation of morphology in each grouping. This comparison was done to suggest, rather than test, patterns of modularity, in a way similar to that for the Cronbach's Alpha.

Howells's data were analyzed by comparing the neurocranial, facial, and basicranial regions, and each of those in combination (Neurocranium = "Skull" + Face; then Base + Face; then Base + Skull). These partitions were tested across sex and population for matrix structure. The complete dataset, all 21 measurements, was also tested across these axes. Circumpolar population skulls were compared to the remainder of Howells's data to test the relationship of this very derived morphology to the global sample.

Hanihara's data were analyzed by comparing the same neurocranial "skull" and facial regions, with the addition of mandibular data. Similarly to the Howells's data, the individual regions and their combinations were analyzed (Neurocranium = "Skull" + Face; then Mandible + Face; then Mandible + Skull). These partitions were tested for structural proportionality within the partitions using the Flury hierarchy. There was no

testing across sex or population here, as all individuals in this subset of Hanihara are male and Asian. The Fortext dataset was tested in a similar way.

Results

H₀1: There are no observable differences in mandibular and cranial multivariate analyses.

As expected this hypothesis is refuted. First it is shown that there are differences in the integration pattern of areas within the skull in Howells's data; then it is shown that the mandible is not integrated with either the full skull, or parts therein.

The series of tables and graphs below are organized to show Cronbach's Alpha (α) (used as an explanatory tool only), then a series of comparisons showing relationships in the covariance matrices by the Flury hierarchy. Results are displayed in tabular form, then discussed. The possible, though extremely unlikely hypothesis that the morphology of the mandible as represented in morphometric statistical matrix is a simple extension of the matrix of the remainder of the skull is refuted.

Results from Cronbach's Alpha (α)

Comparison of All 47 Measurements in the Howells Dataset

"All measurements" is all Howells's craniometric data, and analysis of these data yields a very high Cronbach's Alpha (α ; 0.9424) (see Table 3-3). Cronbach's Alpha (α) is extremely high here (normally acceptable levels are from 0.7 to 0.8) because the number of points used to define the structure of the skull is redundant, basically encompassing not only all three dimensions, but also subset-measurements within those dimensions. As

outlined previously, Cronbach's Alpha (α) is susceptible to numbers of points—over-specified models lead to overly high p-values. Tables 3-4 and 3-5 show little difference in males versus females across Howells's full dataset; the model is over-specified in both cases, meaning again a great many measured points in Howells's data are not only redundant for defining shape, but are biologically uninformative.

Table 3-3. Cronbach's Alpha – All Measurements in the Howells Dataset

Cronbach's α	A	Plot Alpha
Entire set	0.9424	

Table 3-4. Cronbach's Alpha – Males in the Howells Dataset

Cronbach's α	A	Plot Alpha
Entire set	0.9107	

Table 3-5. Cronbach's Alpha – Females in the Howells Dataset (multivariate sex=2)

Cronbach's α	A	Plot Alpha
Entire set	0.9095	

Table 3-6 presents the results for size-corrected Howells data (size removal using PAST; allometric size removal option). The analysis again uses the complete Howells dataset, using all 47 variables. It shows how the over-specification of the above model drops upon size removal, suggesting a major factor of the relationships across the skull is overall size (male $n=1463$, female $n=1141$).

Table 3-6. Cronbach's Alpha – Size-Corrected Data for the Entire Howells Dataset Males and Females

Cronbach's α	α	Plot Alpha
Entire set	0.7408	

The following comparisons presented in Tables 3-7, 3-8, and 3-9 are the results for the neurocranial skull, face, and base regions in Howells. Again the neurocranial “skull” and face regions are the same as used by Polanski and Franciscus (2006; seven measurements, preserved three-dimensional structure, and derived from large samples). The cranial base is also comprised of seven points, one of which is the same as the neurocranial (basion-bregma height [BBH]). In the broad sense (as discussed earlier) inclusion of redundant points can be an issue in rigorous statistical testing—here Cronbach's Alpha (α) is not used rigorously, only to suggest patterns. Although the numbers of points are the same, there is an unexpected lower degree of integration in the neurocranial “skull” (Table 3-7). This is not found in the face or the base (Tables 3-8 and 3-9).

Table 3-7. Cronbach's Alpha – Comparison of the Neurocranial “Skull” Only

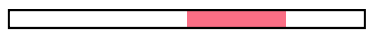






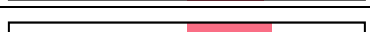
Cronbach's α	A	Plot Alpha
Entire set	0.5588	
Excluded Column	A	Plot Alpha
Column 4	0.3565	
Column 5	0.7046	
Column 6	0.7404	
Column 7	0.4373	
Column 8	0.4032	
Column 9	0.4280	
Column 10	0.4727	

Table 3-8. Cronbach's Alpha – Comparison of the Face Only

















Cronbach's α	α	Plot Alpha
Entire set	0.7769	
Excluded Column	α	Plot Alpha
Column 12	0.7586	
Column 13	0.7752	
Column 14	0.7556	
Column 15	0.7347	
Column 16	0.7759	
Column 17	0.7127	
Column 18	0.7102	

Table 3-9. Cronbach's Alpha – Comparison of the Base Only

Cronbach's α	α	Plot Alpha
Entire set	0.7622	
Excluded Column	α	Plot Alpha
Column 20	0.7212	
Column 21	0.6903	
Column 22	0.7163	
Column 23	0.7532	
Column 24	0.7327	
Column 25	0.7445	
Column 26	0.7559	

The comparisons showing a lack of integration in the neurocranium support results from both Ackermann (2002, 2005) and from Polanski and Franciscus (2006). Results here support Ackermann in demonstrating a higher degree of integration in the face, while also supporting Polanski and Franciscus in describing the human cranium as more modular and less integrated overall. The results here are contra Mitteroecker and Bookstein (2008) suggesting tight integration across the cranium and are contra findings that cranial integration level is similar across a broad taxonomic range of primates. If as

was discussed above modularity increases in evolution, it would seem that higher modularity, hence lower integration across modules, would be a necessary consequence in ongoing evolution in the Hominoidea (Lieberman, Mowbray, and Pearson, 2000).

While not conclusive, the lower level of integration demonstrated here strongly indicates that analyses relying on Howells's data, particularly that deriving from the neurocranium, should be regarded with caution. As an aside, note that throughout these comparisons of skull and face (see Tables 3-7, 3-8, and 3-9 above), the Plot Alpha graphs show the increase in model r when certain variables are extracted. Removal of these (although unlabeled here) breadth measurements consistently causes a rise in r , indicating a better model fit when width measurements are excluded. As earlier discussed and later tested in Chapter 5, this better fit results from the fact the skull varies across the globe more in width measurements than length and height; thus removal of the proportionately higher-loading measurements causes spurious similarity to increase (see recent results in Martínez-Abadías et al., 2009). This is not germane only to the present study: as discussed later, when width measurements are removed, matrices and comparisons of matrices remaining will consistently seem more similar than they actually are—removal of this axis as in analysis using two-dimensional radiographs will be proportionately more compromised than the removal of either of the other axes. The axis of breadth is the least removable axis if, for instance, discrimination of populations is the goal.

Table 3-10 reports the comparison of the sum of Skull + Face + Base (21 measurements). Cronbach's Alpha changes, dropping from that obtained for the complete Howells dataset (47 measurements). This result probably reflects loss of "intermediary" (in other words, over-specified) linking points across the skull, which are unnecessary for

defining morphology. Nonetheless, the very high Cronbach's Alpha suggests there is still redundancy of points used.

Table 3-10. Cronbach's Alpha – Skull+Face+Base (“intermediary” points removed from the Howells data)



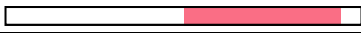

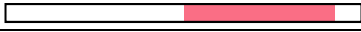

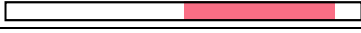

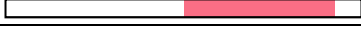





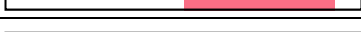







Cronbach's α	α	Plot Alpha
Entire set	0.8635	
Excluded Column	A	Plot Alpha
Gol	0.8447	
xfb facbreadth	0.8843	
Xcb	0.8967	
bnl.bas.nas	0.8473	
Bbh	0.8471	
frc nas-breg	0.8511	
pac.breg.lamb	0.8579	
bpl.bas.pros.l	0.8532	
obh.orb.hei	0.8622	
obb.breadth	0.8599	
nph.fac.height	0.8516	
nlb.nas.breadth	0.8627	
mab.ext.pal.breadth=ectomolare	0.8543	
zmb.fac.breadth	0.8522	
bbh 2	0.8471	
Aub	0.8470	
Asb	0.8536	
Bpl	0.8532	
Mdb	0.8573	
Mdh	0.8602	
Fol	0.8611	

Figure 3-2 shows that the Scree Plot has selected three rather than five significant PCA axes as in the 47 corrected measurements from Howells's original data (not shown), probably reflecting simple directionality (length-width-height) of the measurements as variation in multiple axes begins to compress to fewer.

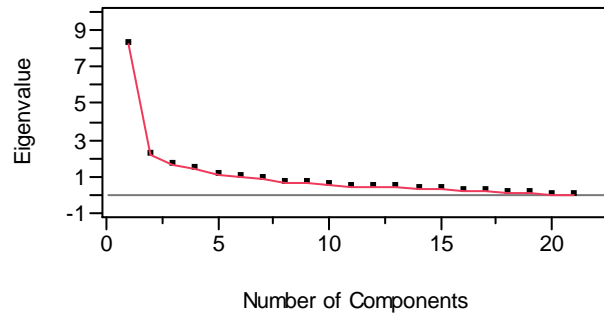


Figure 3-2. Scree Plot for the 47 Corrected Measurements of Howells Data

Results from the CPC Model

Howells's data was used to test the relationship of the three cranial regions (exclusive of the mandible) below. The Flury hierarchy results show no relationship across all three regions, meaning integration is not primary in skull (see Table 3-11 below). This comparison underlies the comparisons that follow showing the pattern of modularity in the neurocranium, face, and base in Howells's data.

Table 3-11. Flury Decomposition of Three Cranial Regions (Step-Up and Model Building Approaches)

Model						
Higher	Lower	Chi Sqr	df	p-val	CS/df	AIC
Equality	Proport	5822.539	2	<0.0001	2911.270	26470.524
Proport	CPC	13810.338	12	<0.0001	1150.861	20651.985
CPC	CPC(5)	81.028	2	<0.0001	40.514	6865.647
CPC(5)	CPC(4)	109.519	4	<0.0001	27.380	6788.619
CPC(4)	CPC(3)	387.004	6	<0.0001	64.501	6687.100
CPC(3)	CPC(2)	1452.100	8	<0.0001	181.513	6312.096
CPC(2)	CPC(1)	896.816	10	<0.0001	89.682	4875.996
CPC(1)	Unrelated	3911.180	12	<0.0001	325.932	3999.180
Unrelated						112.000

In tables such as Table 3-11, the lower the AIC criterion in the final column, the more robust the model is. If the AIC shows at levels other than unrelated, that is the level of matrix integration. Here results show no similarity across matrix (modular) structure, $AIC = 112$. The p-value for any shared matrix structure is zero. Robustly defined modules can be expected to exhibit this lack of integration when their covariance structure is compared to other modules. (Full discussion of the AIC criterion appears in Appendix C.) The summation of the above indicates there are different levels of integration and possible modularity across the three regions in Howells's data.

Results from Partial Least Squares (PLS)

Figure 3-3 and Table 3-12 show the explanation of morphology of the face by the neurocranium in Howells, $n = 2643$. This low figure of 30.61 suggests little explanation of the morphology of the face by the skull and decoupling of the face and skull following Polanski and Franciscus (2006). A high value of explanation of the face by the skull would not be a prediction of modularity.

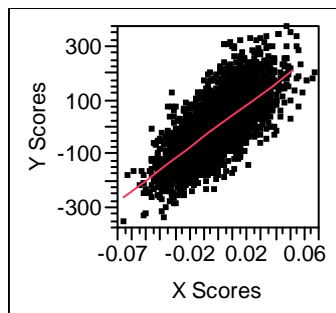
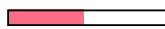
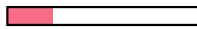
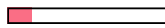
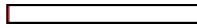
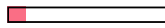
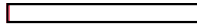
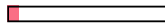
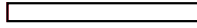
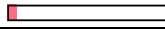
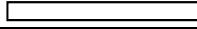
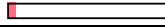
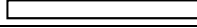
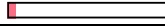
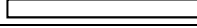


Figure 3-3. Scores Graph for Partial Least Squares Analysis of Facial Morphology Explained by the Neurocranium

Table 3-12. Partial Least Squares – Percent Variation Explained by the Neurocranium

No.	X	X-Plot	Cumulative X	Y	Y-Plot	Cumulative Y
1	47.02		47.02	23.65		23.65
2	16.01		63.04	2.839		26.49
3	11.39		74.43	2.145		28.64
4	7.189		81.61	1.195		29.83
5	6.565		88.18	0.587		30.42
6	6.092		94.27	0.15		30.57
7	5.728		100	0.039		30.61

Results for Fortext Mandibles and Crania

The results here are from analysis of the literature-derived and lab-collected Fortext dataset (n = 150). The data landmark descriptions were listed previously, comprising six mandibular and six cranial points from six global populations. The Flury hierarchy reported in Table 3-13 and Figure 3-4 that follows below show the mandible and skull are not integrated units. The mandible and skull have very different trajectories. Again, the higher the AIC, the lower the comparability of matrices.

Table 3-13. Flury Decomposition of the Matrices of the Skull and Mandible

Model						
Higher	Lower	Chi Sqr	df	p-val	CS/df	AIC
Equality	Proport	97.991	1	<0.0001	97.991	414.017
Proport	CPC	121.289	5	<0.0001	24.258	318.026
CPC	CPC(4)	0.062	1	0.8035	0.062	206.737
CPC(4)	CPC(3)	16.627	2	0.0002	8.313	208.675
CPC(3)	CPC(2)	25.741	3	<0.0001	8.580	196.048
CPC(2)	CPC(1)	61.369	4	<0.0001	15.342	176.307
CPC(1)	Unrelated	90.939	5	<0.0001	18.188	122.939
Unrelated	—					42.000

Figure 3-4 illustrates the parallel coordinate plot of the mandible and cranium in 144 individuals, from the global Fortext sample, for all measurements. The plot provides a visual confirmation of the lack of integration of skull and mandible measurements. Each of the six mandibular (measurements 1–6) and six cranial measurements (measurements 7–12) across all individuals is plotted against all other individuals. Ideally this plot would show a 12-peaked dark band composed of all point relationships in parallel (see the JMP [SAS, Inc.] information in Appendix C).

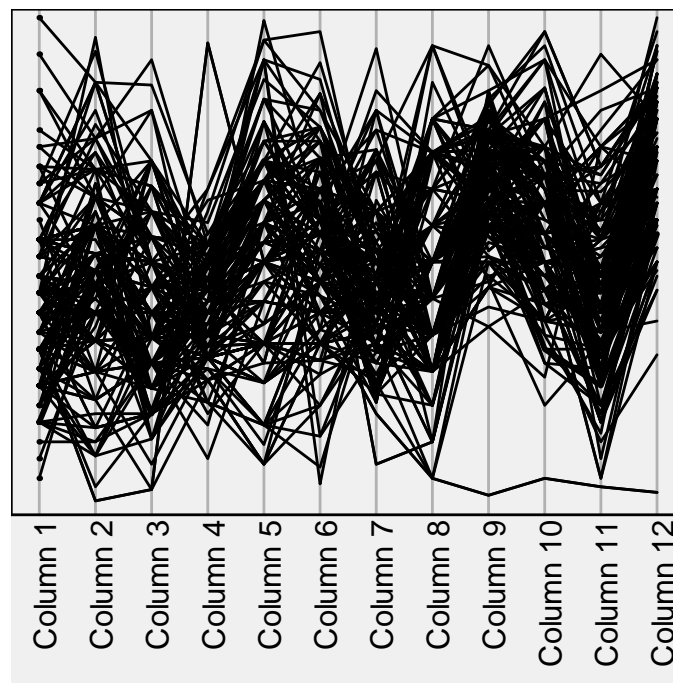


Figure 3-4. Parallel Coordinate Plot of the Mandible and Cranium in 144 Individuals

Figure 3-5 depicts the PLS prediction of the morphology of mandible by the skull.

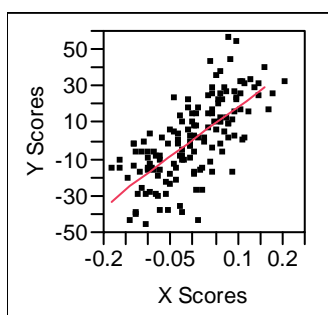


Figure 3-5. PLS Scores Plot for Mandible by Skull

Table 3-14 shows the percent of variation (28.95%) in the mandible explained by the skull in the Fortext dataset. The cross-validation (not illustrated) in PLS selected multiple factors affecting morphology, rather than the one or possibly two expected in an integrated structure. The PLS here supports the results from the Flury hierarchy (Table 3-11) in showing a relatively low explanatory value for the neurocranium on the face and thus there is little significant shared modular structure between the skull and the face or the mandible. In summation these results show the mandible and cranium and face and neurocranium are not integrated structures.

Table 3-14. Partial Least Squares – Percent Variation in the Mandible Explained by the Skull

No.	X	X-Plot	Cumulative X	Y	Y-Plot	Cumulative Y
1	45.63	<div><div style="width: 45.63%;"></div></div>	45.63	20.89	<div><div style="width: 20.89%;"></div></div>	20.89
2	17.84	<div><div style="width: 17.84%;"></div></div>	63.47	4.093	<div><div style="width: 4.093%;"></div></div>	24.98
3	14.56	<div><div style="width: 14.56%;"></div></div>	78.04	2.393	<div><div style="width: 2.393%;"></div></div>	27.37
4	10.02	<div><div style="width: 10.02%;"></div></div>	88.06	0.944	<div><div style="width: 0.944%;"></div></div>	28.32
5	5.338	<div><div style="width: 5.338%;"></div></div>	93.39	0.498	<div><div style="width: 0.498%;"></div></div>	28.81
6	6.606	<div><div style="width: 6.606%;"></div></div>	100	0.136	<div><div style="width: 0.136%;"></div></div>	28.95

Tables 3-15 and 3-16 present results from multiple analyses of the Flury hierarchy in tabular form. The same general pattern is observed across the Howells data as for the Hanihara data (and for the Fortext data, though not presented here). The cranial regions

of mandible, skull, base, and face do not achieve proportionality when compared to each other. This result is expected of modular structures; if the matrices are proportional they are integrated within themselves and fail the criterion of intra-modular rather than inter-modular integration.

The same pattern is observed when partitions such as the face plus base or skull plus mandible (and so forth) are tested across sex or population: no proportionality. However, at the level of individual regions of the skull—mandible, face, base, neurocranium—invariance to allometric and/or populational axes emerges. ***This is in the face and base, not the neurocranial skull or mandible.*** This result is further evidence for internal trajectories in population and sex that are resistant or invariant across these axes and thus may highly influence phylogenetic analyses.

Table 3-15. Flury Hierarchy – Howells Dataset

Sample	# Measurements	N	C's α	Population	Sex	Flury across Sex CPC	Across Pop CPC
How.Whole Skull21 S/F/B	21	2461	N/A	All	Mixed	NS ¹	NS
How.Skull7 / Face7	14	2461	N/A	All	Mixed	NS ¹	NS
How.Skull7 / Base7	14	2461	N/A	All	Mixed	NS ¹	NS
How.Base7 / Face7	14	2461	N/A	All	Mixed	NS ¹	NS
HowSkull7	7	2461	0.5543	Global	Mixed	2PC	2PC
HowFace7	7	2461	0.776	Global	Mixed	PROP ²	PROP
HowBase7	7	2461	0.762	Global	Mixed	PROP	PROP
Whole Skull in Circumpolars / Skull in Global	21	115/2346	N/A	Circumpolar / Global	Mixed	NS ¹	NS
Face in Circumpolars / Face in Global	7	115/2346	N/A	Circumpolar / Global	Mixed	NS ¹	CPC
"Skull" ⁴ in Circumpolars / Skull in Global	7	115/2346	N/A	Circumpolar / Global	Mixed	NS ¹	NS
Base in Circumpolars / Base in Global	7	115/2346	N/A	Circumpolar / Global	Mixed	NS ¹	CPC
Whole Skull21 S/F/B across Sex	21(20)	2461	N/A	Global	Males vs Females	PROP	PROP

¹ NS means no structural similarity, that the matrices are completely unrelated.

² PROP denotes integrated pattern (different only on size—see discussion).

³ See Table 3-16 for comparisons with complete data.

⁴ Neurocranium, 7 measurements.

⁵ See Table 3-16 for comparisons with complete data.

Table 3-16. Flury Hierarchy – Complete Set Hanihara’s Data

Sample	# Measurements	N	C's α	Population	Sex	Flury Within	Flury Across Sex CPC	Across Pop CPC
HA. Whole Skull 21 S/F/M	21(20)	115	/	Asian	Male	N/A	NS	NS
Skull7 / Face7	7	115	/	Asian	Male	NS	/	/
Skull7 / Mandible6	6	115	/	Asian	Male	NS	/	/
Mandible7 / Face7	7	115	/	Asian	Male	NS	/	/
HanSkull7	7	115	0.513	Asian	Male	/	2 PC	2 PC
HanFace7	7	115	0.795	Asian	Male	/	PROP	PROP
HanBase7	7	115	0.726	Asian	Male	/	PROP	PROP
HanSkull7+ Hanface7	14	115	/	Asian	Male	NS	/	/
HanSkull7+ HanMandible6	13	115	/	Asian	Male	NS	/	/
HanFace7+ HanMandible6	13	115	/	Asian	Male	NS	/	/

These results follow the expected pattern for modularity. Combinations of two regions of the skull across populations and sex always show matrix dissimilarity using the Flury hierarchy. These results are reflected in the Cronbach’s Alpha where obtained. The Flury hierarchy results show also that the cranial base and face maintain structural relationships across sex and population, within all test sets. Males and females within test sets maintain proportionality of the matrices.

H₀2: No mandibular and/or cranial multivariate or morphometric male/female differences exist across sex.

In Test 1, H₀2 is rejected.

Using the Fortext dataset, Figure 3-6 shows males are more variable in the whole skull using 12 measurements of skull and mandible (6 and 6). The hypothesis is rejected at <0.0001 . Figure 3-7 shows the skull across sex in the Howells dataset (size-corrected) is demonstrably different, $p < <0.00011$.

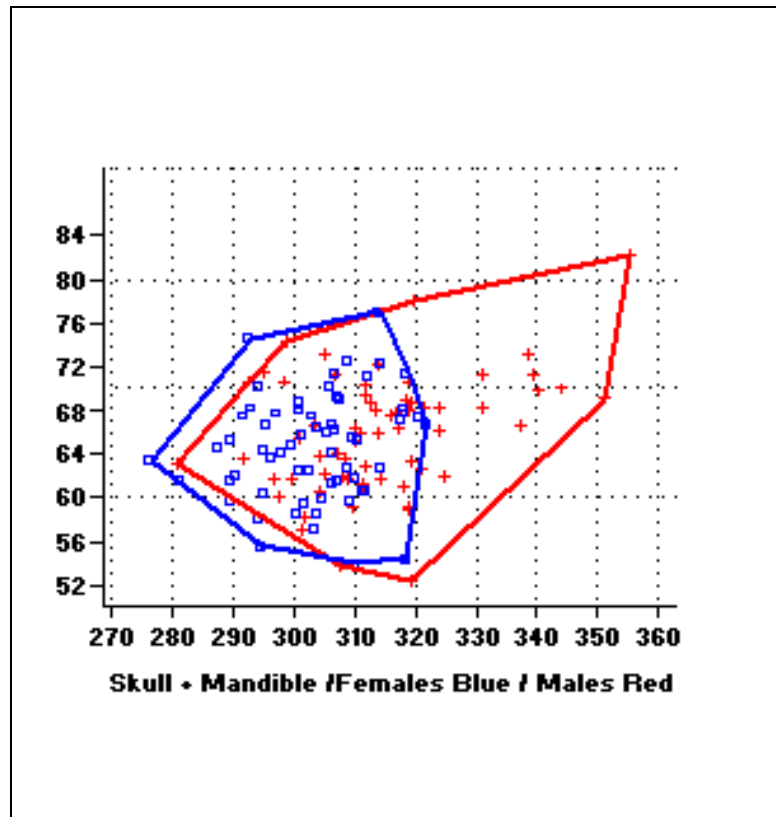


Figure 3-6. Fortext Male/Female

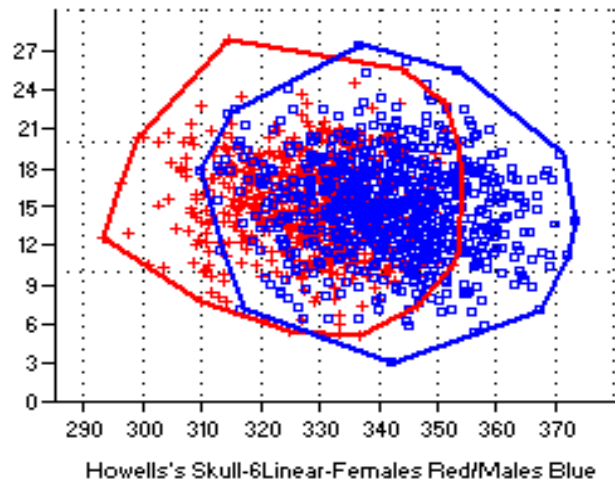


Figure 3-7. Howells Male/Female

Table 3-17 shows the Flury hierarchy results for the whole skull in the Howells dataset, males and females, all 21 measurements of the neurocranium, face, and base combined.

Table 3-17. Flury Hierarchy for Whole Skull, Males versus Females Howells Dataset

Model						
Higher	Lower	Chi Sqr	df	p-val	CS/df	AIC
Equality	Proport	24.355	1	<0.0001	24.355	78.396
Proport	CPC	13.987	6	0.0298	2.331	56.041
CPC	CPC(5)	0.762	1	0.3828	0.762	54.054
CPC(5)	CPC(4)	11.000	2	0.0041	5.500	55.292
CPC(4)	CPC(3)	3.692	3	0.2967	1.231	48.292
CPC(3)	CPC(2)	11.738	4	0.0194	2.934	50.600
CPC(2)	CPC(1)	3.251	5	0.6613	0.650	46.863
CPC(1)	Unrelated	9.611	6	0.1420	1.602	53.611
Unrelated	—					56.000

Here results show a range of between three and one CPCs shared, nowhere near approximating proportionality of modular structure, AIC= 48.292 or 46.863. The results in Table 3-17 are expected. While not proving the regions of the neurocranium, basicranium, and face are modules, Table 3-17 shows that the pattern of all three regions together (forming the skull) is very different for males as compared with females. This result would be expected in both sex and population, as whole skulls are easily discriminated along population and sex in large samples.

Results from Multivariate Analysis – Howells's Data

Figures 3-8 and 3-9 show Howells's data are bimodal for the skull, supporting results obtained from the Flury Hierarchy above.

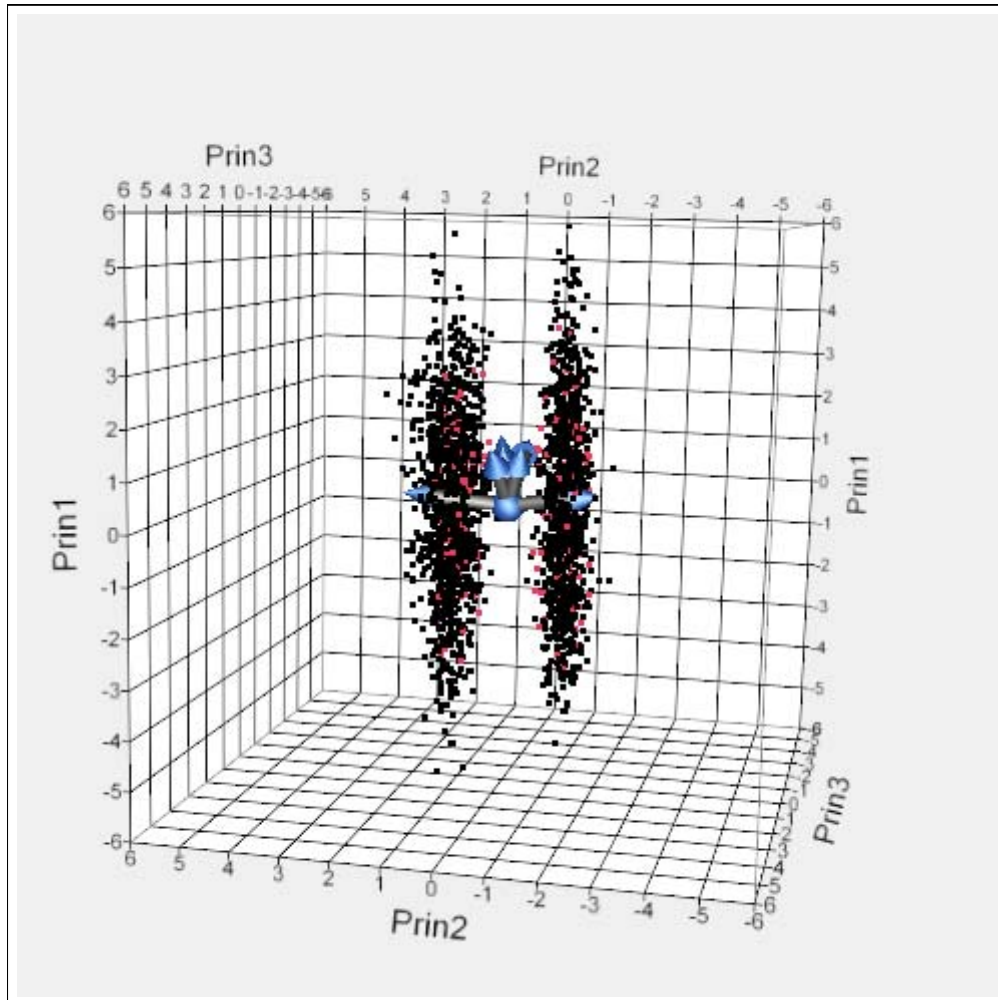


Figure 3-8. Bimodal Distribution of 3D Points in Males versus Females for the Howells Dataset. First three principal components are shown (80% of total variation).

Figure 3-9 shows there are few outliers in the Howells dataset (for the skull, <1%).

These results suggest the variables used are defining morphological male-female differences adequately.

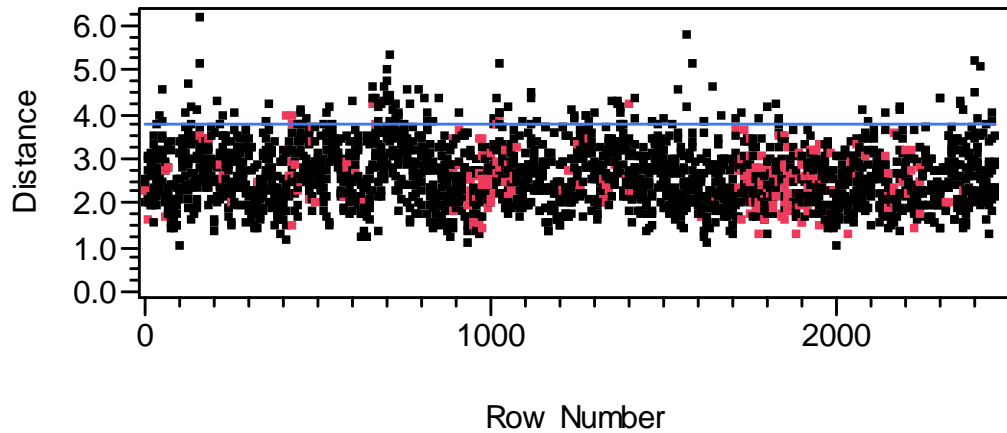


Figure 3-9. Analysis (Mahalanobis Distances) Shows Few Outliers, Suggesting Model Is Well Specified. This result supports the bimodality visible in Figure 3-7.

In contrast to the neurocranium, Figure 3-10 shows the integrated (non-bimodal) distribution of 3D points of the face (length-width-height; seven points) within males and females in the Howells dataset (combined $n = 2461$). Table 3-18 illustrates the results from Figure 3-10 and the tabular information in Tables 3-15 and 3-16.

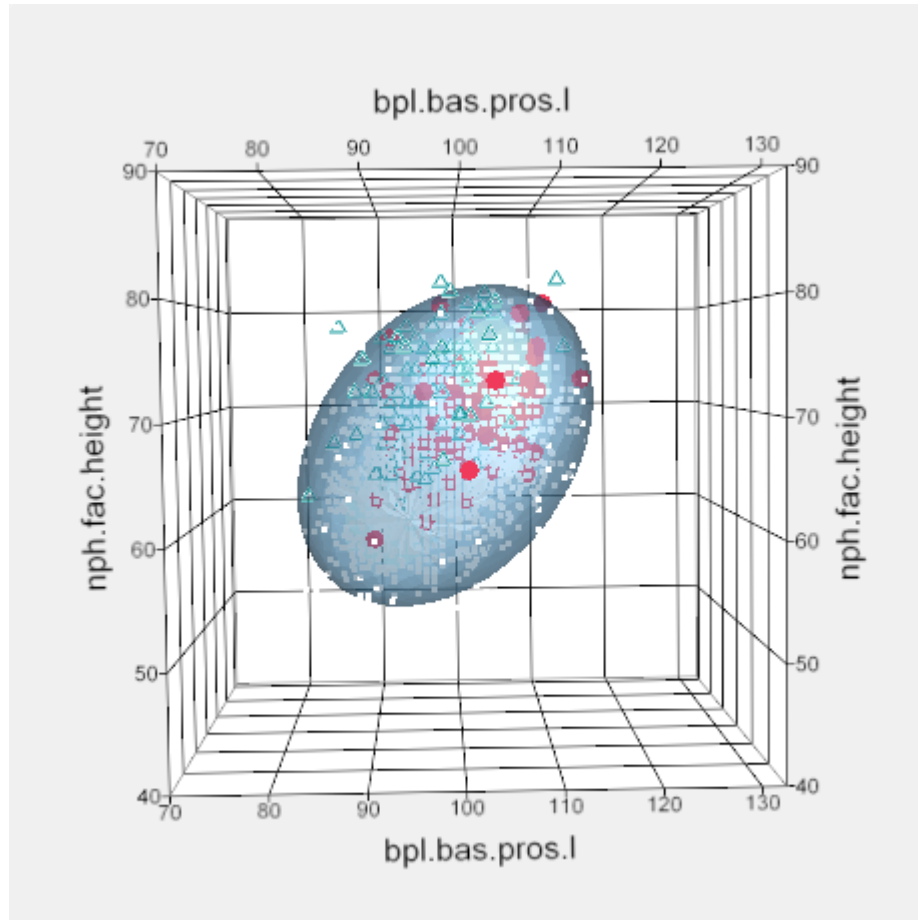


Figure 3-10. Three-Dimensional Plot of the Face Using the Howells Data

Table 3-18. Flury Decomposition of Chi Square (Step-Up and Model Building Approaches)
Howells Data, Cranial Base, 7 Measurements

Model						
Higher	Lower	Chi Sqr	Df	p-val	CS/df	AIC
Equality	Proport	92.040	50	<0.0001	3.682	1133.774
Proport	CPC	263.172	150	<0.0001	1.754	1091.734
CPC	CPC(5)	28.897	25	0.2682	1.156	1128.563
CPC(5)	CPC(4)	93.769	50	0.0002	1.875	1149.666
CPC(4)	CPC(3)	89.203	75	0.1256	1.189	1155.897
CPC(3)	CPC(2)	137.664	100	0.0075	1.377	1216.693
CPC(2)	CPC(1)	175.228	125	0.0020	1.402	1279.029
CPC(1)	Unrelated	253.801	150	<0.0001	1.692	1353.801
Unrelated	—					1400.000

The summation of Figure 3-10 and Table 3-18 suggests that across global samples the whole skull varies across males and females and population. However within the skull there are regions (such as the face illustrated here) which remain remarkably stable across these axes. Within Hanihara's data the pattern is the same—no two macromodular regions achieve matrix proportionality when comparing the two, suggesting modularity is not across any two regions together but only within individual regions. And, when compared to Howells's face and base, Hanihara's facial and base modules *individually* are proportional. This result indicates invariance of these regions to sex and population.

H₀3: No mandibular and/or cranial multivariate or morphometric modular craniomandibular population differences exist across samples from circumpolar populations.

This hypothesis is examined below, first through PCA, then discriminant function, finally through the Flury hierarchy.

Principal Component Analysis (PCA)

Figures 3-11, 3-12, and 3-13 show the results from the PCAs of global samples using Morphologika 2.5. The analyses are single-vector decomposition, which removes all size (including the size component remaining after procrustes superimposition; see Appendix C). In the plots the black diamonds show results for circumpolar populations. Tables 3-19, 3-20, and 3-21 show the eigenvalues for the principal components composing up to 80% of the variation.

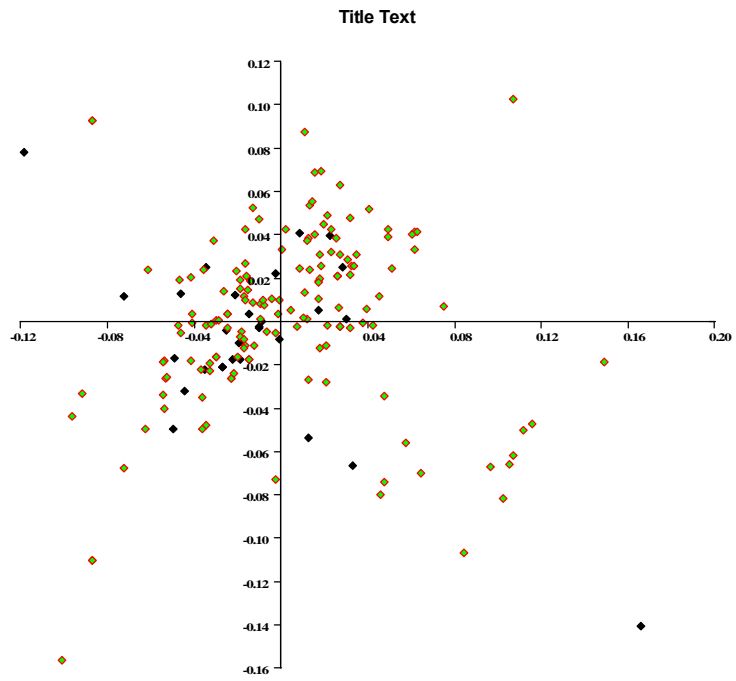


Figure 3-11. Results for Cranial Base (14 measures). Black diamonds are circumpolar samples.

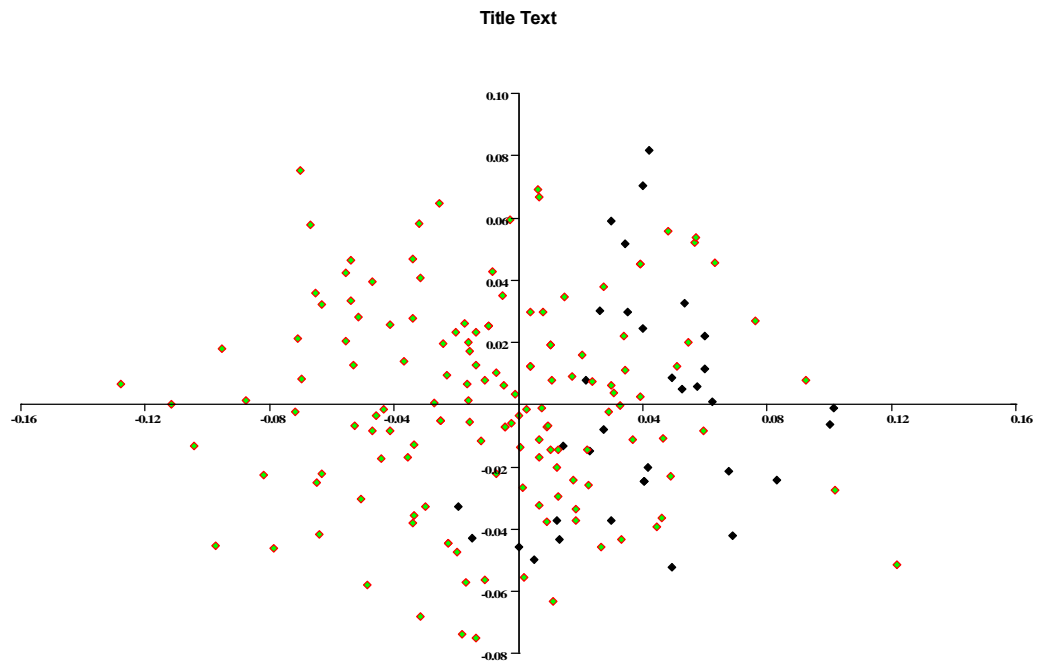


Figure 3-12. Results for Face (14 measures). Black diamonds are circumpolar samples.

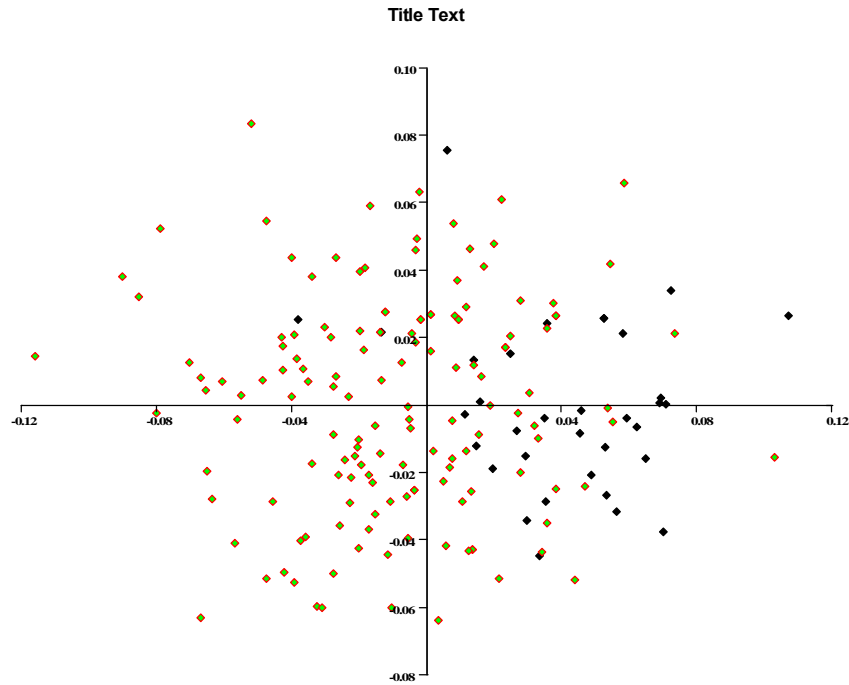


Figure 3-13. Results for Mandible (14 measures). Black diamonds are circumpolar samples. This figure shows that mandibular integration approximates that of the base and face, but the circumpolar group more tightly together.

Table 3-19. PC Eigenvalues for Cranial Base

Principal Component	Eigenvalue	Percent (%)	Cumulative Percent (%)
PC 1	0.002103	16.83972	16.83972
PC 2	0.001646	13.18395	30.02367
PC 3	0.00131	10.48695	40.51062
PC 4	0.001012	8.105903	48.61653
PC 5	0.000759	6.07876	54.69529
PC 6	0.000695	5.562744	60.25803
PC 7	0.000597	4.779552	65.03758
PC 8	0.000495	3.964628	69.00221
PC 9	0.000404	3.237592	72.2398
PC 10	0.000367	2.938723	75.17853
PC 11	0.000346	2.770166	77.94869
PC 12	0.000312	2.502292	80.45098

Table 3-20. PC Eigenvalues for Face

Principal Component	Eigenvalue	Percent (%)	Cumulative Percent (%)
PC 1	0.001994	36.50947	36.50947
PC 2	0.001087	19.89802	56.40748
PC 3	0.000789	14.45031	70.85779
PC 4	0.000465	8.517634	79.37543
PC 5	0.000401	7.350813	86.72624
PC 6	0.000254	4.649654	91.37589

Table 3-21. PC Eigenvalues for Mandible

Principal Component	Eigenvalue	Percent (%)	Cumulative Percent (%)
PC 1	0.001513	22.06238	22.06238
PC 2	0.000943	13.75039	35.81276
PC 3	0.000563	8.20804	44.0208
PC 4	0.00049	7.150076	51.17088
PC 5	0.000439	6.397389	57.56827
PC 6	0.000365	5.323624	62.89189
PC 7	0.000331	4.833545	67.72544
PC 8	0.000262	3.824679	71.55012
PC 9	0.000228	3.324341	74.87446
PC 10	0.000183	2.667585	77.54204
PC 11	0.000164	2.394656	79.9367
PC 12	0.000153	2.229978	82.16667
PC 13	0.000139	2.024806	84.19148
PC 14	0.000113	1.651043	85.84252
PC 15	0.000106	1.551501	87.39402
PC 16	9.91E-05	1.444321	88.83834
PC 17	8.4E-05	1.225039	90.06338

The plots and PCA eigenvalues suggest rough similarity for the face and mandible in loadings on the axes and scatter of the circumpolar individuals. The high loading on PC1 and the positioning of the circumpolar individuals suggest that particularly the face (35%) and the mandible (22%) are responding to high biomechanical force on PC1. This is most likely the factor being represented in the high loading of the mandible and face together on the (canonical correlation) PC1 axis in Table 3-22. Figure 3-14 shows the regression of PC1 and centroid size; there is no significant contribution of size to PC1, indicating a factor beyond size is being sampled ($p = 0.9751$). PC1 in the cranial base is much less explanatory than in the other macromodules (16%), possibly indicating the cranial base is not responding to biomechanical effects, as indicated by the broader scatter of circumpolar individuals in the plot (Figure 3-13 and Table 3-19, above).

Table 3-22. Face and Mandible Responding Together to High Biomechanical Force on PC1

Eigenvalue	Percent (%)	Cumulative Percent (%)	Canonical Correlation
3.0536386	54.3582	54.3582	0.86793321
1.65714284	29.4990	83.8572	0.78971888
0.57686344	10.2688	94.1260	0.60483855
0.32997752	5.8740	10<0.0001	0.498104
3.9453e-16	<0.0001	10<0.0001	0
1.8254e-16	<0.0001	10<0.0001	0
7.3567e-17	<0.0001	10<0.0001	0

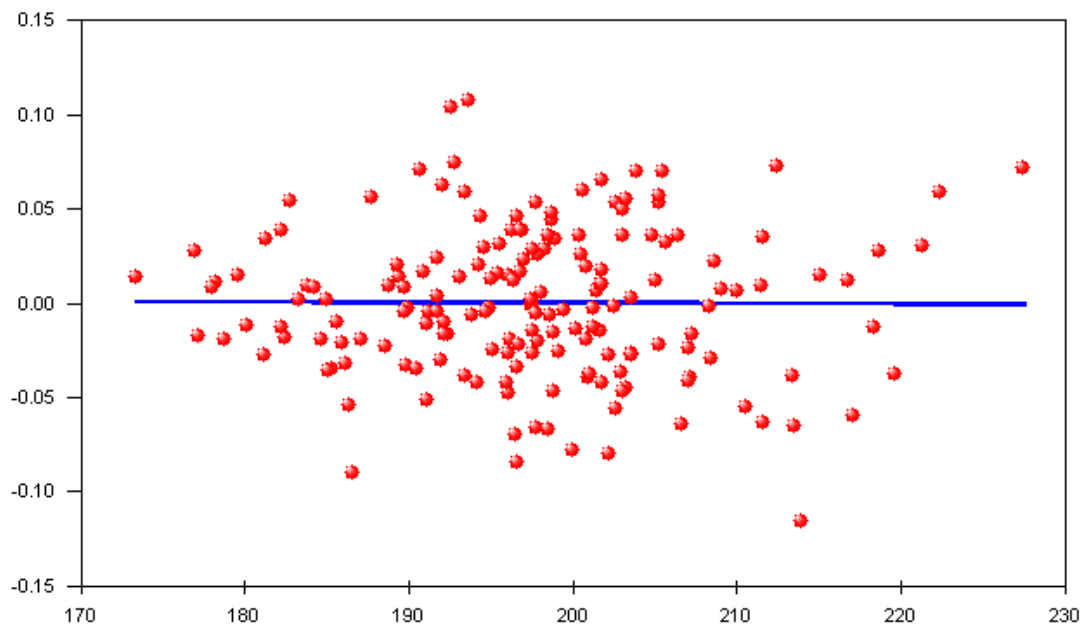


Figure 3-14. Single Variable Decomposition (SVD), Regression of PC1 and Centroid Size Showing No Significant Contribution of Size to PC1

Discriminant Analysis

The discriminant analysis presented below in Table 3-23 and Figures 3-15 and 3-16 (as well as Figure 3-17 in the next section) show circumpolar populations are consistent outliers to other populations in the skull and mandible. This is a graphic demonstration of the distinctive circumpolar morphology, which while no more distinguishable than the Australian skulls and mandibles from others overall, shows why the highly biomechanically loaded skull in these populations has been considered unique in the past.

Across the global samples the face and base remain stable across sex and population. It is only in the comparison of the individual regions to the rest of the global samples for each region of the skull that the differences emerge. Table 3-23 shows the

misclassification of circumpolar (GRE, Greenland Circumpolar, Fortext, cranium and mandible) morphology is very low, given the distinctive pattern encountered there.

Table 3-23. Counts for Group Membership for Actual Rows by Predicted Columns from Discriminant Function

	Aus	GRE	Lap	Nor	Uga
Aus	23	0	0	0	0
GRE	0	22	0	2	0
Lap	0	1	20	2	2
Nor	0	3	5	35	5
Uga	1	1	0	3	19

The plots below in Figures 3-15 and 3-16 show the difference of the circumpolar populations from others. The discriminant function is used here to describe the differences in the proposed modular regions in the circumpolar versus other populations only to underscore the fact that all other populations have similar structure in the matrices when compared (stability in the face and base and lack of stability in the neurocranium and mandible).

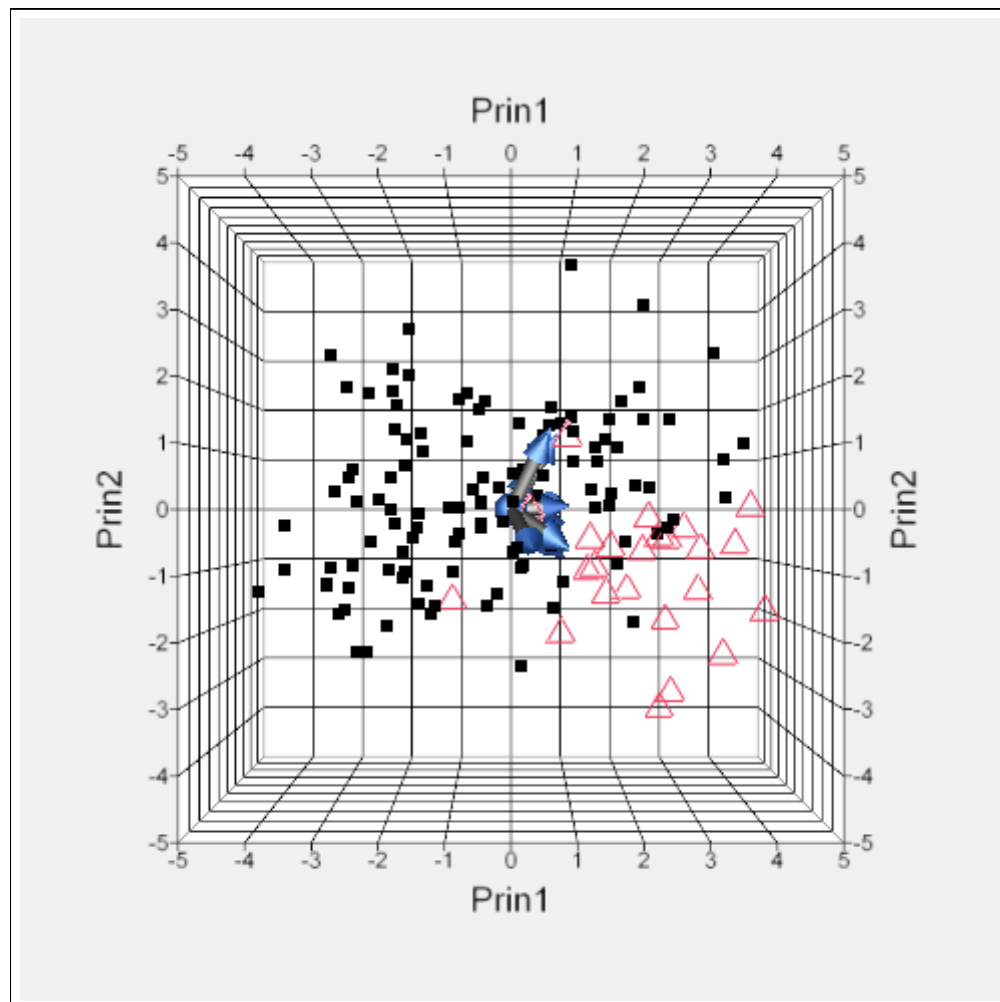


Figure 3-15. Face, 3D Scatterplot. Triangles are circumpolar populations.

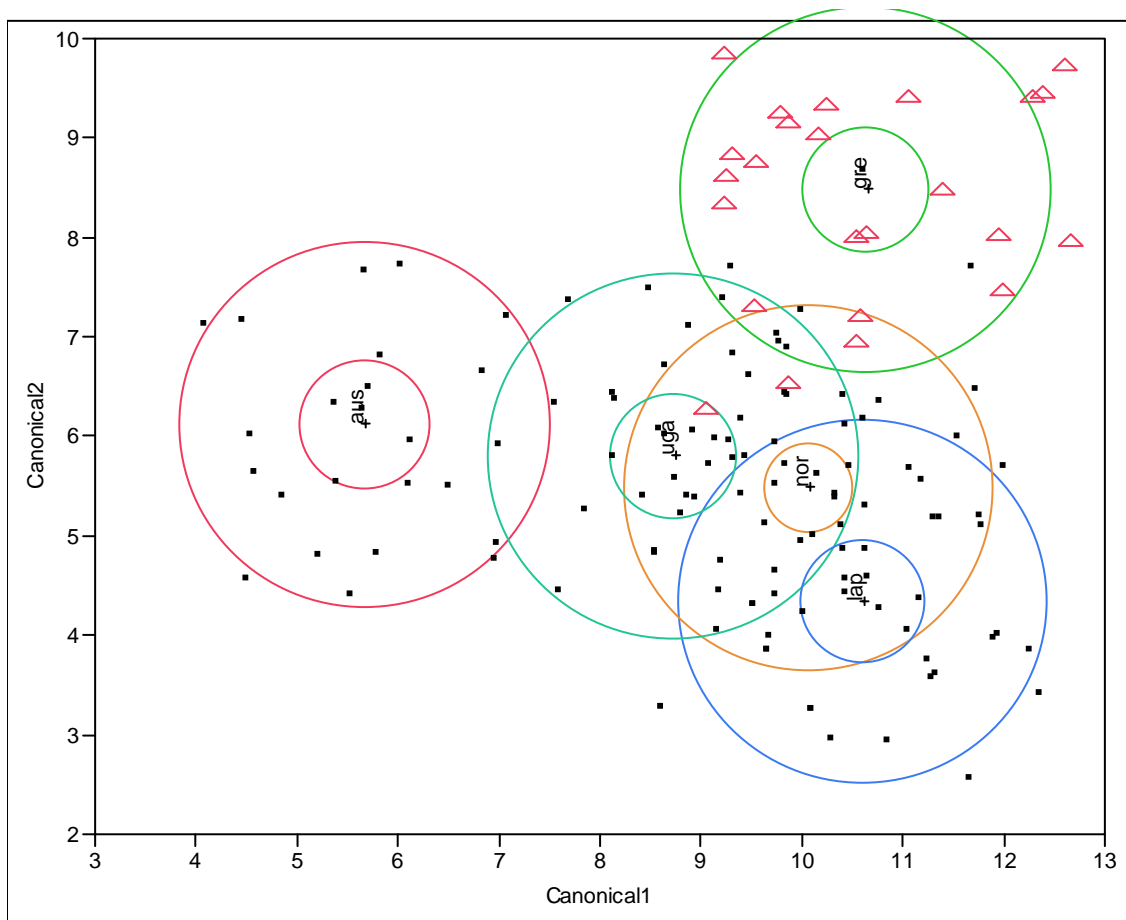


Figure 3-16. Skull, Canonical Plot Using Linear Discriminant Method (GRE=Circumpolar)

Discriminant Analysis Mandible 6 Measurements

In support of Harvati and Weaver (2006), Figure 3-17 shows the mandible in circumpolar populations is even more distinct than the skull, and that also there is a highly explanatory factor driving the PCA. Similarly to the face illustrated above, this result is hypothesized here as the result of biomechanical force.

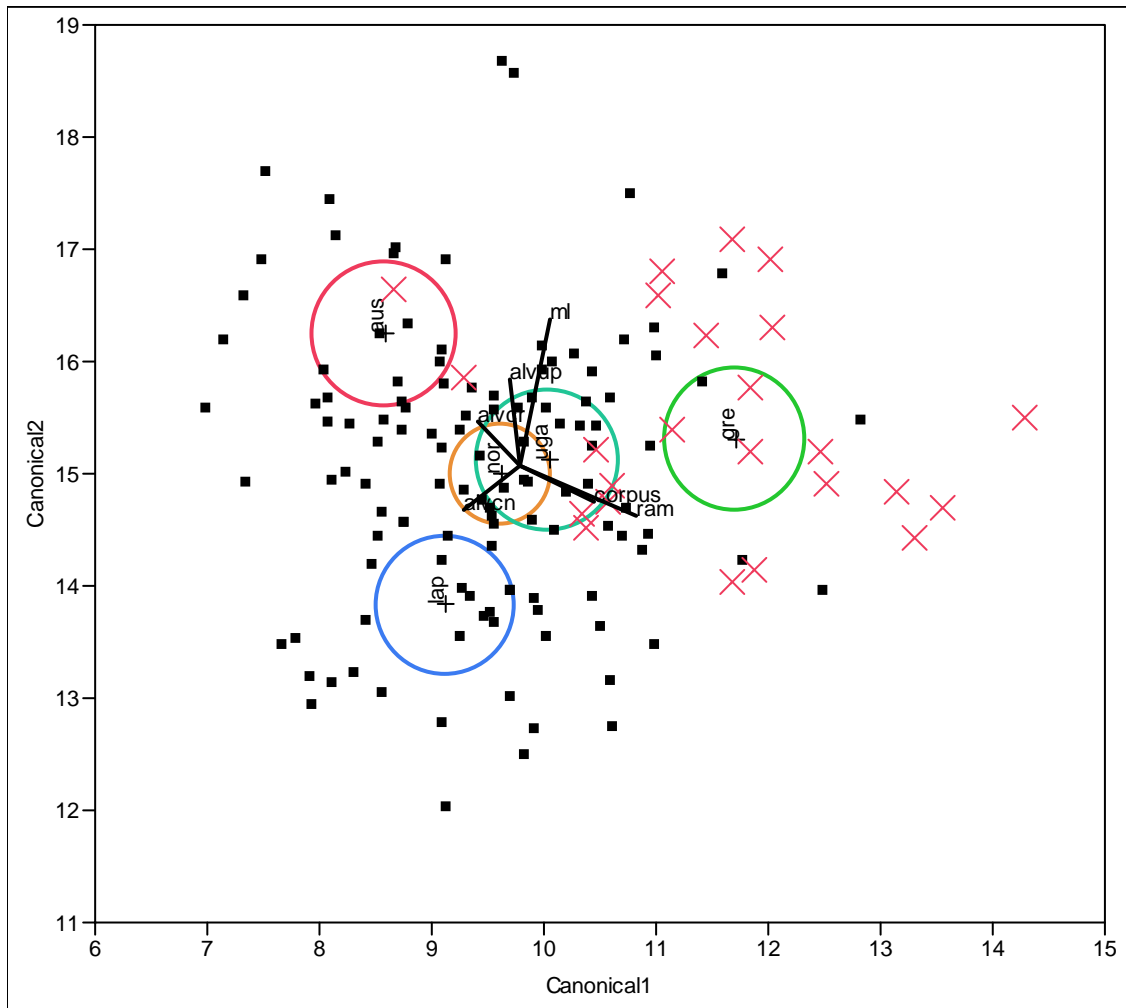


Figure 3-17. Mandible, Canonical Plot Discriminant Analysis Linear Method

Flury Hierarchy, Circumpolar

Similarities in matrix structure hypothesized as the signal of modularity found in the other global populations from Howells, Fortext, and Hanihara are less pronounced in the circumpolar individuals. Here the face does not achieve proportionality in all circumpolar populations. Using Howells's data, we see that in circumpolars there are differences in the face, base, and neurocranial skull when compared to all other global populations.

However, when data from circumpolar populations is later examined in Chapter 4

with a three-dimensional morphometric analysis, the face does achieve

proportionality. It may be that more complex three-dimensional analysis is describing morphology more fully than the seven points for each cranial region here. Circumpolars are different compared to other populations (see Tables 3-19 through 3-22). The differences are less when the whole skull (all measurements) is compared across populations since we can see there are several principal components in common. Tables 3-24 through 3-27 underscore the fact that circumpolar populations generally follow the pattern in the Flury hierarchy seen in other global populations. However, an exception is that the face, probably through the influence of biomechanics, does not achieve the proportionality of the face in other global samples. As was suggested in the PCA analyses above, the cranial base is more similar to that found in the other global samples; near proportionality is shown (Table 3-23). Unlike all other comparisons using all other samples in the neurocranium alone AND in the face alone, however, there is nonstructural similarity of the PCs—non- related structure. Broadly this result shows the variability of the skull is in the face and neurocranium, again probably as the result of biomechanics in the most highly loaded modern human population.

Table 3-24. Whole Skull, Flury Decomposition of Chi Square (Step-Up and Model Building Approaches) for Circumpolars

Model						
Higher	Lower	Chi Sqr	df	p-val	CS/df	AIC
Equality	Proport	16.812	1	<0.0001	16.812	662.128
Proport	CPC	308.888	18	<0.0001	17.160	647.317
CPC	CPC(17)	0.439	1	0.5075	0.439	374.428
CPC(17)	CPC(16)	7.350	2	0.0254	3.675	375.989
CPC(16)	CPC(15)	1.134	3	0.7689	0.378	372.639
CPC(15)	CPC(14)	6.002	4	0.1990	1.500	377.505
CPC(14)	CPC(13)	7.574	5	0.1813	1.515	379.503
CPC(13)	CPC(12)	11.621	6	0.0710	1.937	381.929
CPC(12)	CPC(11)	10.183	7	0.1785	1.455	382.308
CPC(11)	CPC(10)	8.997	8	0.3426	1.125	386.126
CPC(10)	CPC(9)	16.813	9	0.0517	1.868	393.129
CPC(9)	CPC(8)	30.840	10	0.0006	3.084	394.316
CPC(8)	CPC(7)	15.908	11	0.1446	1.446	383.477
CPC(7)	CPC(6)	30.409	12	0.0024	2.534	389.568
CPC(6)	CPC(5)	14.542	13	0.3368	1.119	383.159
CPC(5)	CPC(4)	25.824	14	0.0273	1.845	394.617
CPC(4)	CPC(3)	24.505	15	0.0570	1.634	396.793
CPC(3)	CPC(2)	37.915	16	0.0016	2.370	402.288
CPC(2)	CPC(1)	53.071	17	<0.0001	3.122	396.373
CPC(1)	Unrelated	33.302	18	0.0153	1.850	377.302
Unrelated	—					380.000

Table 3-25. Cranial Base Only, Flury Decomposition of Chi Square (Step-Up and Model Building Approaches) for Circumpolars

Model						
Higher	Lower	Chi Sqr	df	p-val	CS/df	AIC
Equality	Proport	27.600	1	<0.0001	27.600	78.403
Proport	CPC	23.385	6	0.0007	3.897	52.803
CPC	CPC(5)	4.369	1	0.0366	4.369	41.418
CPC(5)	CPC(4)	0.881	2	0.6438	0.440	39.049
CPC(4)	CPC(3)	1.131	3	0.7695	0.377	42.169
CPC(3)	CPC(2)	7.057	4	0.1329	1.764	47.037
CPC(2)	CPC(1)	3.195	5	0.6699	0.639	47.980
CPC(1)	Unrelated	10.784	6	0.0953	1.797	54.784
Unrelated	—					56.000

Table 3-26. Neurocranium, Flury Decomposition of Chi Square (Step-Up and Model Building Approaches) for Circumpolars

Model						
Higher	Lower	Chi Sqr	df	p-val	CS/df	AIC
Equality	Proport	68.118	1	<0.0001	68.118	402.640
Proport	CPC	291.229	6	<0.0001	48.538	336.521
CPC	CPC(5)	0.905	1	0.3414	0.905	57.292
CPC(5)	CPC(4)	1.005	2	0.6049	0.503	58.387
CPC(4)	CPC(3)	3.643	3	0.3027	1.214	61.381
CPC(3)	CPC(2)	14.798	4	0.0051	3.699	63.739
CPC(2)	CPC(1)	13.247	5	0.0212	2.649	56.941
CPC(1)	Unrelated	9.694	6	0.1381	1.616	53.694
Unrelated	—					56.000

Table 3-27. Face Only, Flury Decomposition of Chi Square (Step-Up and Model Building Approaches) for Circumpolars

Model						
Higher	Lower	Chi Sqr	df	p-val	CS/df	AIC
Equality	Proport	5.364	1	0.0206	5.364	96.270
Proport	CPC	25.706	6	0.0003	4.284	92.906
CPC	CPC(5)	3.588	1	0.0582	3.588	79.201
CPC(5)	CPC(4)	1.286	2	0.5256	0.643	77.613
CPC(4)	CPC(3)	4.307	3	0.2302	1.436	80.327
CPC(3)	CPC(2)	19.071	4	0.0008	4.768	82.019
CPC(2)	CPC(1)	17.314	5	0.0039	3.463	70.948
CPC(1)	Unrelated	19.634	6	0.0032	3.272	63.634
Unrelated	—					56.000

Discussion

The complexity of the relationship of the macromodules of the skull was addressed above in a series of hypotheses. Complexity was partitioned by examining model-free hypotheses, which looked at the statistical relationship of cranial modules and did not attempt functional explanation. The summary of the results from four primary datasets

(the Howells dataset, the Hanihara dataset, the Fortext dataset, and the Morphometric dataset) and four major analytical techniques (Cronbach's Alpha, Canonical Variate Analysis, PLS analysis, and Flury hierarchy) is as follows:

1. No comparison across all datasets showed the highest level of integration *across* all macromodular partitions of the skull at once. That is, no combination of all three regional, or any two macromodular regions in combination, ever showed proportionality of covariance matrix structure. If this had been the case, modularity for those regions would have been rejected by the currently used standard definitions of modularity (through internal integration). For example, if it had been demonstrated there was proportionality of matrices across the neurocranium, basicranium, and face in Howells's data, the conclusion would have been that the skull is primarily integrated rather than modular. This first test necessarily preceded the following tests.
2. Analysis showed that the mandible, while probably not a module, nevertheless does not integrate with either the basicranium or the face in matrix structure. This non-proportionality would of course, be expected of a true module, but variability across sex and population in all datasets used here suggests the mandible is probably composed of two modules (examined under functional hypotheses in the next chapter, Chapter 4).
3. Results generally follow predictions of parts of the skull as exhibiting similar levels of integration. PC1 scores for the three regions from Morphologika are as

follows: base = 0.168; face = 0.365; mandible = 0.220. These results suggest broadly similar levels of explanation of morphology by PC1. These results also suggest general correspondence to results from levels of heritability and levels of (genetic) variation in the regions of neurocranium, basicranium, and face as suggested by Martínez-Abadías and colleagues (2009). However, this dissertation's results differ from results in the study by Martínez-Abadías et al. (2009) by suggesting there is little or no contribution of explanation by sexual dimorphism or population for the face or cranial base. Broadly the results here suggest the face is the most integrated, followed by the mandible, and then the cranial base. This conclusion may be a representation of biomechanical function, which is tested in Chapter 4.

4. Results here reinforce prior results suggesting matrix identity, when found, is a function of small sample sizes (Marroig and Cheverud, 2000). That is to say, according to the literature, differences in covariance matrices are to be expected in most cases; any fully identical matrices result from small samples, not biological identity. While true in the most extreme sense as detailed earlier, this observation is an oversimplification. *Large* sample-size matrices which are “equal” (exhibiting equality) are unexpected; however large sample matrices which are proportional, and hence differing in an (allometric) scaling factor are not necessarily so. The patterning of matrix similarity (proportion) in the Howells data using the Flury hierarchy is not found randomly in small samples. It is found as predicted by patterns of modularity: similar modules across sex and population have similar structure—which remains invariant across these axes. As is detailed in the next

chapter, cranial relationships of modules can best be described as belonging to a class of invariant organizations in the skull, and this property can be used for robust definitions of modularity.

5. Across the world the skull varies more in width than in length. In the Howells dataset Cronbach's Alpha goes up in both males and females when width is excluded. Other comparisons show cranial widths as the most highly correlated dimension, and all results here correspond to those from Martínez-Abadías and colleagues (2009) showing width as the driving dimension in cranial variation. As is shown in Chapter 5, this practice makes analyses of three dimensional skulls by two-dimensional models problematic.
6. Circumpolar populations are outliers in the above analyses. When matrices derived from these populations in the Howells data are compared to the matrices of non-circumpolar populations, the matrices are not proportional. There is relationship at the level of several shared PCAs in the skull (neurocranium; see data above), but not proportion. The patterning of the differences is stronger in the face. This finding may be an artifact of using seven linear measurements as a proxy for three-dimensionality (a hypothesis tested in Chapter 4). It may be that in some populations the functional modular relationships that hold stable across all other global comparisons break down if the level of force through the masticatory apparatus is sufficient—after all these populations are unique in masticatory loading. Circumpolar populations with extremely high biomechanical loading were shown to be a possible exception to the pattern found in all other populations. In some arctic populations the face, and less so the base, does not remain stable in

population or sexually dimorphic comparisons. These results basically mirror those found in recent work by Babb and others (2010) suggesting a significant relationship of robusticity with hard-to-process diets. Their work suggests robusticity is primarily correlated with shape, is not inherited, and can be influenced by high masticatory loading. Earlier it was suggested attributes of robusticity suggest it is the primary way shape can accommodate higher levels of force (function): robusticity maximizes the way a shape is maintained, with an allometric increase rather than reorganization. Interestingly, Babb et al. (2010) showed that other populations outside the circumpolar region with even more demanding diets can have lower degrees of robusticity, so robusticity is not necessarily related to force only. It is the hypothesis being tested herein that the unique aspect of shape in circumpolar skulls does not directly result from robusticity—that skulls usually tend to become more robust without changing shape, and that change in shape emerges when functional response cannot further increase. If this hypothesis is correct, then populations (such as the circumpolar populations) who further increase loading—i.e., further anterior dental loading through chewing hide—in a skull already fully responding to tough diet will change shape. In this case function provides the basic organizational pattern of modules in all human groups, but sufficient cultural response can swamp the signal of modularity. In the next chapter the predictability of the morphology of the skull by various factors is explored, and it is shown that circumpolar populations are actually more integrated in the skull than other populations, probably as a result of skull-wide response to loading.

7. This analysis supports Polanski and Franciscus (2006) in finding the face and neurocranium are different modules. However, the analysis presented above supports the face as being more integrated in modern humans, contra Polanski and Franciscus. This dissertation's analysis also differs from Bookstein, in finding the integration is not primarily in the vault and face. Bookstein et al. (2003) found warp scores were highest for the vault and face. He also found lower correlations for the vault and cranial base ($r < 0.68$) and the face and cranial base. Results here for the Howells data suggest that the base and face are integrated areas. Results further suggest that the base and face together are more integrated than the neurocranium and the face together (see Canonical Vector Analysis [CVA] scores in Appendices). This contradiction probably results from the analysis in Bookstein et al. (2003) being carried out in two dimensions and this dissertation's analysis, in three. Absent that, the face and skull differ. This analysis is different from analyzing just the neurocranium as above here. When the breadth axis is removed, skulls become more similar because the Y-axis is the most variable.

Conclusions

Traditional regions of the skull are not necessarily modules. The splanchnocranial, dermatocranial, basicranial, and mandibular regions all pass the first of three proposed definitions of modules by testable property, being integrated within themselves more than across. The splanchnocranial and basicranial regions past the second test, invariance to sex and population effects on matrix structure. The neurocranium and mandible fail this second test, being more variable across these axes. All regions are tested for the third quantifiable property, definition by function, in Chapter 4.

CHAPTER 4

FUNCTIONAL MODULAR PROPERTIES: TESTING HYPOTHESES OF MODULAR STRUCTURE

This chapter tests the formation of modules of the skull as organized by function. Two of the “macromodular” partitions (the face and base) of the skull analyzed in Chapter 3 have characteristics one would expect of functional modules. In this chapter the attribute of functionality is included as a necessary testable property of modules. Individual functions are ascribed to prospective modular and non-modular regions of the skull. Relationships of function to form are tested using stepwise model building techniques. Testing the statistical inferences drawn from functional modular form thus forms the final of the three tests of modularity by property—integration within modules, invariance, and function.

Modularity is not a traditional or random partitioning of the skull. To this point modular definition by property has generally been carried out by simple quantification of levels of integration within prospective modules, then comparison to other prospective modules (see discussions in Polanski and Franciscus, 2006; Mitteroecker and Bookstein, 2007; Klingenberg et al., 2003; Ackermann, 2005; Wagner et al., 2007; Good, de Montjoye, and Clauset 2009). Localized integration is but one aspect of what a module is; without a defined function a module can encompass any aspect of morphology. Chapter 2 emphasized outlining how modules must be defined by both attribute and property, with the working definition being modules are inherited patterns of integration exhibiting invariance across axes of population and sex. Expected attributes and properties that can

be used to define modules were discussed, including sequential transformation, delineation from other modules, internal integration, and other factors. These factors are used here as control factors for defining modules by function, with the attributes being used to define areas that can be measured to produce modules.

In Chapter 3 the hypothesized modular property of invariance was tested, with mixed results—although the mandible and neurocranium exhibited aspects of modular structure, *in toto* the pattern exhibited by these regions in the skull suggests otherwise. Results in Chapter 4 build on the hierarchy introduced in the model-free hypotheses in Chapter 3. Here model-bound hypotheses of the relation of function to modular formation are tested.

Definition of modules by quantifiable properties is a necessary first step towards a useful biological entity. Previous discussion has shown biological definition must include modules possessing an inherited pattern of relationship, set in the framework of being less randomly organized than non-modular regions. Further extending the definition, it is proposed a definable function is a further necessary condition (see González-José et al. [2005] for background). Modules can thus be described as functional expressions of morphology demonstrating the adage “form represents function.” This dissertation addresses those points in a sequence where “one form becomes another,” as the function of the module changes through time. As new functions emerge, morphology changes. As discussed in earlier chapters such changes probably usually occur at the modular level to prevent the deleterious genome-wide effects in systemic change of integrated systems.

Currently the neurocranium, the basicranium, and the splanchnocranium are implicitly treated as modules in (non-functional) definitions. The difficulty begins with ascribing modularity to any one of these regions, but most particularly to the splanchnocranium (face or viscerocranium), which is capable of being partitioned in many ways: into areas defined by biomechanical functions; into superior and inferior *or* anterior and posterior portions (Bastir and Rosas, 2004; Rosas and Bastir, 2004); into pharyngeal arch derivations (as outlined in Chapter 2); into Enlow's anterior fossa–middle cranial counterpart or architectonic areas (Hans and Enlow, 1996); into mandible and maxilla colloquially.

Some of this uncertainty in defining the facial module derives from prior research which suggested the basicranium as more of a stable region and the face as more of a “plastic” or “evolvable” region (see discussion in Martínez-Abadías et al., 2009). This model basically tracks back to assumed differences related to functional mastication (Vidarsdóttir et al., 2002). This idea was demonstrated to be incorrect; it is actually the face which is the most heritable (stable; 81% of traits; 0.26 mean heritability [Martínez-Abadías et al., 2009]). Interestingly Martínez-Abadías and colleagues found the neurocranium to be the least heritable region of the skull, results which support analysis here showing the neurocranium as a non-module.

Several key questions are posed in this chapter:

1. How can the skull be defined in functional terms? What are robust repeatable definitions of points for each functional module, including the mandible?

2. Do functional modules compose the entirety of the skull? That is, does the skull consist of modules alone, or are there “extra-modular regions”?
3. Are functional modules invariant across sex and population?
4. Can modules be shown as invariant across the axes of sex and population in extreme cases such as circumpolar populations—Eskimos or Aleutian Islanders—when function (particularly biomechanical force) is controlled for?
5. Finally, if modules ARE invariant across sex and population, at what level does population and/or sex become a driving factor in morphology? When some or all modules are combined into macromodules for example?

Functional Definitions

As detailed in Chapter 2 several interconnected factors must be considered as instrumental in driving the evolution of the modern human face: ethmomaxillary expansion, neurocranial reorganization/expansion, and increased flexion of the cranial base for orthograde, masticatory changes (Franciscus and Trinkaus, 1995; Lieberman, Mowbray, and Pearson, 2000; Lieberman, Ross, and Ravosa, 2000), dental reduction (Brace, 1963, 1979, 1991), reduction of craniofacial robusticity (Rak, 1986; Lahr and Wright, 1996), reduction of prognathism (Franciscus and Trinkaus, 1995; Trinkaus, 2003), inferior and anterior rotation of the mandible or facial retraction (Hans and Enlow, 1996; Wolpoff, 2000; Rosas, 2001; González-José et al., 2008). All the above factors affect multiple elements of cranial and mandibular morphology. They are interconnected in effect and probably represent function across several modules at once. Throughout the Pleistocene, then, functional changes are occurring that have been implicitly or explicitly modeled as producing modules of the skull (González-José et al., 2008). But it is difficult

to describe the changes in individual modules, given sample sizes through the Pleistocene and specimen preservation.

The hypothesis here is that cranial morphology represents areas selected for by function, such as respiration (Franciscus and Trinkaus, 1988), which may be combined with areas that may or may not be modules into macromodules. These macromodules might exist above the level directly selected by function, and might include non-functional areas (the macromodules of mandible and neurocranium for example). Alternatively, these areas may be functional but not modules in the sense that modules are internally integrated and pursue independent pathways in ontogeny (Bastir et al., 2006). For instance, as was discussed in Chapter 2, structural organization predicts it is unlikely selection acted directly for cranial base angle; it is a byproduct of selection for expansion of the brain and/or the neurocranium, lengthening cranium, and orthograde (see discussions of cranial base angles in Lieberman, Ross, and Ravosa 2000). The degree of anterior and inferior mandibular rotation is another example being that it is eventually constrained by the position of the larynx and pharynx (Hall, 1999), which in turn is responding to changing requirements for respiration. In development of present morphology, the factor here, anterior rotation, was thus constrained by the selection acting on two modules, the face and the cranial base.

The skull thus results from direct selection and indirectly selected structural organization (or canalization, as discussed in Chapter 2). This structural pattern overall can be considered organization by function coupled with organization by canalization or

epigenetic process. In this view function creates the modules and their overall relationship responds to factors such as respiration, cortical expansion, ecogeographical patterning, and mechanical forces (Rothhammer and Silva, 1990; Franciscus and Long, 1991; Wood and Lieberman, 2001; Franciscus, 2003; Giesen et al., 2003; see also Chapter 2 of this dissertation for more detail). The difficulty then is in showing how a modular skull can respond to extra-modular factors such as these. It is suggested here that responses to whole-body factors such as ecogeographical patterning involve more than one module. This finding might indicate that the variability of modules found in Martínez-Abadías et al. (2009) showing areas of non-heritability within cranial regions is actually measuring response to these (extra-modular) factors.

The modeling of function as the overarching factor in modularity begins with analyzing factors operating across large regions of the skull. Donald Enlow's solution to this problem of modular definition is to suggest that it is the function of occlusion which unites the different regions into complexes which then develop in balance. Under his view it is function that allows modules to form, and also remain discrete yet interconnected. (It is sometimes overlooked that Enlow's model is explicitly functional; much research has ignored this fact and simply tests predictions of architectonic or counterpart balance derived therein [Bastir et al., 2004; Bastir and Rosas, 2005; Martínez-Abadías et al., 2009]). Moreover, Enlow's model is population-specific. Enlow used Angle Class relationships to define mandibular or maxillary retrognathism as generalized tendencies in broad population groupings (Angle Class 2 being maxillary prognathism, Class 3 being mandibular prognathism [Angle, 1887]). Enlow's model

suggests cranial organization at the broadest scale is functional: all developing skulls exhibit the counterpart principle dictated by function, with degrees of prognathy/retrognathy as deviations from the perfectly functional (and idealized) occlusion.

What is most important in Enlow's model is not that it explains dolichocephaly and brachiocephaly as the driving descriptors of skulls from around the world (predictions from this model have been demonstrated as non-explanatory anyway [Martínez-Abadías et al., 2009]), or even that it is secondarily explanatory (Mitteroecker and Bookstein, 2008). The importance of Enlow's original model is that it provides a more explanatory model than simplified cranial shape. Enlow found that functional organization supersedes effects of population, ecogeographical patterning, or respiration exhibiting differential expression across groups. Enlow understood response through modular organization is functional—which explains why modules may remain invariant across sex and population. Hierarchy of organization would predict occlusion is a primitive inviolate function which constrains modules that develop later to act (and evolve) in concert. Under this view there would be organizational principles underlying modularity itself, an idea tested in this dissertation's Chapter 5.

Enlow's model predicts population effects in cranial organization emerge in major divisions of the skull. It does not predict modules within these major regions of the skull themselves vary by population. Enlow's model thus roughly explains the results from Chapter 3 that show the stability of the face and cranial base across population and sex. If these are modules, it is not unexpected they remain invariant to a degree, being driven by independent functions. The neurocranium, consisting of more than one module and

anchoring muscles for another (facial) module, does not exhibit this invariance as it probably represents more than one functional area (results from Martínez-Abadías and colleagues [2009] show a decoupling of the face and neurocranium; see also González-José et al., 2005 on the multiplicity of modules in the cranium).

Being multifactorial, factors such as occlusion are accomplished by modules acting in unison. The modules themselves may not vary by population or sex, yet the whole masticatory complex can. An example may be found in the Aleuts; it may be high dental loading that makes discrimination of Aleut gnathic complex from other populations possible (Nicholson and Harvati, 2006). Rather than the face itself being organized or integrated differently from other populations, it may be that extremely high paramasticatory force (chewing hides to soften) in the mandible and face combined with extremely high masticatory requirements for diet can swamp the signal of modularity, which usually prevents the crossing of boundaries of integration. If so, circumpolar populations are the only populations that deviate from the pattern of modularity in the face and base found in Chapter 3.

If, as current modular theory assumes, modules evolve because of changing functional requirements, then it is function defining the form (maintaining the form through time as outlined above), irrespective of population or sex. This argument has been used to explain the neutral axis of the orbit at approximately 90 degrees to the posterior maxillary (PM) plane so that a level field of vision is maintained no matter how the rostrum's morphology is configured (Bromage, 1992). The PM plane is defined as the line connecting two termini on midsagittal plane: the most posteroinferior point on the

maxillary tuberosities and the point on the anteriormost extent of the greater wings of the sphenoid. The angle to this line between the two points is invariant to a great degree. The PM plane is an example of an invariant cranial property. The configuration of the angle is not affected by sex or population. In a simplified case such as this it is easy to see the functional requirements for effective vision have served to maintain that orientation.

Is the Mandible a Module?

The question “Is the mandible a module?” was answered in the broad sense in Chapter 3. It was shown that as expected, the mandible did not integrate in the Flury hierarchy of matrix comparisons with the face, neurocranium, or base to any significant degree. That satisfies a basic property of modules: by definition if an area is a module, it is less integrated across other areas than within itself. However, it is doubtful the mandible as a whole is a module. In the *Rodentia*, the mandible is composed of two modules (Atchley, Plummer, and Riska 1985a,b; Leamy 1993; Cheverud et al., 1997; Mezey et al., 2000; Klingenberg et al., 2003), and under counterpart analysis generally the mandible belongs to two different modular systems (Hans and Enlow, 1996; Bastir 2008). The summation of the results also suggests the mandible is not a module. The mandible varied significantly across population and sex, suggesting in the broad sense that morphology was responding to the integrated paths in the skull in a different pattern from that of the base and face, areas which remained relatively stable across population and sex. The role of extreme or dual function in the mandible causing a pattern to diverge from modularity in other regions of the skull is examined below.

This chapter tests how regions of relative stability in the skull respond differentially to functional factors such as biomechanics. This is germane because much current research

seeks to define such areas of modularity in the Hominoidea, Hominidae, and Homininae. It is suggested regions of the skull (modules) have differential patterns in other hominoids, hominines, and maybe even within modern human populations. Given the function of mastication, analyses that do not include the mandible as part of the facial skeleton may be seriously lacking in predictive value. An analysis of the facial module that doesn't include the mandible may lack as much as 50% of morphology, given the high degree of integration in the face overall (Ackermann, 2002). Considering the embryological beginnings of an integrated splanchnocranium, failure to include this morphology can mean failure in analysis. The mandible matures later than the basicranium (midline and then lateral) and the neurocranium (Bastir et al., 2006).

Predictions

The summary of the previous sections allows a series of predictions and testable hypotheses to be made. Given that population, allometry, biomechanics, ecogeographical patterning, and degree of cranial base flexion all have been shown to contribute to mandibular, facial, and cranial architecture, all should be considered when trying to describe patterns of modularity in the skull. The prediction is thus made that these functional aspects will differentially drive portions of the skull. To test this prediction is thus to test the functional definition of modularity at the taxonomic level of species, within modern humans. (Chapter 5 tests this prediction at different taxonomic levels.)

The prediction here is that the shape of regions of the skull, described using three-dimensional centroids of data derived using Morphologika 2.5, can be predicted from the functional variables above. Thus it is predicted that the morphology of regions of the face and cranial base shown to be invariant across population and sex in Chapter 3 can be

highly explained by a combination of the functional variables from above. This explanation is a necessary criterion for a definition of module by property. For the purposes of this test, a model $r > 0.7$ is considered adequate.

A corollary prediction is that circumpolar populations will exceed others in definition of morphology of functional modules. Although there are pronounced differences in the skull matrices of circumpolar populations as shown in Chapter 3, it is suggested morphology will follow the general pattern of modularity in other human populations. In the broad sense this may be unlikely, given Harvati and Weaver (2006) demonstrated the major source of variation in the mandible derived from partitioning high dental-loading populations such as the circumpolar against other global populations, finding PC1 accounting for 25.04% of the total variance describing the overall shape of the mandible, with PC2 separating her circumpolar populations from others.

Functions Driving Modules

While there are multiple factors affecting modules as discussed, the primary two are the biomechanical vectors and the cranial base angle (CBA). These factors were discussed as representatives of particulate and integrationist models in Chapter 2, together forming the way most morphology of the masticatory and cranial complexes was viewed previously. Biomechanical vectors and loading produce a large part of mandibular morphology, and the CBA has been apportioned a major role in representing structural cranial formation (see below).

As discussed in Chapter 1, the masticatory apparatus has been schematically represented in the past, with the mandible being viewed as a simple bent beam, as a simple bent beam with differentiated areas extending for muscle attachment, and as a

simple bent beam with attached muscle insertions and representative stress points at expected areas of greatest loading. Finally, representation culminates in this same bent beam with the addition of the areas of muscle insertion on the cranium included (Symons, 1951; Greaves, 1978; Weijs, 1989; Wieshampel, 1993; Antón, 1994; Killiardis, 1995; Spencer, 1998). The biomechanically expressed function of the mandible here is addressed by use of a proxy, bending strength of the mandible using beam analysis (see full details in Appendix B).

Cranial Base Angle

Cranial flexion (as a reflection of orthogrady) influences the basicranium and hence the entire skull (see Figure 4-1). The CBA correlates with facial form—Polanski and Franciscus (2006) found the nasion-basion axis of the CBA to be a demarcation of the face and neurocranium. Enlow's model suggests this portion, underlying both the anterior and middle cranial fossae, is an important boundary for facial hafting. Lieberman, Mowbray, and Pearson (2000) note the breadth of the cranial base is affecting cranial volume, mostly through effects on brain volume. There are interactions with the face, because the neurocranial base width affects the facial width (also supported by studies of cranial modification, as discussed in Chapter 2. Cranial width is driving global variation the axes of length-width-height, discussed in Chapters 3 and 5; see also Martínez-Abadías et al., 2009).

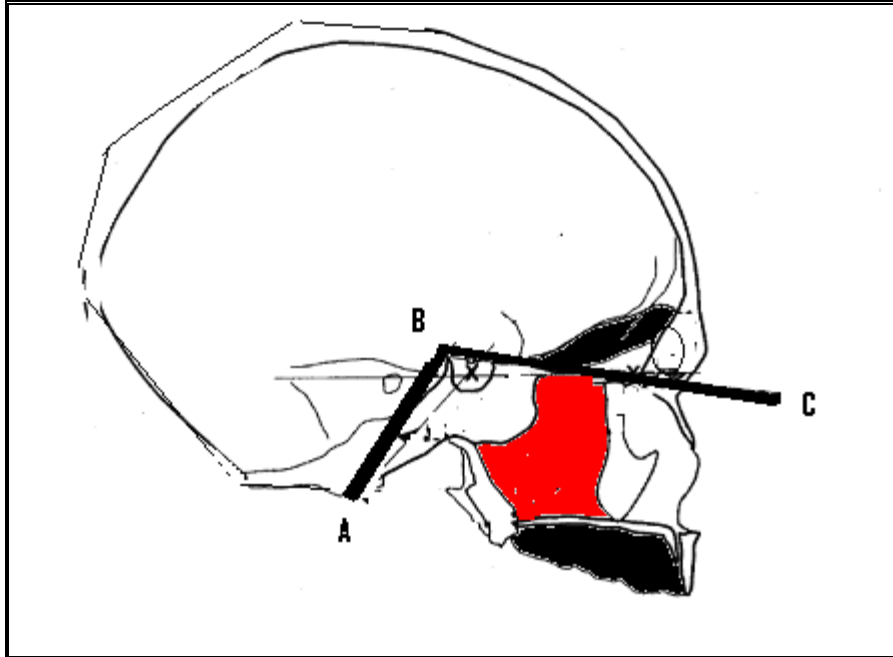


Figure 4-1. Cranial Base Angle (CBA). C is sella, B is nasion, and A is basion.

Lieberman, Mowbray, and Pearson (2000) also note that in the basicranium the cranial base length-width-height and sella-nasion-basion (SNB) flexion are mutually independent (see Figure 4-1 above for an illustration of the CBA). Their neuro-basiscranial (NBC) measurement explains 25% of the facial variation (exclusive of mandible), leaving the other 75% of facial morphology to be accounted for by other factors, such as ecogeographical patterning, biomechanics, allometry, and spatial effects being described here.

Importantly, Lieberman, Mowbray, and Pearson (2000) also find that many of their observations are sample-specific, supporting results from Bastir and Rosas (2004) demonstrating there may be population effects early in ontogeny.

Model-Bound Hypotheses

The predictions above are formalized into hypotheses. These hypotheses are model-bound based on function in the skull:

H₀₁: Similar patterns of functional factors affect modules or macromodules of skull.

H₀₂: Circumpolar populations will be similar to others in predictive factors producing morphology.

(If H₀₂ is accepted, function MAY NOT be a predictive factor for modularity.)

Methods

The above hypotheses were tested in a subset of all digitized skulls from the global sample in Morphologika 2.5. In the subset, 140 individuals exhibited sufficient morphology to reflect all functional factors. The details of morphometric applications are in Chapter 3 and in Appendix D. Table 4-1 consists of the entire three-dimensional digitized database of points collected at AMNH and NMNH; M14, F14, and B14 are three-dimensional midline and bilateral landmark sets within the database comprising the mandible, face, and cranial base. Landmark point numbers within each regional subset are the same and have the same number of midline and bilateral points within each subset. This strategy allows robust Flury hierarchical comparisons of the matrices derived from PCA (see Chapter 3 and Appendices B and D). The balance of midline and bilateral points are the same within each region in order to preserve dimensionality to the highest degree possible. (See Chapter 5 and Mitteroecker and Bookstein [2008] for critiques of modularity integration tests using point sets without the same number of points.)

Table 4-1. Landmark Points for Morphometric Measurements

Point Number	Landmark	Region of the Skull/Number of Measurements
1	Mental foramen left side (lmf)	M14
2	Mental foramen right side (rmf)	M14
3	Post-condyle (postcon)	M14
4	Lateral condyle (latcon)	N/A
5	Incisura semilunaris (semilunaris)	N/A
6	Coronoid tip (corotip)	M14
7	Indented ramus	N/A
8	First molar superior side (M/1 superior)	N/A
9	Infradentale	M14
10	Mental foramen left side (lmf)	N/A
11	Pogonion	M14
12	First molar inferior side (M/1 inferior)	N/A
13–15	Alveolar line (alv)	N/A
16	Gonion left side (l gonion)	M14
17	Minimum ramus breadth (mrb)	N/A
18	Internal ramus – mandibular foramen (mandfor)	M14
19–21	Mentum osseum	N/A
22	Mental foramen left side (lmf)	N/A
23	Mental foramen right side (rmf)	N/A
24	Coronoid tip (cortip)	M14
25	Lateral condyle (latcon)	N/A
26	Post-condyle (postcon)	M14

Point Number	Landmark	Region of the Skull/Number of Measurements
27	Gonion right side (r gonion)	M14
28	Mandibular foramen right side (rmandfor)	M14
29	Lingual tuberosity right side (ling tub r)	M14
30	Lingual tuberosity left side (ling tub l)	M14
31	Third molar distal side (distal M/3)	N/A
32–43	Dental measurements excluded	—
44	First molar lingual side (ling M/1)	F14
48	Third molar labial side (M/3 labial)	F14
49	Cranial height	N/A
50	Mental foramen left side (lmf)	N/A
51	Nasion 63 (nas=63)	F14
52	Glabella	F14
53	Cranial length – opisthocranium (cranial length opi)	N/A
54	Cranial breadth – euryon right side (r cbr eur)	N/A
55	Cranial breadth – euryon left side (l cbr eur)	N/A
56	Bizygomatic right side (r bizygo)	F14
57	Bizygomatic left side (l bizygo)	F14
58	Porion right side (r por)	B14
59	Porion left side (l por)	B14
60	Bottom of left orbit (left orbit)	F14
61	Left infraorbitale (l infraorb)	F14
62	Right infraorbitale (r infraorb)	F14
63	Nasion check = 51	N/A
64	Left supraorbitale (l supraorb)	F14

Point Number	Landmark	Region of the Skull/Number of Measurements
65	Right supraorbitale (r supraorb)	F14
66	Right nasal capsule (r nasal cap)	F14
67	Left nasal capsule (l nasal cap)	F14
68	Infraspinale	F14
69	Right nasal aperture (r nasal aperture)	F14
70	Left nasal aperture (l nasal aperture)	F14
71	Top nasal	F14
72	Incision	F14
73	Internal temporal fossa (internal tempfossa)	F14
74–76	Temporal lines (templines)	N/A
77	Bregma	N/A
78	Right infraorbitale (r infraorb)	N/A
79	Nasion	N/A
80	Right porion (r porion)	N/A
81	Posterior foramen magnum (formag post)	B14
82	Opisthion (opi)	B14
83	Left pterygomaxillary tubercle (l ptm)	B14
84	Right pterygomaxillary tubercle (r ptm)	B14
85	Left pharyngeal tubercle (l phar tub)	B14
86	Right pharyngeal tubercle (r phar tub)	B14
87	Incision	N/A
88	Right foramen rotundum (r for rot)	B14
89	Left foramen rotundum (l for rot)	B14
90	Right ovale (r ovale)	B14

Point Number	Landmark	Region of the Skull/Number of Measurements
91	Left ovale (l ovale)	B14
92	Right foramen spinosa (r spin)	N/A
93	Left foramen spinosa (l spin)	N/A
94	Left palate (l palate)	B14
95	Right palate (r palate)	B14
96	Left glenoid (l glenoid)	B14
97	Right glenoid (r glenoid)	B14
98	Left hypoglossal (l hypo)	B14
99	Right hypoglossal (r hypo)	B14
100	Styloid process left side (l stylo)	N/A
101	Styloid process right side (r stylo)	N/A

Table 4-2 identifies the major functional predictive factors for morphology.

Biomechanical predictors include $I_{\max} * I_{\min}$ and angle (of the mandibular corpus). Orbital size (Orbit; orb) although problematic if used as a proxy for body size (see appendices for discussion). Cranial Base Angle is included here as Cranang. The bending strength of the mandible at M1 ($I_{\max} * I_{\min}$), the area of the mandibular corpus in cross-section, the long axis of mandibular corpus section (angle) were used as representatives of different aspects of biomechanical force in the mandible. (Biomechanical details in Appendix B.) Sex, sample, and sex by sample interaction were included. (Readers may wish to refer to Table 4-2 while they review the stepwise fit tables that follow below.)

Table 4-2. Major Functional Predictive Factors for Morphology

Character	Definition
Orbit	Orbital area
L _{max}	$I_{\max} * I_{\min}$ (moment of bending strength at M1)
Cranang	Cranial base angle
Manar	Area of mandibular corpus
Angle	Angle of mandibular corpus section long axis
Sample	Effect of sample
SX*SAM	Sex by sample interaction
M14	Shape of mandible defined by 14 points in Morphologika v2; centroid
F14	Shape of face defined by 14 points in Morphologika v2; centroid
B14	Shape of base defined by 14 points in Morphologika v2; centroid
SKULL28	Shape of skull defined by 28 points in Morphologika v2; centroid
ENTIRE.SKULL42	Shape of skull defined by all 42 points (M14+F14+B14) in Morphologika v2; numbers after entity refer to numbers of points used

Note: Numbers after entity in left column refer to the number of points used in the measurement.

Much research on modularity uses the cranial base as the interface between the face and base (because it is the hafting for the face; Hans and Enlow, 1996; Polanski and Franciscus, 2006; Bastir and Rosas, 2002, 2005). However, the proposed module frequently includes congruent points in both facial AND basilar matrices, thus confounding results and leading to interpretive difficulties (see discussion in Polanski and Franciscus, 2006). Here the points are all in the proposed module (mandible, face, base) and are not shared with any other module. Skull28 is made up of the points from Face14 and Base14 grouped as a representation of the entire skull without the mandible. Skull42 is all midline and bilateral points of the mandible, face, and base. The three primary regions tested are mandible, face, and cranial base.

The shape of proposed modules was derived from the shape centroids from PCA analysis (single variable decomposition [SVD] method, the most robust). Morphometrics

provides the methodology to test relationships as exemplars of three-dimensional coordinate systems. Landmark data in three dimensions is perturbed about mean form. Perturbation models address the problems of reflection, translation, scaling, and rotation as groups of three-dimensional points are compared. If groups of points are correctly registered (centroids standardized as to scaling, reflective properties, and translation) within the hemispheres of a three-dimensional sphere, then a perturbation model can be applied. This model predicts that change in landmark groups occurs as a perturbation of three-dimensional space as defined by landmark group, within which the points are assumed to be able to “randomly” move independently of other landmarks. Perturbations are examined as the deviations from isotropy, in which all landmarks are assumed to exhibit equal spacing in three dimensions. The proposed functional variables and the centroids from the regions of the mandible, face, and cranial base were loaded into a stepwise regression using the stepwise variable selection procedure (option mixed forward and backwards, 0.05 significance to stay, 0.05 to leave in JMP [from SAS 2009]). Stepwise regression selects subsets of effects for a regression model, then sequentially extracts variables in model building, finally producing a model based on minimum and maximum designated p-values for model inclusion. Models were judged adequate in explanation if model r was greater than 0.7 ($r > 0.7$). Many of the models tested below far exceeded this criterion. Details about the statistical underpinnings, applications, and implications of the use of MANOVA, Morphologika, and stepwise variable selection and reduction appear in Appendices B, C, and D.

Results for Whole Skull

The results in Table 4-3 show poor prediction of the skull (Skull42) by the model ($r = 0.5433$). The effects of sample, size, and orb are significant. This result shows yet again the fact the whole skull is not a module. Not only does the whole skull have differential areas of integration within, but the whole skull also is predictable by population and sex, and not by function. Therefore the whole skull fails all three tests of modularity.

Table 4-3. Stepwise Fit – Skull42 (42 landmark points, combination of the face, base, and mandible)

Current Estimates							
SSE	DFE	MSE	R Square	R Square Adj	Cp	AIC	
12901.744	125	103.21395	0.5433	0.5324	11.279284	602.0844	
Parameter		Estimate	nDF	SS	“F Ratio”	“Prob>F”	
Intercept		298.388709	1	0	0.000	>0.9999	
Sample{5&7&8&9&6&3&4-2&1}		-8.3979149	1	5998.144	58.114	<0.0001	
Sample{5-7&8&9&6&3&4}		0	1	198.8513	1.941	0.1660	
Sample{7&8&9-6&3&4}		0	2	381.5066	1.874	0.1579	
Sample{7&8-9}		0	3	470.281	1.538	0.2080	
Sample{7-8}		0	4	860.7994	2.163	0.0722	
Sample{6-3&4}		0	3	678.0774	2.256	0.0853	
Sample{3-4}		0	4	681.2361	1.686	0.1575	
Sample{2-1}		0	1	31.8126	0.307	0.5808	
Sex{2-1}		-5.3254644	1	3548.165	34.377	<0.0001	
Cranang		0	1	30.28178	0.292	0.5901	
Orb		32.037819	1	4987.389	48.321	<0.0001	
Manar		0	1	119.3517	1.158	0.2480	
I _{max}		0	1	150.0533	1.459	0.2294	
I _{min}		0	1	97.69754	0.946	0.3326	
Angle		0	1	74.49471	0.720	0.3977	
Step History							
Step	Parameter	Action	“Sig Prob”	Sequence SS	R Square	Cp	p
1	Orb	Entered	<0.0001	6305.082	0.2232	100.02	2
2	Sample{5&7&8&9&6&3&4-2&1}	Entered	<0.0001	5497.629	0.4178	45.658	3
3	Sex{2-1}	Entered	<0.0001	3548.165	0.5433	11.279	4

Results for Skull Exclusive of Mandible

The results presented in Table 4-4 show several key points. Although the overall r is low (0.6744), results show the skull is primarily driven by the integration with the mandible and sample. It is expected that a combination of two possible modules (face and base together as one unit here) would still be affected by sample because the skull as a whole can be discriminated across populations easily (Howells, 1989). A comparison to the entire skull from above (Skull42; see Table 4-3) shows sex has dropped out as a predictive factor, which is expected; in the results for Skull42, this variable is only weakly predictive, less so overall than sample. This finding also indicates that, across sex, skull shape with mandible included is more similar in males and females than simply the skull itself. This result further supports results introduced in Chapter 2 indicating the mandible itself is a less useful discriminator for sex than the remainder of the skull. So inclusion of mandibular information, as here, should force discrimination to drop (see Chapter 2 and Humphrey et al. [1999] for further discussion).

Hypothesis testing here assumes the skull as a whole responds to factors such as population and sex which gradually become less significant as lower levels of hierarchy are reached, finally becoming non-predictive at the modular level or below. The results in Table 4-4 thus suggest it is modules in combination—"macromodules" such as the cranial base and face together—that respond together to ecogeographic or populational effects rather than modules in and of themselves. This response would seem to make intuitive sense, as ecogeographical response is not inherited as modules are. Therefore response cannot be intramodular; it must either be intermodular or as some yet unexplained factor within modules.

Table 4-4. Stepwise Fit – Skull28 (28 landmark points, whole skull exclusive of mandible)

Current Estimates							
SSE	DFE	MSE	R Square	R Square Adj	Cp	AIC	
4493.2824	125	35.946259	0.6744	0.6639	7.2039638	470.5646	
Parameter		Estimate	nDF	SS	“F Ratio”	“Prob>F”	
Intercept		80.2325419	1	0	<0.0001	>0.9999	
Sample{5&8&4&1.06&6&7-9&3&2&1}		-2.8097161	1	886.0208	24.648	<0.0001	
Sample{5-8&4&1.06&6&7}		0	1	86.15173	2.424	0.1220	
Sample{8-4&1.06&6&7}		0	2	91.63207	1.280	0.2816	
Sample{4&1.06-6&7}		0	3	103.8754	0.962	0.4129	
Sample{4-1.06}		0	4	121.3905	0.840	0.5024	
Sample{6-7}		0	4	146.3164	1.018	0.4008	
Sample{9&3-2&1}		0	1	12.7491	0.353	0.5536	
Sample{9-3}		0	2	13.69048	0.188	0.8289	
Sample{2-1}		0	2	74.78003	1.041	0.3562	
Sex{2-1}		0	1	135.1015	3.844	0.0522	
Cranang		0.19465329	1	177.4378	4.936	0.0281	
Orb		6.20675075	1	160.1822	4.456	0.0368	
Manar		0	1	3.055475	0.084	0.7719	
I _{max}		0	1	8.561696	0.237	0.6274	
I _{min}		0	1	13.73422	0.380	0.5386	
Angle		0	1	38.08147	1.060	0.3052	
(I _{max} -260336)*(I _{min} -160897)		0	3	116.7735	1.085	0.3581	
Mand14		0.67999433	1	4240.384	117.965	<0.0001	
Step History							
Step	Parameter	Action	“Sig Prob”	Sequence SS	R Square	Cp	p
1	Mand14	Entered	<0.0001	8091.159	0.5864	35.572	2
2	Sample{5&8&4&1.06&6&7-9&3&2&1}	Entered	<0.0001	853.6252	0.6482	13.406	3
3	Cranang	Entered	0.0215	200.1951	0.6628	9.7387	4
4	Orb	Entered	0.0368	160.1822	0.6744	7.204	5

Results for Mandible

The results in Tables 4-5 and 4-6 are interesting in that when the base and face are analyzed for their predictive value on the mandible separately, sex and population are strong predictors (Table 4-5). When the modules of face and base are combined, the

effect of sex drops out (Table 4-6). This finding means that although the mandible is probably not a module, the way the mandible varies in comparison to the remainder of the skull is by population. This result might be an example of how ecogeographical patterning works, with response not showing up at the modular level, but above, with differences not found in males and females from a given spatial locus. At the level below this (intermodular, as reported in Table 4-5) male and female skulls vary equally in the way the mandible fluctuates with (or is predicted by) the remainder of the skull; this is the level at which the variability of the mandible to the axes of both sex and population demonstrated in Chapter 3 emerges.

Table 4-5. Stepwise Fit – Mand14 (including base and face)

Current Estimates							
SSE	DFE	MSE	R Square	R Square Adj	Cp	AIC	
2878.9939	123	23.406455	0.7156	0.7499	6.19309	416.696	
Parameter		Estimate	nDF	SS	“F Ratio”	“Prob>F”	
Intercept		32.6647412	1	0	0.000	>0.9999	
Sample{5&7&9&8&6&4-3&1&2}		-1.991454	3	513.4855	7.313	0.0001	
Sample{5&7-9&8&6&4}		-0.5553606	2	333.1826	7.117	0.0012	
Sample{5-7}		0	1	14.73156	0.627	0.4298	
Sample{9-8&6&4}		-2.4062921	1	215.7463	9.217	0.0029	
Sample{8-6&4}		0	1	0.580087	0.025	0.8757	
Sample{6-4}		0	2	31.51855	0.670	0.5138	
Sample{3-1&2}		0	1	2.130763	0.090	0.7642	
Sample{1-2}		0	2	24.53239	0.520	0.5959	
Sex{1-2}		-1.2153623	1	156.9644	6.706	0.0108	
Cranang		0	1	2.168238	0.092	0.7622	
Orb		0	1	30.91704	1.324	0.2521	
Manar		0	1	30.96887	1.327	0.2517	
I _{max}		0	1	42.33329	1.821	0.1797	
I _{min}		0	1	63.50708	2.752	0.0997	
Angle		0	1	26.34003	1.126	0.2906	
Face14		0.72710973	1	1766.641	75.477	<0.0001	
Base14		0.45508496	1	441.1701	18.848	<0.0001	
Step History							
Step	Parameter	Action	“Sig Prob”	Sequence SS	R Square	Cp	p
1	Face14	Entered	<0.0001	8121.154	0.6728	41.636	2
2	Base14	Entered	<0.0001	484.078	0.7129	23.09	3
3	Sample{9-8&6&4}	Entered	0.0009	429.6365	0.7485	10.855	6

Table 4-6. Stepwise Fit – Mand14 (with face and base joined as Skull28)

Current Estimates							
SSE	DFE	MSE	R Square	R Square Adj	Cp	AIC	
4005.9568	123	32.568755	0.6681	0.6519	9.0325338	459.6404	
Parameter		Estimate	nDF	SS	"F Ratio"	"Prob>F"	
Intercept		40.6865481	1	0	0.000	>0.9999	
Sample{5&7&9&8&6&4-3&1&2}		-1.6638576	4	816.73	6.269	0.0001	
sample{5&7-9&8&6&4}		-1.0636551	3	749.8319	7.674	0.0001	
Sample{5-7}		0	1	8.765894	0.268	0.6059	
Sample{9-8&6&4}		-3.3008527	2	403.7891	6.199	0.0027	
Sample{8-6&4}		0	1	0.467118	0.014	0.9053	
Sample{6-4}		0	2	4.139345	0.063	0.9394	
Sample{3-1&2}		0	1	42.98442	1.323	0.2523	
Sample{1-2}		0	2	78.95282	1.216	0.2999	
Sex{2-1}		-1.6670721	2	261.1111	4.009	0.0206	
Cranang		0	1	29.86615	0.916	0.3403	
Orb		0	1	101.45	3.170	0.0775	
Manar		0	1	25.18724	0.772	0.3814	
I _{max}		0	1	35.18977	1.081	0.3005	
I _{min}		0	1	35.72234	1.098	0.2968	
Angle		0	1	44.72273	1.377	0.2428	
Skull28		0.63394243	1	3356.725	103.066	<0.0001	
Sample{5&7&9&8&6&4-3&1&2}*Sex{2-1}		0	1	42.77429	1.317	0.2534	
Sample{5&7-9&8&6&4}*Sex{2-1}		0	1	12.42046	0.379	0.5391	
Sample{5-7}*Sex{2-1}		0	2	74.39689	1.145	0.3271	
Sample{9-8&6&4}*Sex{2-1}		-0.542264	1	14.12671	0.434	0.5114	
Sample{8-6&4}*Sex{2-1}		0	2	61.8639	0.949	0.3900	
Sample{6-4}*Sex{2-1}		0	3	77.86192	0.793	0.5002	
Sample{3-1&2}*Sex{2-1}		0	2	50.16696	0.767	0.4665	
Sample{1-2}*Sex{2-1}		0	3	79.50195	0.810	0.4908	
Step History							
Step	Parameter	Action	"Sig Prob"	Sequence SS	R Square	Cp	p
1	Skull28	Entered	<0.0001	7078.115	0.5864	29.831	2
2	sample{9-8&6&4}*sex{2-1}	Entered	<0.0001	986.7544	0.6681	9.0325	7

The results in Tables 4-7 and 4-8—showing that the face and mandible are the only predictors of significance for the base and that the base, mandible, and orbit are the only significant predictors for the face—are important as they suggest the pattern of modularity in the skull is the most predictive of morphology. The predictive value of the base on the face is lower than that for the mandible, possibly as a result of retained biomechanical effects. The prediction of the base is quite poor, $r = 0.4774$. As is shown in Chapter 5, it is likely that the cranial foramina provide an understanding into the basic organizational system of the skull. It may be the use of multiple foramina in the definition of the cranial base used here is driving the poor prediction; as is later shown the foraminal pattern is not predictable by modular or functional constraints. Later (Chapter 5) results suggest none of the predictors used here work on the foraminal pattern, which is to be expected if that pattern is indeed primitive.

Table 4-7. Stepwise Fit – Face14

Current Estimates						
SSE	DFE	MSE	R Square	R Square Adj	Cp	AIC
2041.3476	126	16.201172	0.7184	0.6933	4.9434551	365.998
Parameter		Estimate	nDF	SS	“F Ratio”	“Prob>F”
Intercept		17.4420132	1	0	0.000	>0.9999
Sample{5&6&7&8&4&9&3&1.06-2&1}		0	1	33.85875	2.108	0.1490
Sample{5-6&7&8&4&9&3&1.06}		0	2	56.55974	1.767	0.1752
Sample{6&7-8&4&9&3&1.06}		0	3	81.99699	1.716	0.1672
Sample{6-7}		0	4	140.3222	2.251	0.0674
Sample{8-4&9&3&1.06}		0	4	92.48473	1.447	0.2225
Sample{4&9-3&1.06}		0	5	99.78496	1.244	0.2930
Sample{4-9}		0	6	106.2738	1.098	0.3674
Sample{3-1.06}		0	6	99.78797	1.028	0.4106
Sample{2-1}		0	2	66.03962	2.073	0.1302
Sex{2-1}		0	1	2.521843	0.155	0.6948
Cranang		0	1	0.105994	0.066	0.9359
Orb		4.48552813	1	83.13281	5.131	0.0252
Manar		0	1	9.293434	0.572	0.4510
I _{max}		0	1	14.08279	0.868	0.3532
I _{min}		0	1	25.91909	1.608	0.2072
Angle		0	1	3.882678	0.238	0.6264
Mand14		0.50459375	1	1546.116	95.432	<0.0001
Base14		0.18877569	1	72.9113	4.500	0.0358
Sample{5&6&7&8&4&9&3&1.06-2&1}*Sex{2-1}		0	3	46.56781	0.957	0.4154
Sample{5-6&7&8&4&9&3&1.06}*Sex{2-1}		0	4	81.6643	1.271	0.2851
Sample{6&7-8&4&9&3&1.06}*Sex{2-1}		0	5	99.7058	1.243	0.2934
Sample{6-7}*Sex{2-1}		0	6	160.4115	1.706	0.1254
Sample{8-4&9&3&1.06}*Sex{2-1}		0	6	176.0356	1.887	0.0884
Sample{4&9-3&1.06}*Sex{2-1}		0	7	135.6574	1.210	0.3025
Sample{4-9}*Sex{2-1}		0	8	126.9812	0.978	0.4564
Sample{3-1.06}*Sex{2-1}		0	8	116.4459	0.892	0.5254
Sample{2-1}*Sex{2-1}		0	4	77.74135	1.208	0.3111
(I _{max} -260336)*(I _{min} -160897)		0	3	65.99553	1.370	0.2552

Table 4-7 (cont.)

Step History							
Step	Parameter	Action	"Sig Prob"	Sequence SS	R Square	Cp	p
1	Mand14	Entered	<0.0001	4554.284	0.6728	11.739	2
2	Orb	Entered	0.0153	100.6889	0.6877	7.4775	3
3	Base14	Entered	0.0358	72.9113	0.6984	4.9435	4

Table 4-8. Stepwise Fit – Base14

Current Estimates							
SSE	DFE	MSE	R Square	R Square Adj	Cp	AIC	
1982.7694	127	15.612357	0.4885	0.4774	9.9041397	360.213	
Parameter		Estimate	nDF	SS	"F Ratio"	"Prob>F"	
Intercept		45.3697071	1	0	0.000	>0.9999	
Sample{1.06&8&5&6&7&3&4&9-1&2}		0	1	12.61948	0.087	0.3707	
Sample{1.06&8&5&6-7&3&4&9}		0	2	56.32404	1.827	0.1651	
Sample{1.06&8&5-6}		0	3	56.51477	1.213	0.3080	
Sample{1.06-8&5}		0	4	86.92232	1.410	0.2346	
Sample{8-5}		0	5	148.9029	1.981	0.0861	
Sample{7&3&4-9}		0	3	84.04348	1.830	0.1452	
Sample{7&3-4}		0	4	86.3847	1.401	0.2377	
Sample{7-3}		0	5	114.6152	1.497	0.1957	
Sample{1-2}		0	2	15.0388	0.478	0.6214	
Sex{2-1}		0	1	16.70525	1.071	0.3028	
Cranang		0	1	14.39981	0.922	0.3389	
Orb		0	1	7.339902	0.468	0.4951	
Manar		0	1	2.1698	0.138	0.7109	
I _{max}		0	1	0.297785	0.019	0.8908	
I _{min}		0	1	0.160484	0.010	0.9197	
Angle		0	1	2.366437	0.151	0.6987	
Mand14		0.26480387	1	276.9554	17.739	<0.0001	
Face14		0.19524231	1	84.43283	5.408	0.0216	
Step History							
Step	Parameter	Action	"Sig Prob"	Sequence SS	R Square	Cp	p
1	Mand14	Entered	<0.0001	1786.694	0.4636	13.606	2
2	Face14	Entered	0.0216	84.43283	0.4855	9.9041	3

Figures 4-2 through 4-7 and Tables 4-9 through 4-16 show selected results in support of the stepwise analysis displayed above. The pattern of prediction of the cranial regions from the other regions is broadly supported in the partial least squares (PLS) results below. The relationship of the mandible and face is tighter ($r = 0.820$) than either the base and face or the base and mandible (both r s approximately 0.6). Explanation of the mandible by the face is approximately 67%; by the base it is approximately 46%. The explanation of the morphology of the face by the base is also relatively good, approximately 53% (not illustrated). The stepwise results mirror this pattern; the mandible and face integrate strongly (selected with high value for prediction), but neither, while significant, are strong predictors of the base.

Finally the results from the PCA factor analysis below of all three regions show an extremely high contribution of PC1, 81% of total variation (Table 4-15). These data are size-corrected, hence removing the allometric effect on the uncorrected PC1 axis, so the pattern of equal influence of each region on the others would be expected to approximate one-third to one-third to one-third of total variation, assuming equal-sided figures. While it is not possible to prove this pattern here, it may be thought that this extremely high loading on the size-corrected PC1 axis represents modularity. Given that the mandible may not be a module, it might be expected that this proportion actually overestimates modularity. The more sampling of true modules, the more their integration overall should drop.

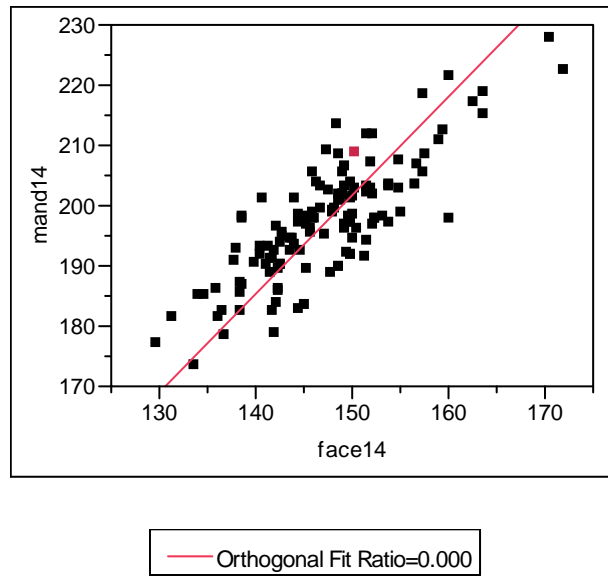


Figure 4-2. Bivariate Fit of Mand14 by Face14 (JMP plot)

Table 4-9. Orthogonal Regression of Face14 and Mand14

Variable	Mean	Standard Deviation
Face14	147.2518	7.24394
Mand14	197.2115	9.673278
Correlation	Intercept	Slope
0.8202	-42.5166	1.628015

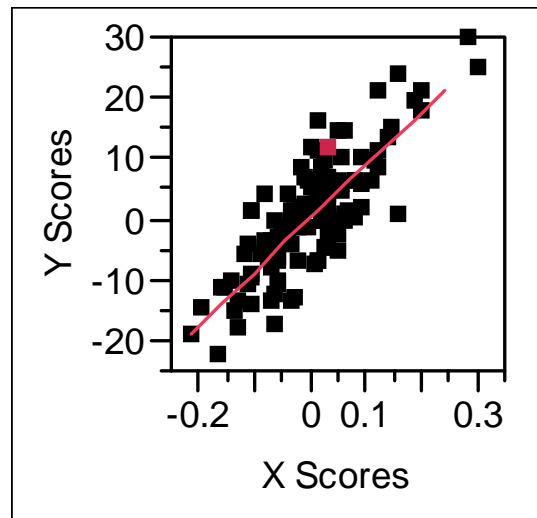


Figure 4-3. Partial Least Squares Scores for Face14 and Mand14 (JMP plot)

Table 4-10. Partial Least Squares – Percent Variation Explained for Face14 and Mand14

No.	X	X-Plot	Cumulative X	Y	Y-Plot	Cumulative Y
1	100	<div style="width: 100%; height: 10px; background-color: #ff0000;"></div>	100	67.28	<div style="width: 67.28%; height: 10px; background-color: #ff0000;"></div>	67.28

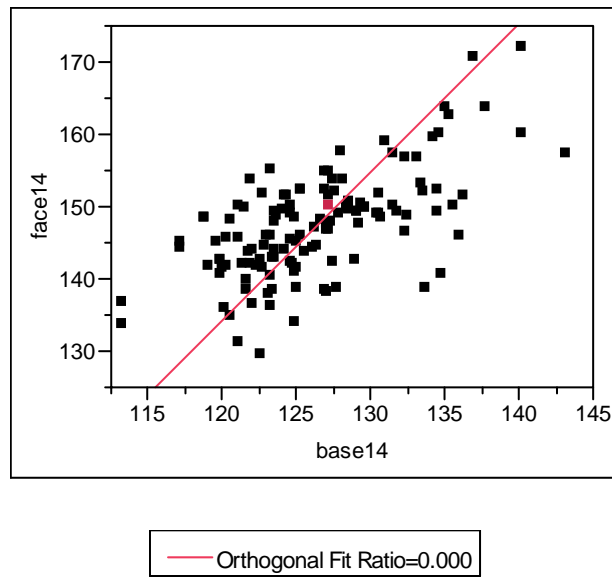


Figure 4-4. Bivariate Fit of Face14 by Base14 (JMP plot)

Table 4-11. Orthogonal Regression of Face14 and Base14

Variable	Mean	Standard Deviation
Base14	126.3419	5.465818
Face14	147.2518	7.24394
Correlation	Intercept	Slope
0.6432	-113.093	2.06064

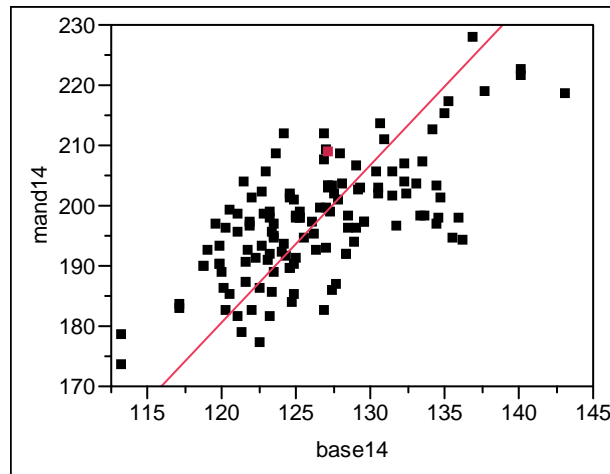


Figure 4-5. Bivariate Fit of Mand14 by Base14 (JMP plot)

Table 4-12. Orthogonal Regression of Mand14 and Base14

Variable	Mean	Standard Deviation
Base14	126.3419	5.465818
Mand14	197.2115	9.673278
Correlation	Intercept	Slope
0.6809	-131.179	2.599222

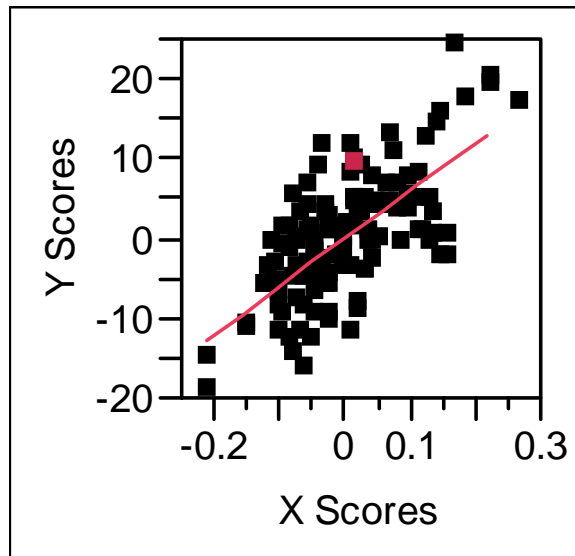


Figure 4-6. Partial Least Squares Scores for Mand14 and Base14 (JMP plot)

Table 4-13. Partial Least Squares – Percent Variation Explained for Mand14 and Base14

No.	XX-Plot	Cumulative X	YY-Plot	Cumulative Y
1	<div style="width: 100%; height: 10px; background-color: red;"></div>	100	<div style="width: 46.36%; height: 10px; background-color: red;"></div>	46.36


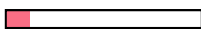
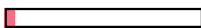
Tables 4-14, 4-15, and 4-16 and Figure 4-6 display the correlations across the three primary regions of the skull. The results show tighter integration in the mandible and face rather than in the mandible and base. These results broadly support those from Ackermann (2005), contra Polanski and Franciscus (2006), suggesting a tight pattern of integration in the face. Figure 4-6 shows the parallel ellipsoid plot of the 42 points of the mandible, face, and base. As discussed and illustrated in Chapter 3, a tight relationship of

points in these plots is indicated by a dark horizontal band. The deviance from this pattern is shown by the trendline in red, which nowhere approximates a tightly bound relationship. Table 4-16 is the pairwise comparisons of the three regions, mandible, face, base, included to show the plot correlation bars; results broadly mirror those from the earlier regressions above.

Table 4-14. Multivariate Correlations across Face, Base, and Mandible

	Mand	Face	Base
Mand	>0.9999	0.8202	0.6809
Face	0.8202	>0.9999	0.6432
Base	0.6809	0.6432	>0.9999

Table 4-15. Principal Components / Factor Analysis on Correlations across Face, Base, and Mandible

Number	Eigenvalue	Percent	Cumulative Percent
1	2.4323	81.078 	87.078
2	0.3904	13.012 	94.090
3	0.1773	5.910 	100.000

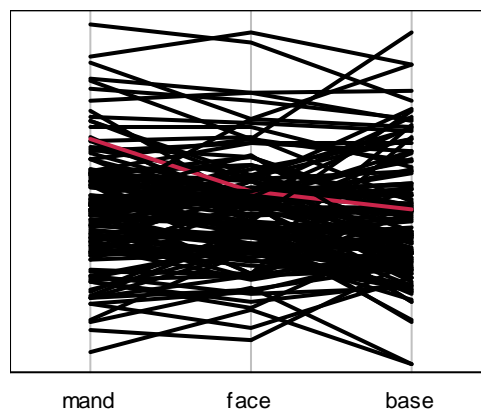





Figure 4-7. Ellipsoid 3D Parallel Coordinate Plot of the Mandible, Face, and Base (JMP plot)

Table 4-16. Pairwise Correlations among Mandible, Face, and Base

Variable	by Variable	Correlation	Count	Sig Prob	Plot Correlation
Face	Mand	0.8202	130	< .0001	
Base	Mand	0.6809	130	< .0001	
Base	Face	0.6432	130	< .0001	

The series of comparisons in the stepwise analysis and PLS shows that the face and base meet the modular definition of formation by function and by absence of effects caused by population (sample) and/or sex. The mandible fails this test, AND, although the base and face separately meet the modular definition, together as “Skull28” they vary by sample. These results suggest the skull is wholly made up of modules, which, although within themselves are invariant, across themselves in combination they respond to ecogeographical and paramasticatory force.

Table 4-17 presents the results from above in tabular form, augmented by results from other partitions of the skull.

Table 4-17. Effects of Functional Factors on Partitions of the Skull

Structure	Orbit	I _{max}	Manar	Cranag	Sex	Sample	SX* SAM	M14 / RAM	S	F14	B14	Model r ²	n
Entire.Skull42	***	*	*	—	***	***	—	N/A	N/A	N/A	N/A	.519	129
Skull28	***	*	*	.02 weak	*weak	***	—	***	N/A			.645	130
Mand14	*	—	—	—	*	***	—	N/A	***	***	***	.641	130
Alaskan Mand14	*	.001***	.03*	—	*	N/A	N/A	N/A	***			.9603	27
Alaskan Skull28	—	—	—	—	—	N/A	N/A	***	—			.8674	27
Non-Alaskan Mand14	* weak	—	—	*	*	N/A	N/A	N/A	***			.463	115
Non-Alaskan Skull28	***	—	—	—	*	N/A	N/A	***	—			.4651	115
Mand14 Males	—	—	—	*weak	N/A	****	N/A	—	***			.668	
Mand14 Females	—	—	—	—	N/A	***	N/A	—	***			.4232	
Face14	***	*	.08	—	—	—	—	***	—	N/A	* weak	.752	130
Base14	—	***	***	—	—	—	—	*	—	*	N/A	.542	130
Mand14	—	.030*	.059*	—	*	***	—	N/A	***	***	***	.752	130
Superior Face	—	—	—		*	***	*	Corlow ****				.342	130
Skull28	***	*	*		*	***	—	***	N/A			.645	130
Corpus8	—	*	*	—	—	***		N/A / N/A / ***	***			.6451	130
Ramus8	*	—	—	—	*	—	—	N/A / *** / N/A	*			.674	130
Anterior Face	*					*						.326	130
Posterior Face	***	—	—		***	***	***		N/A			.441	130

* > 0.05; > 0.01; *** < 0.01; **** < 0.001

Discussion

H_{o1}: Similar patterns of functional factors affect modules or macromodules of skull.

This hypothesis is not supported. There is a differential pattern of factors reflecting function in the tested regions of skull and mandible. In the entire skull (Skull42) predictor factors include orbital area, sample, and sex. Orbital area is a predictor in almost all partitions, failing significance only in circumpolar populations. Orbital area is a significant predictor of the morphology of the mandible itself though not nearly as strong as for the skull, with orbit much more significant for the skull (skull $p < 0.001$; mandible $p < 0.05$). The skull as a whole is not predicted by the cranial base angle, but the skull exclusive of the mandible (Skull28) is.

Both skull and mandible are weakly predicted by sex ($p < 0.05$), while sample is highly predictive of both ($p < 0.01$). Predictor variables for the mandible alone differ in that the only significant contributory factors are skull shape, sex, sample, and orbital area. When the skull is partitioned into mandible and cranium, both partitions are somewhat explained by the model, with both cranial and mandibular shape predicted about equally by the model (mandibular $r = 0.641$; cranial $r = 0.643$). Interestingly, there is a divergence of trajectories not predicted by the model. While the skull is weakly predicted by both bending strength at M1 and mandibular corpus area, neither predictor is significant of the mandible as a whole. As will be discussed further, partitioning the mandible into corpus and ramus shows that these effects are operating in the mandible but only on the corpus; the ramus is not responding to these factors.

These results generally support some differences in male versus female morphology, but this analysis suggests an essential conservancy of shape across sex, roughly similar

shape being exhibited in males and females (Humphrey et al., 1999; Cheverud, 1998). However, Bastir (2002) reported a higher degree of explanation by sex in mandibular shape, 37% of total variance. As discussed in Chapter 5, it is probable those results stemmed from the fact that Bastir performed a two-dimensional analysis, compared to the three-dimensional analysis here. Interestingly, his values for male and female centroids are two-thirds of the ones generated here, as predicted in the two-dimensional versus three-dimensional analysis (male = 386.4; female = 366). (See Appendix D for centroid numbers for males and females—male mean = 527.9; female mean = 508.6.)

Besides sample, the explanation of the mandible in females is only by relationship to the skull. In other words, the female mandible reflects the overall skull shape more than population, body size, or biomechanical force. This observation generates the hypothesis that larger loading masticatory populations will be more differentiated in males versus females, again tested in H_02 here. The shape of the mandible, as discussed above, is predicted primarily by sex, sample, orbital size, and most importantly, skull shape. Figure 4-8 illustrates the non-isomorphy of the effect of the base and face on the male mandible, the near isomorphy in the female mandible.

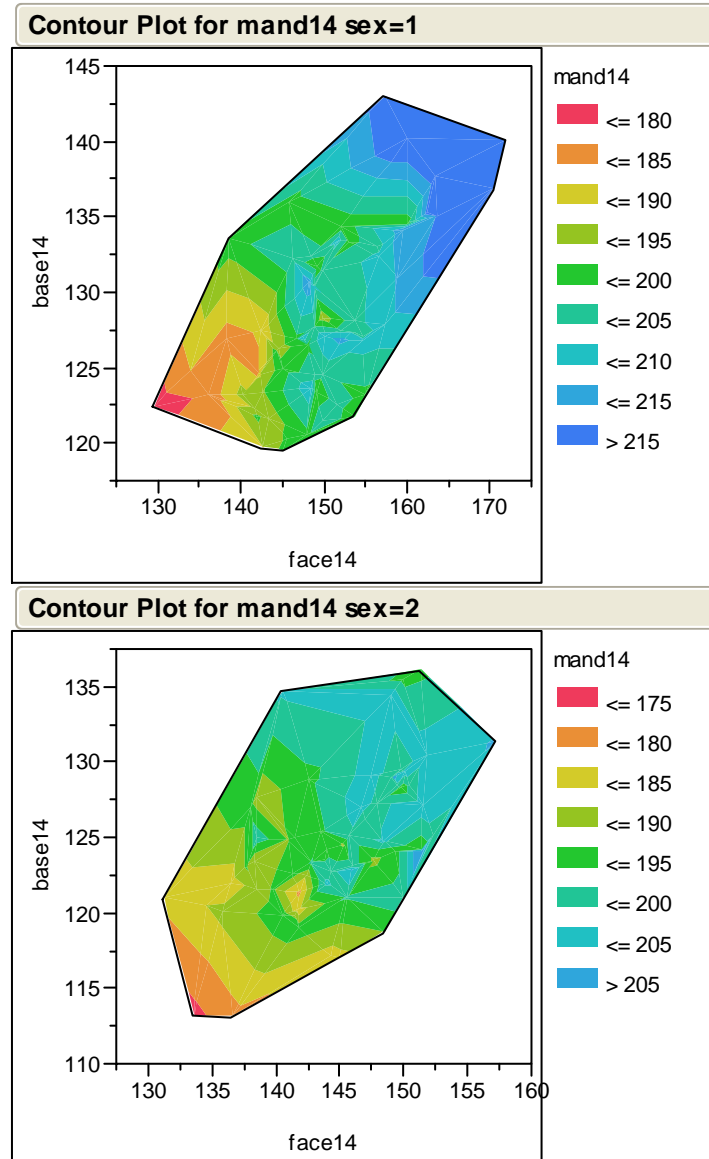


Figure 4-8. Contour Plots for the Mandible in Males (sex = 1) and Females (sex = 2).

The face primarily responds to the influence of both the cranial base and the mandible, with both factors maintaining significance, although the predictive value of the base on the face is much reduced compared to the mandible (mandible $p = 0.0001$ as compared with base $p = 0.052$). Model robusticity increases to $r = 0.715$. Interestingly, both bending strength of the mandible and size of corpus maintain significance (though

weakly), and as expected orbital size remains predictive. Most interestingly, both sex and sample, and sex by sample interaction, become non-significant. As previously discussed this finding is hypothesized to result as valid modules are sampled.

The cranial base responds to both mandibular and facial shape, and though, as in the case of the face, the mandible remains highly predictive, the face is much less so. Bending strength of mandible and size of corpus are still predictive. Model robusticity is much reduced compared to that for the face and mandible, $r = 0.542$. Also most interestingly, both sex and sample, and sex by sample interaction, become non-significant. As discussed further below, this finding is also hypothesized to result as valid modules are sampled.

H₀2: Circumpolar populations will be similar to others in predictive factors producing morphology.

This hypothesis is also rejected. The predictive model for the shape of the mandible is the highest in circumpolar populations ($p = 0.9603$), and orbital area, bending strength of mandible, sex, and corpus area are also predictors. These results contrast highly with those for the mandible in non-circumpolar areas (and results in those populations generally are the same for the global mandibular comparisons). In the non-circumpolar populations cranial base angle is a weakly significant predictive factor.

These results also support Nicholson and Harvati (2006) who demonstrated a major source of variation in the mandible derived from partitioning high dental loading populations such as the circumpolar against other global populations. They found PC1 accounting for 25.04% of the total variance, describing the overall shape of the mandible

with PC2 separating circumpolar populations from all others. The explanation of robust mandibles generally showing higher prediction of morphology from model factors is also supported by results from partitioning male and female mandibles here. Males are approximately $r = 0.6$; females, $r = 0.4$.

At the same time, the mandible itself is the only predictor of significance for the skull in Alaskan populations, suggesting that in more robust populations morphology is tightly integrated, possibly organized to produce anterior loading. These results broadly support Hylander (1979, 1985) and Antón (1995).

It would thus seem that circumpolar mandibles with higher paramasticatory loading do exhibit morphology that allows partitioning from non-circumpolar populations (see Figure 4-17). However, even in these populations, biomechanical vectors are not strong enough predictors of shape to overcome the effects of other integrated regions of the skull. The face and base are significant predictors of mandibular morphology as in all populations, but somewhat less so in circumpolar populations.

Discussion

One of the initial questions addressed in this dissertation was why the biomechanical model fails to robustly explain mandibular morphology. The analysis conducted here shows the biomechanical effects are never as explanatory as cranial modularity, if we consider cranial integration as having two aspects at different hierarchical levels, modularity and/or integration. Even when the circumpolar populations (whose explanation by the biomechanical model is very good) are compared, it is integration or modularity with other parts of the skull that is more significant than biomechanics. The

question therefore is what occurs at levels below traditional modules of the skull. This question is addressed in Chapter 5.

Finally, the Flury hierarchy of the different relationships outlined above is shown in Tables 4-18, 4-19, and 4-20. The Flury hierarchy of the whole skull of circumpolar populations compared to noncircumpolar populations shows the extreme differences of circumpolar populations in morphology. This result is not unexpected given the extreme differences in circumpolar skull and facial morphology, and the fact that matrix similarities across the skull as a whole are not similar (see Chapter 3, Table 3-15).

Table 4-18. Flury Hierarchy of Whole Skulls of Circumpolar and Non-Circumpolar Populations (CPC shows Eskimos compared to skull of others, CPC=2)

Model						
Higher	Lower	Chi Sqr	df	p-val	CS/df	AIC
Equality	Proport	68.118	1	<0.0001	68.118	402.640
Proport	CPC	291.229	6	<0.0001	48.538	336.521
CPC	CPC(5)	0.905	1	0.3414	0.905	57.292
CPC(5)	CPC(4)	1.005	2	0.6049	0.503	58.387
CPC(4)	CPC(3)	3.643	3	0.3027	1.214	61.381
CPC(3)	CPC(2)	14.798	4	0.0051	3.699	63.739
CPC(2)	CPC(1)	13.247	5	0.0212	2.649	56.941
CPC(1)	Unrelated	9.694	6	0.1381	1.616	53.694
Unrelated	—					56.000

The Flury hierarchy of the mandible in circumpolar populations compared to all other global samples presented in Table 4-19 shows these differences are somewhat less than in the skull overall, but it still does not show a pattern comparable to that observed in modules.

Table 4-19. Flury Hierarchy of Mandible in Circumpolar Populations Compared to All Other Samples (Mand14)

Model						
Higher	Lower	Chi Sqr	df	p-val	CS/df	AIC
Equality	Proport	8.582	1	0.0034	8.582	295.335
Proport	CPC	207.661	19	<0.0001	10.930	288.753
CPC	CPC(18)	79.094	1	<0.0001	79.094	119.093
CPC(18)	CPC(17)	0.000	2	>0.9999	0.000	41.998
CPC(17)	CPC(16)	0.000	3	>0.9999	0.000	45.998
CPC(16)	CPC(15)	0.000	4	>0.9999	0.000	51.998
CPC(15)	CPC(14)	0.000	5	>0.9999	0.000	59.998
CPC(14)	CPC(13)	0.000	6	>0.9999	0.000	69.998
CPC(13)	CPC(12)	0.000	7	>0.9999	0.000	81.998
CPC(12)	CPC(11)	0.000	8	>0.9999	0.000	95.998
CPC(11)	CPC(10)	0.000	9	>0.9999	0.000	111.998
CPC(10)	CPC(9)	0.000	10	>0.9999	0.000	129.998
CPC(9)	CPC(8)	0.000	11	>0.9999	0.000	149.998
CPC(8)	CPC(7)	0.000	12	>0.9999	0.000	171.998
CPC(7)	CPC(6)	0.000	13	>0.9999	0.000	195.998
CPC(6)	CPC(5)	0.000	14	>0.9999	0.000	221.998
CPC(5)	CPC(4)	0.000	15	>0.9999	0.000	249.998
CPC(4)	CPC(3)	0.000	16	>0.9999	0.000	279.998
CPC(3)	CPC(2)	0.000	17	>0.9999	0.000	311.998
CPC(2)	CPC(1)	0.000	18	>0.9999	0.000	345.998
CPC(1)	Unrelated	-0.002	19	>0.9999	0.000	381.998
Unrelated	—					420.000

Finally, as was observed in other modular comparisons, even in circumpolar as well as non-circumpolar populations, modularity (or essential conservancy of modular shape) is observed (see Table 4-20 below). In Chapter 3 it was shown that all populations except circumpolar maintained invariance in the face and cranial base to axes of sex and population. Here it is shown that when the full three-dimensional dataset for Morphologika is used, this pattern remains operant even in the circumpolar populations.

The facial module result below demonstrates this, and it also holds for the base (not illustrated).

Table 4-20. Flury Hierarchy of Circumpolar Facial Module

Model						
Higher	Lower	Chi Sqr	df	p-val	CS/df	AIC
Equality	Proport	3.266	1	0.0707	3.266	25.656
Proport	CPC	22.388	14	0.0710	1.599	24.390
CPC	CPC(13)	0.000	1	<0.0001	0.000	30.002
CPC(13)	CPC(12)	0.000	2	>0.9999	0.000	32.002
CPC(12)	CPC(11)	0.002	3	>0.9999	0.001	36.002
CPC(11)	CPC(10)	0.000	4	>0.9999	0.000	42.000
CPC(10)	CPC(9)	0.000	5	>0.9999	0.000	50.000
CPC(9)	CPC(8)	0.000	6	>0.9999	0.000	60.000
CPC(8)	CPC(7)	0.000	7	>0.9999	0.000	72.000
CPC(7)	CPC(6)	0.000	8	>0.9999	0.000	86.000
CPC(6)	CPC(5)	0.000	9	>0.9999	0.000	102.000
CPC(5)	CPC(4)	0.000	10	>0.9999	0.000	120.000
CPC(4)	CPC(3)	0.000	11	>0.9999	0.000	140.000
CPC(3)	CPC(2)	0.000	12	>0.9999	0.000	162.000
CPC(2)	CPC(1)	0.000	13	>0.9999	0.000	186.000
CPC(1)	Unrelated	-0.002	14	>0.9999	0.000	212.000
Unrelated	—					240.000

Summary

This chapter tested a series of model-bound functional predictions and relationships of modules of the skull through two hypotheses. The first hypothesis stated there would be no differences in predictive functional factors for the mandible and the skull. Testing this hypothesis was a necessary first step in examining the hierarchical relationship of the modules of the skull. As was the case in Chapter 3 where it was first tested to see if the mandible could simply be regarded as another cranial element, here in Chapter 4 it was

necessary to see if factors affecting cranial form were identical for the mandible and skull. Had that been the case, further analysis would have been uninformative.

Rejection of the hypotheses was not unexpected, given the results from Chapter 3. The results rejecting H_01 were not trivial insofar as it is necessary, in order to explain modular structure, to first examine shape and factors affecting that shape at all levels of analysis, here starting “top down,” and proceeding to finer and finer levels of analysis. One of the major results was that much of the total variability in macromodules occurs by sample, which is not unexpected because population differences are hypothesized to develop early in ontogeny (Bastir and O’Higgins, 2006; Gonzalez et al., 2010). These results support Bastir et al. (2005), O’Higgins and Jones (1998), O’Higgins et al. (2001), Strand-Vittarsdóttir et al. (2002). Differences in the predictive factors affecting each module were observed and described. Following and building upon the results rejecting H_01 , it was shown different predictive factors affected the traditional modules of face and base, suggesting these two are possible valid modules.

Modular theory predicts modules arise as a means for functional independence of somatic systems. As was discussed in Chapter 2, independence is a prerequisite for structures to evolve while maintaining overall homeostasis. Each developing function can operate semi-independently, but the point is each module must have some degree of different functionality or modular definition is impossible. Here, first macromodules and then modules were described as having different factors producing shape (in being produced by different functions). Second, these different functional effects manifest as covariance matrix differences, as the functions producing the principal components are

not equal. After the covariance matrices are formed, there are several ways to compare their levels of integration; here the Flury hierarchy was used to show the increasing proportionality of structure as modules and parts of modules are compared. This proportionality does not exist for non-modules.

In this dissertation's analysis, the mandible differs from both the facial and cranial base modules, although, as expected— given a higher degree of spatial and functional integration beginning in ontogeny—the mandible and face enjoy a closer (less significantly different) relationship than the mandible and the base.

There are many defining attributes of modules including autonomous genetic organization, hierarchical organization, specific location, connection to other modules, and sequential transformations in development (Raff, 1996; McCollum, 1999; also see Chapter 2). Here it has been demonstrated that robustly defined modules exhibit three properties as well as shared attributes, internal integration, invariance across axes of sex and population, and functional autonomous definition. The mandible and neurocranium are different from face and base individually in that they vary by population and sex, and thus they might be more properly classed not as modules, but as areas possibly formed of two modules. A new definition proposes they are structures integrated with both the face and base together to form macromodules.

CHAPTER 5

MODULAR APPLICATION AND IMPLICATIONS

Research presented here has demonstrated that some regions of skull exhibit three properties that can be used to define them as modules. The properties of internal integration, invariance, and definition by function have been applied to four regions of the skull using four datasets and four primary means of analysis. The four regions, neurocranium, face, cranial base, and mandible have been tested using data from W.W. Howells, I. Hanihara, Fortext (a database constructed from the literature), and three-dimensional digitized data collected at the AMNH and NMNH. Statistical analysis has combined Cronbach's Alpha, the Flury hierarchy, stepwise linear regression, and Partial Least Squares (PLS) to examine patterns and expression of modularity both as statistical probability and biological reality.

The definition of modules by properties has been detailed as a necessary first step in avoiding circularity of analysis, non-repeatability of results, and general confusions in biological science over the meaning of modularity. Several definitions of modules have been used here—areas of integration, areas exhibiting invariance, and areas defined by functional relationships. All these definitions together produce a meaningful biological entity. In this chapter is added a fourth definition, delineation from similar modules in different taxa, which adds the temporal dimension to modular definition. The commonality of all these definitions taken together is that they apply to structure(s) that, in John Hawks's words (speaking on canalization as a useful character for phylogenetic reconstruction), “have a clean distribution of variation—they should vary relatively little within species, but relatively much between species” (Hawks 2006).

If modules fail these basic definitions they are not well defined and useless both as a conceptualizing principle and as a biological reality for two main reasons. First it is possible modules vary highly within species, but if that variability exceeds the patterned variation in morphology (by canalization) at a certain level they become random, and hence incomparable to those in other species. Conversely (and more difficult to test) modules may fail definition in not varying between species, but if they do not then (at least at some level) function never changed and the conception of modularity itself is obviated.

Attributes define “how” entities are; properties measure what they are. Any entity can be defined by attribute, but without a quantifiable property the entity is not a testable unit. The thrust of the dissertation is that modularity provides the only conceptual framework for hypothesis testing in biological morphology that is robust. This is saying nothing new: modularity in the broad sense is simply categorization of structure into constituent parts. What is relatively new is the attempt to explain modularity as the means by which new functions can emerge without systemic disruption (discussed in Chapter 2). Building on this idea, the definition of modules as areas of greater internal integration than external (discussed in Chapters 2 and 3), as areas of relative invariance, and as areas representing function (discussed in Chapters 3 and 4) follows naturally. The final step is to examine a module (here the facial) in other taxa.

All modular definitions by property used herein derive from current discussions and applications of modularity in the literature. These definitions by property are just necessary extensions of modular definitions by attribute into the past and into intraspecies

analysis of patterned expression. It is necessary to understand extant morphology before comparing it to fossil representatives. All biological structures and change in those structures need two organizing aspects, qualification and quantification, that is to say, attribute and property. Without a defined entity which exhibits both, analysis cannot proceed. Attribute cannot be quantified; either “it is or it isn’t” a vertebrate. Similarly, properties cannot be qualified—a measurement approximating 150mm is no “more or less” an average cranial breadth than it is the average rostral length in *Canus familiaris*.

This chapter extends the definition by property for modules to different taxa, looks for the reason why the mandible is not a module, examines patterning that may underlie modularity itself, and finally shows that the way modularity itself is measured influences the way it is defined. Without these final extensions, even definition of modularity by property is uninformative: it requires functional differences from other modules for modules to have meaning, it requires a reason why the mandible is not a module rather than simply showing it isn’t, it requires some form of explanation for emergence of the current pattern of modularity, and finally it needs to be assessed as to how measurement itself affects definition. Hawks (2006) observes, “We should be aware that the kinds of characters that tend to be most useful for phylogenetic reconstruction will have certain evolutionary characteristics.” This chapter attempts to define those characteristics.

Earlier chapters demonstrated that some regions of skull exhibit three properties that can be used to define them as modules. The face and cranial base are internally integrated, they remain invariant to the axes of sex and population when assessed by their covariance structure, and they can be defined by function in their relationship to other areas of the skull. The neurocranium, in contrast, was shown to be internally integrated,

but was shown to be bimodal in distribution across sex, and non-proportional in covariance structure across sex and population. This variability (in contrast to the patterned variation of modules) likely results from the neurocranium either consisting of more than one module (response to ecogeographical patterning suggests this) or could possibly result from under-definition by use of Howells's data. That is unlikely given it was shown in Chapter 3 that the Howells data actually has redundancy; Cronbach's Alpha gives results commensurate with too many, rather than too few, measured points. The mandible itself is discussed separately below, but it primarily fails the tests of modularity in not being internally integrated, not being invariant to the axes of sex and population, and probably being representative of more than one function (also tested below).

The discussion in this chapter is divided into four sections:

1. Mandibular Modularity

This section further details results from earlier chapters that demonstrated the modern mandible is not a module. These results generally support earlier research in other taxa suggesting the mandible is comprised of two modules (Atchley et al., 1985; Leamy 1993; Cheverud et al., 1997; Mezey et al., 2000; Klingenberg et al., 2003). Results herein broadly support earlier research in suggesting there are two major developmental areas, the ramus and the corpus in humans (or the alveolar process and ramus in Rodentia), with the **difference being that in humans neither area can be adequately defined as a module**. Additionally, the results to this point of the investigation show the contribution of biomechanical force to the morphology of the mandible is relatively small, thus addressing the original question taken up by this

dissertation: why is the biomechanical model insufficient to explain mandibular morphology? The results here show biomechanical vectors are not highly explanatory of morphology, and they are most likely secondary to modular structure in formation of morphology.

2. Modular Taxon Specificity

The second section expands the current definition of modules because it includes taxon-specificity among the properties of modules detailed in earlier chapters. As modules represent changing functional organization through time, as previously discussed, this taxon-specificity may be assumed to be a necessary property of modules.

3. Cranial Nerve Patterning and Foramina

The third section builds on taxon specificity to theorize and test cranial organization that may underlie modularity itself. In this section it is demonstrated that the cranial nerve patterning in development of the skull is the equivalent of a module in that it is invariant, highly explained by model formation, and functional in providing the original structure underlying all succeeding functions. It is hypothesized here that the cranial nerve (CN) patterning, being primitive, represents fundamental organization antecedent to present modularity, being a source of constraint therein. If so, this might mean that unlike modules, CN patterning, if primitive in the Hominidae, is probably specific to the sub-family level.

4. Dimensionality

Last, the fourth section discusses dimensionality as a factor that must be addressed in modular study. A robust definition of a three-dimensional structure requires a three-dimensional definition. The underlying principle is that globally the skull varies more on the width axis than the other two axes. Analysis that removes this source of variability or treats it as inconsequential may be compromised. It is shown here that changes in dimensionality of measurements can change results when PCA is performed for individuals representing taxa in the Flury hierarchy analysis. This phenomenon indicates that three-dimensional analysis covariance structure is not the same as that derived from two dimensions. Covariance matrices derived from this reduced source of information (two dimensions) are not equivalent to matrices constructed in three dimensions. By extension this observation means phylogenetic analyses failing to control for this factor are possibly compromised.

Mandibular Modularity

The first question addressed in this dissertation concerned the morphology of the mandible. Definitions for morphology were discussed in light of biomechanical and integrative models. The original suggestion was that the mandible could not be explained solely with a biomechanical model and that the summation of morphology might be better explained through integration with the remainder of the cranium. This question was then addressed by inclusion of the mandible as a possible module. Results presented in earlier chapters have shown the mandible, although partially integrated with the remainder of the cranium, does not fit a robust definition of a module, showing high variability across sex and population and possibly dual functions. The question then

becomes whether the mandible is composed of two modules, as suggested to be the pattern in Rodentia (Atchley et al., 1985; Leamy, 1993; Cheverud et al., 1997; Mezey et al., 2000, Klingenberg et al., 2003), one module combined with a non-modular area, or two non-modular areas. This dissertation's results support previous research in suggesting that in humans, as well as in other taxa, there are two major developmental areas in the mandible, as proposed by earlier lines of research (Lin 1993; Hans and Enlow, 1996; Nicholson and Harvati, 2006). It may be more likely the corpus is a module given presence of the alveolar process and lack of nasopharyngeal spatial requirements which are exhibited by the ramus. The ramus in turn, probably responds directly to biomechanical effects in transmitting force for *mm temporalis*. Corpus and ramal areas have been distinguished as separable morphological units in *H. heidelbergensis* (Rosas, 2001), and prediction under an integrated architectonic model suggests the ramal width should correlate with nasopharyngeal requirements as well as body mass and the middle cranial fossa (Hans and Enlow, 1996; Estenson, 1999). Here the mandibular regions of corpus and ramus are tested for shared covariance structure and by stepwise regression. Two 8-point subsets (of the original 14-point datasets in Chapters 3 and 4) were constructed for each area (see Appendix C). Table 5-1 presents the comparisons of the ramus versus the corpus. There is no shared proportional covariance structure, as would be expected from the internal structure in a single module. This result disproves the idea that the mandible is a unitary unit, but does not prove the ramus and corpus are modules, as modules are expected to exhibit this differential Flury structure.

Table 5-1. Flury Hierarchy of the Ramus Compared with the Corpus

Model						
Higher	Lower	Chi Sqr	df	p-val	CS/df	AIC
Equality	Proport	0.943	1	0.3315	0.943	60.449
Proport	CPC	50.234	12	0.0000	4.186	61.506
CPC	CPC(11)	9.272	1	0.0023	9.272	35.272
CPC(11)	CPC(10)	0.000	2	1.0000	0.000	32.000
CPC(10)	CPC(9)	0.000	3	1.0000	0.000	28.000
CPC(9)	CPC(8)	0.000	4	1.0000	0.000	38.000
CPC(8)	CPC(7)	0.000	5	1.0000	0.000	46.000
CPC(7)	CPC(6)	0.000	6	1.0000	0.000	56.000
CPC(6)	CPC(5)	0.000	7	1.0000	0.000	68.000
CPC(5)	CPC(4)	0.000	8	1.0000	0.000	82.000
CPC(4)	CPC(3)	0.000	9	1.0000	0.000	98.000
CPC(3)	CPC(2)	0.000	10	1.0000	0.000	116.000
CPC(2)	CPC(1)	0.000	11	1.0000	0.000	136.000
CPC(1)	Unrelated	0.000	12	1.0000	0.000	158.000
Unrelated	—					182.000

The bivariate plot and correlation table below show a high degree of correlation and explanation of the morphology of the corpus by the ramus. There is approximately 57% explanation of form with a correlation between the two regions of 0.7571 (see Figures 5-1 and 5-2 ; Tables 5-2 and 5-3).

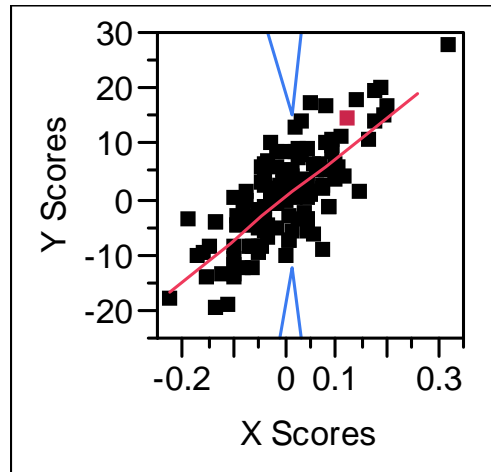
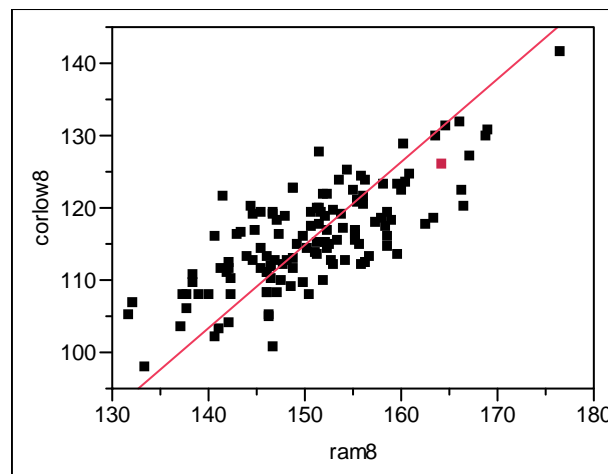


Figure 5-1. PLS Scores

Table 5-2. Partial Least Squares – Percent Variation Explained, Corpus by Ramus

No.	X	X-Plot	Cumulative X	Y	Y-Plot	Cumulative Y
1	100	<div style="width: 100%; height: 10px; background-color: red;"></div>	100	57.32	<div style="width: 57.32%; height: 10px; background-color: red;"></div>	57.32



— Orthogonal Fit Ratio=0.000

Figure 5-2. Bivariate Fit of Cor8 By Ram8

Table 5-3. Orthogonal Regression of Cor8 By Ram8

Variable	Mean	Standard Deviation
Ram8	150.732	8.138105
Cor8	115.7191	7.056548
Correlation	Intercept	Slope
0.7571	-56.9167	1.145316

Tables 5-4 and 5-5 show the stepwise fit for the ramus (Ram8) and the corpus (Cor8). These results show that both the corpus and the ramus respond to both population and sex in expression of morphology. These results indicate neither the mandible itself nor the two major divisions into corpus and ramus exhibit the stability and invariance of modules.

It is possible to hypothesize that areas as responsive to biomechanical vectors as these areas are never modules; see the discussion of the neurocranium in Chapter 4. Table 4-17 showed that highly loaded facial structures such as the face in circumpolar populations are well explained by biomechanics, experiencing loading throughout, yet retain modular invariance. The simple increase in biomechanical force vectors in the circumpolar population increases the predictability of the mandible by biomechanics (more than 95% of all variability in the mandible is explained). At the same time the facial and cranial base modules do not become variable. This result suggests that biomechanical force vectors cannot swamp the phylogenetic signal of modularity, even in the most highly loaded populations. The face and base remain invariant across sex and population even within the circumpolar populations (in three-dimensional analysis) while the mandible (and ramus and corpus individually) does not. These results broadly support the high degree of explanation of morphology in circumpolar populations through masticatory and paramasticatory use originally demonstrated in Hylander's (1976) predictions. However, here it is shown that, although predictive, biomechanical factors are less predictive than integrative ones; biomechanical vectors do not swamp integration.

The results in Tables 5-4 and 5-5 show that although the ramus and corpus are separate areas, they do not meet robust definitions of modularity, being highly influenced by sample (stepwise regression control probability r = approximately 0.7 for both).

Table 5-4. Stepwise Fit for Factors Producing Ramus

Current Estimates							
SSE	DFE	MSE	R Square	R Square Adj	Cp	AIC	
2007.1707	120	16.726423	0.7651	0.7474	7.7438811	375.8031	
Parameter		Estimate	nDF	SS	“F Ratio”	“Prob>F”	
Intercept		-4.715491	1	0	0.000	1.0000	
Sample{5&7&9-3&6&8&4&1&2&1.06}		-0.9927091	6	830.8722	8.279	0.0000	
Sample{5-7&9}		0	1	23.58807	1.415	0.2366	
Sample{7-9}		0	2	65.33669	1.985	0.1419	
Sample{3&6&8-4&1&2&1.06}		-1.070922	5	678.8177	8.117	0.0000	
Sample{3-6&8}		-2.90634	1	273.1306	16.329	0.0001	
Sample{6-8}		0	1	0.538472	0.032	0.8585	
Sample{4&1-2&1.06}		-1.3653516	3	479.0327	9.546	0.0000	
Sample{4-1}		3.26677628	1	341.6649	20.427	0.0000	
Sample{2-1.06}		-6.0616017	1	127.1545	7.602	0.0067	
Sex{2-1}		0	1	7.215257	0.429	0.5136	
Cranang		0	1	0.003316	0.000	0.9888	
Orb		0	1	1.602357	0.095	0.7584	
Manar		0	1	15.43624	0.922	0.3388	
I _{max}		0	1	18.95125	1.134	0.2890	
I _{min}		0	1	27.31404	1.642	0.2026	
Angle		0	1	18.35571	1.098	0.2968	
Base14		0.34818632	1	243.9122	14.582	0.0002	
Face14		0.2608278	1	165.6274	9.902	0.0021	
Cor8		0.63119075	1	165.6274	47.879	0.0000	
Step History							
Step	Parameter	Action	“Sig Prob”	Sequence SS	R Square	Cp	p
1	Cor8	Entered	0.0000	4896.925	0.4372	87.915	2
2	Face14	Entered	0.0000	644.1144	0.6486	52.13	3
3	Sample{4-1}	Entered	0.0010	415.5331	0.6972	35.754	7
4	Sample{3-6&8}	Entered	0.0005	247.0804	0.7261	23.26	8
5	Base14	Entered	0.0009	205.531	0.7502	13.203	9
6	Sample{2-1.06}	Entered	0.0067	127.1545	0.7651	7.7439	10

Table 5-5. Stepwise Fit for Factors Producing Cor8

Current Estimates							
SSE	DFE	MSE	R Square	R Square Adj	Cp	AIC	
2064.4703	125	16.515763	0.6768	0.6683	10.180753	369.4623	
Parameter		Estimate	nDF	SS	“F Ratio”	“Prob>F”	
Intercept		18.0910935	1	0	0.000	1.0000	
Sample{5&7&1.06&6&8&4&9-3&1&2}		-2.8919439	2	698.6086	21.150	0.0000	
Sample{5&7&1.06-6&8&4&9}		0	7	91.03599	0.778	0.6072	
Sample{5-7&1.06}		0	7	91.03599	0.778	0.6072	
Sample{7-1.06}		0	7	91.03599	0.778	0.6072	
Sample{6&8&4-9}		0	7	91.03599	0.778	0.6072	
Sample{6-8&4}		0	7	91.03599	0.778	0.6072	
Sample{8-4}		0	7	91.03599	0.778	0.6072	
Sample{3&1-2}		-1.3819942	2	698.6086	0.2150	0.0000	
Sample{3-1}		0	7	91.03599	0.778	0.6072	
Sex{2-1}		0	1	51.08017	3.146	0.0786	
Cranang		0	1	5.696978	0.0343	0.5591	
Orb		0	1	27.20721	1.656	0.2005	
Manar		0	1	1.111233	0.067	0.7965	
I _{max}		0	1	5.492894	0.331	0.5662	
I _{min}		0	1	14.27024	0.863	0.3547	
Angle		0	1	0.752352	0.045	0.8320	
Base14		0.51117493	1	984.0705	59.584	0.0000	
Face14		0.18700363	1	77.4748	4.691	0.0322	
Step History							
Step	Parameter	Action	“Sig Prob”	Sequence SS	R Square	Cp	p
1	Face14	Entered	0.0000	3514.327	0.5471	57.448	2
2	Sample{3&1-2}	Entered	0.0000	767.2658	0.6665	13.066	4
3	Base14	Entered	0.0322	77.4748	0.6786	10.181	5

In the results above, the biomechanically influenced variables—I_{max}, I_{min}, manar—fail to achieve significance as predictors for either the ramus or the corpus. This finding confirms results introduced in Chapter 4 showing relatively little effect on mandibular morphology from biomechanical vectors in non-circumpolar populations.

Modular Taxon Specificity

The second section extends the definition for modularity to include taxon-specificity. Results introduced below suggest the facial module in *Homo* exhibits a unique pattern that differs from the module in non-*Homo* taxa. Results here tend to support recent research suggesting modules can be used for phylogenetic analysis (González-José et al., 2008). Looked at from a perspective of evolutionary sequence, modules are taxon-specific representations of changing function and structural organization of the skull. Phylogenetic modeling using modules can provide a way to assess variation through time in taxa without using the entire skull all at once.

Here a comparison is made of the facial module from 180 samples digitized with Morphologika 2.5 of modern humans to the facial module in non-*Homo* and archaic *Homo* individuals, using a three-dimensional analysis and Flury hierarchical comparisons. Results below show the facial module meets all definitional requirements for modularity introduced previously (definition by function; invariance; delineated function in an analytical model [$r > 0.7$]). Here it is shown that the facial module also meets the definition of a taxon-specific modular structure. This result is demonstrated below as supported by the similarity of the module to 12 archaic representatives of *Homo* (with Neandertals included) and discrimination from the archaic non-genus *Homo* representatives.

This section details the testing of the final criterion proposed for a robust definition of modularity, taxon-specificity. As was previously discussed, current research has begun to emphasize the fact that modules can be used to model evolutionary process, and recently the broad outlines of hominine evolution have been recreated in a cladistic analysis using modular characters in combination (González-José et al., 2008). Although the main

import of the article was to demonstrate the applicability of the use of continuous variables to cladistic analysis, results were interesting in showing how change in modules represents changing functions through time. Here, three-dimensional data were extracted from the publication, portioned, and reanalyzed here as modules.

Figure 5-3 is the lateral view of the anterior facial module and mandibular region in modern humans ($n = 180$).

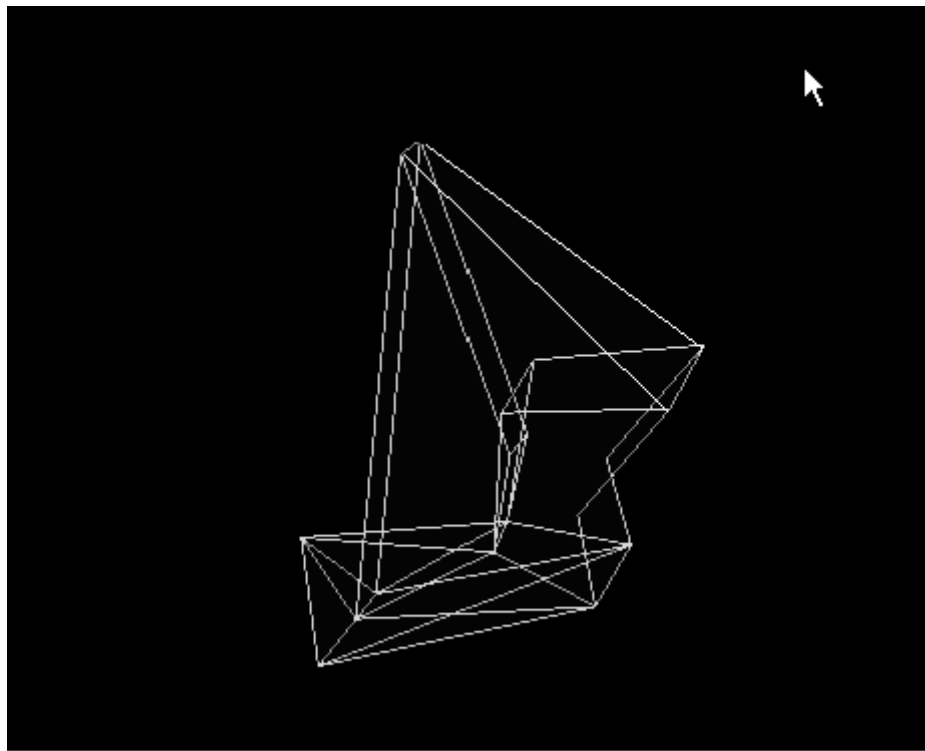


Figure 5-3. Anterior facial block and mandible, 24 landmarks (screen capture from Morphologika 2.5).

The modules used by González-José et al. (2008) are all ones mentioned previously in Chapter 2 as exemplifying the major reorganizational factors operating during the Pleistocene to form the skull in *Homo*—facial retraction (anterior rotation); flexure of the

cranial base; changes in the masticatory apparatus; and increasing globularity of the skull.

Table 5-6 lists the points defining anterior rotation in González-José et al. (2008).

Table 5-6. Points used by Gonzalez-José et al. (2008) for face, in Common with This Dissertation's Morphologika Dataset

Landmark No.	Name	Definition
1	Prosthion	The midline point at the most anterior point on the alveolar process of the maxillae
2	Ectomolare	The most lateral point on the alveolar border (left)
3	Subspinale	The most posterior point in the concavity between the anterior nasal spine and prosthion, i.e., apical base
4	Alare	The most lateral point on the margin of the nasal aperture (left)
5	Nasion	The midline point where the two nasal bones and the frontal intersect
6	Maxillofrontale	The point where the anterior lacrimal crest of the maxilla meets the frontomaxillary suture (left)
7	Frontomolare orbit	The point where the fronto-zygomatic suture crosses the inner orbital rim (left)
8	Glabella	The most anterior midline point on the frontal bone, usually above the frontonasal suture
9*	Opisthocranium	The posterior-most point of the skull in the medial sagittal plane; the farthest chord length from glabella
10	Posterior nasal spine	The posterior terminus of the palatal plane
11	Alveolar point	Posterior limit of the maxillary alveolar arch at the pterygoalveolar suture (left)

* Landmark 9 opisthocranium was included in González, et al.-José et al.'s facial module to provide a reference point for anterior rotation. It was excluded here as it is not part of the facial module. All other points reflect the anterior facial block from the Morphologika 2.5 database illustrated in Figure 5-3 above.

The implication of the article is important because, while the sample sizes are small, it is an effort to begin to tease apart factors operating independently to a degree to produce morphology, and, as has been shown here, analysis can be compromised if explicit level of hierarchical analysis is lacking. The data from González-José et al. (2008) are used here (see Table 5-6 above) to test the idea the face not only meets the criteria for a module previously discussed, but also has a different modular pattern than that of terminal Pliocene and Pleistocene non-*Homo* individuals, and a similar modular pattern

to later Plio-Pleistocene representatives of *Homo*. Published three-dimensional coordinates of the face using data from González-José et al. (2008) using Morphologika 2.5 were loaded into Morphologika 2.5 by this researcher and compared to the three-dimensional modern human sample used in Chapters 3 and 4. (Full details for Morphologika 2.5 in terms of usage, program, and data analysis are in Appendix D.) The Flury hierarchy was used to compare the covariance matrices from the fossils to the covariance from the modern humans. The results in Tables 5-8 and 5-9 suggest hierarchical comparisons can be extended to other taxonomic levels besides species. Other results expanding on results here appear below in the Dimensionality section of this chapter.

Table 5-7. List of Specimens (from Gonzalez-José et al. 2008)

<i>Non-Homo</i>	<i>Homo</i>
CTL-004 Gorilla gorilla 9–0 { Ggor}	KNMER 1470 <i>Homo rudolfensis</i> 2.5–1.8 Hrud
CTL-006 Pan troglodytes 8–0 { Ptro A.L. 444-2 (reconstruction) Australopithecus afarensis \$3.7–3.0 Aafa	KNMER 1813 <i>H. habilis</i> 2.1–1.5 Hhab
Sts 5 <i>A. africanus</i> ca. 3.0–2.5 Aafr	KNMER 3733 <i>H. ergaster</i> 2–1 Herg
KNMER-406 <i>Paranthropus boisei</i> \$2.3–1.4 Pboi-406	Zhoukoudian { <i>H. erectus</i> 1.8–0.03 Here
OH 5 <i>P. boisei</i> \$2.3–1.4 Pboi-OH5	D2700 <i>H. erectus</i> / <i>H. ergaster</i> 1.8 Here-Herg
SK 48 <i>P. robustus</i> ca. 1.5–2.0 Prob	Steinheim <i>H. heidelbergensis</i> 0.8–0.2 Hhei-S
WT 17000 <i>P. aethiopicus</i> ca. 2.7–2.3 Paet	Kabwe, Broken Hill 1 <i>H. rhodesiensis</i> 0.8–0.2 Hrho
	Atapuerca 5 <i>H. heidelbergensis</i> 0.8–0.2 Hhei-A
	Gibraltar 1, Forbes' Quarry <i>H. Neandertalensis</i> 0.2–0.03 Hnea-G
	La Chappelle-aux-Saints 1 <i>H. Neandertalensis</i> 0.2–0.03 Hnea-LC
	La Ferrassie 1 <i>H. Neandertalensis</i> 0.2–0.03 Hnea-LF
	Patagonian, Rý 'o Negro#797 <i>H. sapiens</i> 0.2–0 Hsap

Table 5-8. Flury Hierarchy of Modern *Homo sapiens* versus non-*Homo* (12 facial measurements)

Model						
Higher	Lower	Chi Sqr	df	p-val	CS/df	AIC
Equality	Proport	26.842	1	0.0000	26.842	125.152
Proport	CPC	78.360	7	0.0000	11.194	100.310
CPC	CPC(6)	19.950	1	0.0000	19.950	35.950
CPC(6)	CPC(5)	0.000	2	0.9999	0.000	18.001
CPC(5)	CPC(4)	0.000	3	1.0000	0.000	22.000
CPC(4)	CPC(3)	0.000	4	1.0000	0.000	28.000
CPC(3)	CPC(2)	0.000	5	1.0000	0.000	36.000
CPC(2)	CPC(1)	0.000	6	1.0000	0.000	46.000
CPC(1)	Unrelated	0.000	7	1.0000	0.000	58.000
Unrelated	—					72.000

Table 5-9. Flury Hierarchy of Modern *Homo sapiens* against Pleistocene *Homo*

Model						
Higher	Lower	Chi Sqr	df	p-val	CS/df	AIC
Equality	Proport	0.209	1	0.6475	0.209	14.725
Proport	CPC	7.494	7	0.3793	1.071	9.515
CPC	CPC(6)	0.022	1	0.8825	0.022	16.022
CPC(6)	CPC(5)	0.000	2	1.0000	0.000	18.000
CPC(5)	CPC(4)	0.000	3	1.0000	0.000	22.000
CPC(4)	CPC(3)	0.000	4	1.0000	0.000	28.000
CPC(3)	CPC(2)	0.000	5	1.0000	0.000	36.000
CPC(2)	CPC(1)	0.000	6	1.0000	0.000	46.000
CPC(1)	Unrelated	0.000	7	1.0000	0.000	58.000
Unrelated	—					72.000

The results in Tables 5-8 and 5-9 show the Flury hierarchical comparisons of the principal component eigenvectors of 180 modern humans to, first, the PCA eigenvectors of the non-*Homo* individuals from González-José et al. (2008), followed by comparison to the *Homo* individuals. Although the results are very preliminary, the comparison above shows there is a quantifiable difference in the module of the face at taxonomic levels above the species. In the *Homo sapiens*–non-*Homo* comparison there is shared matrix

structure at the level of six principal components. In the within *Homo–Homo sapiens* comparison there is proportionality or near proportionality of the matrices suggesting conserved invariance of facial shape. Although González-José and colleagues (2008) do not suggest it, this taxon-specificity should be a defining characteristic of modules, as genera-level or above morphological change results in major reorganizational configurations. This idea was discussed in depth in Chapters 2 and 3. Further exploration of the pattern of modularity is discussed below in the section on dimensionality.

Cranial Nerve Patterning and Foramina

In eutherian mammals, development of the central nervous system (CNS) precedes subsequent development, providing a stable unified structure (Smith K, 1996; de Graaf-Peters and Hadders-Algra, 2006). As discussed above this is the fundamental organizational system for both the splanchnocranium and basicranium. Therefore the facial and basicranial foraminal patterning developing early in ontogeny can be expected to maintain aspects of constraint through life. Recent results suggest this pattern is observable and loads differently in multivariate space than in mechanically influenced regions of the skull (Anderson, 2000). Konisberg and colleagues (1993) have shown that cranial modification affecting cranial modules does not produce significant differences in foraminal position. Foraminal patterning is an example of what Mitteroecker and Bookstein (2008) describe as conserved developmental processes in hominoids. In addition to providing the probable pattern antecedent to modularity in the skull, the foramina are unique in all being robust “Type 1” points as described by O’Higgins (1999), possessing biological relevance, repeatability, and surety of measurement

gathering. They are thus highly valid Type 1 points necessary for repeatability of measurements and replication of results.

Figure 5-4 illustrates the area bounded by the facial foramina, and Figure 5-5 presents a frontal view of the foramina as derived from Morphologika 2.5. Figure 5-6 shows the positioning of the supraorbital, infraorbital, and mental foramina (the illustration is misleading, as the Morphologika 2.5 illustration shows, because in lateral view the foramina form a straight line, and in frontal view they nearly form a rectangle). Interestingly, the basicranial and facial foramina maintain an angle of 90 degrees to each other, another possible example of invariant relationships in the skull.

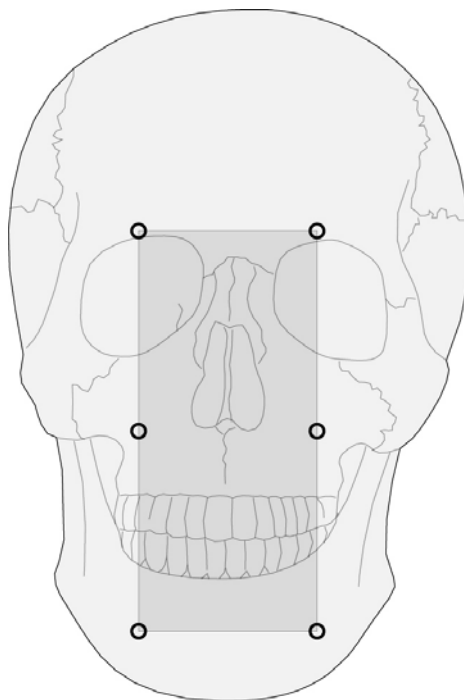


Figure 5-4. Area Bounded by Facial Foramina

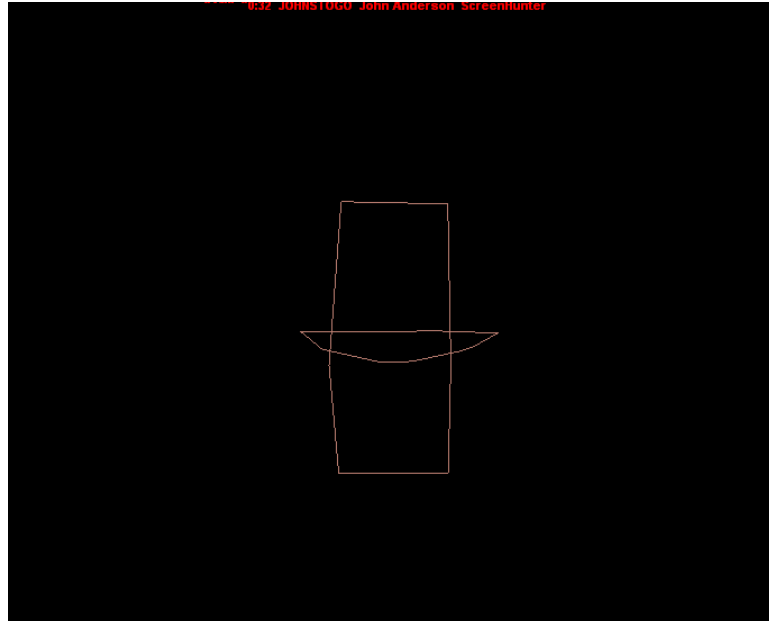


Figure 5-5. Anterior View of Constrained Area Bounded by Facial Foramina (screen capture from Morphologika 2.0)

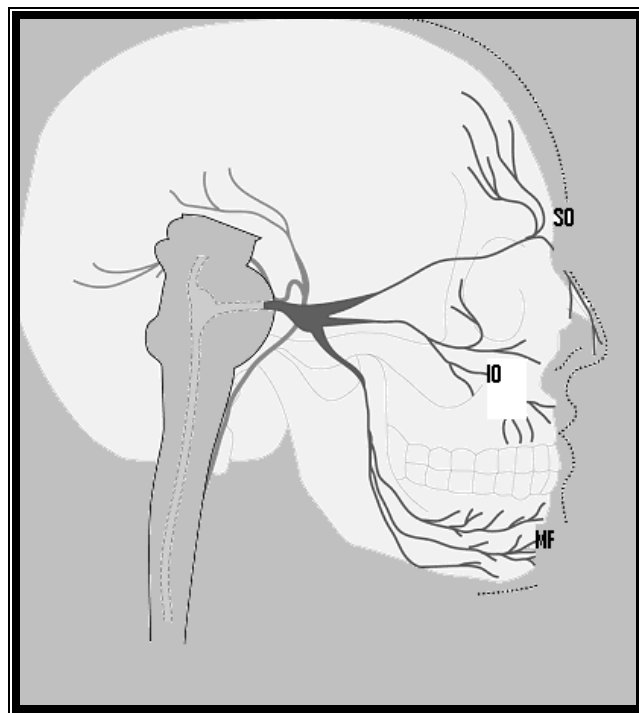


Figure 5-6. Lateral View of Supraorbital (SO), Infraorbital (IO), and Mental Foramina (MF)

Table 5-10 shows that the foramina pattern in the skull does not respond to any of the functional, population, or structural predictors for the skull.

Table 5-10. Stepwise Fit for Foramina Pattern in Morphologika 2.5 (stepwise fit for foramina16, probability to enter 0.05 and probability to leave 0.05; 5 rows not used due to excluded rows or missing values)

Current Estimates							
SSE	DFE	MSE	R Square	R Square Adj	Cp	AIC	
1417.963	122	11.622647	0.8936	0.8512	8.6120671	309.5829	
Parameter		Estimate	nDF	SS	“F Ratio”	“Prob>F”	
Intercept		25.2037797	1	0	0.000	1.0000	
Sample{5&7&8&4&6&9&3-2&1}		0	1	0.625615	0.053	0.8176	
Sample{5-7&8&4&6&9&3}		0	1	14.95626	0.640	0.5293	
Sample{7&8-4&6&9&3}		0	2	17.46541	0.495	0.6867	
Sample{7-8}		0	3	32.22666	0.686	0.6030	
Sample{4&6&9-3}		0	4	59.11045	1.283	0.2805	
Sample{4-6&9}		0	4	69.64111	1.209	0.3094	
Sample{6-9}		0	5	109.4111	1.617	0.1487	
Sample{2-1}		0	6	3.755106	0.159	0.8529	
Sex{2-1}		0	2	22.37209	1.940	0.1663	
Cranang		-0.1190353	1	62.85785	5.408	0.0217	
Orb		0	1	18.75862	1.622	0.2052	
Manar		0	1	0.391624	0.033	0.8552	
I _{max}		0	1	0.242081	0.021	0.8859	
I _{min}		0	1	0.004115	0.000	0.9851	
Angle		0	1	1.7931	0.153	0.6962	
Skull28		0.78547706	1	8269.066	711.461	0.0000	
Ufac9		0	1	20.12994	1.742	0.1893	
Step History							
Step	Parameter	Action	“Sig Prob”	Sequence SS	R Square	Cp	p
1	Skull28	Entered	0.0000	8206.328	0.8781	12.269	2
2	Cranang	Entered	0.0217	62.85785	0.8836	8.6121	3

This is a highly explanatory model and probably samples the primitive architecture of *Homo*. It may well be expected that cranial base angle is explanatory, as this angle also

develops early in ontogeny and is constrained in *Homo*. The only other model as explanatory as this one was the biomechanical model for the face and mandible of circumpolar populations. The other predictor is also interesting: Skull28 is the shape of most of the facial, neurocranial, and mandibular regions together, and the pattern shows a relationship with the foramina of the skull, probably by fundamentally preceding all later growth. (The caveat is some of the foramina are mirrored in the comparative sample).

It is interesting that, out of all the comparisons of factors influencing models, two stand out. The pattern of prediction of circumpolar facial and mandibular morphology by biomechanics was extremely strong ($r > 0.9$). Here, the pattern of prediction, by very different factors for the possible underlying structure of the skull, is nearly equally high ($r > 0.85$).

These results could in a way be considered as a return to the original question addressed in the thesis—why the biomechanical model is a necessary, yet insufficient, model for prediction of the mandible and face. Results in this thesis have shown that generally biomechanics are not good predictors of morphology, becoming strong only in extreme cases such as the circumpolar populations. It is hard to posit a pattern in the skull that is less influenced by biomechanics than foraminal pattern, as it completely precedes the development of all muscles. One way to regard these results is to regard them as the poles of variation in the skull. It may be at the hierarchical level below that of modularity when whole skull integration again becomes the chief organizing factor. This might mean the cranial foramina pattern and cranial base angle may represent the fundamental integration pattern in the skull of *Homo*. Results here, coupled with the results on

circumpolar prediction of morphology by biomechanics, show why the dichotomy between biomechanical analysis and structural analysis exists. At one extreme of the spectrum biomechanical model is more explanatory than any other. At the other extreme, at the level of fundamental integration patterns in the skull, the structural model is highly explanatory. In between these poles is where modularity operates most efficiently. Support for this idea is drawn from recent research suggesting phenotypic change occurs most efficiently when change is neither constrained by earlier developing, canalized relationships nor by recent adaptations (Eroukmanoff and Svensson, 2008). As was discussed in Chapter 2 current evolutionary theory predicts change occurs at the level of “least resistance,” here hypothesized as in, not across, modules.

Dimensionality

Dimensionality of measurements is the final factor that must be addressed in modular study. A robust definition of a three-dimensional structure requires a three-dimensional definition. Across the world the skull varies more on the axis of width than on the axes of length and height (Wolpoff 2000; demonstrated in Chapter 3). This fact has implications for modular definition and study in that much analysis simply removes this source of variability and analyzes three-dimensional structure in two dimensions (Bastir et al., 2006; Bookstein et al., 2003; Bastir and Rosas, 2005; Gonzalez et al., 2010). When lateral radiographs are employed it is thus the most variable axis which is removed, and, as was discussed in Chapter 3, this factor alone makes analysis of morphological structure somewhat problematic. The question that has not been previously addressed is to what degree use of two-dimensional analysis is commensurate with that derived from three

dimensions. It is shown here that phylogenetic hypotheses of modular relationship derived from two-dimensional analysis are not equivalent to those from three dimensions.

There are two main aspects to this basic problem of dimensionality. First, as discussed before, lateral radiographs are missing the most variable axis (the mediolateral axis; here referred to as the Y-axis). Second, there is a related problem which seems superficially the same—much research simply records and uses data from one side of the skull, recording three-dimensional coordinates from but one-half of the skull and sometimes mirroring (González-José et al., 2008).

Therefore there are three primary methods for collecting dimensional data for the skull:

1. Data collected from one side of the skull in three dimensions (such as the original data from González-José et al. [2008], 46 points, used in Figure 5-7)
2. Data collected from both sides of the skull in three dimensions (in this study represented by mirrored data; González-José et al.'s [2008] data mirrored to make a three-dimensional skull, under the assumption of bilateral symmetry, used in Figure 5-8)
3. Data collected from one side of the skull in two dimensions only (as is typically done with lateral radiographs; here represented by complete removal of the mediolateral Y-axis from analysis; simple analysis of González-José et al.'s [2008] data without the Y-axis, used in Figure 5-9).

It is readily apparent that datasets 1 and 3 do not define the same object in the same way. The collection of one side of the skull in three dimensions (Method 1) is not the same as never collecting the Y-axis data in the first place (as in Method 3) because the

additional Y-axis dimension contributes—slightly, if bilateral points are few—to representational position variability. Therefore lateral radiographs which never had Y-axis data will give different results from a three-dimensional representation of the same three-dimensional object. In the broad sense a three-dimensional structure analyzed in two dimensions is missing 33% of information if the three dimensions are roughly equivalent in size. This point is illustrated by the fact that biological structure is usually analyzed in PCA after the isometric removal of size based on all three axes (O’Higgins et al., 1999). Removal of the isometric commonality of all measurements in three dimensions and then analyzing two dimensions is not the same as removing the allometric commonality from two dimensions originally. The PCA structure is not the same. By extension, this means phylogenetic analyses failing to control for this factor are likely to be compromised. In order to explicate the effect of dimensionality on phylogenetic hypotheses, a series of comparisons of various taxonomic relationships is depicted below. The data matrices in this part are not analyzed; the illustrations are only used to show how hypothesized taxonomic relationships can change with dimensionality of measurements. Obviously the PCA covariance matrices underlying the displays change as well, but full statistical analysis of them is not performed in this first part of this section.

Data used are derived from the published source González-José et al. (2008). There are two primary analyses:

1. The first analysis depicts the relationships of taxa using individual specimens to represent taxa ($n = 20$). The analysis shows positioning of representative members of taxa after procrustes removal and PCA in Morphologika 2.5.

Specimens included are *Homo sapiens*; *Gorilla gorilla*; *Pan troglodytes*; *Aust. Afarensis*; *Aust. africanus*; *P. boisei*406; *P. boisei*405; *P. aethiopicus*; *P. robustus*; *H. rudolphensis*; *H. Habilis*; *H. ergaster* (*KnM-Er 3733*) / *H. erectus* / *Dmanisi 2600* / *H.s.n Gibralter, La Chappele, La Ferrasie* / *H. hei Broken Hill, Stenheim, Atapuerca* 5. The formal species attributions for these 20 individuals are controversial in some cases (González-José et al., 2008). The graphic display of this list is in Figure 5-7.

2. The second analysis conducts Flury hierarchy comparisons of modules composed of three-dimensional representations of the skull versus those from two dimensions. Results show caution must be used not only to define modules used to form hypotheses of taxonomy, but also to define the numbers of points and their dimensionality.

Analysis 1

The plots below are intended to graphically display where the specimens would be placed in relationship to one another in two-dimensional and three-dimensional analyses.

In Figure 5-7, note how the *Homo sapiens* clusters with the three Neandertals, with Dmanisi being highly different. Figure 5-8 plots three-dimensional mirrored data, the same three-dimensional data plotted in Figure 5-7 but with the difference that the Y-axis is mirrored one side to the other to construct a fully three-dimensional skull (see Method 2 for collecting dimensional data above). Figure 5-8 illustrates that changing dimensionality causes little difference in the generalized positional relationship from the original 46-point combined modules in González-José et al. (2008; shown as Figure 5-7):

Dmanisi remains removed from the cluster of *Homo sapiens* and the Neandertals. In other words, there is not much change in the plot due to mirroring the data to make three dimensions.

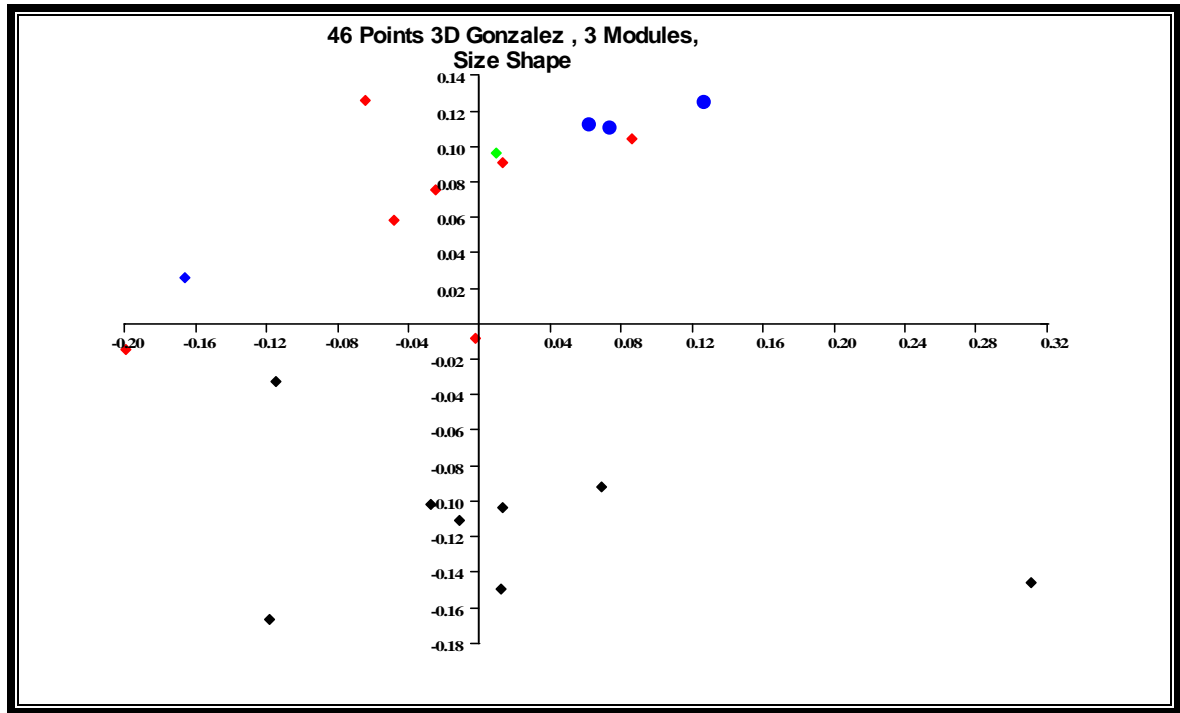


Figure 5-7. Positional relationships using all 46 measurements from González-José et al. (2008)

Legend:

- ◆ Blue diamond = Dmanisi 2600
- Blue circles = Neandertals
- ◆ Red diamonds = Homo
- ◆ Black diamonds = Non-Homo
- ◆ Green diamond = Homo sapiens

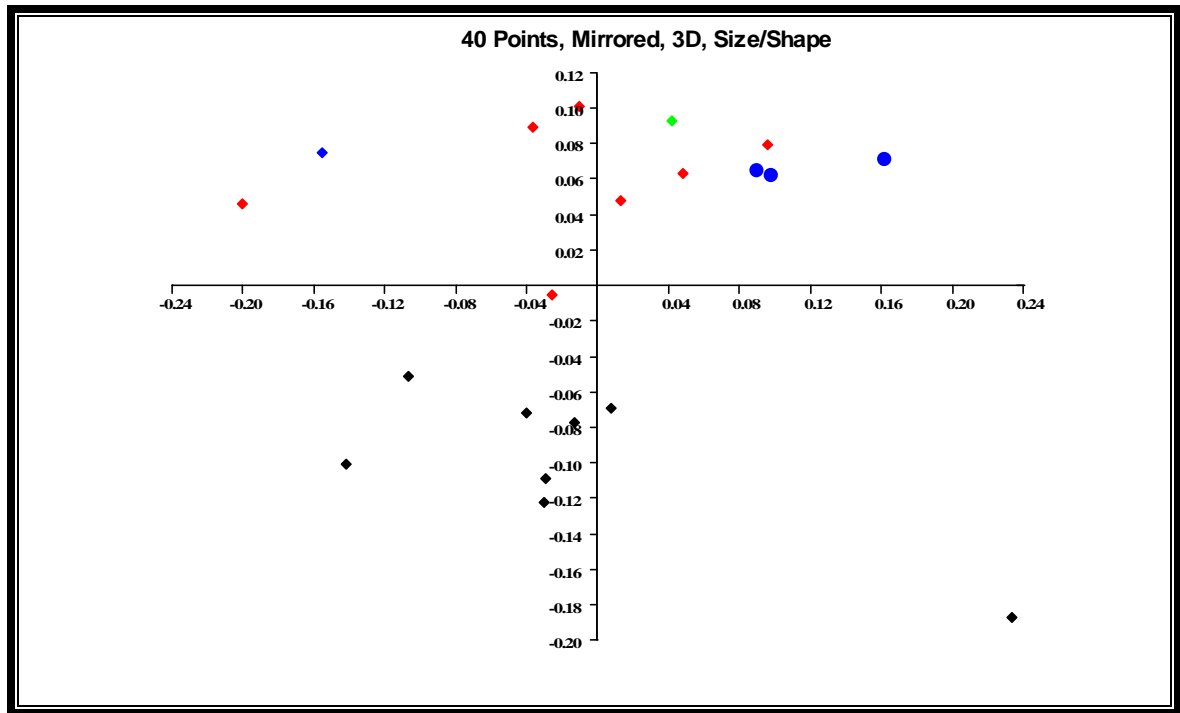


Figure 5-8. Three-Dimensional, 40 Points Used (both sides with Y-axis, mirrored)

Legend:

- ◆ Blue diamond = Dmanisi 2600
- Blue circles = Neandertals
- ◆ Red diamonds = Homo
- ◆ Black diamonds = Non-Homo
- ◆ Green diamond = Homo sapiens

Finally Figure 5-9 shows what occurs simply as a result of dimensionality.

Comparison of Figure 5-9 to Figure 5-8 and 5-7 shows that simple removal of the mediolateral Y-axis changes the positional relationships. Not only is the formerly close relationship of *Homo sapiens* to Neandertals in nearly all other graphs broken, but Dmanisi now clusters even further from *Homo sapiens* and the Neandertals, in being even more separated on both the Y- and X-axes. The point here is not to present a full statistical analysis; obviously there would be differences in the covariance matrices

underlying these visuals. The visuals are simply used as an illustration to warn against regarding dimensionality as a trivial factor in two- versus three-dimensional morphometrics.

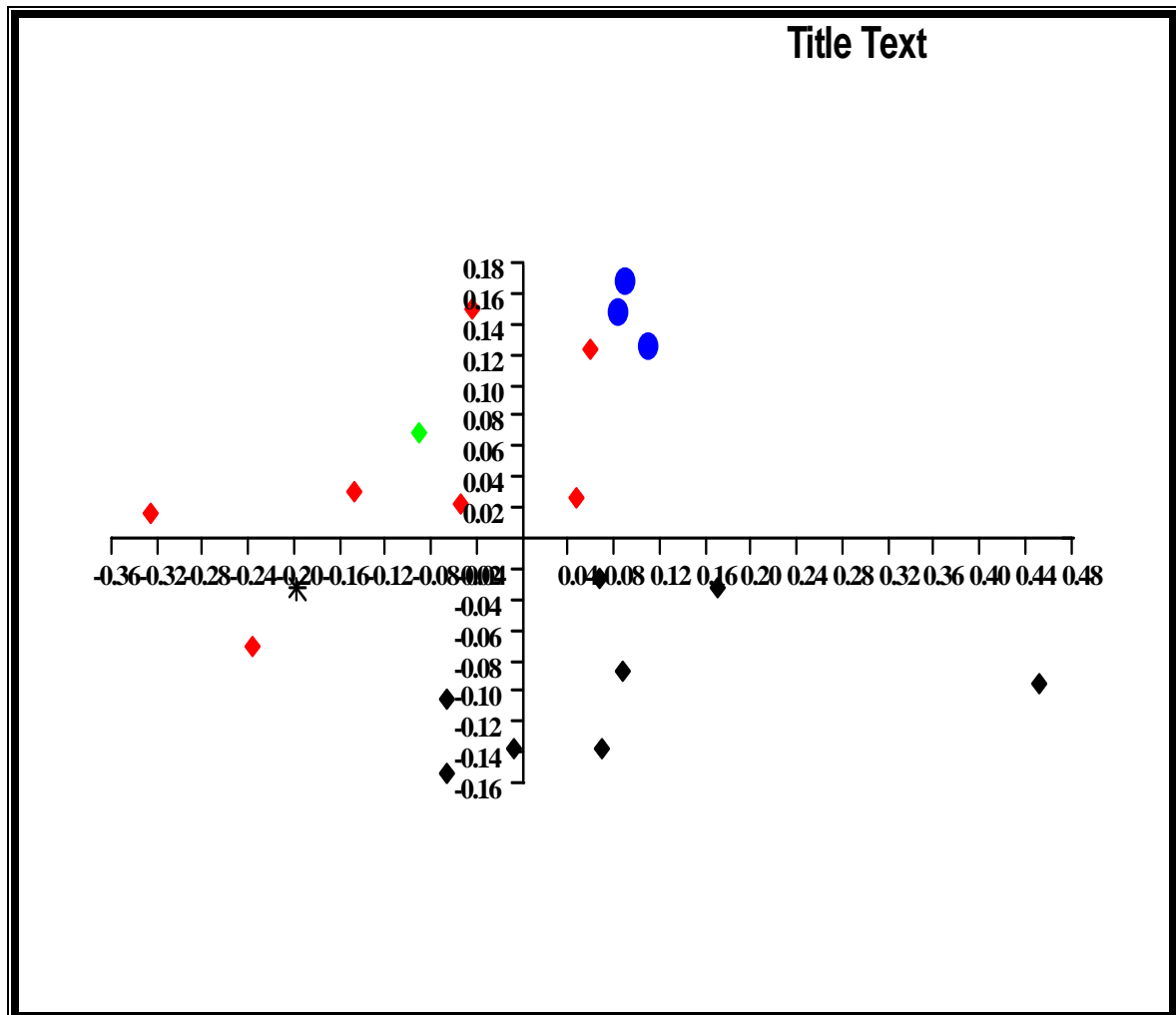


Figure 5-9. Bilateral Facial without Y-axis (same as Figure 5-8 with Y-axis removed)

Legend:

- * Black asterisk (star) = Dmanisi 2600
- Blue circles = Neandertals
- ◆ Red diamonds = Homo
- ◆ Black diamonds = Non-Homo
- ◆ Green diamond = Homo sapiens

Analysis 2

The second analysis conducts Flury hierarchy comparisons of modules composed of a three-dimensional representation of the skull versus that from two dimensions. Results show caution must be used to define not only modules used to form hypotheses of taxonomy, but also to define the numbers of points and their dimensionality as well.

Analysis 2 also deals with modularity and dimensionality. The next comparisons in Tables 5-11 and 5-12 show that the facial module is proportional in (archaic) *Homo* to later, modern *Homo sapiens* and that modern *Homo sapiens* is not proportional to non-*Homo*.

The same comparisons through the Flury hierarchy break down when the same specimens are compared but the matrices compared are composed of unilateral one-side-only matrices. The data are exactly the same in both the first set of comparisons and the second (Comparisons 4 and 5, displayed as Tables 5-13 and 5-14), with the exception that the right-side mirrored data are removed. These results, together with the results on modular definitions and dimensionality in Analysis 1 (above) show that overall dimensionality of measurements can greatly influence phylogenetic hypotheses.

Table 5-11. Flury Hierarchy Comparing Face—Modern Humans against Archaic *Homo* (three-dimensional, 12 measures)

Model						
Higher	Lower	Chi Sqr	df	p-val	CS/df	AIC
Equality	Proport	0.209	1	0.6475	0.209	14.725
Proport	CPC	7.494	7	0.3793	1.071	9.515
CPC	CPC(6)	0.022	1	0.8825	0.022	16.022
CPC(6)	CPC(5)	0.000	2	1.0000	0.000	18.000
CPC(5)	CPC(4)	0.000	3	1.0000	0.000	22.000
CPC(4)	CPC(3)	0.000	4	1.0000	0.000	28.000
CPC(3)	CPC(2)	0.000	5	1.0000	0.000	36.000
CPC(2)	CPC(1)	0.000	6	1.0000	0.000	46.000
CPC(1)	Unrelated	0.000	7	1.0000	0.000	58.000
Unrelated	—					72.000

Table 5-12. Flury Hierarchy Comparing Face—Modern humans against Archaic *Homo* (two-dimensional unilateral 8 measures with Y-axis removed)

Model						
Higher	Lower	Chi Sqr	df	p-val	CS/df	AIC
Equality	Proport	10.478	1	0.0012	10.478	40.879
Proport	CPC	21.740	7	0.0028	3.106	32.401
CPC	CPC(6)	8.661	1	0.0033	8.661	24.662
CPC(6)	CPC(5)	0.000	2	0.9999	0.000	18.001
CPC(5)	CPC(4)	0.000	3	1.0000	0.000	22.000
CPC(4)	CPC(3)	0.000	4	1.0000	0.000	28.000
CPC(3)	CPC(2)	0.000	5	1.0000	0.000	36.000
CPC(2)	CPC(1)	0.000	6	1.0000	0.000	46.000
CPC(1)	Unrelated	0.000	7	1.0000	0.000	58.000
Unrelated	—					72.000

The results displayed in Tables 5-11 and 5-12 show that phylogenetic hypotheses of relationship are highly influenced by dimensionality of measurements used to test the hypotheses. By excluding the Y-axis data from the original PCA to form the covariance structure tested in the Flury hierarchy, results would indicate that matrix proportionality

is not achieved in modern versus archaic *Homo*. This is not the case; the results in Analysis 2 (above) already demonstrated this. These results reiterate that excluding the most variable dimension in human skulls skews all downstream results in analysis.

Building on this finding, it is shown below that modular analysis within a given taxa (here modern humans) is also highly affected by the dimensionality of the measurements used in the construction of the modules. Although the mandible is not a module, the hierarchical structure of analysis when using a 14-landmark dataset (Table 5-13) compared to a 9-landmark unilateral dataset (Table 5-14) shows a tendency to approach matrix proportionality simply through measurement dimension. Although neither mandibular dataset achieves the proportionality expected of a module, the unilateral mandibular measurement dataset approaches close to proportionality as the Y-axis is removed. This finding means that unlike the facial dataset illustrated above, the variability in the mandible in human groups is highly driven by width. The point is that simply using variable dimensions can cause groups to be more or less similar, both in their display and in the covariance structure itself.

Tables 5-13 and 5-14 show that matrix comparisons are dimension-specific. The mandible almost becomes a module when analyzed in two dimensions.

Table 5-13. Flury Hierarchy of Man14 (3D)

Model		Chi Sqr	df	p-val	CS/df	AIC
Higher	Lower					
Equality	Proport	8.582	1	0.0034	8.582	295.335
Proport	CPC	207.661	19	0.0000	10.930	288.753
CPC	CPC(18)	79.094	1	0.0000	79.094	119.093
CPC(18)	CPC(17)	0.000	2	1.0000	0.000	41.998
CPC(17)	CPC(16)	0.000	3	1.0000	0.000	45.998
CPC(16)	CPC(15)	0.000	4	1.0000	0.000	51.998
CPC(15)	CPC(14)	0.000	5	1.0000	0.000	59.998
CPC(14)	CPC(13)	0.000	6	1.0000	0.000	69.998
CPC(13)	CPC(12)	0.000	7	1.0000	0.000	81.998
CPC(12)	CPC(11)	0.000	8	1.0000	0.000	95.998
CPC(11)	CPC(10)	0.000	9	1.0000	0.000	111.99
CPC(10)	CPC(9)	0.000	10	1.0000	0.000	129.998
CPC(9)	CPC(8)	0.000	11	1.0000	0.000	149.998
CPC(8)	CPC(7)	0.000	12	1.0000	0.000	171.998
CPC(7)	CPC(6)	0.000	13	1.0000	0.000	195.998
CPC(6)	CPC(5)	0.000	14	1.0000	0.000	221.998
CPC(5)	CPC(4)	0.000	15	1.0000	0.000	249.998
CPC(4)	CPC(3)	0.000	16	1.0000	0.000	279.998
CPC(3)	CPC(2)	0.000	17	1.0000	0.000	311.998
CPC(2)	CPC(1)	0.000	18	1.0000	0.000	345.998
CPC(1)	Unrelated	-0.002	19	1.0000	0.000	381.998
Unrelated	—					420.000

Figure 5-14. Flury Hierarchy of Man9 (2D)

Model		Chi Sqr	df	p-val	CS/df	AIC
Higher	Lower					
Equality	Proport	63.205	1	0.0000	63.205	546.754
Proport	CPC	483.536	14	0.0000	34.538	485.550
CPC	CPC(13)	0.000	1	0.9937	0.000	30.013
CPC(13)	CPC(12)	0.000	2	1.0000	0.000	32.013
CPC(12)	CPC(11)	0.012	3	0.9997	0.004	36.013
CPC(11)	CPC(10)	0.000	4	1.0000	0.000	42.002
CPC(10)	CPC(9)	0.000	5	1.0000	0.000	50.002
CPC(9)	CPC(8)	0.000	6	1.0000	0.000	60.002
CPC(8)	CPC(7)	0.000	7	1.0000	0.000	72.002
CPC(7)	CPC(6)	0.000	8	1.0000	0.000	86.002
CPC(6)	CPC(5)	0.000	9	1.0000	0.000	102.002
CPC(5)	CPC(4)	0.000	10	1.0000	0.000	120.002
CPC(4)	CPC(3)	0.000	11	1.0000	0.000	140.002
CPC(3)	CPC(2)	0.000	12	1.0000	0.000	162.002
CPC(2)	CPC(1)	0.000	13	1.0000	0.000	186.002
CPC(1)	Unrelated	0.002	14	1.0000	0.000	212.002
Unrelated	—					240.000

Summary

Formerly it was shown when modules are used to form phylogenetic hypotheses these hypotheses must be tested by properly defined modules. Even when properly defined, results are influenced by the dimensionality of modules as measured. The dimensionality of the measurements themselves can drive results.

CHAPTER 6

SUMMARY AND CONCLUSIONS

This dissertation began with the basic question of why a biomechanical model did not suffice to define the mandible in modern humans. It ends with the position that as currently defined, modules are untestable quantities. In order to arrive at this conclusion it was necessary to show that the mandible is integrated with the skull and that increasing complexity of modeling through several historical periods of cranial research was necessary to demonstrate this integration. In conjunction with biomechanics, integration was then defined as the primary operant factor in production of the human skull. The mandible, as part of the integrated skull, was here described as part of a complex system that changed through both direct selection and stabilizing selection through the Pleistocene. Some of this selection resulted from biomechanics, some not. Systemic change was described as avoided by the action of the sister factor to integration, modularity. Modularity was defined as areas of heritable functional integration. The question of the production of mandibular morphology beyond biomechanics became reframed as the position of the mandible in a modularized system. Biomechanical force reflects function within an integrated system—it cannot explain the system, which is hierarchical.

This being said, it remained to be seen whether modularity or integration is more explanatory for the morphology of the skull, including the mandible. It was demonstrated that the skull was more modular than integrated, a necessity whether the skull is partitioned as traditionally defined or in terms of modules. Modules were then described as representative of function, with such semi-autonomous functional regions requiring

further robust definition to be accepted as true modules. Localized areas of invariance in the skull were then tested to the degree to which they conformed to a definition of modularity, defined as expected areas of relative invariance to effects of sex and population within a species. This definition assumes at least some degree of maintenance of morphological form as defined by function; basic functional requirements are assumed to be the same across sex and population within a species. These regions of invariance were then defined by properties as well as attributes, finally producing a definition of a module as an heritable area of localized functional integration which tends to remain stable (invariant) within species.

The above definition of modularity in a single species (*Homo sapiens sapiens*) was compared to examples of other taxonomic levels (by testing taxon-specificity in the face). The underlying logic here was that modules can be expected to differ though phyla as they represent changing functional reorganization of the skull. The various properties of function—internal integration, invariance across population and sex—were coupled with variance through time in evolving taxa to ultimately provide a new definition of modularity. Next it was demonstrated that some parts of the skull are modular, while other parts are not, and that even in the highest loading biomechanical populations some regions remain modular and invariant across population and sex. Penultimately it was demonstrated there are patterns of organization underlying modules—cranial nerve patterning for example. Finally it was shown that even correctly defined modules can be subjected to unsatisfactory analysis if dimensionality of their measurements (three-dimensional) is not preserved; phylogenetic hypotheses of relationship can be skewed by simply using two-dimensional data. Modular testing must be in three dimensions.

Conclusions

Three-dimensional morphometrics used as an analytic tool in biology is still a relatively new endeavor. As is common with the introduction of such new processes and applications, manipulation has outstripped modeling; it always takes some time for integration of theory and methods. Using three-dimensional modeling for study of modularity is a prime example, because presently there exists no robust definition of a module. Modularity without measuring is only a concept. This dissertation has sought to provide the way to define modules through properties, without which statistical analysis is unsatisfactory. It is easy to extract “modules” from two- or three-dimensional data and analyze and compare them. It is much less easy to define the modules *a priori* through properties as well as attributes.

As was demonstrated herein it is necessary to form and test hypotheses of modularity which not only reflect areas of statistically defined integration, but biological reality as well. This is but a first pass at describing temporal and spatial complexity in biology. Definitions of modularity need both attributes and properties: without attributes we cannot categorize entities, without properties we cannot statistically compare them. Evolutionary theory predicts structural change in morphology will follow constrained paths such as lines of least resistance; it also predicts patterns of morphology build on prior states such as basic neurocranial developmental patterns.

No amount of complex mathematical modeling divorced from biological realities will ever be able to completely describe cranial shape. For an appreciation of the complexity and ultimate unsatisfactory results of strictly mathematical modeling see the Santa Fe Institute’s working paper “Extreme Degeneracies Characterize the Module Identification Problem for Complex Networks” (Good, de Montjoye, and Clauset 2009). This paper sets

forth the asymptotic properties of mathematical models of modularity and shows optimum modular partitioning at best produces models which degenerate into multiple equal probabilities. This finding means we must reference other quantifiable properties as necessary conditions for biological modularity—invariance, taxon specificity, function—in addition to mathematically defined integration. All these properties are indispensable for meaningful scientific definition. Both the appreciation that constraint plays a role in prior states and awareness that modularity remains the heritable, stable, integrated pattern in evolutionary change are necessary to define the hierarchical transition from skulls showing high variability in the singular to patterned variation in the aggregate. Modularity provides the means to establish where variability leaves off and patterned variation commences. Modules are inherited patterns of functional integration.

APPENDIX A

SAMPLE COMPOSITIONS BY LOCATION

In this dissertation, the data analyzed in Chapters 3, 4, and 5 come from these sources:

- ◆ W.W. Howells (1996) dataset, $n = 2554$
- ◆ T. Hanihara (used with permission), $n = 113$
- ◆ Fortext (a lab-collected and literature-derived dataset prepared by this author for the dissertation), $n = 150$
- ◆ A morphometric three-dimensional dataset (collected at the American Museum of Natural History [AMNH], the National Museum of Natural History [NMNH], and the Maxwell Museum of Anthropology), $n = 180$

Details about the locations from which these samples are drawn and their composition follow in the sections below.

W.W. Howells 1996 Data

The 2,554 individuals in Howells's study of human craniometric variation come from these 28 locations (illustrated on http://arts.anu.edu.au/bullda/howells_map2.png):

1. Europe, Oslo, Medieval Norse
2. Central Europe, Hungary, Zalavar
3. Central Europe, Carinthia, Austria, Berg
4. East Africa, Kenya, Teita
5. West Africa, Mali, Dogon
6. South Africa, Zulu

7. South Australia, Lake Alexandrina Tribes
8. Tasmania, Tasmanian
9. Melanesia, New Britain, Tolai
10. Oahu, Hawaii, Polynesia, Mokapu
11. Easter Island, Polynesia
12. Chatham Islands, Polynesia, Moriori
13. North America, Early Archaic
14. Santa Cruz Island, California, North America
15. Peru, South America, Yauyos
16. Northern Hokkaido, Japan
17. Southern Japan, northern Kyushu
18. Haikou City, China, Hainan
19. Taiwanese Aborigines, Atayal
20. Phillipine Islands
21. Late Period Guam
22. Gizeh, Egypt, 26th–30th Dynasties
23. South Africa, San
24. Andaman Islands
25. Southern and Southeastern Hokkaido, Japan, Ainu
26. Siberia, Buriat
27. Inugsuk, Greenland, Eskimo
28. Shang Dynasty, China, Anyang

T. Hanihara Data

The 113 individuals in the Hanihara dataset are all male and all from locations in Japan.

Fortext Data

The recent *H. sapiens* mandibular sample Fortext ($n = 256$; $n_{\text{complete}} = 150$) comprises two datasets, one deriving from direct measurement and observation of mandibles (originals and casts) and one composed of literature-derived metric values.

The osseous sample that was directly measured comprises:

1. Modern European-derived American individuals ($n = 35$)
2. Prehistoric Amerindian individuals ($n = 57$)

These specimens are housed in the Maxwell Museum of Anthropology, Albuquerque, NM, and the Phoebe Hearst Museum of Anthropology, University of California, Berkeley, CA.

The osseous sample is supplemented with literature-derived (scaled photographic) values for the following populations:

1. Aboriginal Australians, $n = 25$ (Milicerowa, 1955)
2. Greenland Eskimo, $n = 32$ (Fürst and Hansen, 1915)
3. Lapps, $n = 25$ (Schreiner, 1935)
4. Later 19th–early 20th century Norwegians, $n = 29$ (Schreiner, 1939)
5. Medieval Norwegian, $n = 22$ (Schreiner, 1946)
6. Ugandans, $n = 31$ (Gorny, 1957)

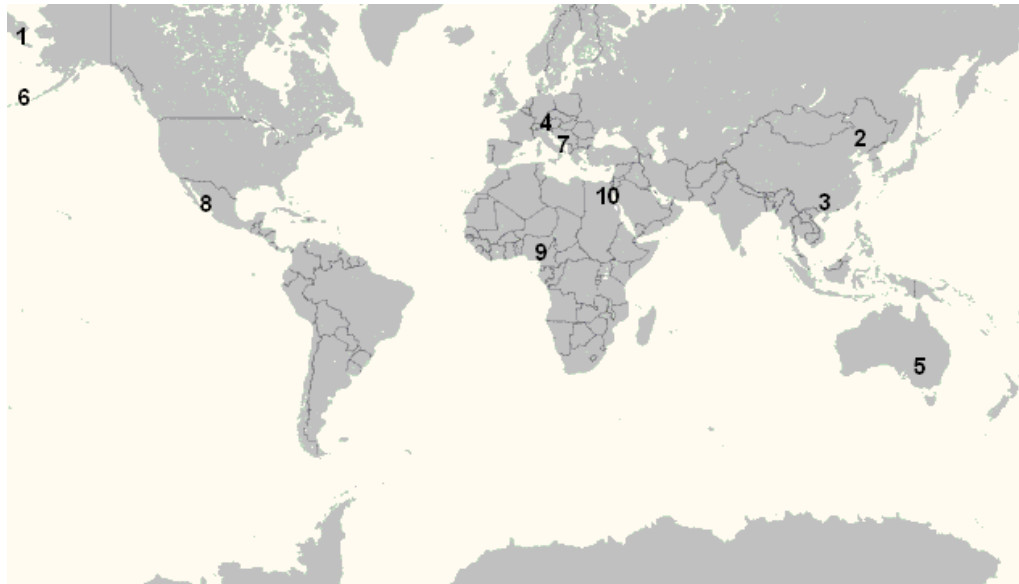
Figure A-1 illustrates the geographic spread of this collection. Not all individuals exhibited all points; where subsets of full samples were used, it is noted in the text and in statistical tables.



Figure A-1 Locations of Fortext Populations

Morphometric 3D Data

Data collected with Morpologika 2.5 came from three museums: the National Museum of Natural History (NMNH) of the Smithsonian Institution in Washington, DC, the American Museum of Natural History (AMNH), in New York, NY, and the Maxwell Museum of Anthropology, Albuquerque, NM. Figure A-2 illustrates the locations of the morphometric three-dimensional data collected at NMNH and AMNH. (The numbers in the figure correspond to the numbers in the text for the NMHN and AMNH sections following the figure.)



**Figure A-2. Locations for NMNH and AMHN Individuals Measured
(1–5 NMNH collections; 6–10 AMHN collections)**

NMNH Collections

1. Aleutian Islands (latitude 57° 25' 35" N, longitude 153° 50' 30" W), Aleuts, n = 20 (Hrdlička, 1945)
2. Mongolia (latitude 45° 45' 0" N, longitude 106° 16' 0" E), Mongolians, n = 2045.75
3. Southern China, n = 20
4. Germany, n = 20 (primarily from a pre-WWII tuberculosis sanatorium; crania were sectioned)
5. Australians, n = 20

AMHN Collections

6. Point Hope, Alaska, Alaskan Islanders, n = 20
7. Greeks, n = 20
8. Mexico City, Mexico (northern Mexico), n = 20

9. West Africans, n = 20

10. Egypt, 2nd Dynasty, Nubians, n = 20

Maxwell Collections

The Maxwell samples came from three collections:

- ◆ The documented collection in the UNM Anthropology repository (Euroamericans from the body donation and Office of the Medical Investigator programs), n = 20
- ◆ UNM Prehistoric Amerindians (with cranial deformation), n = 20
- ◆ Spencer R. Atkinson Collection from the University of the Pacific Dental School, San Francisco¹, highly admixed population, n= 20

¹ These individuals were opportunistically gathered by Spencer Atkinson from the streets of Mexico City in the early 1900s (see details in McCabe 1997).

APPENDIX B METHODOLOGY

Five types of methodology are described in this appendix:

- ◆ Biomechanical Modeling / Molding
- ◆ Cranial Base Angle and Radiography
- ◆ Photography
- ◆ Fortext
- ◆ Howells Measurements

Biomechanical Modeling / Molding

The biomechanical model is functionally multifactorial, including lever arms, pivot points, locations of great bending strengths, and materials composition. The biomechanically expressed function of the mandible here is addressed by use of a proxy, the bending strength of the mandible using beam analysis. Prior studies have modeled the M1 position as being the most reflective of positioning of force-transmission in biomechanical modeling (Benveniekus, 1995), and, in the present study, loading vectors were assessed at M1 force-production vectors such as I_{\max}/I_{\min} -theta (bending and torsional strength; see Figure 4-1) of the mandible, which strongly correlate with *mm. temporalis* and *masseter* moment arms for force production and hence regions of the neurocranium as well as mandibular corpus dimensions. Second moments of area around the superoinferior (I_y) and labiolingual (I_x) axes were calculated. Modeling was done as a solid beam, following Dobson and Trinkaus (2002). The implications of solid beam versus ellipsoid (hollow and solid) are discussed therein.

Figure B-1 shows the relation of bending strength of the mandible at M2 that is used here as a proxy for biomechanical force. Cross-sectional moments of inertia (I_{\max}/I_{\min} -theta) are digitized after non-adhesive silicone molding of the mandibular periosteal contours of the corpus at M/2. Periosteal molds of the mandible at M1 were sectioned through the midline, traced on scaled paper, then scanned and analyzed using a macro written by Teri Rosenbaum of the University of Utah (see Figure B-2). I_{\max}/I_{\min} was calculated using Scion Image.

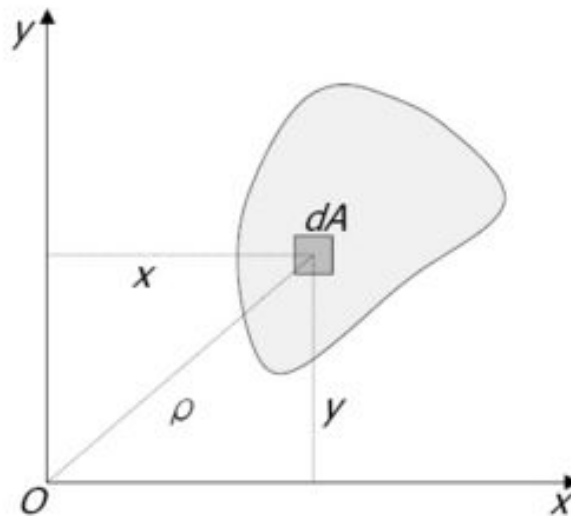


Figure B-1. Illustration of axes used to calculate Polar J (Polar $J = I_{\max} + I_{\min}$)

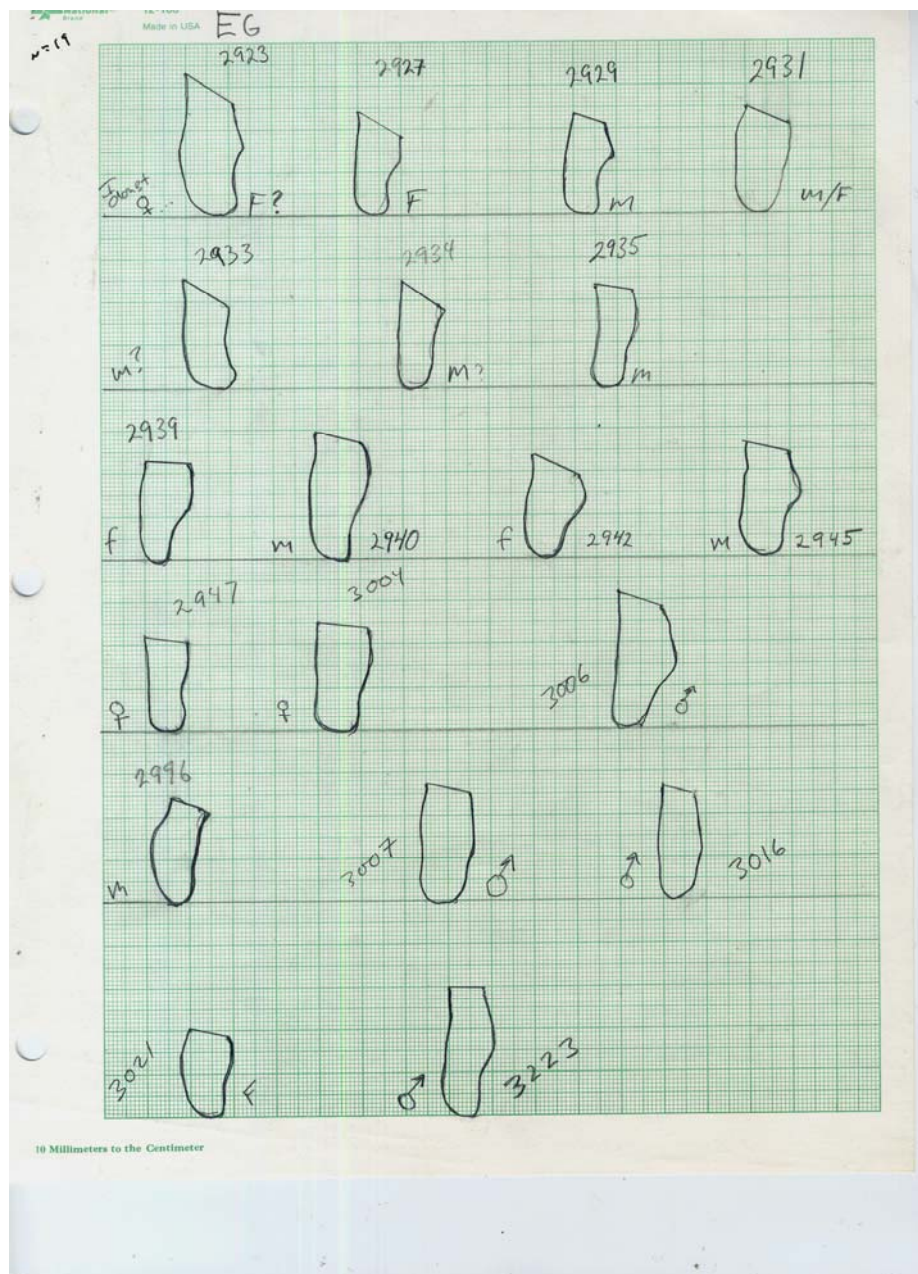


Figure B-2. Sample Illustration of Mandibular Molds (showing periosteal contours of Egyptian mandibula in the NMNH collection)

To form the molds, Siliconix material resin is mixed with polymer and allowed to set to the desired consistency, then wrapped around the corpus. Because teeth will prevent a full encirclement of the corpus at this position, after setting up the molded impressions,

they are then removed, so that the previously taken measures across lingual and buccal digitized distances across M2 at the alveolar plane can then be verified. Each silicone impression is then bisected through the coronal plane to provide a perfectly flat surface for placement on graph paper. The measure across the lingual-buccal position at M2 is then used to orient the ends of the mold, after which the internal surface of the mold is traced to the paper. Next, the resultant shape is digitized using a two-dimensional digitizer, thus describing the relative bending strength and torsional orientation of the corpus at M2.

Cranial Base Angle and Radiography

Cranial flexion (as a reflection of orthogrady) influences the basicranium and hence the entire skull (see Figure 4-2). Frontal and lateral cephalometry of the skull was accomplished with the skull in standard fixed position, immobilized by insertion of steel pins into the left and right external auditory meatii. Crania are radiographed in *norma lateralis* to establish the cranial base angle. Frankfurt Horizontal position for the cephalometry is checked by leveling the skull to the left orbitale and the right and left porion positions (standard method). Position from the x-ray machine is constant, and correction for parallax is checked by scaling the cephalometric films to the previously collected digitized measures of the frontal and sagittal measures of the skull and mandible.

The position of the mandible in anatomical position is assured by anchoring the mandible in occlusion to the skull by a series of several expandable rubber straps, which are checked three times during the cephalometry. Radiography, when possible, used existing facilities associated with collections accessed. When a collection did not have an

x-ray machine, a portable x-ray machine from Washington University was used (provided through the kindness of Dr. Erik Trinkaus).

Shape in the skull (defined as form with size removed) is defined by using landmarks with known homologies, through prior knowledge of processes of morphogenesis. O'Higgins (2000) discusses a hierarchy of landmarks such that Type I results from the meeting of structure and knowledge of histology; Type II results from the use of easily defined points, with or without strict biological interpretation (e.g., easily replicated projecting features); and Type III results from there being present at least one deficient coordinate such as a point placement on a rounded bump or within a fossa. The great majority of landmarks used here (see the list in Table 4-1) are Type I.

Photography

Photography of the skull is accomplished with the skull remaining in fixed position after radiography, with a 35mm camera set at a fixed distance. This methodology is used to provide exact orbital area for estimate of body mass following Kappelman (1996). Correction for parallax will be made by comparison to digitized measures and the frontal cephalometry. Additionally, if completeness of the skeleton allows, femoral head measures (cubed) were taken to provide a secondary estimate of body mass, following Trinkaus and Ruff (1995).

Fortext

Quantification of mandibular ramal morphology was carried out using sliding calipers, with accuracy to ± 0.1 mm. Where published data and radiographs were used, scaled photographs and radiographs in *norma lateralis* were analyzed to 0.1 mm. Comparison of

results obtained were verified for accuracy by comparison to published data for those specimens.

Osteometric Points

The following standard osteometric points were employed:

- ◆ Infradentale (Martin, 1928)
- ◆ Superiormost condyle (Twisselmann, 1973)
- ◆ Superiormost coronoid, defined as the coronoid portion of Twisselmann (1973:17, #24)
- ◆ Distal border M3 (Twisselmann 1973:17, # 3; Franciscus and Trinkaus, 1995)
- ◆ Least indented anterior ramus (Twisselmann, 1973:17, # 9; Franciscus and Trinkaus, 1995)
- ◆ Least indented posterior ramus (Twisselmann, 1973:17, #9; Franciscus and Trinkaus, 1995)
- ◆ Most inferior point on the incisura semilunaris (Twisselmann, 1973:17, #10)

Standard Measures

The following standard measures were used (also see Figure B-3):

- ◆ Mandibular length (ML), the direct midsagittal distance from infradentale to a transverse line drawn between the centers of the mandibular condyles (Franciscus and Trinkaus, 1995)

- ◆ Dental arcade length (DAL), the midsagittal distance from infradentale to the middle of a line drawn tangential to the distal surfaces of the distal M3 roots (Martin, 1928, #80)
- ◆ Minimum ramus breadth (RAM), the minimum anteroposterior width of the ramus (Martin, 1928, #71a; Franciscus and Trinkaus, 1995)
- ◆ Superior coronoid-condylar distance (C-C), the maximum breadth taken from the superiormost point of the coronoid to the condylar midpoint in the sagittal plane (Twisselman, 1973:17, #12)
- ◆ Depth of semilunaris incisura (CCD), the depth of incisura taken from a line between the superiormost points of the condyle and coronoid processes to the most inferior point on the incisura (Twisselman, 1973:17, #11)
- ◆ Incisure area (INCISURE), calculated as the result of CCD multiplied by C-C, as employed by Schultz (1933) and Weidenreich (1936).

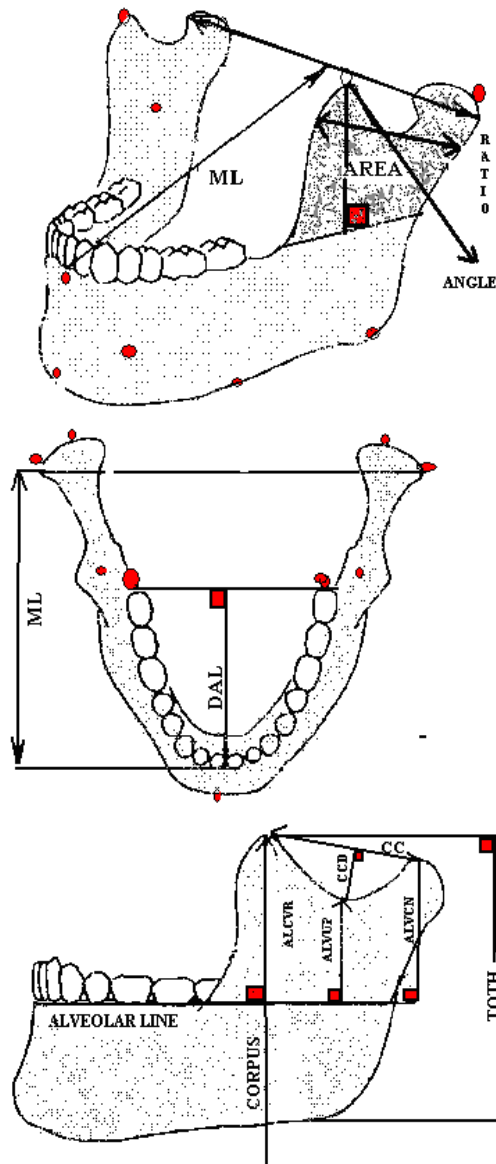


Figure B-3. Illustration of Mandibular Points Used In Fortext

Key:

ML	Mandibular Length
RAM	Ramus Breadth
CORPUS	Corpus Depth
ALVCR	Aveolar Line to Coronoid
ALVCN	Alveolar Line to Condyle
ALVUP	Alveolar Line to Bottom Mandibular Notch

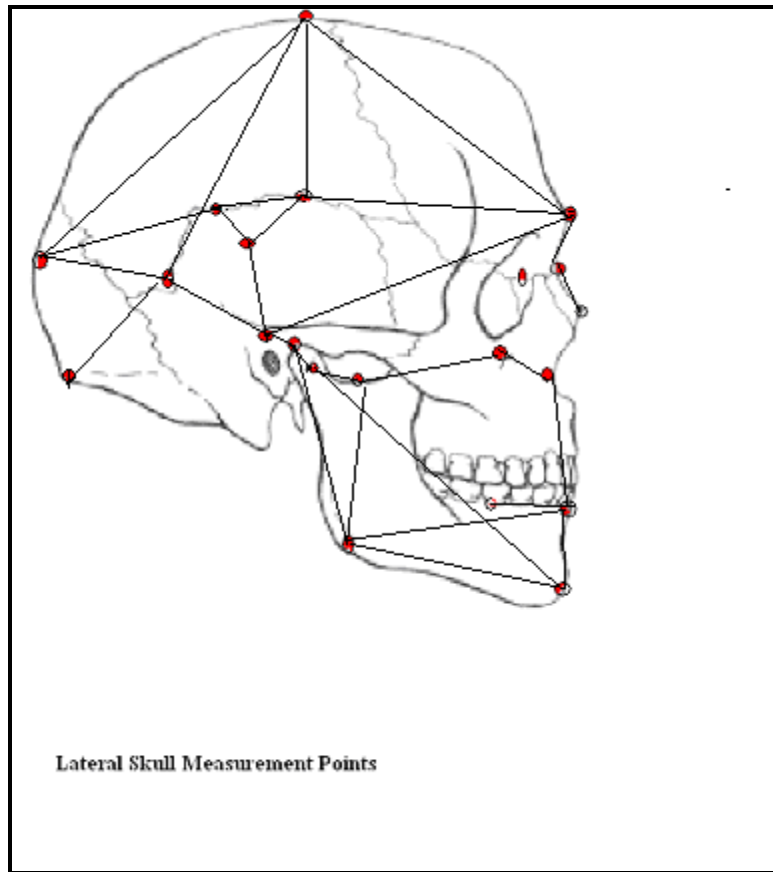


Figure B-4. Illustration of Cranial and Mandibular Points Used In Fortext¹

Key:
 GOL Maximum Cranial Length (M1), #1
 NPL Nasion-Porion Length (M43), #12
 XCB Maximum Cranial Breadth, #5
 ZYB Superior Facial Breadth (M43), #8
 NPH Nasion-Prosthion (M48), #13
 NLB Nasal Aperture Breadth (M54)

¹ Not all measurements points were used in all analyses.

Additional Measurement Definitions

This dissertation's research methods used both traditional anthropometric and clinically derived, architectonic measurements. A set of functionally defined points, lines, angles, and areas was derived from clinical research and evolutionary theory (Martin, 1928; Weidenreich, 1936; Twiesselman, 1973; Howells, 1989; Enlow, 1996). This second dataset is necessary, because traditional anthropomorphic measures do not include many internal cranial measures or measures derived from a model of architectonic integration.

Howells Measurements

Table B-1 lists 47 of the original 77 craniometric measurements for more than 2,500 individuals from 28 populations (Howells, 1973, 1989) used in this dissertation. No analysis here uses any more than the 47 below. See text for subsets of measurements used in specific analyses. Table B-2 lists the codes for population affiliation for each individual (each population is coded by values 1-28).

Table B-1. Howells Craniometric Measurements Used

Variable No.	Variable Abbreviation	Variable Definition
1	POP	Population affiliation for each individual, coded as 1-28. See Table B-2 for coding designations.
2	SEX	Designation of male or female for each individual: Male = 1, Female = 2. Populations are represented by both males and females.
3	GOL	Glabello-occipital length
4	NOL	Nasio-occipital length
5	BNL	Basion-nasion length
6	BBH	Basion-bregma height
7	XCB	Maximum cranial breadth
8	XFB	Maximum frontal breadth
9	STB	Bistephanic breadth
10	ZYB	Bizygomatic breadth

Variable No.	Variable Abbreviation	Variable Definition
11	AUB	Biauricular breadth
12	WCB	Minimum cranial breadth
13	ASB	Biasterionic breadth
14	BPL	Basion-prosthion length
15	NPH	Nasion-prosthion height
16	NLH	Nasal height
17	OBH	Orbit height, left
18	OBH	Orbit breadth, left
19	JUB	Bijugal breadth
20	NLB	Nasal breadth
21	MAB	Palate breadth, external
22	MDH	Mastoid height
23	MDB	Mastoid breadth
24	ZMB	Bimaxillary breadth
25	SSS	Zygomaxillary subtense
26	FMB	Bifrontal breadth
27	NAS	Nasio-frontal subtense
28	EKB	Biorbital breadth
29	DKS	Dacryon subtense
30	DKB	Interorbital breadth
31	NDS	Naso-dacryal subtense
32	WNB	Simotic chord (least nasal breadth)
33	SIS	Simotic subtense
34	IML	Malar length, inferior
35	XML	Malar length, maximum
36	MLS	Malar subtense
37	WMH	Cheek height
38	SOS	Supraorbital projection
39	GLS	Glabella projection
40	FOL	Foramen magnum length
41	FRC	Nasion-bregma chord (frontal chord)
42	FRS	Nasion-bregma subtense (frontal subtense)
43	FRF	Nasion-subtense fraction
44	PAC	Bregma-lambda chord (parietal chord)
45	PAS	Bregma-lambda subtense (parietal subtense)
46	PAF	Bregma-subtense fraction
47	OCC	Lambda-opisthion chord (Occipital chord)

Table B-2. Population Coding Used

Population Code	Population
1	Norse: (Medieval), Europe, Oslo
2	Zalavar: Central Europe, Hungary
3	Berg: Central Europe, Carinthia, Austria
4	Teita: East Africa, Kenya
5	Dogon: West Africa, Mali
6	Zulu: South Africa
7	Lake Alexandrina Tribes: South Australia
8	Tasmanian: Tasmania
9	Tolai: Melanesia, New Britain
10	Mokapu: Oahu, Hawaii, Polynesia
11	Easter Island: Polynesia
12	Moriori: Chatham Islands, Polynesia
13	Arikara: (Early) North America
14	Santa Cruz Island: California, N. America
15	Yauyos: Peru, South America
16	Hokkaido: North Japan
17	North Kyushu: South Japan
18	Hainan: Haikou City, China
19	Atayal: Taiwan Aborigines
20	Phillipine: Phillipine Islands
21	Guam: Late Period
22	Egypt: Gizeh, 26th–30th Dynasties
23	San: South Africa
24	Andaman: Andaman Islands
25	Ainu: S. and SE. Hokkaido, Japan
26	Buriat: Siberia
27	Eskimo: Inugsuk, Greenland
28	Anyang: Shang Dynasty, China

APPENDIX C STATISTICS

Each of the four sections detailing statistical procedures and applications used in this dissertation's analysis consists of two parts. The first describes the necessity and appropriateness of the technique. Second, there is a graphical representation (usually a flow chart) of the expectations and limitations of the technique used. The four statistical procedures covered in this appendix are as follows:

- ◆ Cronbach's Alpha
- ◆ Flury Hierarchy
- ◆ Stepwise Linear Regression
- ◆ Partial Least Squares (PLS)

Cronbach's Alpha

The initial problem addressed in this dissertation is the identification of areas of integration and their patterning. As a preliminary technique for the identification of areas of integration, the decision was made to identify areas of the skull with significantly higher or lower areas of correlations of measurements. In order to test for internal consistency of cranial measures and compare average correlations within and across areas of the skull in Howells's and Hanihara's datasets, Cronbach's Alpha (α) was used. Cronbach's Alpha is a popular reliability statistic (Cronbach, 1951). Cronbach's Alpha determines the internal consistency or average correlation of items in a sample to gauge reliability of estimates. Computation of alpha is based on the reliability of a test relative

to other tests with same number of items and then measuring the same structure (Hatcher, 1994). Cronbach's α is defined as

$$\alpha = (k/(k-1)) * [1 - \Sigma(s_i^2/s_{sum}^2)]$$

where the s_i^{*2} 's denote the variances for the k individual items and s_{sum}^{*2} 's denotes the variance for the sum of all items. Cronbach's α will generally increase when the correlations between the items increase, causing the coefficient also to be called the internal consistency or the internal consistency reliability of the test. Cronbach's α is used only as an exploratory measure of the relationship of variables within the macromodules (putative modules) here. As noted in the text, the statistical power of Cronbach's α is weak (high Type II error), and it is uninformative if used for different numbers of measured points, being sensitive to the numbers of comparisons. In this dissertation, it is used only with similar numbers of points, and only to examine relationships and form, not to test, hypotheses. Figure C-1 summarizes the technique's proper application and the types of conclusion that can be drawn from the results.

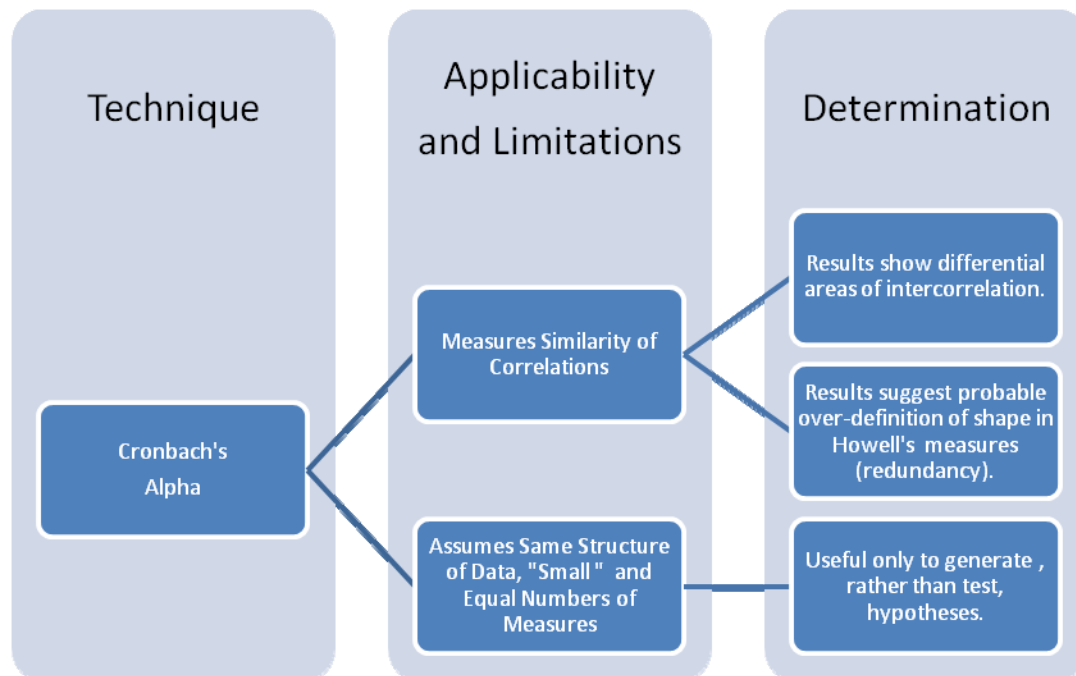


Figure C-1. The Application of Cronbach's Alpha

Flury Hierarchy

The second major statistical problem addressed in this dissertation was how to robustly compare integration patterns across the skull. Traditionally covariance matrices have been compared for the probability of being identical (or exhibiting equality as referred to here). Given large numbers of measurements this comparison has been described as highly unlikely, with such results either spurious or only found in cases where very small numbers of points are measured in construction of the matrices (Ackermann and Cheverud, 2000). Another informative approach is to compare results when changing membership of given points in constructing matrices and bootstrapping; the theory predicts less and less relationship of matrices as the correct placement of boundaries between modules is reached (Klingenberg et al., 2001). The approach used here is somewhat different: *a priori*–constructed modules (and/or macromodules) are compared for structural similarity using the Flury hierarchy.

Rather than mathematically establishing boundaries between modules, the Flury hierarchy is used here to compare matrices derived from sets of non-overlapping cranial points. Thus, while the boundaries between modules are not identified as such, regions are not redundant in points used. The Flury hierarchy—as applied by Arnold and Phillips (1999) and illustrated in Figure C-2—is used here to compare the structure of two (or more) covariance matrices in a hierarchical fashion.

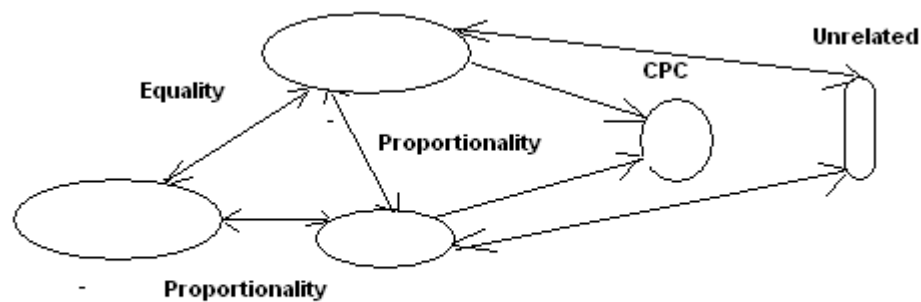


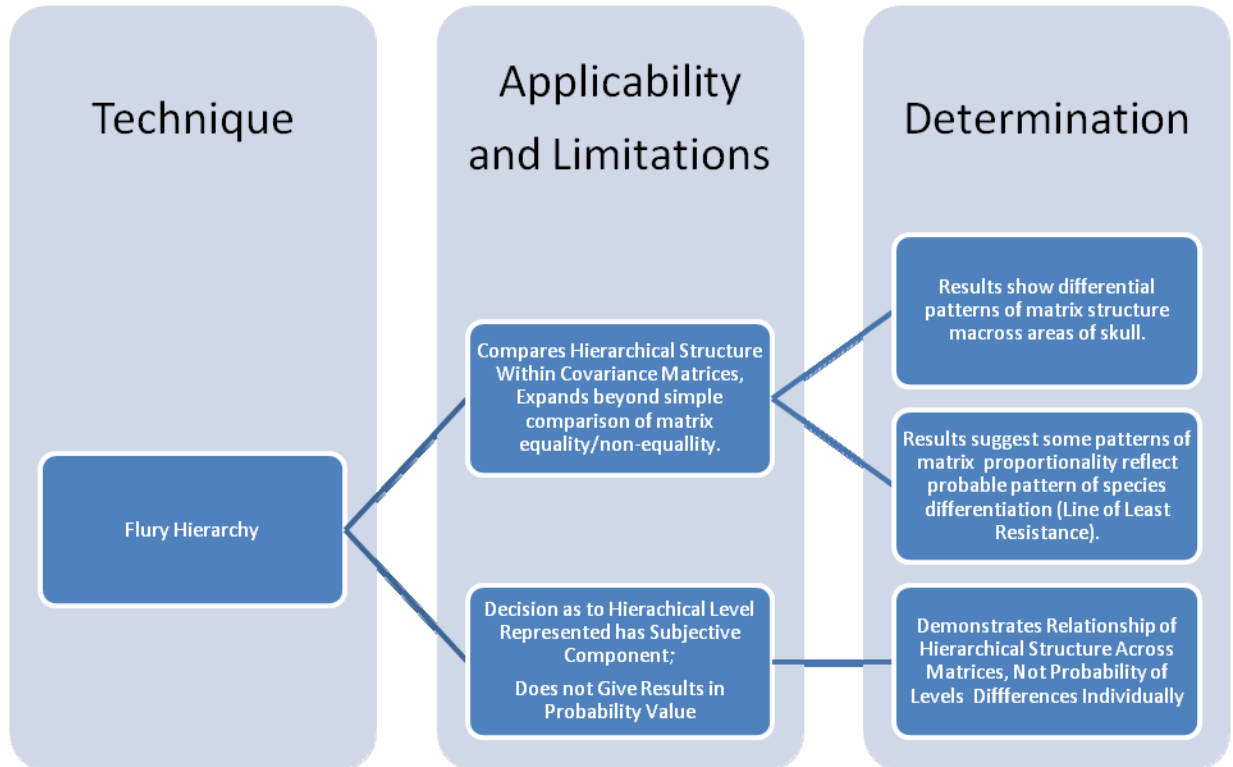
Figure C-2. Flury Hierarchy (redrawn from Arnold and Phillips 1999)

Hierarchy provides a means to assess covariance structure (as seen in Figure C-2). The large oblate spheroids preserve the same shape as the smaller, and are representative of matrices exhibiting equality. The smaller oblate spheroid is proportional to both the larger examples, differing only in size. The “true” spheroid represents matrices sharing common principal components with the left side exemplars; the ‘lozenge’ on the right represents matrices with unrelated structure (here demonstrated by possessing straight lines, smaller size, and 90° rotation of the long axis).

The hierarchy operates on the fact that covariance matrices can share more complex relationships between one another than just being equal or not. In fact, covariance matrix equality in large datasets is extremely unlikely (Marroig and Cheverud, 2000). As discussed in Chapters 2 and 3, matrices share structure up to and including equality, with the assumption being made that matrices exhibiting proportionality or higher are representing scaled exemplars of the same entity (e.g., allometrically scaled). For example, one matrix might be identical to another except that each element of the matrix is multiplied by a single constant (similar eigenvectors, different eigenvalues; proportionality). This is the pattern expected in the “lines of least resistance” argument for speciation discussed in the text; covariance matrices from same-species phenotypes can be assumed to be represented by scaled similar modules, and functional differences across species mean the shape of modules and their attendant covariance matrices are different and non-proportional (Erouhmanoff and Svensson, 2008).

The Flury hierarchy is an expression of log-likelihood ratio; models can be built up or down and tested with the maximizing Akaike Information Criterion (AIC; see Akaike, 1974). The AIC works as a trade-off between precision and complexity. Overspecified models are overly complex for the degree of precision they require and their AIC is consequently too high. Well-fit models thus have lower AICs than higher. The AIC is not a test on the model in the sense of hypothesis testing; rather it is a tool for model selection. Here, the AIC in combination with p-values of the matrices being compared is used to show the level of matrix comparability or structure. A low AIC indicates good fit; a low p-value indicates the model is rejected, as overspecified. Nonetheless, the converse is not necessarily true—a high p-value (acceptance given false) does not mean that the

given model is not overspecified (a Type II error). Figure C-3 summarizes the proper application of the Flury hierarchy.



C-3. The Application of the Flury Hierarchy

Stepwise Linear Regression

The third major use of statistical inference in the dissertation was stepwise linear regression (also known as stepwise discriminant function). After regions of the skull were shown to exhibit differential areas of integration through the use of Cronbach's Alpha, the Flury hierarchy was used to examine the covariance matrices for structural similarities across multiple partitions of the skull. Results showed that some regions of the skull could be considered modules under the definition of possessing proportional covariance structure (see Chapter 3 of this dissertation).

The next step was to find the predictor variables for morphology in the modular and non-modular regions. The assumption was non-modular regions should have different predictor values (such as sex and population) than modular regions. The decision was made to analyze the pattern in which various factors affect the observed regions. Morphology of each part of the skull *in toto* and by subset (macromodule or module) was predicted by Stepwise Linear Regression. Stepwise linear regression is an approach to selecting a subset of effects for prediction in a regression model, which is an example of general linear models for prediction of the best linear model from a number of possible models. The use of these model-building techniques begins with the specification of the design for a comprehensive “whole model.” Less comprehensive submodels are then tested to determine if they adequately account for the outcome under investigation. Finally, the simplest of the adequate is adopted as the “best.”

In Chapter 4, several factors were used to predict the morphology of the centroids (defined as point matrices for individuals from the global samples as defined in Appendix A, standardized as to scaling, reflective properties, and translation). The predictor variables included biomechanical force (using I_{\max}/I_{\min} as a proxy), the effect of mandibular size (mandibular area), and other factors defined in Chapter 4. The explanatory power of the regression was considered sufficient if r was greater than 0.7; several regressions equaled or exceeded this value. Stepwise regression can sometimes be misleading in that the significance levels on the statistics for models can violate standard statistical assumptions given the model sometimes is used to select the “best” of *a priori*-defined models rather than tested within a fixed model. It is based on methods (e.g., F-tests for nested models) that were intended to be used to test pre-specified

hypotheses. Figure C-4 summarizes the benefits and limitations of stepwise linear regression.

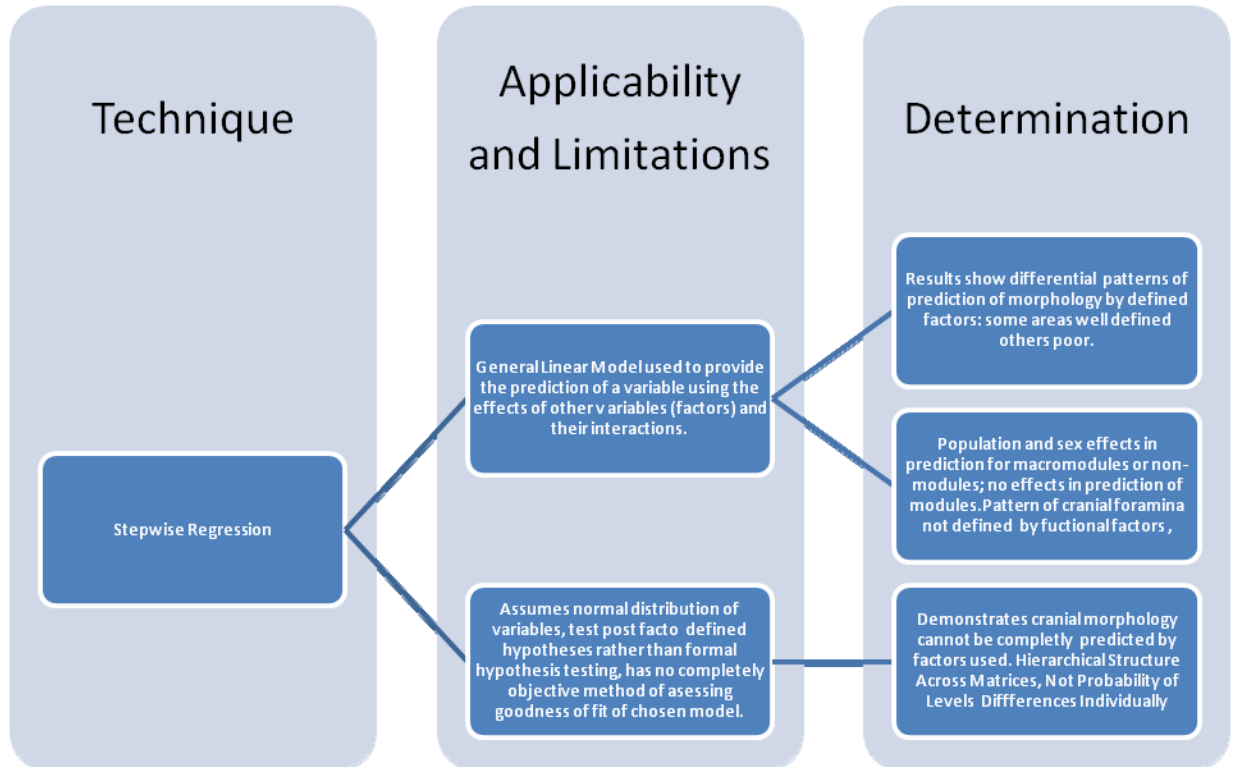


Figure C-4. The Application of Stepwise Linear Regression

Partial Least Squares (PLS)

Partial least squares (PLS) regression can be used to find the fundamental relations between two matrices (X and Y); that is, PLS is a latent variable approach to modeling the covariance structures in these two spaces. A PLS model will try to find the multidimensional direction in the X matrix that explains the maximum direction in the Y space. PLS regression is an important step in PLS path modeling, a multivariate data analysis technique that employs latent variables. This technique is often referred to as a form of variance-based or component-based analysis. If factors are few in number and are

not significantly collinear, PLS provides a good explanation of one variable by another.

Figure C-5 summarizes this statistical technique.

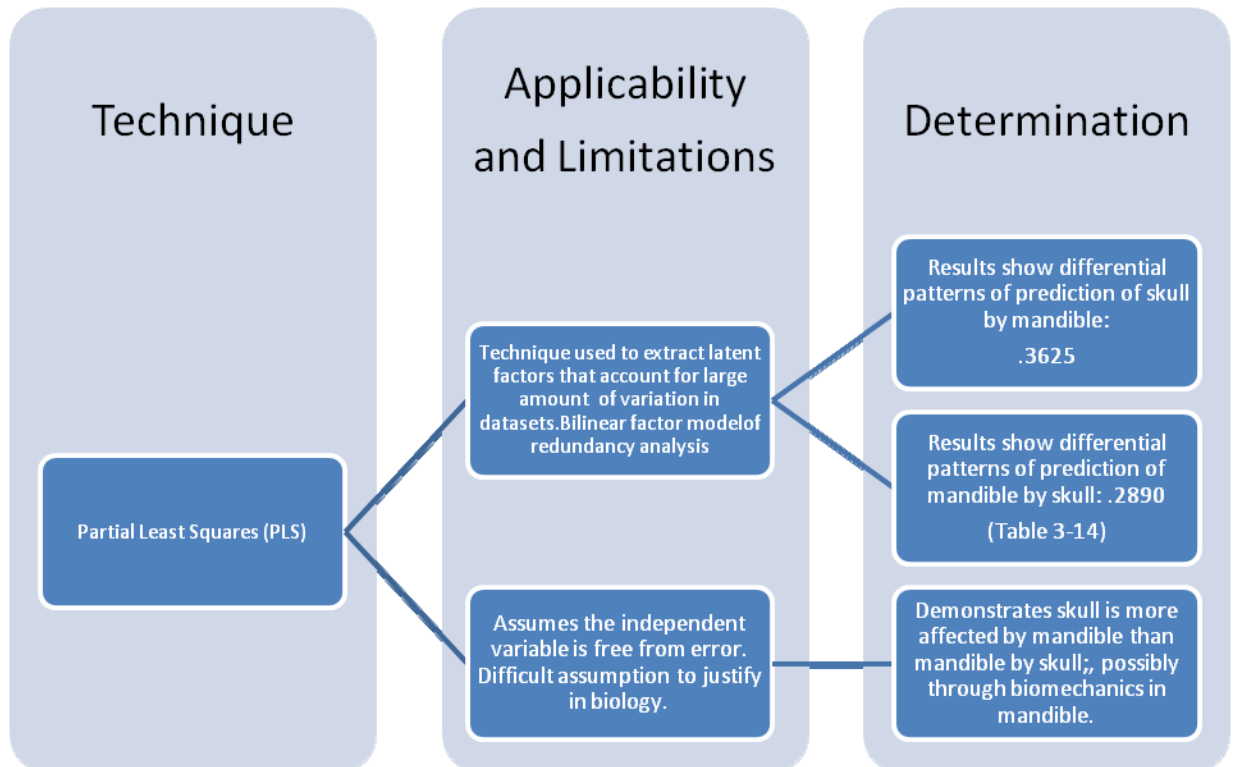


Figure C-5. The Application of PLS Regression

APPENDIX D

MORPHOLOGIKA 2.5

This appendix is organized into two sections:

- ◆ Morphometrics
- ◆ Digitizing

Morphometrics

Morphometrics provides the methodology to test three-dimensional relationships as exemplars of three-dimensional coordinate systems. Landmark data in three dimensions is perturbed about mean form. Perturbation models address the problems of reflection, translation, scaling, and rotation as groups of three-dimensional points are compared. If groups of points are correctly registered (standardized as to scaling, reflective properties, and translation) within the hemispheres of a three-dimensional sphere, then a perturbation model can be applied. This model predicts that change in landmark groups occurs as a perturbation of three-dimensional space as defined by landmark group (shape), within which the points are assumed to be able to “randomly” move independently of other landmarks. Perturbations are examined as the deviations from isotropy, in which all landmarks are assumed to exhibit equal spacing in three dimensions. If these assumptions are allowed, it is possible to use Procrustes superimposition techniques in which the sum of squared distances of equivalent landmarks in each landmark grouping (such as the skull or mandible) is minimized by using the formula:

$$S^2 = \sum_{i=1}^n \sum_{j=i+1}^n (X_i' - X_j')^2$$

The mean distance between all sets of points at a given location in 3D space is thus removed. This formula is used to create the centroid for each specimen, and then centroid sizes are compared. This technique works because the variability common to all points—the summation of Euclidian distances to the centroid (mean of all points per specimen)—is removed. This removal causes specimens to group based on centroids; it is essentially a size-removal technique, if size is considered the initial underlying reason all points have a relationship to the mean. (This methodology gives essentially the same results as the Darroch and Mossiman [1985] size-removal technique.) This technique minimizes the sum of squared distances between equivalent landmarks of forms; if all landmarks have a relationship to their centroid, removing the relationship leaves the landmarks without this extra source of variability. The centroids of the specimens themselves are then modeled as points and assumed to have an isotropic distribution in Kendall's shape space. Deviations from this assumption are then analyzable in terms of their covariance structure. Statistical analysis is thus performed on the data matrix formed by the aligned landmark sets. Kendall's shape space configurations are then treated as a linear space, in which standard statistical techniques can be applied directly.

In order to statistically analyze relationships of non-isotropic distributions of points in principal component analysis (PCA), a plane tangent to the curved Kendall's shape space is established. Figure D-1 shows that PC1 and PC2 are easily visualized as in a plane tangent to the Kendall's sphere. In order to construct an orthogonal axis to that plane, PC3, it would be necessary to go into the sphere itself; hence representation here is of necessity two-dimensional. Techniques used in PAST and Morphologika 2.5 allow use of the PCA in Morphologika 2.0 as either full size-removal single-vector deconstruction

(SVD) or an option to preserve size-shape relationship. The more robust SVD methodology is used for this thesis.

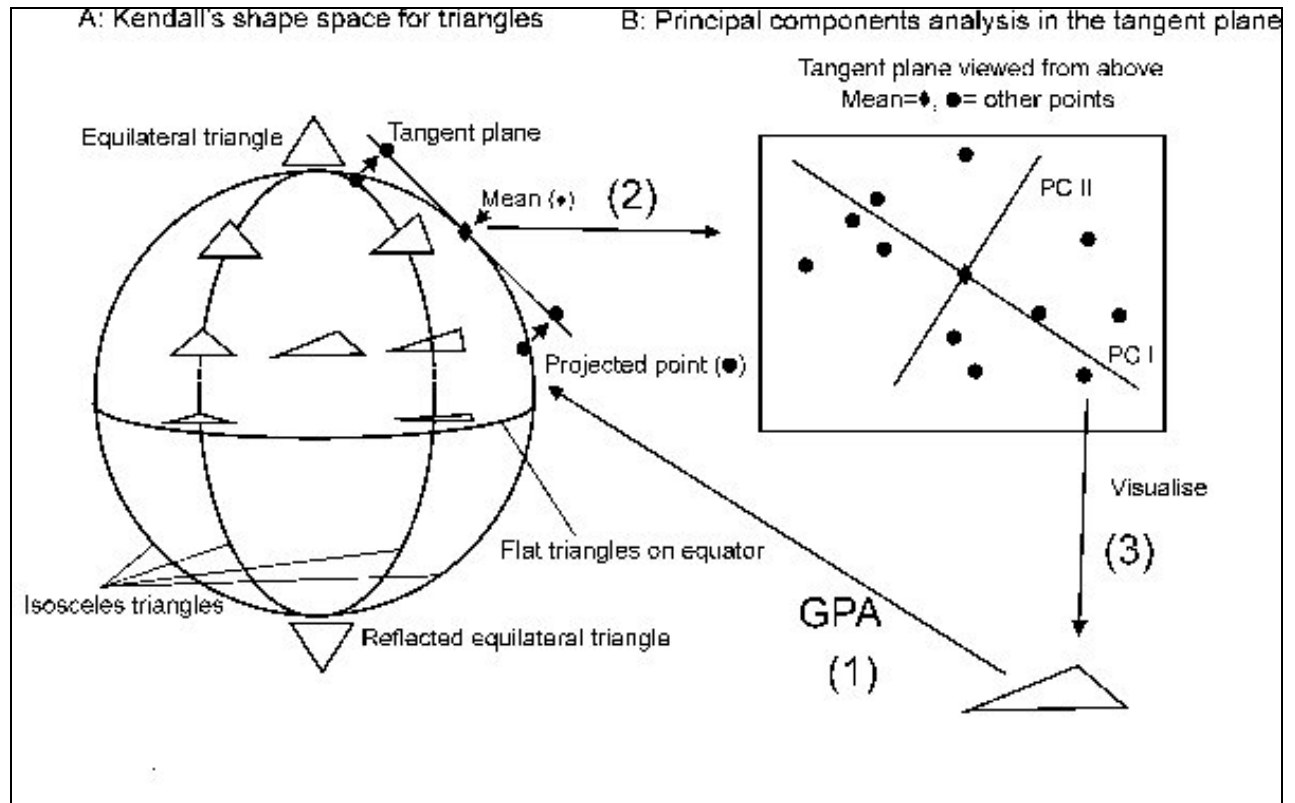


Figure D-1. The projection of three-dimensional coordinates into tangent two-dimensional space can be analyzed using multivariate techniques. Also the projection forms thin plate splines (TPS) when extracted to two dimensions (figure from Morphologika 2.5 with permission from Paul O'Higgins).

Digitizing

Methodology consists of immobilization of the mandible in fixed position to the digitizer. Three-dimensional coordinates of the skull and mandible are recorded using a Calypso three-dimensional spacer digitizer, accurate to 0.001 mm. Immobilization is initially achieved by the anchoring of the mandible using non-adhesive modeling clay at three points: the mental symphysis and both genial regions,. The internal and external

mandibular measures are then digitized, with the position of the left mental foramen repeatedly checked to insure continued immobility of the object. After the mandibular measures are taken, the remainder of the skull is placed in anatomical position atop the mandible, with the condyles in position in the glenoid fossa and the teeth in occlusion; the posterior skull supported by a column of clay to maintain perfect occlusion. (While this orientation is not in Frankfort Horizontal [FH], because all skulls are measured using the same methodology, conversion of orientation to FH later is of little trouble).

Immobility of the mandible is checked by verifying the position of the left mental foramen, and then a series of external cranial vault and facial measures are taken, with constant rechecking of the mandibular and cranial immobility. After placement of the skull into occlusion, nasion, left porion, and infraorbital foramen are used as constant reference points to check cranial immobility atop the mandible. The inferior facial and basicranial measures are then digitized, with the cranial immobilized in a fixed position relative to the digitizer. Nasion, porion, and infraorbital foramen are again used as the checkpoint for the inverted cranium, which will allow rotation of the series of inferior points into congruence with the previously gathered mandibular and external cranial and facial measure dataset.

Zero point in the research for this dissertation was as follows:

AMNH	+82.900	+145.200	+37.600
NMNH	+00107.500	+00145.000	+00039.200

Morphologika 2.5 allows visual inspection of shapes produced by the centroids, as well as examination of the effects of allometry. Figures D-2, D-3, and D-4 are some

screen captures from Morphologika 2.5. Figure D-2 is a lateral view of a 14-point three-dimensional model of the mandible, and Figure D-3 is an oblique view of same. Figure D-4 is a view of the anterior facial block. Table D-1 lists the three-dimensional points used for digitizing in Morphologika 2.5.

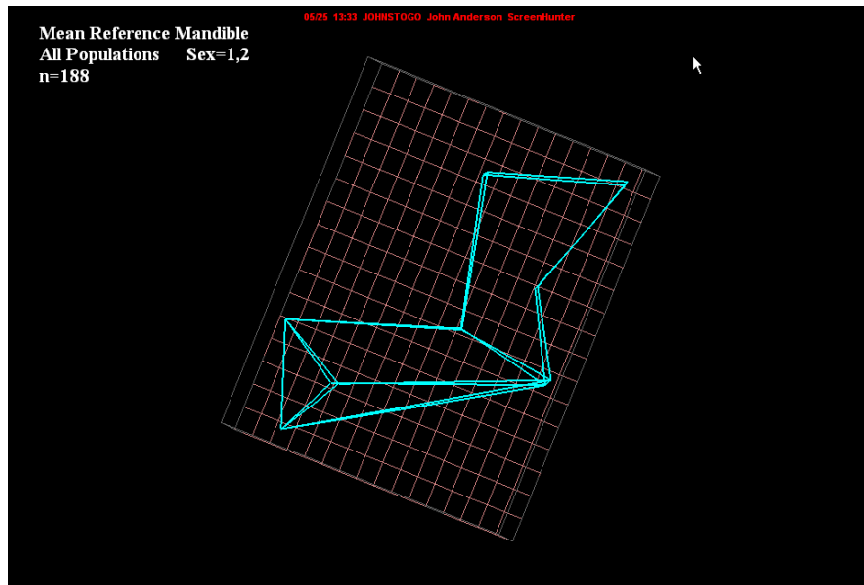


Figure D-2. Lateral mandible Analyzed in Chapters 3, 4, and 5

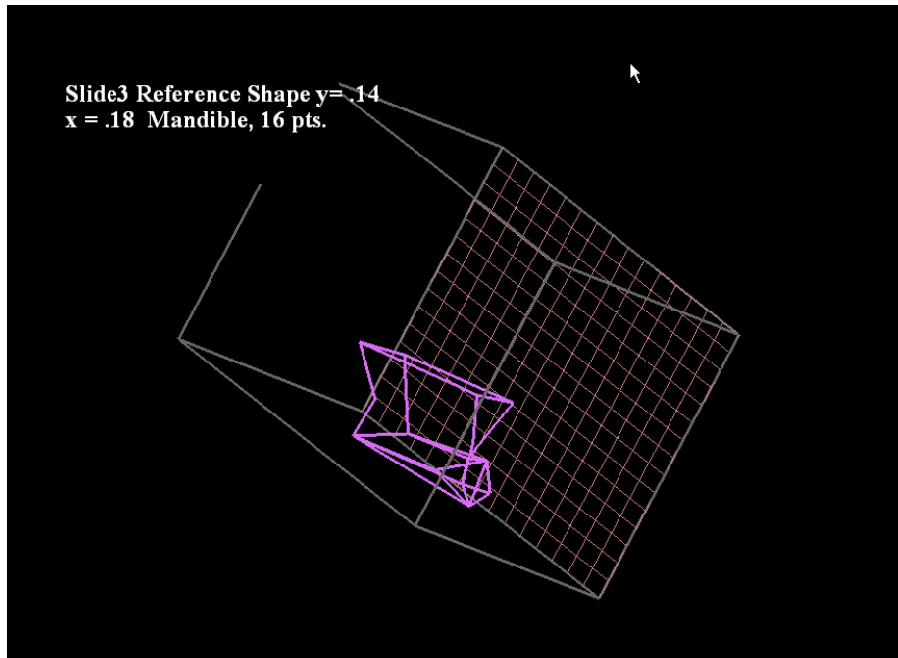
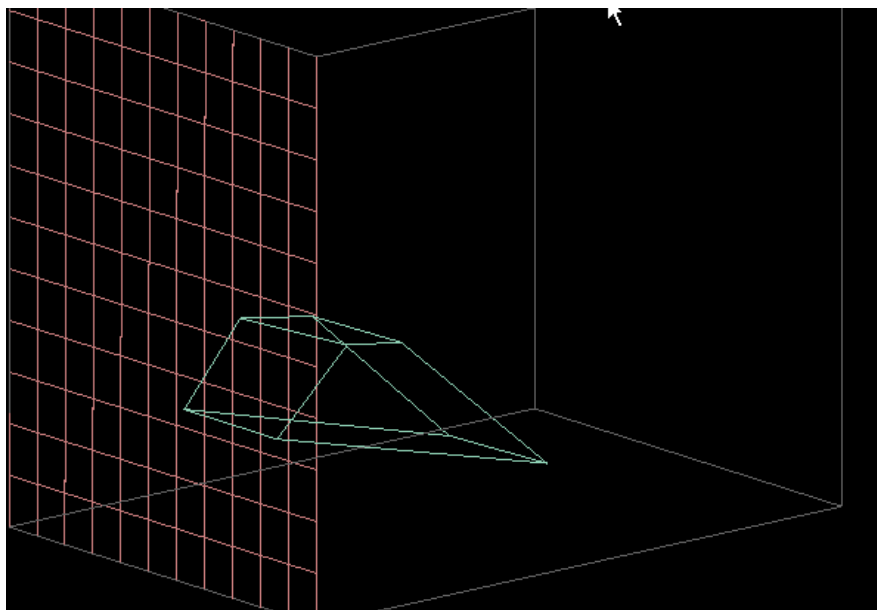


Figure D-3. Oblique View Mandible Analyzed in Chapters 3, 4, and 5 (16 points)



D-4. Anterior Facial Block, Analyzed in Chapters 4 and 5

Table D-1. Morphologika 2.5 Digitizing Points

Point No.	Digitizing Point
Points on the Mandible	
1	Posterior condyle left (ML)
2	Mid-condyle left (CC)
3	Lateral condyle
4	Bottom incisura notch, middle
5	Coronoid tip
6	Most indented ramus (MRB)
7	Height at M1superior
8	Height at symphysis superior infradentale
9	Mental foramen left
10	Mental symphysis midline inferior, pogonion (ML)
11	Height at M1 inferior
12	Alveolar plane (1 = anterior)
13	Alveolar plane (1 = middle)
14	Alveolar plane (1 = posterior)
15	Gonial angle (gonion)
16	Most indented posterior ramus (MRB)
17	Internal ramus (mandfor = top of entry left)
18	Mentum osseum right
19	Mentum osseum left
20	Mentum osseum top
21	Mental foramen left
22	Mental foramen right
23	Right side coronoid tip (other half bicoronoid)
24	Right side condyle posterior (same position as #1)
25	Outer condyle right middle (#2)
26	Right lateral condyle (other part of bicondylar width; same as #3)
27	Right side gonion
28	Right side top of mandibular foramen
29	Lingual tuberosity right side
30	Lingual tuberosity left side
31	Mental foramen left
32	Left M3 distal
33	M3 mesial
34	M2 mesial
35	M1 distal
36	M1 mesial
37	P4 mesial
38	P3 mesial
39	Canine distal

Point No.	Digitizing Point
40	Canine mesial
41	Lateral incisor distal
42	lateral incisor mesial
43	Central incisor distal
44	Central incisor medial
Breadths	
45	Canine base labial
46	Canine base lingual
47	M1 lingual left
48	M1 labial
49	M1 lingual alveolar border (across from #6)
50	M2 lingual
51	M2 labial
52	M3 lingual
53	M3 labial
54	Note on condition of dentition
Skull (note skull condition and any modification)	
55	Mental foramen left (check nasion)
56	Cranial length glabella
57	Cranial length opisthocranium
58	Cranial breadth right
59	Cranial breadth left
60	Bizygomatic right
61	Bizygomatic left
62	Porion right
63	Porion left
64	Bottom of orbit left (for Frankfort Horizontal)
65	Infraorbital foramen left
66	Infraorbital foramen right
67	Nasion
68	Supraorbital foramen left
69	Supraorbital foramen right
70	Nasal capsule right at ethmoidal suture
71	Nasal capsule left at ethmoidal suture
72	Infraspinal
73	Maximum lateral flare nose right
74	Maximum lateral flare nose left
75	Maximum height nasal aperture
76	Incision
77	Internal zygomatic left side
78	Orbitale left (will give orbital breadth)

Point No.	Digitizing Point
79	Temporal line anterior left at coronal suture
80	Temporal line anterior right at coronal suture
81	Temporal line left 15° from idealized 90° of measure at suture
82	Temporal line left 30° from idealized 90° of measure at suture
83	Temporal line left 45° from idealized 90° of measure at suture
84	Temporal line left 90° from idealized 90° of measure at suture
Crania (without mandible)	
85	Infraorbital foramen left
86	Nasion
87	Porion left
88	Foramen magnum posterior (opisthion)
89	Foramen magnum anterior (basion)
90	PTM left
91	PTM right
92	Pharyngeal tubercle left
93	Pharyngeal tubercle right
94	Incision (internal incisor point)
95	Palate breadth on suture left
96	Palate breadth on suture right
97	Glenoid depth left

APPENDIX E

CRANIAL BREADTH DISCRIMINANT ANALYSIS

The following analysis reinforces results from Hallgrímsson et al. (2007); Martínez-Abadías, et al. (2009) and Betti, et al. (2010), showing that cranial widths drive much of the variation in human skulls and are decoupled to a degree from length and width measurements. As outlined in Chapter 5, this has significance for studies which examine modularity in terms of two dimensions. Usually two-dimensional analysis uses lateral imaging such as lateral radiographs for data collection. If the breadth of the skull is the primary axis of variation, results describing three-dimensional structures such as the skull are likely to be compromised. This is particularly true for studies of population relationships based on phenotypic traits using two dimensions only (Gonzalez, et al., 2010) and even more so if climate is included as a factor (Betti, et al., 2010).

The following sequence shows sequential variable sequencing in addition of variables in discriminant function.

- ◆ The first variable distinguishing populations is facial breadth (XCB).
- ◆ The second is cranial breadth (FCB).
- ◆ The third is asterionic breadth (AUB).

This demonstrates the pattern of variation in the skull as a whole is driven by breadth measurements, and suggests removal of breadth in two-dimensional analyses is the most damaging axis of removal.

The discriminant function in Table E-1 is performed on the 21-variable subset derived from W.W. Howells's 47-measure dataset, the details for which are provided in Chapter 3 and Appendices A and B. Given the extremely large Howells dataset, all measures here

are strong predictors ($p = 0.0$). The importance is seen in the f-value, unmistakably much larger for the breadth measures.

Table E-1. Discriminant Function Analysis Illustrating Effect of Breadth Measurements

Measurements	F Ratio	Prob > F
GOL (glabello-occipital length)	79.938	0.0000000
XFB (facial breadth, #2)	524.828	0.0000000
XCB (cranial breadth, #1)	996.148	0.0000000
BNL (basion-nasion length)	78.418	0.0000000
BBH (basion-bregma height)	88.810	0.0000000
FRC (nasion-bregma chord)	52.709	0.0000000
PAC (bregma-lambda chord)	44.295	0.0000000
BPL (basion-prosthion length)	60.888	0.0000000
OBH (orbit height)	56.917	0.0000000
OBB (orbit breadth)	56.342	0.0000000
NPH (facial height)	79.525	0.0000000
NLB (nasal breadth)	54.195	0.0000000
MAB (external palate breadth)	34.149	0.0000000
ZMB (bimaxillary breadth)	32.991	0.0000000
BBH 2	88.810	0.0000000
AUB (biauricular breadth)	168.889	0.0000000
ASB (biasterionic breadth)	73.720	0.0000000
MDB (mastoid breadth)	21.063	0.0000000
MDH (mastoid height)	25.109	0.0000000
FOL (foramen magnum length)	27.312	0.0000000

LITERATURE CITED

- Ackermann RR. 2002. Patterns of covariation in the hominoid craniofacial skeleton: implication for paleoanthropological models. *J Hum Evol* 42:147–187.
- Ackermann RR. 2005. Ontogenetic integration of the hominoid face. *J Hum Evol* 48:175–197.
- Ackermann RR, Cheverud JM. 2000. Phenotypic covariance structure in Tamarins (Genus *Saguinus*): a comparison of variation patterns using matrix correlation and common principal components analysis. *Am J Phys Anthropol* 111:489–502.
- Ackermann RR, Cheverud JM. 2004. Detecting genetic drift versus selection in human evolution. *Proc Natl Acad Sci USA* 101:17946–17951.
- Akaike H. 1974. A new look at the statistical model identification. *IEEE Trans Automatic Control* 19:716–723.
- Anderson JY. 1996. Neanderthal and modern human ramal proportions. *Am J Phys Anthropol* 24S:163.
- Anderson JY. 1998. Mandibular morphology in human populations: an examination of primary muscle attachment and architectonic models for development of the ramus. *Am J Phys Anthropol* 26S:64.

- Anderson JY. 2000. Regional cranial stability: constancy of the mid-mandibulo-facial region as defined by foraminal determinants. *Am J Phys Anthropol* 30S:96.
- Anderson LC, Kosinski TF, Mentag PJ. 1991. A review of the interosseous course of the nerves of the mandible. *J Oral Implantol* 17:394–407.
- Angle EH. 1887. Notes on orthodontia, with a new system of regulation and retention. Washington DC: International Medical Congress.
- Antón S. 1989. Intentional cranial vault modification and induced changes in the cranial base and face. *Am J Phys Anthropol* 79:253–267.
- Antón S. 1994. Mechanical and other perspectives on Neandertal craniofacial morphology. In: Corruccini, RS, Ciochon RL, editors. *Integrative paths to the past: festschrift in honour of FC Howell*. Englewood Cliffs, NJ: Prentice Hall. p. 673–692.
- Arambourg C, Hoffstetter R. 1963. Le gisement de Temifine. *Arch Inst Paleont Hum* 32:1–191.

- Arnold SJ, Phillips PC. 1999. Hierarchical comparison of genetic variance-covariance matrices. II. Coastal inland divergence in the garter snake *Thamnophis elegans*. *Evolution* 53:1516–1527.
- Atchley WR, Hall BK. 1991. A model for development and evolution of complex morphological structures. *Biol Rev* 66:101–57.
- Atchley WF, Plummer AA, Riska B. 1985a. Genetics of mandible form in the mouse. *Genetics* 111:555–577.
- Atchley WF, Plummer AA, Riska B. 1985b. Genetic-analysis of size-scaling patterns in the mouse mandible. *Genetics* 111:579–595.
- Avis V. 1959. The relation of temporal muscle to the form of the coronoid process. *Am J Phys Anthropol* 17:99–105.
- Babb K, Freidline SE, Wang SL, Hansen T. 2010. Relationship of cranial robusticity to cranial form: geography and climate in *Homo sapiens*. *Am J Phys Anthropol* 141:97–115.
- Badyaev AV, Foresman KR, Young RL. 2005. Evolution of morphological integration: developmental accommodation of stress-induced variation. *Am Nat* 166:382–95.

- Bastir, M. 2008. A systems-model for the morphological analysis of integration and modularity in human craniofacial evolution. *J Anthropol Res* 86:37–58.
- Bastir M, Rosas A. 2004. Facial heights: evolutionary relevance of postnatal ontogeny for facial orientation and skull morphology in humans and chimpanzees. *J Hum Evol* 47:359–381.
- Bastir M, Rosas A. 2005. Hierarchical nature of morphological integration and modularity in the human posterior face. *Am J Phys Anthropol* 128:26–34.
- Bastir M, Rosas A. 2006. Correlated variation between the lateral basicranium and the face: a geometric morphometric study in different human groups. *Arch Oral Biol* 51:814–824.
- Bastir M, Rosas A. 2008. Mosaic evolution of the basicranium in *Homo* and its relation to modular development. *Evol Biol* (in press).
- Bastir M, Rosas A, Kuroe K. 2002. Morphogenetic determinants of mandibular ramus breadth: a test in modern human populations. *Am J Phys Anthropol* 115:40–41.
- Bastir M, Rosas A, Kuroe K. 2004. Petrosal orientation and mandibular ramus breadth: evidence for an integrated petrosomandibular developmental unit. *Am J Phys Anthropol* 123:340–350.

- Bastir M, Rosas A, O'Higgins P. 2006. Craniofacial levels and the morphological maturation of the human skull. *J Anat* 209:637–654.
- Bastir M, Rosas A, Sheets DH. 2005. The morphological integration of the hominoid skull: a partial least squares and PC analysis with morphogenetic implications for European Mid-Pleistocene mandibles. In: Slice D, editor. *Modern morphometrics in physical anthropology*. New York: Kluwer Academic / Plenum. p. 265–284.
- Beecher RM, Coruccini RS. 1981a. Effects of dietary consistency on maxillary arch breadth in macaques. *J. Dent Res* 60:68.
- Beecher RM, Coruccini RS. 1981b. Occlusal variation related to soft diet in a nonhuman primate. *Science* 218:74–76.
- Bercovitch FB. 1989. Body size, sperm competition, and determinants of reproductive success in male savanna baboons. *Evolution* 43:1507–1521.
- Betti L, Balloux F, Hanihara T, Manica A. 2010. The relative role of drift and selection in shaping the human skull. *Am J Phys Anthropol* 141:76–82.
- Biknevicius AR, Ruff C. 1992. Use of biplanar radiographs for estimating cross-sectional geometric properties of mandibles. *Anat Rec* 237:157–163.

- Biondi C. 1890. Forma e dimensioni della apofisi coronoide nella mandibula umana. *Arch Antropol Ethnol* 20:129–187.
- Boesch C, Boesch-Achermann H. 2000. The chimpanzees of the Taï Forest: behavioural ecology and evolution. Oxford: Oxford University Press.
- Boesch C, Crockford C, Herbinger I, Wittig R, Moebius Y, Normand E. 2008. Intergroup conflicts among chimpanzees in Tai National Park: lethal violence and the female perspective. *Am J Primatol* 70:519–532.
- Bookstein FL, Gunz P, Mitteroecker P, Prossinger H, Schaefer K, Seidler H. 2003. Cranial integration in Homo: singular warps analysis of the midsagittal plane in ontogeny and evolution. *J Hum Evol* 44:167–187.
- Brace CL. 1963. Structural reduction in evolution. *Am Nat* 97:39–49.
- Brace CL. 1979. Krapina, “classic” neanderthals, and the evolution of the European face. *J Hum Evol* 8:527–550.
- Brace CL, Rosenberg KR, Hunt KD. 1987. Gradual change in human tooth size in the late Pleistocene and Post-Pleistocene. *Evol* 41:705–720.

- Brace CL, Smith SL, Hunt KD. 1991. What big teeth you had grandma: human tooth size past and present. In: Kelley MA, Larsen CS, editors. *Advances in dental anthropology*. New York: Wiley-Liss. p 33–58.
- Bromage TG. 1989. Ontogeny of the early hominid face. *J Hum Evol* 18:751–773.
- Bromage TG. 1992. The ontogeny of *Pan troglodytes* craniofacial architectural relationships and implications for early humans. *J Hum Evol* 23:235–251.
- Carlson D. 1985. Craniofacial biology as “normal science.” In: Johnston LE, editor. *New vistas in orthodontics*. Philadelphia: Lea and Febiger. p 12–37.
- Carson EA. 2006a. Maximum likelihood estimation of human craniometric heritabilities. *Am J Phys Anthropol* 131:169–180.
- Carson EA. 2006b. Maximum-likelihood variance components analysis of heritabilities of cranial nonmetric traits. *Hum Biol* 78:383–402.
- Chernoff B, Magwene PM. 1999. Morphological integration: Forty years later. In: Olsen EC, Miller RL, editors. *Morphological integration*. Chicago: University of Chicago Press. p 319–354.

- Cheverud JM. 1982. Phenotypic, genetic, and environmental morphological integration in the cranium. *Evolution* 36:499–516.
- Cheverud JM. 1984. Quantitative genetics and developmental constraints on evolution by selection. *J Theor Biol* 110, 155–171.
- Cheverud JM. 1988. A comparison of genetic and phenotypic correlations. *Evolution* 42:958–968.
- Cheverud JM. 1995. Morphological integration in the saddle-back tamarind (*Saguinus fuscicollis*) cranium. *Am Nat* 145:63–89.
- Cheverud JM. 1996. Developmental integration and the evolution of pleiotropy. *Am Zool* 36:44–50.
- Cheverud, JM. 2004. Modular pleiotropic effects of quantitative trait loci on morphological traits. In: Schlosser G, Wagner G, editors. *Modularity in development and evolution*. Chicago: University of Chicago Press. p 132–153.
- Cheverud J, Kohn L, Konigsberg L, Leigh S. 1992. Effects of fronto-occipital artificial cranial vault modification on the cranial base and face. *Am J Phys Anthropol* 88:323–345.

- Cheverud JM, Midkiff J. 1992. Effects of fronto-occipital cranial reshaping on mandibular form. *Am J Phys Anthropol* 87:167–171.
- Cheverud JM, Routman EJ, Irschick DJ. 1997. Pleiotropic effects of individual gene loci on mandibular morphology. *Evolution* 51:2006–2016.
- Cheverud JM, Kohn LP, Konigsberg LW, Leigh SR. 1993. Effects of annular cranial vault modification on the cranial base and face. *Am J Phys Anthropol* 90:147–168.
- Chinn DJ, Cotes J, Martin A. 2006. Modelling the lung function of Caucasians during adolescence as a basis for reference values. *Ann Hum Biol* 33:64–77.
- Churchill SE. 1996. Particulate versus integrated evolution of the upper body in late Pleistocene humans: a test of two models. *Am J Phys Anthropol* 100:559–583.
- Churchill SE. 1998. Cold adaptation, heterochrony, and neandertals. *Evol Anthropol* 7:46–59.
- Cronbach LJ. 1951. Coefficient alpha and the internal structure of tests. *Psychometrika* 16:297–334.

- Daegling D. 1989. Biomechanics of cross-sectional size and shape in the hominoid mandibular corpus. *Am J Phys Anthropol* 80:91–106.
- Daegling D, Hylander WL. 1998. Biomechanics of torsion in the human mandible. *Am J Phys Anth* 105:73–87.
- Darroch TW, Mossiman JE. 1985. Canonical and principal components of shape. *Biometrika* 72:241–252.
- Demes B, Creel N. 1988. Bite force, diet, and cranial morphology of fossil hominids. *J Hum Evol* 17:657–670.
- Dibbets JMH. 1996. Morphological associations between the Angle classes. *Eur J Orthod* 18:11–118.
- Dobson SD, Trinkaus E. 2002. Cross-sectional geometry and morphology of the mandibular symphysis in Middle and Late Pleistocene Homo. *J Hum Evol* 43:67–87.
- Dullemeijer P, Zweers GA. 1997. The variety of explanations of living forms and structures. *Eur J Morphol* 35:354–364.
- Economos AC. 1981. On the origin of biological similarity. *J Theor Biol* 94:25–60.

Enlow DH. 1966. A morphogenetic analysis of facial growth. *Am J Orthod* 52:283–299.

Enlow DH. 1968. Wolffs law and factor of architectonic circumstance. *Am J Orthod* 54:104, 803.

Enlow DH, Moyers RE, Hunter WS, McNamara Jr. JA. 1969. A procedure for the analysis of intrinsic facial form and growth. *Am J Orthod* 56:6–23.

Enlow DH, Kuroda T, Lewis AB. 1971. Morphological and morphogenetical basis for craniofacial form and pattern. *Angle Orthod* 41:161–188.

Enlow DH, Pfister C, Richardson E, Kuroda T. 1982. An analysis of Black and Caucasian craniofacial patterns. *Angle Orthod* 52:279–287.

Eroukmanoff F, Svensson E. 2008. Phenotypic integration and conserved covariance structure in calopteryid butterflies. *J Evol Biol* 21:514–526.

Estenson TL. 1999. Symmorposis and the respiratory capacity of the upper airway. *Am J Phys Anthropol* 28S:124–125.

Estenson TL, Anderson JY. 1998. The angle of the Neandertal sulcus processus zygomaticus and masticatory muscle function. *Am J Phys Anthropol* 26S:81.

- Estenson TL. 2004. Functional constraints on the morphology of the pharynx [dissertation]. Albuquerque: University of New Mexico.
- Fisher RA. 1930. The genetical theory of natural selection. Oxford, UK: Oxford University Press.
- Flatt T. 2005. The evolutionary genetics of canalization. *Quart Rev Biol* 80:287–295.
- Flury B. 1983. Some relations between the comparison of covariance matrices and principal component analysis. *Comput Stat Data Anal*, 1: 97–107.
- Flury B. 1988. Common Principal Components and Related Multivariate Models. New York: Wiley.
- Franciscus RG. 2003. Comparing internal nasal fossa dimensions and classical measures of the external nasal skeleton in recent humans: inferences for respiratory airflow dynamics and climatic adaptation. *Am J Phys Anthropol* 36S:169
- Franciscus RG, Long JC. 1991. Variation in human nasal height and breadth. *Am J Phys Anthropol* 85:419–427.

Franciscus RG, Trinkaus E. 1988. Ethmomaxillary morphology and the emergence of *Homo erectus*. *Am J Phys Anthropol* 75:517–527.

Franciscus RG, Trinkaus E. 1995. Determinants of retromolar space presence in Pleistocene *Homo* mandibles. *J Hum Evol* 28:577–595.

Fürst CM, Hansen CC. 1915. *Crania Greenlandica*. Höst: Copenhagen.

Giesen EBW, Ding M, Dalstra M, van Eijden TMGJ. 2003. Architectural measures of the cancellous bone of the mandibular condyle identified by principal components analysis. *Calcif Tissue Int* 73:225–231.

Good B, de Montjoye YA, Clauset A. 2009. Extreme degeneracies characterize the module identification problem for complex networks. Santa Fe Institute working paper 2009-09-039.

González-José R, Escapa I, Neves WA, Rubén C, Pucciarelli HM. 2008. Cladistic analysis of continuous modularized traits provides phylogenetic signals in *Homo* evolution. *Nature* 6891:1–5.

González-José R, Ramírez-Rozzi F, Sardi M, Martínez-Abadías N, Hernández M, Pucciarelli H. 2005. Functional-craniology approach to the influence of economic strategy on skull morphology. *Am J Phys Anthropol* 128:757–771.

- González-José R, Van der Molen S, González-Pérez E, Hernández M. 2004. Patterns of phenotypic covariation and correlation in modern humans as viewed from morphological integration. *Am J Phys Anthropol* 123:69–77.
- Gonzalez PN, Perez IC, Bernal V. 2010. Ontogeny of robusticity of craniofacial traits in modern humans: a study of South American populations. *Am J Phys Anthropol* (in press).
- Górny S. 1957. Crania Africana, Uganda. *Mater Pr Anthropol* 14:1–400.
- Goswami A. 2007. Cranial modularity and sequence heterochrony in mammals. *Evol Dev* 9:290–298.
- Gould SJ, Garwood RA. 1969. Levels of integration in mammalian dentitions: an analysis of correlations in *Nesophontes micros* and *Oryzomys couesi*. *Evol* 23:276–300.
- de Graaf-Peters V, Hadders-Algra M. 2006. Ontogeny of the human central nervous system: what is happening when? *Early Hum Dev* 82:257–266.
- Greaves WS. 1978. The jaw lever system in ungulates: a new model. *J. Zool. Soc. London* 184:271–285.

- Hall BK. 1999 [1998]. *Evolutionary developmental biology*. Dordrecht, The Netherlands: Kluwer.
- Hallgrímsson B, Lieberman DE, Liu W, Ford-Hutchinson AF, Jirik FR. 2007. Epigenetic interactions and the structure of phenotypic variation in the cranium. *Evol Dev* 9:76–91.
- Hallgrímsson B, Willmore K, Hall BK. 2002. Canalization, developmental stability, and morphological integration in primate limbs. *Am J Phys Anthropol* 119:131–158.
- Hammer Ø. 2007. Spectral analysis of a Plio-Pleistocene multispecies time series using the Mantel periodogram. *Palaeogeogr Palaeoclimatol Palaeoecol* 243:373–377.
- Hammer Ø, Harper DAT, Ryan PD. 2001. PAST: Paleontological Statistics Software Package for education and data analysis. *Palaeontol Electron* 4:9.
- Hanken J, Hall BK. 1998. *The skull – vols 1, 2 3*. Chicago: University of Chicago Press.
- Hans MG, Enlow DE. 1996. *Essentials of facial growth*. Philadelphia: Saunders Co.
- Harvati K, Weaver TD. 2006. Human cranial anatomy and the differential preservation of population history and climate signatures. *Anat Rec* 288A:1225–1233.

Hatcher L. 1994. A step-by-step approach to using the SAS^(R) system for factor analysis and structural equation modeling. Cary, NC: SAS Institute.

Hawks J. 2007 (Jul 20). Not so fast, says one anthropologist. Message posted to http://johnhawks.net/weblog/reviews/early_modern/movement/modern_human_skeletal_manica_2007.html.

Hawks J. 2006 (Jan 5). Canalization. Message posted to http://johnhawks.net/weblog/reviews/genomics/evo-devo/canalization_flatt_review_2005.html.

Hershkovitz I, Speirs MS, Frayer D, Nadel D, Wish-Baratz S, Arensburg B. 1995. Ohalo II H2: A 19,000-year-old skeleton from a water-logged site at the Sea of Galilee, Israel. *Am J Phys Anthropol* 96:215–234.

Houston WJB. 1988. Mandibular growth rotations—their mechanisms and importance. *Eur J Orthod* 10:369–373.

Howells WW. 1973. Cranial variation in man. Cambridge, MA: Harvard University Press.

Howells WW. 1989. Skull shapes and the map. Cambridge, MA: Harvard University Press.

Hrdlička A. 1940a. Mandibular and maxillary hyperostoses. *Am J Phys Anthropol* 27:1–55.

Hrdlička A. 1940b. Lower jaw. *Am J Phys Anthropol* 27:281–308.

Hrdlička A. 1940c. Lower jaw: further studies. *Am J Phys Anthropol* 27:383–467.

Hrdlička A. 1945. The Aleutians and Commander Islands and their inhabitants. Philadelphia: Wistar Institute of Anatomy and Biology.

Huggare J, Houghton P. 1996. Associations between atlantoaxial and craniofacial anatomy. *Growth Dev Aging* 60:21–30.

Humfrey GM. 1866. On the growth of the jaw. *Trans Camb Philo Soc* 11:1–5.

Humphrey LT, Dean MC, Stringer C. 1999. Morphological variation in great ape and modern human mandibles. *J Anat* 195:491–513.

Hunter J. 1771. The natural history of the human teeth explaining their structure, use, formation, growth and disease. London: J. Johnson.

Hylander WL. 1976. An in-vivo analysis of the bite force utilizing rosette strain gauges.

Am J Phys Anthropol 44:187–188.

Hylander WL. 1977. The adaptive significance of Eskimo craniofacial morphology. In:

Dahlberg AA, Graber TM, editors. Orofacial growth and development. Paris:

Mouton. p 129–170.

Hylander WL. 1979. The functional significance of primate mandibular form. J Morphol

160:223–240.

Hylander WL, Johnson KR. 1994. Jaw muscle function and the wishboning of the

mandible during mastication in macaques and baboons. Am J Phys Anthropol

94:523–547.

Isberg AM, McNamara JA, Carlson DS, Isacsson G. 1986. Coronoid process elongation

in rhesus monkeys after experimentally induced hypomobility. Oral Surg Oral

Med Oral Pathol 70:704–710.

Jantz RL, Owsley DW. 2003. Reply to Van Vark et al.: Is European Upper Paleolithic

cranial morphology a useful analogy for early Americans? Am J Phys Anthropol

121:185–188.

- Kaifu, Y. 1998a. Attritional occlusion. *Anthropol Sci* 106: 128–135.
- Kaifu, Y. 1998b. Alveolar prognathism and tooth wear. *Anthropol Sci* 106:136–144.
- Kappelman J. 1996. Evolution of body mass and relative brain size in fossil hominids. *J Hum Evol* 30:243–276.
- Kean MR, Houghton P. 1987. The role of function in the development of human craniofacial form—a perspective. *Anat Rec* 218:107–110.
- Kieser J. 1999. Biomechanics of masticatory force production. *J Hum Evol* 36:575–581.
- Kiliardis S, Engstrom C, Chavez L. 1995. Craniofacial morphology, occlusal traits, and bite force in persons with advanced occlusal tooth wear. *Am J Orthod Dentofac Orthop* 107:1184–1187.
- Klingenberg CP. 2004. Integration, modules and development: molecules to morphology to evolution. In: Pigliucci M, Preston K, editors. *Phenotypic integration: studying the ecology and evolution of complex phenotypes*. New York: Oxford University Press. p 213–230.

- Klingenberg CP. 2005. Developmental constraints, modules and evolvability. In:
Hallgrímsson B, Hall BK, editors. Variation: a central concept in biology. San
Diego: Academic Press. p 219–247.
- Klingenberg CP, Badyaev AV, Sowry SM, Beckwith NJ. 2001. Inferring developmental
modularity from morphological integration: analysis of individual variation and
asymmetry in bumblebee wings. *Am Nat* 157:11–23.
- Klingenberg CP, Leamy LJ. 2001. Quantitative genetics of geometric shape in the mouse
mandible. *Evolution* 55:2342–2352.
- Klingenberg CP, Mebus K, Auffray J-C. 2003. Developmental integration in a complex
morphological structure: how distinct are the modules in the mouse mandible?
Evol Dev 5:522–531.
- Klingenberg CP, Zimmermann M. 1992. Dyar Rule and multivariate allometric growth in
9 species of waterstriders (heteroptera, gerridae). *J Zool* 227:453–464.
- Kohn LP, Leigh S, Cheverud JM. 1995. Asymmetric vault modification in Hopi crania.
Am J Phys Anthropol 98:173–195.
- Konigsberg LW, Kohn LP, Cheverud JM. 1993. Cranial deformation and non-metric
trait variation. *Am J Phys Anthropol* 90:35–48.

- Kuratani S. 2005. Evolutionary developmental biology and vertebrate head segmentation: a perspective from developmental constraint. *Theor Biosci* 122:230–251.
- Lahr MM, Wright RVS. 1996. The question of robusticity and the relationship between cranial size and shape in *Homo sapiens*. *J Hum Evol* 31:157–191.
- Leakey MG, Spoor F, Brown FH, Gathogo PN, Kiarie C, Leakey LN, McDougall I. 2001. New hominin genus from eastern Africa shows diverse middle Pliocene lineages. *Nature* 410:433.
- Leamy LJ, Routman EJ, Cheverud JM. 1999. Quantitative trait loci for early- and late-developing skull characters in mice: a test of the genetic independence model of morphological integration. *Am. Nat.* 153:201–214.
- Lieberman DE. 1996. How and why recent humans grow thin skulls: Experimental data on systemic cortical robusticity. *Am J Phys Anthropol* 101:217–236.
- Lieberman DE. 1998. Sphenoid shortening and the evolution of modern human cranial shape. *Nature* 393:158–162.

- Lieberman DE. 2007. Palaeoanthropology: homing in on early Homo. *Nature* 449:291–292.
- Lieberman DE, McBratney BM, Krovitz G. 2002. Evolution and development of cranial form in Homo sapiens. *Proc Natl Acad Sci USA* 99:1134–1139.
- Lieberman DE, McCarthy RC. 1999. The ontogeny of cranial base angulation in humans and chimpanzees and its implication for reconstructing pharyngeal dimensions. *J Hum Evol* 36:487–517.
- Lieberman DE, Mowbray KM, Pearson OM. 2000. Basicranial influences on overall cranial shape. *J Hum Evol* 38:291–315.
- Lieberman DE, Ross CR, Ravosa M. 2000. The primate cranial base: ontogeny, function and integration. *Yeast Phys Anthropol* 43:117–169.
- Lin Y-F. 1993. Study on morphology of mandibular corpus and ramus influencing the eruption of the mandibular first permanent molar. *Bull Tokyo Med Dent Univ* 40:17–28.
- Lockwood CA. 2007. Adaptation and functional integration in primate phylogenetics. *J Hum Evol* 52:490–503.

- Lockwood CA, Fleagle JG. 1999. The recognition and evaluation of homoplasy in primate and human evolution. *Yearb Phys Anthropol* 42:189–232.
- Magwene PM. 2001. New tools for studying integration and modularity. *Evolution* 55:1734–1745.
- Manica A, Amos W, Balloux F, Hanihara T. 2007. The effect of ancient population bottlenecks on human phenotypic variation. *Nature* 448:346–348.
- Mardia KV, Bookstein F, Moreton I. 2000. Statistical assessment of bilateral symmetry of shapes. *Biometrika* 87:285–300.
- Marroig G, Cheverud JM. 2001. A comparison of phenotypic variation and covariation patterns and the role of phylogeny, ecology, and ontogeny during cranial evolution of New World monkeys. *Evolution* 55:2576–2600.
- Marroig G, Cheverud JM. 2005. Size as a line of least evolutionary resistance: diet and adaptive morphological radiation in New World monkeys. *Evolution* 59:1128–1142.
- Martin CP, O'Brien HD. 1939. The coracoid process in the primates. *J Anat* 73:630–642.
- Martin R. 1928. *Lehrbuch der anthropologie in systematischer darstellung mit besonderer berücksichtigung deranthropologischen methoden für studierende, ärzte und*

forschungsreisende. aweiter band: kraniologie, osteologie [2 ed]. Jena: Gustav Fischer.

Martin, R. 1937 [1962]. Lehrbuch der anthropologie. Berlin: Fischer.

Martínez-Abadías N, Esparza M, Sjøvold T, González-José R, Santos M, Hernández M. 2009. Heritability of human cranial dimensions: comparing the evolvability of different cranial regions. *J Anat* 214:19–35.

Martínez-Abadías N, González-José R, González-Martín A, Van der Molen S, Talavera A, Hernández P, Hernández M. 2006. Phenotypic evolution of human craniofacial morphology after admixture: a geometric morphometrics approach. *Am J Phys Anthropol* 129:387–398.

Martínez-Abadías N, Esparza M, Sjøvold T, Gonzalez-Jose R, Santos M, Hernandez M, Klingenberg CP. 2008. Detecting natural selection in modern human skulls [meeting abstract]. *Am J Phys Anthropol* 46S:150.

Martone VD, Enlow D, Hans M, Broadbent H, Oyen O. 1991. Class I and Class III malocclusion sub-groupings related to headform type. *Angle Orthod* 62:35–43.

Mayr, E. 1947. Ecological factors in speciation. *Evolution* 1:263–288.

- McCabe T. 1997. Implications of intermixture on human cranial morphology [dissertation]. Albuquerque: University of New Mexico.
- McCarthy R. 2001. Anthropoid cranial base architecture and scaling relationships. *J Hum Evol* 40:41–66.
- McCarthy R, Lieberman DE. 2001. Posterior maxillary (PM) plane and anterior cranial architecture in primates. *Anat Rec* 264:247–260.
- McCollum M. 1999. The robust australopithecine face: a morphogenetic perspective. *Science* 284:301–305.
- McCollum, M. 2008. Nasomaxillary remodeling and facial form in robust *Australopithecus*: a reassessment. *J Hum Evol* 54:2–14.
- McCown, TD, Keith A. 1939. The Stone Age of Mount Carmel: the fossil human remains from the Levallois-Mousterian. 2 vols. Oxford, UK: Clarendon Press.
- Mezey JG, Cheverud JM, Wagner GP. 2000. Is the genotype-phenotype map modular? statistical approach using mouse quantitative trait loci data. *Genetics* 156:305–311.

- Milicerowa H. 1955. *Crania Australica* [Materia i Prace Antropologiczne, No. 6].
Wrocaw: Polska Akademia Nauk Zaklud Antropologii.
- Mitteroecker P, Bookstein F. 2007. Conceptual and statistical relationship between modularity and morphological Integration. *Syst Biol* 56:818–886.
- Mitteroecker P, Bookstein F. 2008. The evolutionary role of modularity and integration in the hominoid cranium. *Evolution* 62: 943–958.
- Mitteroecker P, Gunz P, Bernhard M, Schaefer K, Bookstein F. 2004. Comparison of cranial ontogenetic trajectories among great apes and humans. *J Hum Evol* 46:679–697.
- Moss M. 1962. The functional matrix. In: Kraus B, Reidel R, editors. *Vistas in orthodontics*. Philadelphia: Lea and Febiger. p 85–98.
- Moss M. 1997a. The functional matrix hypothesis revisited. 1. The role of mechanotransduction. *Am J Orthod Dentofacial Orthop* 112:8–11.
- Moss M. 1997b. The functional matrix hypothesis revisited. 2. The role of an osseous connected cellular network. *Am J Orthod Dentofacial Orthop* 112:221–226.

Moss M. 1997c. The functional matrix hypothesis revisited. 3. The genomic thesis. *Am J Orthod Dentofacial Orthop* 112:338–342.

Moss M. 1997d. The functional matrix hypothesis revisited. 4. The epigenetic antithesis and the resolving synthesis. *Am J Orthod Dentofac Orthop* 112:410–417.

Moss M, Young RW. 1960. A functional approach to craniology. *Am J Phys Anthropol* 45:281–292.

Müller GB, Wagner GP. 1996. Homology, Hox genes, and developmental integration. *Am Zool* 36:4–13.

Nicholson E, Harvati K. 2006. Quantitative analysis of human mandibular shape using three-dimensional geometric morphometrics. *Am J Phys Anthropol* 131:368–383.

O'Higgins P. 1999. Ontogeny and phylogeny: some morphometric approaches to skeletal growth and evolution. In: Chaplain MAJ, Singh GD, McLachlan JC, editors. *On growth and form: spatio-temporal pattern formation in biology*. New York: John Wiley & Sons. p 373–393.

O'Higgins P. 2000. Study of morphological variation in the hominid fossil record: biology, landmarks and geometry. *J Anat* 197:103–120.

- O'Higgins P, Bastir M, Kupczik K. 2006. Shaping the human face. *Int Cong Ser* 1296:55–73.
- Olson EC, Miller RL. 1958 [1999]. *Morphological integration*. Chicago: University of Chicago Press.
- Orr HA. 2005. Turned on: a revolution in the field of evolution? *New Yorker* Oct 24:85–88.
- Osborn JW. 1996. Features of the human jaw which maximize the bite force. *J Biomech* 29:589–595.
- Phillips PC, Arnold SJ. 1999. Hierarchical comparison of genetic variance-covariance matrices. I. Using the Flury hierarchy. *Evolution* 53: 1506–1515.
- Pigliucci M. 2006. Genetic variance-covariance matrices: critique of the evolutionary quantitative genetics research program. *Biol Philos* 21:1–23.
- Pinhasi R. 2000. The position of the Nazlet Khater specimen among prehistoric and modern African and Levantine populations. *J Hum Evol* 39:269–288.
- Polanski JM, Franciscus RG. 2006. Patterns of craniofacial integration in extant Homo, Pan, and Gorilla. *Am J Phys Anthropol* 131:38–49.

- Raff RA. 1996. The shape of life: genes, development, and the evolution of animal form. Chicago: University of Chicago Press.
- Rak Y. 1986. The Neanderthal: a new look at an old face. *J Hum Evol* 15:151–164.
- Rak Y. 1998. Does any Mousterian cave present evidence of two hominid species? In: Akazawa T, Aoki K, Bar-Yosef O, editors. Neandertals and modern humans in Western Asia. New York: Plenum Press. p 353–366.
- Rak Y, Ginzburg A, Geffen E. 2002. Does Homo neanderthalensis play a role in modern human ancestry? The mandibular evidence. *Am J Phys Anthropol* 119:199–204.
- Rak Y, Ginzburg A, Geffen E. 2007. Gorilla-like anatomy on Australopithecus afarensis mandibles suggests Au. afarensis link to robust australopiths. *Proc Nat Acad Sci* 104:6568–6572.
- Ravosa MJ, Shea BT. 1994. Pattern in craniofacial biology: evidence from the Old World Monkeys (Cercopithecidae). *Int J Primatol* 15:801–828.
- Renaud S, Auffray J-C, Michaux J. 2006. Conserved phenotypic variation patterns, evolution along lines of least resistance, and departure due to selection in fossil rodents. *Evolution* 60:1701–1717.

- Richards GD, Jabbour RS, Anderson JY. 2003. Medial mandibular ramus: ontogenetic, idiosyncratic, and geographic variation in recent Homo and fossil hominids [BAR International Series 1138]. Oxford: BAR Hedges.
- Rohlf FJ, Slice D. 1990. Extensions of the procrustes method for the optimal superimposition of landmarks. *Syst Zool* 39:40–59.
- Rohlf FJ, Corti M. 2000. The use of two-block partial least-squares to study covariation in shape. *Syst Biol* 49:740–753.
- Rosas A. 1995. Seventeen new mandibular specimens from the Atapuerca/Ibeas Middle Pleistocene hominid sample (1985–1992). *J Hum Evol* 28:533–560.
- Rosas A. 1997. A gradient of size and shape for the Atapuerca sample and Middle Pleistocene hominid variability. *J Hum Evol* 33:319–331.
- Rosas A. 2001. Occurrence of neanderthal features in mandibles from the Atapuerca-SH site. *Am J Phys Anthropol* 114:74–91.
- Rosas A, Bastir M. 2002. Thin-plate spline analysis of allometry and sexual dimorphism in the human craniofacial complex. *Am J Phys Anthropol* 117:236–245.

- Rosas A, Bastir M. 2004. Geometric morphometric analysis of allometric variation in the mandibular morphology from the hominids of Atapuerca, Sima de los Huesos site. *Anat Rec* 278A:551–560.
- Rosas A, Bastir M, Alarcón JA, Kuroe K. 2008. Thin-plate spline analysis of the cranial base in African, Asian and European populations and its relationship with different malocclusions. *Arch Oral Biol*.
- Rosas A, Bastir M, Martinez-Maza C. 2002. Morphological integration and predictive value of the mandible in the craniofacial system of hominids: a test with the Atapuerca SH mandibular sample. *Coll Antropol* 26:171–172.
- Rosas A, Martinez-Maza C, Bastir M, Garcia-Tabernero A, Lalueza-Fox C, Huguet R, Ortiz JE, Julia R, Soler V, Torres TD, Martinez E, Cañaveras JC, Sanchez-Moral S, Cuezva S, Lariol J, Santamaria D, de la Rasilla M, Fortea J. 2006. Paleobiology and comparative morphology of a late Neandertal sample from El Sidrón, Asturias, Spain. *Proc Natl Acad Sci USA* 103:19266–19271.
- Ross C, Henneberg M. 1995. Basicranial flexion, relative brain size, and facial kyphosis in *Homo sapiens* and some fossil hominids. *Am J Phys Anthropol* 98:575–593.
- Ross CF, Ravosa MJ. 1993. Basicranial flexion, relative brain size, and facial kyphosis in nonhuman primates. *Am J Phys Anthropol* 91:305–324.

Roth VL. 1996. Cranial integration in the *Sicuridae*. *Am Zool* 36:14–23.

Rothhammer F, Silva C. 1990. Craniometrical variation among South-America prehistoric populations: climatic, altitudinal, chronological, and geographic contributions. *Am J Phys Anthropol* 82:9–17.

Sarnat BG. 1986. Growth patterns of the mandible: some reflections. *Am J Dentofac Orthop* 90:221–232.

Sarnat BG, Engel MB. 1985. A serial study of mandibular growth after removal of the condyle in the *Macaca rhesus* monkey. *Plastic Recon Surg* 7:364–380.

Schluter D. 1996. Adaptive radiation along genetic lines of least resistance. *Evolution* 50:1766–1774.

Schreiner KW. 1935. *Zur osteologie der Lappen*. Oslo: Instituttet for Sammenlignende Kulturforskning.

Schreiner KW. 1939. *Crania Norvegica I*. Oslo: Instituttet for Sammenlignende Kulturforskning.

- Schreiner KW. 1946. *Crania Norvegica II*. Oslo: Instituttet for Sammenligende Kulturforskning.
- Schultz HE. 1933. Ein Beitrag zur Rassenmorphologie des Unterkiefers. *Zeitschr F Morph U Anthropol* 32:275–366.
- Schwartz JH, Tattersall I. 2000. The human chin revisited: what is it and who has it? *J Hum Evol* 38:367–409.
- Schwartz GT, Conroy GC. 1996. Cross-sectional properties of the *Otaviapithecus* mandible. *Am J Phys Anthropol* 99:613–623.
- Schillaci M. 2008. Human cranial diversity and evidence for an ancient lineage of modern humans. *J Hum Evol* 54:814–826.
- Seddon, RP. 1984. A cephalometric study of the Romano British. *Eur J Orthod* 6:303–312.
- Smith K. 1996. Integration of craniofacial structures during development in mammals. *Am Zool* 36:70–79.
- Smith RJ. 1982. On the mechanical reduction of functional morphology. *J Theor Biol* 96: 99–106.

- Smith RJ. 1984. The plan of the human face: a test of three general concepts. *Am J Orthod* 85:103–109.
- Sofaer JA. 1972. A model relating developmental interaction and differential evolutionary reduction of tooth size. *Evolution* 27:427–434.
- Spencer MA. 1998. Force production in the primate masticatory system: electromyographic tests of biomechanical hypotheses. *J Hum Evol* 34:25–54.
- Spencer MA. 1999. Constraints of masticatory system evolution in anthropoid primates. *Am J Phys Anthropol* 108:483–506.
- Spencer MA, Demes B. 1993. Biomechanical analysis of masticatory system in Neandertals and Inuits. *Am J Phys Anthropol* 91:1–20.
- Sperber GH. 2001. Craniofacial development. London: BC Decker Inc.
- SPSS (Statistical Package for the Social Sciences), Version 11.5 1989–2009.
- Stedman HH, Kozyak BW, Nelson A, Thesier DM, Su LT, Low DW, Bridges CR, Shrager JB, Minugh-Purvis N, Mitchell MA. 2004. Myosin gene mutation correlates with anatomical changes in the human lineage. *Nature* 428:415–418.

- Steppan SJ. 1997. Phylogenetic analysis of phenotypic covariance structure. I. Contrasting results from matrix correlation and common principal components analyses. *Evolution* 51:571–586.
- Strait DS. 2001. Integration, phylogeny, and the hominid cranial base. *Am J Phys Anthropol* 114:273–297.
- Strand-Vidarsdóttir U, O’Higgins P, Stringer CB. 2002. A geometric morphometric study of regional differences in the ontogeny of the modern human facial skeleton. *J Anat* 201:211–229.
- Symons, NB. 1951. Mandibular morphology. *Dent Rec* 71:41–42.
- Trinkaus E. 2003. Neandertal faces were not long; modern human faces are short. *Proc Natl Acad Sci USA* 100:8142–8145.
- Trinkaus E, Milota S, Rodrigo R, Mircea G, Moldovan O. 2003. Early modern human cranial remains from the Pesteră cu Oase, Romania. *J Hum Evol* 45:245–253.
- Trinkaus E, Ruff CB. 1995. Yamashita-cho 1 and early modern human lower limb ontogeny. *Am J Phys Anthropol* 38S:104.

Twisselmann F. 1973. Evolution des dimensions et de la forme de la mandibule, du palais and des dents de l'homme. *Ann Paléontol Vert* 59:173–277.

Van Valen L. 1965. The study of morphological integration. *Evolution* 19:347–349.

Vrba, ES. 1996. Climate, heterochrony, and human evolution. *J Anthropol Res* 52:1–28.

Waddington CH. 1942. Canalization of development and the inheritance of acquired characters. *Nature* 150:563–565.

Waddington CH. 1957. *The strategy of the genes*. New York: Macmillan and Co.

Wagner GP. 1984. On the eigenvalue distribution of genetic and phenotypic dispersion matrices: evidence for a nonrandom organization of quantitative character variation. *J Math Biol* 21:77–95.

Wagner GP. 1989 [2009]. A comparative study of morphological integration in *Apis mellifera*. *J Zool Syst Evol Res* 28:28–61.

Wagner GP. 1996. Homologues, natural kinds and the evolution of modularity. *Am Zool* 36:36–43.

Wagner GP, Altenberg L. 1996. Complex adaptations and the evolution of evolvability. *Evolution* 50:967–976.

Wagner GP, Pavlicev M, Cheverud JM. 2007. The road to modularity. *Nature Rev Genet* 8: 921–931.

Wake, D. 1993. Brain-stem organization and branchiomic nerves. *Acta Anat* 148:124–131.

Wake D, Larson A. 1987. Multidimensional analysis of an evolving lineage. *Science* 238:42–49.

Washburn S. 1947. The relation of the temporal muscle to the form of the skull. *Anat Rec* 99:239–249.

Weidenreich F. 1936. The mandibles of *Sinanthropus pekinensis*: a comparative study. *Palaeontol Sin D* 7:1–163.

Weijjs WA. 1989. The functional significance of morphological variation of the human mandible and masticatory muscles. *Acta Morphol Neerl Scand* 27:149–162.

Weijjs WA, Hillen B. 1986. Correlations between the cross-sectional area of the jaw muscles and craniofacial size and shape. *Am J Phys Anthropol* 70:423–431.

Weiner JS. 2003. The Piltdown Forgery: the classic account of the most famous and successful hoax in science. Oxford, UK: Oxford University Press.

Weinstein K. 2008. Thoracic morphology in Near Eastern Neandertals and early modern humans compared with recent modern humans from high and low altitudes. *J Hum Evol* 54:287–295.

Weishample DB. 1993. Beams and machines: modeling approaches to the analysis of skull form and function. In: Hanken J, Hall BK, editors. *The skull – vol 3*. Chicago: University of Chicago Press. p 303–343.

Welch JJ, Waxman D. 2003. Modularity and the cost of complexity. *Evolution* 57:1723–1734.

Wenzel A, Williams S, Ritzau M. 1989. Relationships of changes in craniofacial morphology, head posture, and nasopharyngeal airway size following mandibular osteotomy. *Am J Orthod Dentofacial Orthop* 96:138–143.

White TD. 1991. *Human osteology*. San Diego: Academic Press.

- Willmore KE, Leamy L, Hallgrímsson B. 2006. Effects of developmental and functional interactions on mouse cranial variability through late ontogeny. *Evol Dev* 8:550–567.
- Wolff J. 1891. *Das gesetz der transformation der knochen*. Berlin: A. Hirschwald.
- Wolpoff M. 2000 [1999]. *Paleoanthropology*. Boston: McGraw-Hill.
- Wolpoff M. 2007. How Neandertals inform human variation. *Am J Phys Anthropol* 139:91–102.
- Wood BA. 1976. Nature and basis of sexual dimorphism in primate skeleton. *J Zool* 180:15–34.
- Wood BA, Li Y, Willoughby C. 1991. Intraspecific variation and sexual dimorphism in cranial and dental variables among higher primates and their bearing on the hominid fossil record. *J Anat* 174:185–205.
- Wood BA, Lieberman DE. 2001. Craniodental variation in *Paranthropus boisei*: a developmental and functional perspective. *Am J Phys Anthropol* 116:13–25.
- Wright S. 1934. The method of path coefficients. *Ann Math Stat* 6:161–215.

Wright RVS. 1992. Correlation between cranial form and geography in *Homo sapiens*:
CRANID – a computer program for forensic and other applications. *Archaeol
Oceania* 27:128–134.

y'Edynak G. 1989. Yugoslav dental reduction. *Am J Phys Anthropol* 78:17–36.

Young NM. 2006. Function, ontogeny and canalization of shape variance in the primate
scapula. *J Anat* 209:623–636.

Zelditch ML. 1987. Evaluating models of developmental integration in the laboratory
rat using confirmatory factor analysis. *Syst Zool* 36:368–380.

Zollikofer CPE, Ponce de León MS. 2002. Visualizing patterns of craniofacial shape
variation in *Homo sapiens*. *Proc R Soc Lond [Biol]* 269:801–807.